Natural Killer Cells and Pre-B Acute Lymphoblastic Leukemia : Evidence for an Unconventional Cytotoxicity Pathway

Simon Nicoletti

université PARIS-SACLAY

NNT : 2017SACLS383

UNIVERSITÉ PARIS SUD
Comprendre le monde, construire l'avenir

Natural Killer cells and pre-B acute lymphoblastic leukemia: evidence for an unconventional cytotoxicity pathway

Thèse de doctorat de l'Université Paris-Saclay
préparée à l'Université Paris Sud

École doctorale n°582
Cancérologie : Biologie – Médecine – Santé (CBMS)
Spécialité de doctorat : aspects moléculaires et cellulaires de la biologie

Thèse présentée et soutenue à Paris, le 6 novembre 2017, par

M. Simon Nicoletti

Composition du Jury :

M. Éric Solary Professeur des Universités – Praticien Hospitalier Université Paris Sud (Institut Gustave Roussy, UMR 1170)	Président
Mme Catherine Blish M.D., Ph.D., Professeure Stanford University (Stanford School of Medicine)	Rapporteur
M. Thierry Walzer Directeur de recherche, ENS, Université de Lyon Centre International de Recherche en Infectiologie	Rapporteur
M. Alain Fischer Professeur des Universités – Praticien Hospitalier Institut Imagine UMR 1163, Collège de France	Examinateur
M. Felipe Suarez Professeur des Universités – Praticien Hospitalier Institut Imagine UMR 1163	Examinateur
M. Olivier Hermine Professeur des Universités – Praticien Hospitalier Institut Imagine UMR 1163	Directeur de thèse
M. Élie Haddad Professeur titulaire CHU Sainte-Justine, Université de Montréal	Co-Directeur de thèse

Thèse de doctorat

À mamie Jeannette,

une grand-mère provençale pleine d’amour et d’élégance

ACKNOWLEDGEMENTS

The study that is presented here is a synthesis of a story that started in August 1st, 2010, when I first arrived in Canada. Since then, many different people contributed to make it more than a research work.

I want to thank Élie Haddad for such incredible relationships. In my work, he made me learn experimental controls, rigor, experimental controls, creativity, experimental controls, analogies, experimental controls, and so much more. More than that, I believe I have been very lucky to meet a pediatrician, physician, with a very simple and direct contact. Someone that, as a patient or a family, I know I would like to meet. Un immense merci Élie, ce travail avec vous a été simplement génial et le meilleur moment de ma vie.

Canada has been an amazingly welcoming country. The very beginning was a complicated start, arriving alone in an unknown land. But I was lucky enough to meet people that I definitely keep in my mind and in my heart.
I want to thank: Silvia Selleri, the Italian source of inspiration to whom I owe many knowledges in science and immunology; Mame Massar Dieng and Vimal Krishnan, incredible friends, a family; Françoise Le Deist, for her help, her rigor, her mentorship, many thanks to her; Isabelle Louis, Panojot Bifsha, François Fontaine, Kathie Béland, Renée Dicaire, Ludovic Durrieu, Joëlle Grégoire-Gauthier, Arnaud Duval, Yuanyi Li, Mark Abramovitz, Zoulfia Allakhverdieva, Didier Doranger, Aurélien Colamartino, Chloé Colas, Hugo Roméro, in my lab. Et quel laboratoire!
I also need to thank my roommates: Matthew Morantz, actually as a part of my family; Marigona Uka, a sweet friend. I wish them both the best. And George Fisher as well.
Looking at these names, you understand Canada and its strength. I'm proud to have been part of it.

Back to France, I have to thank Olivier Hermine for his help and mentorship in this project. Thanks to him, we were able to pursue the work and I was allowed to do my PhD. His humanity and his devotion are precious for patients. Merci Olivier pour ces fulgurances et ces échanges plus qu'enrichissants, parfois tardifs pour ne pas dire nocturnes! Je garde en mémoire un départ dans la nuit parisienne en vélo, comme un moment privilégié.
I want to thank in my lab: Mathilde Lamarque and her delicious cakes; Hervé Souchet, a sailor climbing partner; Morgane Cheminant, very efficient and a clever mind; Moussab Tatfi,

a surprising friend. The lab 217 was an amazing atmosphere. Thank you to Francine Côté, a bridge between Montreal and Paris, Joël Babdor, a climbing friend sharing interesting ideas.
Thanks to all the members of the team Hermine: Flavia Guillem, Geneviève Courtois, Guillemette Fouquet, Leila Maouche-Chrétien, Lucile Couronné, Yves Lepelletier… and all the others.
I also need to thank many people from Imagine institute, Olivier Pellé and Aude Magerus for their help with the Fortessa, asso YR2I, and colleagues and friends from many labs (Benoît, Antoine, David, Clarisse, Christelle…).
In Lyon, I thank Laurent Jacqueroud, a true friend with whom we have been through the challenging steps of the MSc before we started our PhD. Besides, Pierre Cochat, Charles Dumontet, Caroline Moyret-Lalle, Yves Bertrand and Alexandre Belot were very important for me, especially to build a consistent medical and scientific career path.

I also want to thank our collaborators worldwide. Their help is crucial. It makes our science feasible.
Thanks to the ARC Foundation for their financial support for the 4th year of PhD; The Liliane Bettencourt School of Inserm, and the Bettencourt-Schueller Foundation for their scholarship during the medical school.

Thanks to Catherine Blish, Alain Fischer, Eric Solary, Felipe Suarez and Thierry Walzer for their role in the evaluation of this manuscript. It's a great honor and a privilege for me.

My parents and my brother are the cornerstones of my personality. I owe them everything. Merci à la famille Nicoletti, nous quatre, un solide repère, une direction.

I started these acknowledgements writing it was more than a research work. I'm looking forward to the next stopovers.

TABLE OF CONTENTS

LIST OF ABBREVIATIONS AND ACRONYMS

7-AAD : 7-aminoactinomycine
ALL: Acute lymphoblastic leukemia
AML: Acute myeloid leukemia
APAF-1: Apoptotic protease activating factor 1
APC : Allophycocyanine
BCA: Bicinchoninic acid
B-EBV LCL: Epstein-Barr virus-transformed human B-lymphoblastoid cell lines
BID: BH3 interacting domain death agonist
BMMCs: Bone marrow mononuclear cells
BSA : Bovine serum albumin
CCCP: Carbonyl cyanide m-chlorophenylhydrazone
CD: Cluster of differentiation
CFSE : 5-6 Carboxy fluorescein diacetate succimidyl ester
CGD: Chronic granulomatous disease
CIK: Cytokine-induced killer cells
CPDA: Citrate phosphate dextrose adenine solution
CRISPR: Clustered regularly interspaced short palindromic repeats
CTL : Cytotoxic T lymphocytes
DAP10: DNAX-activating protein 10
DCs: Dendritic cells
DHR: Dihydrorhodamine
DKO: Double knockout
DMSO: Dimethylsulfoxide
D-PBS: Dulbecco's phosphate buffer saline
DRs: Death receptors
ECAR: Extracellular acidification rate
E:T ratio: Effector to target ratio
FACS : Fluorescence-activated cell sorting
FADD: FAS-associated death domain protein
FAS: Cluster of differentiation
FBS: Fetal bovine serum
FCC: Flow cytometry-based cytotoxicity assay
FHL: Familial hemophagocytic lymphohistiocytosis
FITC: Fluorescein isothiocyanate
FLICA: Fluorescent labelled inhibitors of caspases
GFP : Green fluorescent protein
GM-CSF: Granulocyte macrophage colony-stimulating factor
GvHD: Graft-versus-host disease
GvT: Graft-versus-tumor
HCMV: Human cytomegalovirus
HIES: Hyper-IgE syndrome
HLA : Human leukocyte antigen
HLH: Hemophagocytic lymphohistiocytosis syndrome
HSCT: Hematopoietic stem cell transplantation
HTS: High throughput sampler

ICAM-1: Intercellular adhesion molecule 1
IFN-γ: Interferon-gamma
ILCs: Innate lymphoid cells
IL-X : Interleukin-X (X depicts a number)
IRES : Internal ribosome entry site
IU: International unit
KIR(L): Killer immunoglobulin-like receptors (ligand)
KO: Knockout
LAMP-1: Lysosomal-associated membrane protein 1
LFA-1: Lymphocyte function-associated antigen 1
MFI : Mean fluorescence intensity
MHC: Major histocompatibility complex
MOMP: Mitochondrial outer membrane permeabilization
MPO: Myeloperoxidase
MTOC: Microtubule-organizing centre
mTOR: mammalian Target of rapamycin
NAC: N-acetylcystein
NADPH oxidase: nicotinamide adenine dinucleotide phosphate-oxidase
NCRs: Natural cytotoxicity receptors
NEMO: NFκB essential modulator
NFκB: Nuclear factor-kappa B
NK: Natural Killer cells
NKAES : Natural Killer activation and expansion system
NSG: Nod/SCID/IL2Rγ$^{-/-}$ mice
OCR : Oxygen consumption rate
OXPHOS : Oxidative phosphorylation
PBMCs: Peripheral blood mononuclear cells
PCA: Principal component analysis
PCR: Polymerase chain reaction
PD-(L)1: Programmed cell death-(ligand) 1
PDX: Patient-derived xenograft
PE : Phycoerythrin
PIDs: Primary immune deficiencies
RAG: Recombination-activating gene
RNAseq: RNA sequencing
ROS: Reactive oxygen species
SCID: Severe combined immunodeficiency
sgRNA: single guide RNA
SLAM: Signaling lymphocyte activation molecule
TCR: T cell receptor
TGF-β: Transforming growth factor-beta
(mb)TNF-α: (membrane-bound) Tumor necrosis factor-alpha
TNFR superfamily: Tumor necrosis factor-receptors superfamily
TRADD: Tumor necrosis factor receptor type 1-associated death domain protein
TRAIL: Tumor-necrosis-factor related apoptosis inducing ligand
UCOEs: Ubiquitous chromatin opening elements
UPR: Unfolded protein response

VSV-G: Vesicular stomatitis virus G-protein
WPRE: Woodchuck hepatitis virus posttranscriptional regulatory element
XHIGM: X-linked immunodeficiency with hyper-IgM
XLP: X-linked lymphoproliferative disease
X-MAID: X-linked moesin-associated immunodeficiency
XMEN: X-linked immunodeficiency with magnesium defect, Epstein-Barr virus infection, and neoplasia syndrome

LIST OF FIGURES

LIST OF SUPPLEMENTAL FIGURES

LIST OF TABLES

LIST OF SUPPLEMENTAL TABLES

CHAPTER 1.

INTRODUCTION AND PROBLEM STATEMENT

1. INTRODUCTION AND PROBLEM STATEMENT

1.1. IMMUNE FUNCTION OF NATURAL KILLER CELLS

In 1975, two articles reported the discovery of large granular lymphocytes capable of killing a target cell spontaneously, without requiring neither a priming step nor the expression of major histocompatibility complex (MHC) molecules on target cells (Herberman et al., 1975). Since then, the so-called Natural Killer (NK) cells have been the subject of intensive investigation, from their ontogeny to their effector functions. It is now well-established that these cells contribute to defending the organism against infections and cancer, and also play a role in immune homeostasis through selective elimination of cells that were involved in the immune response (Lieberman, 2016).

The proportion of systemic NK cells among peripheral blood mononuclear cells (PBMCs) is generally considered to be between 5-15% (Lotze and Thomson, 2009). NK cells are also found in some organs in which they can represent a more significant part of all lymphocytes, such as secondary lymphoid tissues, mucosal tissues, liver (where they can encompass up to 30-50% of all lymphocytes), lungs, skin, uterus, pancreas, joints and central nervous system (Björkström et al., 2016; Shi et al., 2011).

Because they exhibit features reminiscent of innate immunity such as the ability to be rapidly activated and respond to mutated or infected cells, and the absence of priming step requirement or of receptor rearrangement from their germline configuration, NK cells have been considered innate lymphocytes (Caligiuri, 2008; Vivier et al., 2016). However, recent works have challenged this view (Cerwenka and Lanier, 2016; Holmes and Bryceson, 2016; Paust and Andrian, 2011; Sun et al., 2009): adaptative or memory NK cells have been identified in humans in response to cytomegalovirus infection (Schlums et al., 2015) following pioneering work in mice, but also murine hapten-specific liver NK cells (Paust and Andrian, 2011), as well as antigen-specific NK cells in non human primates (Reeves et al., 2015; Walzer and Marçais, 2016). Also, cytokine-induced memory NK cells, that can be generated *in vitro,* show increased proliferation, cell recovery, and effector function *in vivo* (Ni et al., 2012; Romee et al., 2016). Furthermore, the expression of the recombination-activating gene proteins RAG1 and RAG2 (collectively, RAG) and of RAG endonuclease activity during NK cell ontogeny, which play a critical role in T and B cells development as shown in the related severe combined immunodeficiency (SCID) (Fischer et al., 2015), appears to impact NK cell phenotype, fitness and function both in mice (Karo et al., 2014) and humans (Dobbs et al., 2017). Thus, NK cells blur the well-established functional distinctions between

the two arms of the immune system, namely the innate and adaptive immunities (Vivier et al., 2011).

Recently, several groups have redefined the conventional immune dichotomy to further distinguish adaptive lymphocytes from innate-like ones, with evidence for overlapping functions (Bedoui et al., 2016). Among the latter, innate lymphoid cells (ILCs) were conceptually theorized as a large family of cells that mirror the phenotype and activity of differentiated T cells (Eberl et al., 2015; 2014). In this model, NK cells are the counterpart of the cytotoxic $CD8^+$ T cells due to their shared ability to kill infected, stressed, or transformed cells (**Figure 1**).

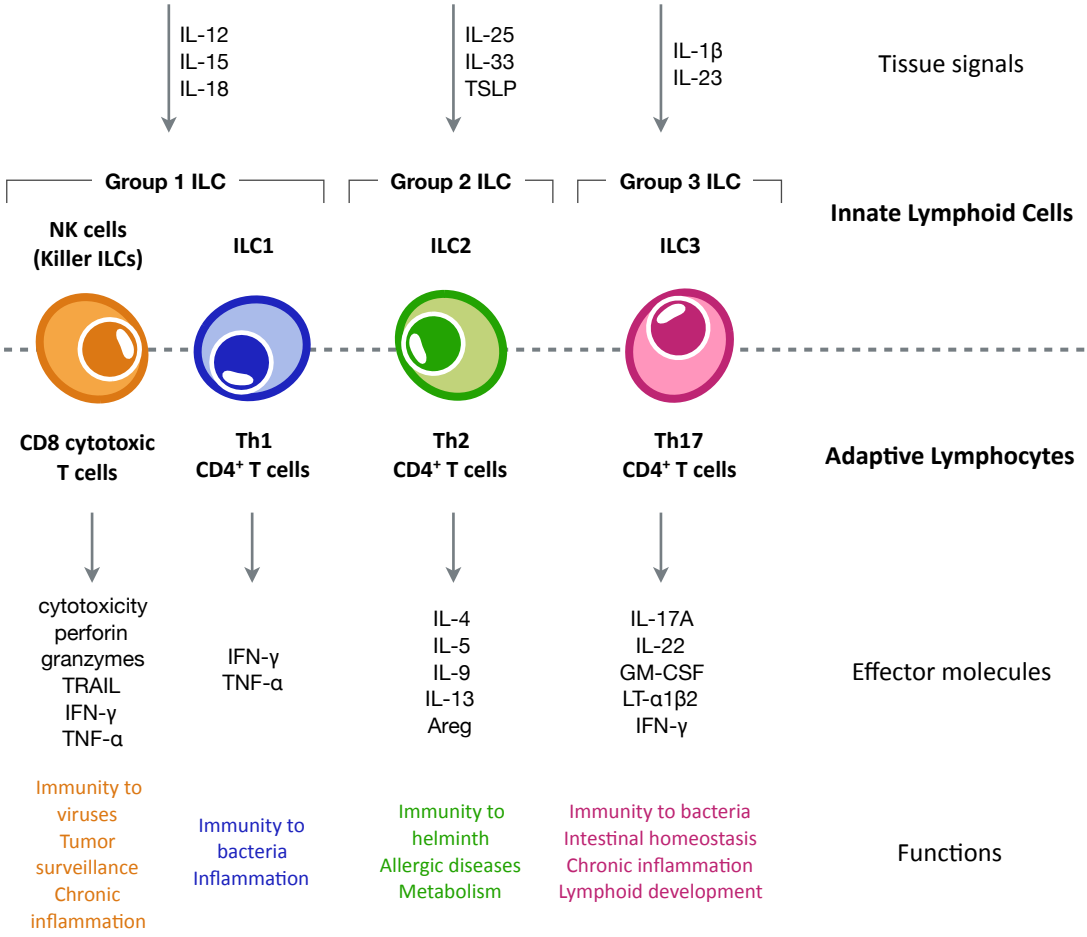

Figure 1. Innate lymphoid cells and their adaptive lymphocytes counterpart: a mirrored model.

Signals from injured or infected tissues activate ILCs whose function will mirror those of $CD8^+$ and $CD4^+$ T cells. The main difference between both cell types is the kinetics of the immune response.

Adapted from Eberl et al., 2015; 2014.

NK cells are the only cytotoxic ILCs and the major circulating subset although all ILC groups can be detected in peripheral blood from children and adults (Vély et al., 2016). As with T-

helper cells, plasticity has been demonstrated among ILCs (Artis and Spits, 2015); for instance, local TGF-β can drive conversion of NK cells into ILC1s with defective cytotoxic function, thus contributing to tumor immunoevasion (Gao et al., 2017).

Overall, many parallels can be drawn between NK cells and $CD8^+$ T cells due to their shared molecular activation pathways and effector responses, and distinct ways of recognizing target cells (Narni-Mancinelli et al., 2011; Sun and Lanier, 2011).

1.2. THE INTERACTION BETWEEN CYTOTOXIC LYMPHOCYTES AND TARGET CELLS

In order to avoid inappropriate immune reaction promoting auto-immunity, i.e. a break of tolerance toward the self, it is of major importance for cytotoxic lymphocytes to efficiently discriminate between infected or transformed cells and normal cells. While $CD8^+$ T cells recognition is restricted to antigens presented by target cells through the major histocompatibility complex (MHC) class I protein, NK cells immune recognition is driven by the "missing self" model, preferentially killing cells with low or no MHC class I expression (Watzl et al., 2014). Such recognition allows NK cells to complement T cell-mediated MHC class I-dependent immunosurveillance through so-called natural cytotoxicity (Kärre et al., 1986).

This unique feature implies that cells which express MHC-I are protected from NK cell-mediated damage by engaging their inhibitory receptors, while cells lacking or with considerably reduced levels of MHC-I are not because they display a "missing-self" phenotype (**Figure 2**). As a corollary, NK cells also target healthy allogenic cells because they lack self-MHC-I molecules (Kärre, 2008).

Nevertheless, the latter model has been expanded by the recognition that both activating and inhibitory receptors play a role in NK cell function: the expression of "induced self" ligands by target cells can overcome the inhibition induced by MHC class I-specific inhibitory receptors (Martinet and Smyth, 2015). Thus, NK cell activation is controlled by a wide range of germline-encoded receptors, either inhibitory or activating, depending on the nature of the signal they transmit. As a result of the engaged immune synapse, effector cells integrate both types of signals in their "decision to kill" (**Figure 2**).

Appropriate progression through critical cell biological steps is essential for the triggering of the effector phase and subsequent target cell death. These checkpoints include three consecutive stages identified respectively as recognition, effector and termination steps (Mace et al., 2014). Cell adhesion to the target cell is the first and crucial step both to ensure the subsequent stages of the immune synapse and to avoid uncontrolled cytotoxic response.

LFA-1 is a key molecule for NK cell adhesion. Indeed, other NK activating receptors induce so-called inside-out signals to dynamically regulate LFA-1 conformation and spatial distribution, highlighting its key role (Bryceson et al., 2009).

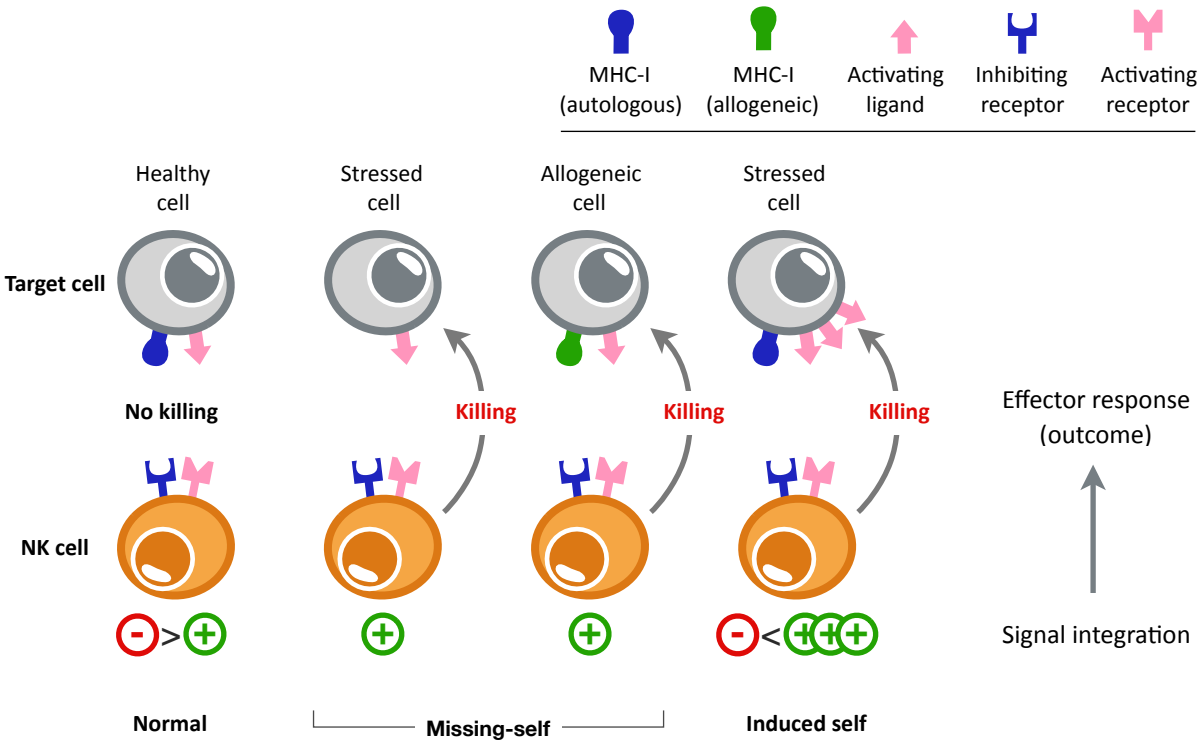

Figure 2. A model of NK cells activation: signal integration and outcome depending on target cell type.
Both activating and inhibiting signals are integrated following the adhesion of NK cells to target cells. Self MHC-I molecule provides strong inhibition through the engagement of inhibitory receptors. In an allogeneic setting or in case of infection or tumoral transformation, activating signals become predominant and trigger NK cell effector response (mainly granule exocytosis). Of note, cytokine production is regulated in the same way.

Overall, the interaction between effector cytolytic cells and target cells is of major importance as it will determine whether the targets have to be eliminated. For NK cells, both activating and inhibiting signals are integrated in an equilibrium that controls the triggering of subsequent effector responses.

1.3. THE MAIN RECOGNIZED EFFECTOR PATHWAYS

We previously emphasized the similarities between NK cells and $CD8^+$ T cells which also share complementary immune functions (Narni-Mancinelli et al., 2011; Sun and Lanier, 2011). The major distinction between the two is the induced pathways for activation after target recognition. As shown by transcriptomic studies in mice (Bezman et al., 2012) and to some extent in humans (Hidalgo et al., 2008), many transcripts are shared between both cell

types while NK-specific ones were found to be principally related to NK receptors (Hidalgo et al., 2008) and were sometimes expressed by other cell types of the immune system, apart from T cells (Bezman et al., 2012).

At the functional level, similarities have been documented as well, especially for granule exocytosis with common molecular requirements, although cytokine production was notably different in its kinetics and frequency (Chiang et al., 2013). Deep immune profiling by mass cytometry also showed that parallels in cytotoxic molecule expression can be drawn between T and NK cells, with granulysin, perforin and various granzymes (A, B, K and M) detected in both cell types (Bengsch et al., 2017).

Moreover, these works established dynamic changes linked to the activation state of the effector cell. Resting NK cells are poor effectors at steady state but can acquire their full effector potential once the have been primed (Narni-Mancinelli et al., 2011), which implies a key role for dendritic cells in secondary lymphoid organs through membrane-bound IL-15 trans-presentation (Huntington et al., 2009; Lotze and Thomson, 2009). Among $CD8^+$ cells, cytotoxic molecule expression patterns are also linked to T cell differentiation (Bengsch et al., 2017).

Focusing on effector functions, NK cells do not require proliferation for acquisition of effector functions but rather exhibit a "pre-armed" state with constitutive expression of perforin, granzyme A, granzyme B and IFN-γ allowing quick response, similarly to memory $CD8^+$ T cells (Narni-Mancinelli et al., 2011). Furthermore, the epigenetic control of NK cell functions, that has been linked to some viral infections like the human cytomegalovirus (HCMV) (Cichocki et al., 2013; Schlums et al., 2015), introduces a supplemental level of complexity in the active regulation of their responses which parallels $CD8^+$ cells.

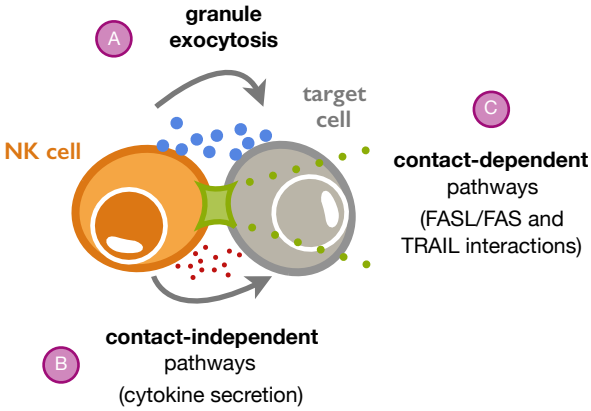

Figure 3. Different effector pathways can be engaged by cytotoxic lymphocytes.
(**A**) Granule exocytosis mainly involves perforin, granzymes and granulysin secretion.
(**B**) Death receptors engagement are part of contact-dependent pathways.
(**C**) Cytokine secretion (TNF-α and IFN-γ) can sensitize target cells to cytotoxic lymphocytes.

Apart from their control, effector pathways potentially engaged by cytotoxic lymphocytes can be categorized depending on their dependence to cell contact. On one hand, the secretion of cytokines (such as TNF-α and IFN-γ) is likely to induce target cell changes

through the local milieu, while, on the other hand, granule exocytosis as well as death receptors pathways rely on a direct cellular contact between effector and target cells (Lieberman, 2016; Martínez-Lostao et al., 2015) (**Figure 3**).

1.3.1. CONTACT-INDEPENDENT PATHWAYS

A vast array of cytokines can be produced by NK cells, including IFN-γ, GM-CSF, TNF-α and IL-10, as well as chemokines such as CCL3, CCL4 and CCL5, and also bactericidal peptides like α-defensins (Chalifour et al., 2004; Clark et al., 2016; Perona-Wright et al., 2009; Rajasekaran et al., 2013; Reefman et al., 2010). Although IFN-γ production has been intensively linked to the control of viruses, however it is interesting to note that NK cells not only release both pro and anti-inflammatory factors, but also chemoattractant mediators and molecules with anti-infectious properties, thus providing a link between NK cell effector and regulatory functions within the immune system.

Cytokine production is not equally shared among NK cell subsets although all NK cells can produce cytokines. Thus, $CD56^{bright}$ cells have been classically defined as an immunoregulatory subpopulation because of their greater (and faster) ability to produce a wide range of cytokines in response to monokine stimulation (Cooper, 2001). However, further work on the regulation of cytokine production upon target cell recognition revealed that the $CD56^{dim}$ subset is a prominent producer in this setting (Fauriat et al., 2010).

Another key question is whether cytotoxicity and cytokine production are differentially controlled by NK cells. Indeed, activation of NK cells by tumor or infected cells classically leads to both phenomenons, and interaction with a susceptible target cell line can induce a pro-inflammatory profile of chemokine and cytokine secretion (Fauriat et al., 2010; Jenkins et al., 2015). Colocalization and trafficking studies of IFN-γ and TNF-α in human NK cells have suggested that compartments and vesicles do not overlap with perforin or other late endosome granule markers (Reefman et al., 2010). However, the definitive answer was provided by a work demonstrating that a dedicated signaling pathway consisting of the tyrosine kinase Fyn, the adaptor ADAP and the CBM signalosome (which consists of the adaptors Carma1, Bcl-10 and MALT1) was exclusively responsible for the production of inflammatory cytokines but not for cytotoxicity, uncoupling both effector responses (Rajasekaran et al., 2013; Vivier et al., 2013).

Importantly, cytokines which are produced by NK cells can impact targets' sensitivity and the outcome of NK mediated cytotoxicity. For instance, IFN-γ and TNF-α were shown to act synergistically to promote NK cell cytotoxicity through NFκB-dependent up-regulation of

ICAM-1 expression in target cells (Wang et al., 2012). Contradictory reports have also been published regarding the role of IFN-γ either sensitizing or altering NK cell mediated cytotoxicity among targets through the up-regulation of various NK ligands such as PD-L1, MHC-I or FAS (Aquino-López et al., 2017). Taken together, this suggests that cytokine effect may vary depending on target cell type.

1.3.2. CONTACT-DEPENDENT PATHWAYS

1.3.2.1. GRANULE EXOCYTOSIS

The main effector mechanisms of cytotoxic lymphocytes are strongly associated with their ability to engage an immune synapse through a membrane cellular contact with target cells. Cytotoxic granule exocytosis is a major contributing pathway to contact-dependent effector function. Pore-forming proteins (perforin and granulysin) and proteases (granzymes) are the two types of molecular effectors contained in specialized secretory lysosomes, the so-called cytotoxic granules (Lieberman, 2016; Voskoboinik et al., 2015). A serglycin matrix holds them in the granule in an acidic environment where they are maintained inactive to avoid self-destruction of the killer cells. Death-inducing enzymes are synthesized as proenzymes which are inactive precursors, and will be processed in an active form only once within the cytotoxic granule (Lieberman, 2016). Cytosolic serpins (serine protease inhibitors which inactivate the granzymes) protect the effector cell from any potential leak from the granules. The granule-mediated death is a well-orchestrated process leading, from the initial cell adhesion and signal transduction from an activating immune synapse, to the cytotoxic granule mobilization and exocytosis (**Figure 4**).

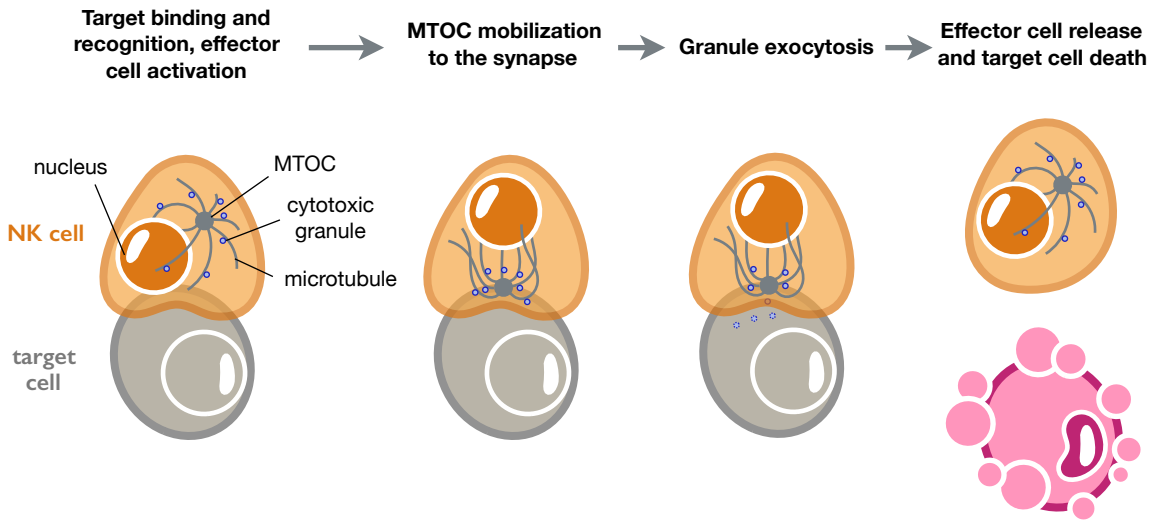

Figure 4. Cytotoxic killing of a cognate target cell through the granule exocytosis.

There are four main steps to this interaction (de Saint Basile et al., 2010; Krzewski and Coligan, 2012; Voskoboinik et al., 2015): (1) the initial cell contact between the killer cell and its target, (2) the mobilization of a microtubule-organizing centre (MTOC, to which cytotoxic granules are anchored) toward the cell contact area, (3) the cytotoxic granule delivery and release of the molecular death-inducing effectors into the synaptic cleft and (4) the target cell death *per se*. At the molecular level, the sequential stages are the following. First, cytotoxic granules move along the microtubules toward the MTOC and the immune synapse (polarization step). Then, they switch to the filamentous actin network and navigate toward the cell membrane (docking step), where they undergo a series of changes and become primed (priming step), before eventually fusing with the cell membrane (fusion step) to release their effector molecules. The synapse is tightly sealed and different mechanisms have been shown to contribute to effector cell protection toward its own death-inducing molecules. Among them, it has been proposed that the lysosomal-associated membrane protein LAMP-1 (CD107a), which is used as a surrogate marker to assess NK cell degranulation (Alter et al., 2004) and plays an important role for perforin trafficking to lytic granules (Krzewski et al., 2013), protects cytotoxic lymphocyte from damage consecutive to degranulation (Cohnen et al., 2013).

Genetic defects impairing granule exocytosis highlight its importance in host defense toward infections but also for immune homeostasis (de Saint Basile et al., 2015): hemophagocytic syndromes (hemophagocytic lymphohistiocytosis syndrome or HLH, also named macrophage activation syndrome) are caused by impaired NK and cytotoxic $CD8^+$ T cell function (Ramos-Casals et al., 2014). HLH is a rare disease which can occur at any age and generally has an infective agent as a trigger. Familial HLH (or FHL) are a subgroup of inherited hemophagocytic syndromes: their study allowed the identification of key molecular effector of granule exocytosis, and demonstration of the link between cytotoxicity and immune homeostasis (de Saint Basile et al., 2010; 2015; Sieni et al., 2014). Several genetic disorders have now been associated with occurrence of HLH (**Table 1**).

PRF1 and *UNC13D* mutations account for ~70% of FHL cases (Sieni et al., 2014). They illustrate genetic defects in cytotoxic granule content (perforin deficiency) or granule priming (Munc13-4 deficiency) and show that alteration of the granule exocytosis pathway at different steps can lead to severe pathology (Feldmann et al., 2003; Stepp et al., 1999).

Of note, the degree of degranulation defect can change, from total abrogation to a relative decrease, particularly with hypomorphic mutations affecting one or multiple genes involved in the pathway. Interestingly, it has been suggested that the importance of the cytotoxic

activity defect correlates with clinical HLH severity (de Saint Basile et al., 2015). This postulate could explain the variable age-onset of the disease, with a higher threshold for triggering the HLH in older people which would be reached through cumulative environmental factors (de Saint Basile et al., 2015; Ramos-Casals et al., 2014).

Table 1. Characteristics of genetic disorders associated with occurrence of HLH.

Subtype	Genetic defect	Affected protein
FHL type 1	*unknown*	unknown
FHL type 2	*PRF1*	Perforin
FHL type 3	*UNC13D*	Munc13-4
FHL type 4	*STX11*	Syntaxin 11
FHL type 5	*STXBP2*	Munc18-2
Griscelli syndrome type 2	*RAB27A*	RAB27A
Chediak-Higashi syndrome	*LYST*	LYST
Hermansky-Pudlak syndrome type 2	*ADTB3A*	AP-3
XLP-1	*SH2D1A*	SAP
XLP-2	*XIAP*	XIAP

FHL and XLP stand for familial hemophagocytic lymphohistiocytosis and X-linked lymphoproliferative disease, respectively.

Released death-inducing molecules include perforin, granzymes and granulysin. Perforin is a protein that oligomerizes to form membrane-spanning pores at the target cell membrane. Granzymes are serine proteases and abundant constituents of the cytotoxic granules, released together with perforin (among others). There are five identified granzymes in humans, namely granzymes A, B, H, K and M (Lieberman, 2016). However, coexpression patterns of cytotoxic molecules reveal that each single $CD8^+$ T cell or NK cell does not express all the types of granzymes, nor perforin or granulysin (at least for unstimulated cells) (Bengsch et al., 2017). Granzymes act synergistically with perforin to induce target cell death (Voskoboinik et al., 2015). To date, no genetic disorders affecting granzymes have been described in humans (Lieberman, 2016). Finally, granulysin is another membrane-perturbing effector whose expression has been reported in many mammals but not in rodents (Lieberman, 2016).

How do these molecular actors interact together? Mechanistically, at the target cell level, once effector cells have degranulated they release these death-inducing molecules in the synapse. Perforin will then form pores in the target cell membrane: whether granzymes enter directly into the cytosol or through an endocytosis process was the subject of debate (Voskoboinik et al., 2015).

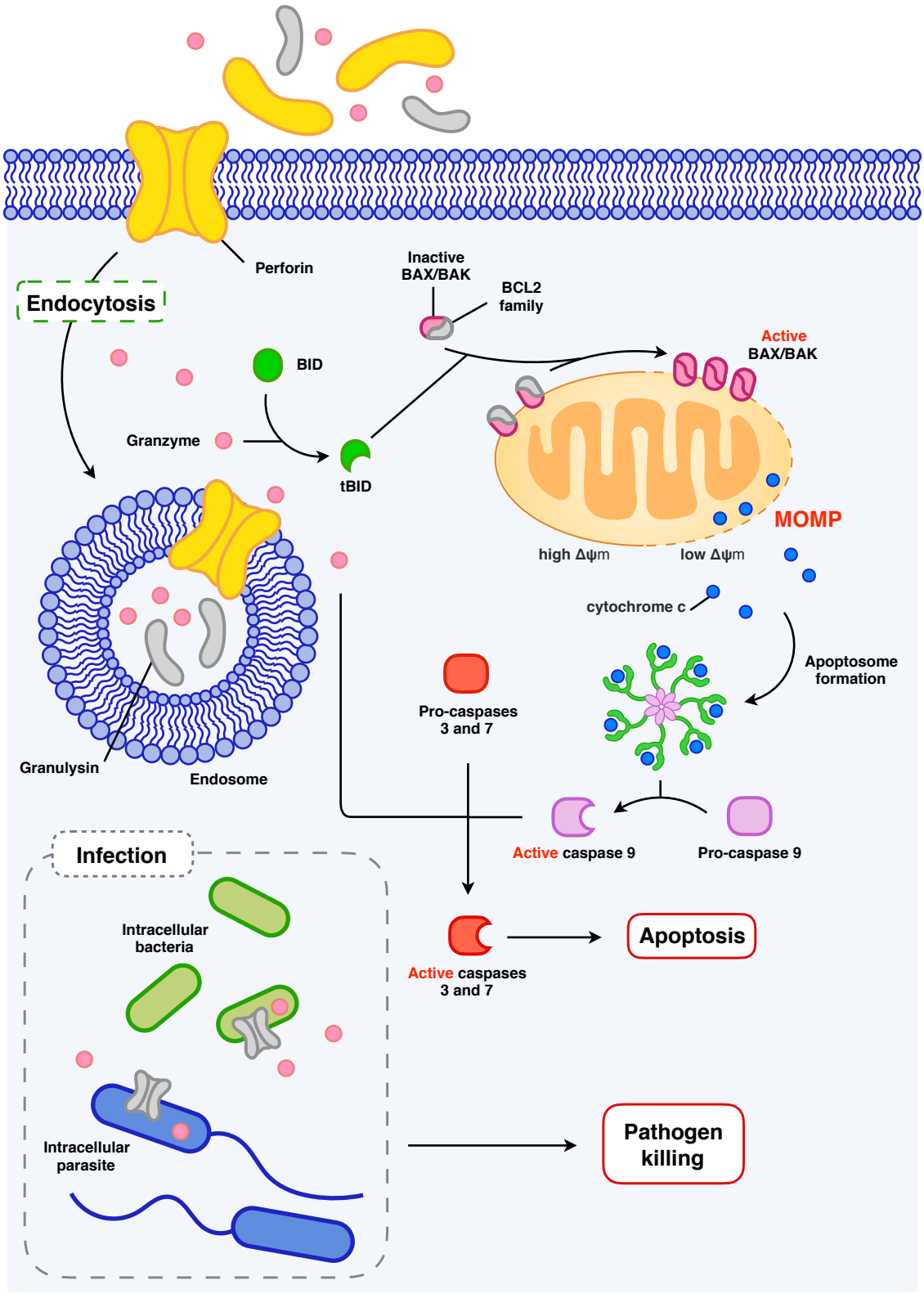

Figure 5. Induced target cell death through the granule exocytosis pathway.
Perforin, granzyme and granulysin are released by cytotoxic lymphocytes in the synapse. Direct entry of granzyme through cell membrane perforin pores and the "endosomolysis" hypothesis are depicted. Once in the cytosol, granulysin acts through a similar mechanism, inducing pores in intracellular bacteria and parasites which allows granzyme to induce pathogen elimination.

Indeed, an "endosomolysis" hypothesis has been suggested proposing a first step where transient pores in the cell membrane trigger the endocytosis of granzyme, perforin and granulysin, and then pore formation in endosomes followed by a second step triggering cytosolic release and subsequent cell death (Thiery et al., 2011). However, the role of granulysin is now appreciated for infection with intracellular bacteria and parasites with a two-step process to deliver granzyme into the pathogen (Dotiwala et al., 2016; Walch et al., 2014) (**Figure 5**).

Perforin and granulysin respective roles are closely related to their biochemical activity: while the former is only active in cholesterol-containing membranes, the latter preferentially disrupts membranes that does not contain cholesterol (which is the case for bacteria, fungi and parasites) (Lieberman, 2016). Granulysin induces a pathogen cell death which is largely oxidative and based on two complementary processes: superoxide anion production and inactivation of the microbial antioxidant defenses (Dotiwala et al., 2016; Lieberman, 2016; Walch et al., 2014). Once delivered in the cytosol of the target cell, granzyme cleaves BID to trigger the intrinsic apoptotic cascade, or activates directly the terminal caspases 3 and 7 (**Figure 5** and **§1.3.2.2**). Overall, these molecular mechanisms are highly relevant in the sense that they confer multiple possible outcomes following the same initial process (granule exocytosis) which are appropriate for various pathogens (virus, bacteria, fungi and parasites) as well as transformed or stressed target cells.

1.3.2.2. DEATH RECEPTORS

Another cytotoxic weapon of the killer cells' arsenal is the expression of death ligands at their cell surface. These death ligands can engage death receptors and induce the so-called death receptor mediated cell death in target cells. Death receptors (DRs) form a subgroup within the TNFR superfamily, characterized by the shared presence among all DRs of an approximately 80 amino acid long cytoplasmic death domain (Ashkenazi and Salvesen, 2014). To date, six human DRs have been identified: TNF-R1, CD95 (Fas/APO-1), TRAIL-R1 (DR4), TRAIL-R2 (APO-2/TRICK/DR5/KILLER), DR3 (TRAMP/APO-3) and DR6 (Walczak, 2013). Their known respective ligands are TNF, CD95L (FasL), TRAIL, TL1A, and APP respectively.

FasL, TRAIL and membrane bound TNF expression have been reported for NK cells in conjunction with their activation profile (Bengsch et al., 2017; Caligiuri, 2008; Caron et al., 1999; Kashii et al., 1999). FasL exposure at the effector cell surface is linked to the mobilization of lysosome-related vesicles distinct from the degranulation-associated ones (He and Ostergaard, 2007; Lettau et al., 2015). TRAIL expression by NK cells plays a role in the

control of cancer cells (Kashii et al., 1999; Takeda et al., 2002) but also in immune homeostasis through the interaction between NK cells and autologous immature dendritic cells (DCs) (Peppa et al., 2013) as well as autologous activated $CD8^+$ T cells (Melki et al., 2010).

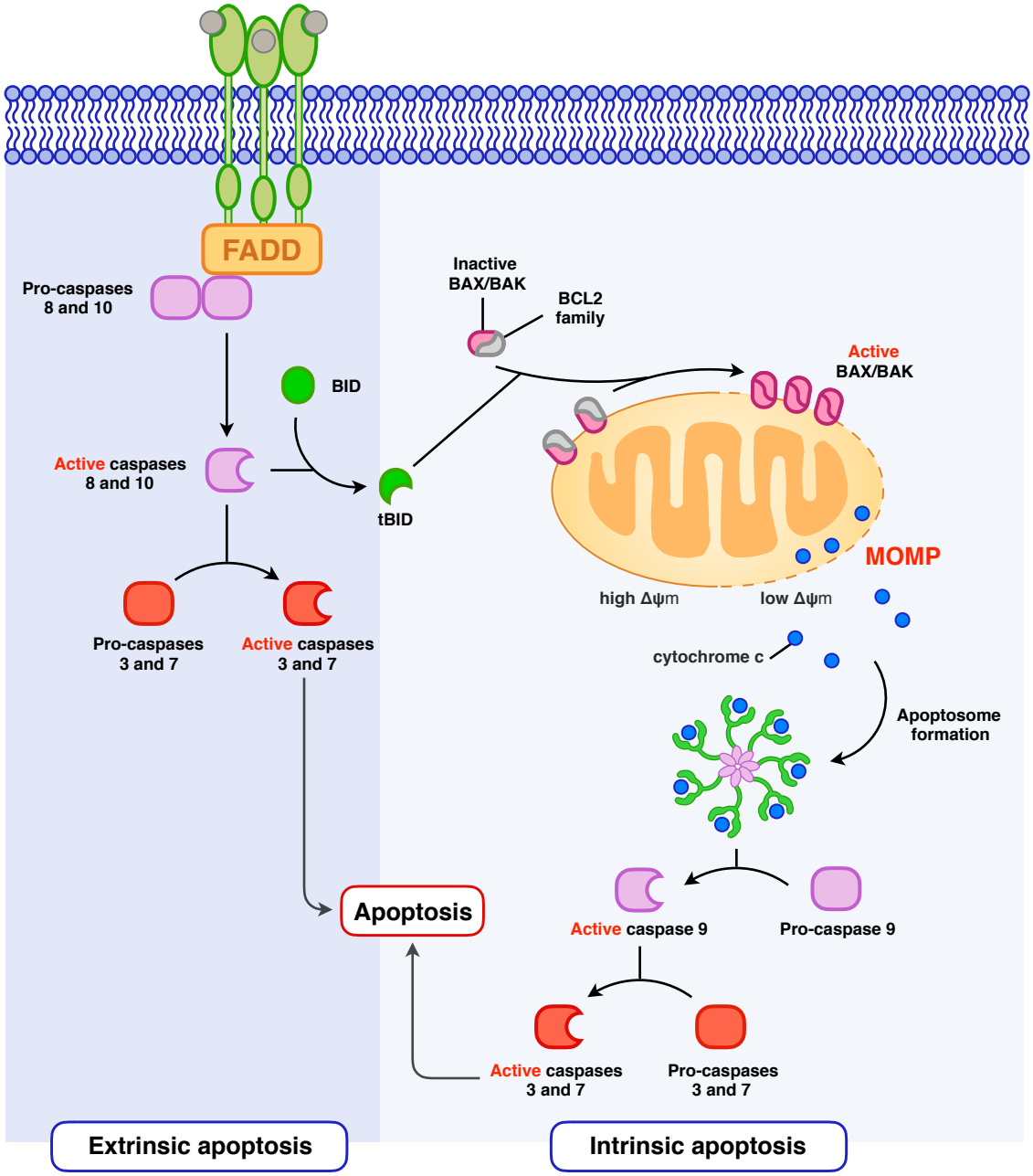

Figure 6. Extrinsic and intrinsic apoptotic signaling pathways.
Once bound to the appropriate ligand, death receptors signal through adaptor molecules such as FADD (FAS-associated death domain protein) and activate initiator caspase-8 and caspase-10. These either directly activate the effector caspase-3 and caspase-7 or will cleave BID, providing a link toward the mitochondria-dependent cell death signalization.
In the latter, truncated BID activate BAX and BAK which will mediate mitochondrial outer membrane permeabilization (MOMP) and subsequent release of cytochrome c. Through its interaction with APAF1 (apoptotic protease activating factor 1), it leads to the apoptosome assembly and caspase-9 activation which will activate then the effector caspase-3 and caspase-7 triggering apoptosis.

DR mediated signaling can induce target cell death through the extrinsic pathway of apoptosis (Ashkenazi and Salvesen, 2014) (**Figure 6**). Of note, DRs can also mediate non-apoptosis-related functions which include regulation of cell proliferation and differentiation, chemokine production and inflammatory responses (Guicciardi and Gores, 2009). Regulation between these signaling pathways is expected to be linked to the adaptor molecules: thus, the FAS-associated death domain protein (FADD) is more likely to trigger cell death, while signaling with the TNF type 1–associated death domain (TRADD) is more likely to activate cell proliferation and inflammation (Lieberman, 2016).

It is interesting to note that granule exocytosis and death receptor mediated pathways both partially overlap and diverge in the molecular mechanisms which are implied in target cell death (**Figures 5** and **6**).

1.4. EFFECTOR CELLS HETEROGENEITY AND DIVERSITY

How cytotoxic effector cells are distinct from each other is an interesting question to address. As previously discussed, $CD8^+$ T cells and NK cells have similarities in their development, homeostasis and immune role (Sun and Lanier, 2011) and can be considered as complementary effectors in their mechanism for target cells recognition.

As opposed to adaptive immunity, innate immune response has been considered as a set of non-specific early defenses, regardless of the threat. Nevertheless, this view has now been challenged. Although the T cell receptor (TCR) confers T cell specificity toward the recognized antigen, not all the NK cells will react to a threat, underlying their heterogeneity and diversity. The latter can be defined at the phenotypic as well as the behavioral levels, both being intrinsically correlated.

Regarding the phenotypic differences, some have been long known: $CD56^{dim}$ $CD16^+$ and $CD56^{bright}$ $CD16^-$ NK cell subsets are classically distinguished as cytotoxic and immunoregulatory cells respectively (Caligiuri, 2008), based on their functional ability to engage cytotoxicity or cytokine production more efficiently. It has been proposed that these two subsets correspond to different stages of NK cell differentiation, with $CD56^{bright}$ $CD16^-$ cells being less mature precursors of $CD56^{dim}$ $CD16^+$ cells, although some groups have found evidence for a different ontogeny between them (Wu et al., 2014). Another distinction can be made whether circulating or tissue resident NK cells are considered, which deeply impact the relative proportion of these two subsets (Björkström et al., 2016). In that regard, liver NK cells are a good example of organ-adapted effector cell function with an important proportion of immunoregulatory NK cells within this specific site of immunosurveillance.

Although NK cells lack a recombined antigen-specific receptor, they express a complex array of germline-encoded receptors whose combinatorial expression defines a massive degree of NK cell diversity. Using a multiparametric study by mass cytometry, it has been estimated that one could distinguish between 6000 and 30,000 phenotypically NK subpopulations within an individual and more than 100,000 NK cell subpopulations within a cohort of 22 people (Horowitz et al., 2013). One can consider that this combinatorial diversity and the multiplicity of activating and inhibitory receptors confers a wide range of triggering thresholds for effector responses.

We have previously discussed cytokine production and cytotoxicity, and it has been shown that they can be uncoupled (Rajasekaran et al., 2013; Vivier et al., 2013). From a "behavioral" point of view, the relative contribution in the killing of target cells varies between individual NK cells. Indeed, in a degranulation-dependent model of cytotoxicity, others demonstrated that a subset of "serial killer" NK cells were responsible for an important proportion of the total number of kills (Choi and Mitchison, 2013; Vanherberghen et al., 2013). Overall, a classification into five categories was proposed based on the contact number and their outcomes: (1) NK cells that don't interact with target cells; (2) NK cells that interact with targets but don't kill them; (3) NK cells that kill all target cells encountered; (4) exhausted NK cells (i.e. that stop killing after a certain number of interactions); and (5) NK cells that kill stochastically (a strong minority of the effector cells).

NK cell subsets also exhibit divergent adaptation with regard to their local environment. For instance, it has been showed that the $CD56^{bright}$ $CD16^{-}$ cells are more resistant to reactive oxygen species-induced stress (Thoren et al., 2007), which was shown responsible for tumoral immune escape (Aurelius et al., 2012).

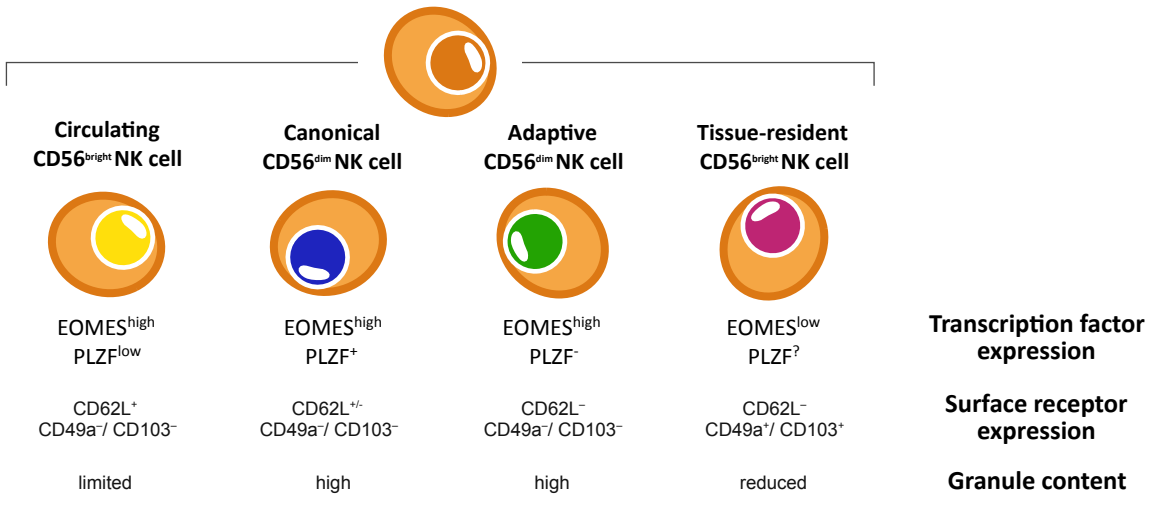

Figure 7. An updated view of human NK cell subsets (proposed by Frank Cichocki *et al.*). Adapted from Cichocki et al., 2015.

Furthermore, HCMV infection drives the expansion of a so-called adaptive subset with distinct functional capacities which include on one hand reduced effector responses toward autologous activated T cells, and on the other hand enhanced function against virus-infected cells (Lee et al., 2015; Schlums et al., 2015).

Among others, Frank Cichocki et al., taking in consideration these recent discoveries, proposed an updated model of NK cell subsets that distinguish four main subgroups with a dichotomic contribution to either immunoregulation or immunosurveillance (**Figure 7**).

These studies provide further evidence of the complexity of NK cell responses at the cellular level.

1.5. PRE-B ACUTE LYMPHOBLASTIC LEUKEMIA AS A TARGET CELL'S MODEL

Among neoplasia, pre-B cell acute lymphoblastic leukemia (pre-B ALL) is the most common form of childhood cancer. Long-term survival has improved to reach 85-90% in children, although intensified systemic and central nervous system-directed chemotherapy causes acute and long-term treatment-related complications (Hunger and Mullighan, 2015; Inaba et al., 2013; Oskarsson et al., 2016). However, relapse, which is observed in about 20% of pediatric and in more than 60% of adult patients (Perova et al., 2014), is still a major concern with a poor prognosis that has not significantly improved since the 80s (Bhojwani and Pui, 2013). Thus, relapsed ALL ranks as the fourth most common childhood malignancy and only 30% of the patients survive (Mullighan et al., 2008).

Pre-B cell ALL development is a complex multistep process and the disease etiology is likely different between young infant and older children or adults, although no single causal mechanism is expected (Greaves, 2006). Following a classical view of cancer development, a prenatal origin has been proposed for ALL arising in childhood (Marshall et al., 2014) while the disease in adults could result from acquired mutations (Hanahan and Weinberg, 2011). This view is supported by the observation of distinct molecular genetics between both groups of patients. For example, *BCR-ABL1* (or Philadelphia chromosome) is detected in over 25% of adult versus only 3% to 5% of pediatric ALL cases (Mullighan, 2012).

A causal link between childhood pre-B ALL and infection has been reported (Greaves, 2006; Greaves and Muschen, 2015; Martín-Lorenzo et al., 2015; Swaminathan et al., 2015). At the pre-B cell stage of B lymphopoiesis, cells exhibit an increase susceptibility to genetic lesions that can be exacerbated by abnormal repetitive or chronic infections, through the associated cytokine signaling and inflammation. However, there is no precise view of the individual species of viruses, bacteria, or other pathogens involved. An infection-triggered selection of

pre-leukemic clones has been suggested by the occurrence, among 2% of the pediatric patients, of a transient clinical phase of aplasia in the few months preceding ALL. This phase, which is expected to favor the emergence of preleukemic clones (Greaves, 2006), was almost always associated with an infection (albeit either cause or effect).

Whether pre-B ALL follows the classical cancer stem cell model has been investigated by several groups. According to this model, tumors are heterogeneous but hierarchically organized entities. In the particular case of hematological malignancies, it is tempting to apply a normal hematopoiesis-derived model in which (immature) cancer stem cells (leukemia stem cells), by analogy with hematopoietic stem cells, retain stemness-related properties, i.e. the ability to self-renewing and differentiation into more differentiated cancer cells. This consideration is important since immature cells are also the most quiescent ones and thus less sensitive to conventional chemotherapy that targets proliferative cells.

While this model seems coherent with acute myeloid leukemias (AML) (Shlush et al., 2017), it does not apply to pre-B ALL (McClellan and Majeti, 2013). Strong evidence was brought by using a xenotransplant model in NOD/scid immunodeficient mice (le Viseur et al., 2008). Sorted blast populations defined with the CD34, CD19 and CD20 surface markers shared the ability to reconstitute and reestablish the complete leukemic phenotype *in vivo*. These results and others establish a clear difference between AML and B-ALL (Belderbos et al., 2017; Rehe et al., 2013): AML arises within the normal HSC compartment and retains a hierarchy similar to normal hematopoiesis while pre-B ALL is highly polyclonal and stochastic in its stemness (**Figure 8**). As a corollary, relapsed ALL clonal diversity is comparable to the one observed at the moment of the diagnosis while clonal survival from diagnosis to relapse is not associated with a mutation burden (Ma et al., 2015; Mullighan et al., 2008).

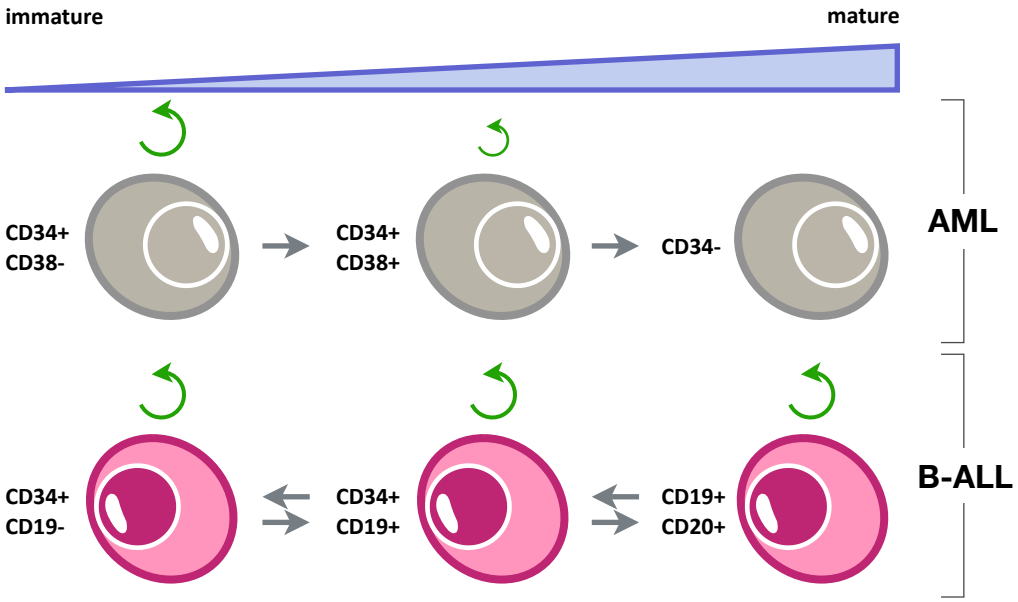

Figure 8. AML and B-ALL cancer stem cell divergent models.

In this work, we have been interested in studying the immune control of pre-B ALL cells (that we used as targets) by cytotoxic lymphocytes and more specifically NK cells.

1.6. PRIMARY IMMUNE DEFICIENCIES TO DECIPHER EFFECTOR LYMPHOCYTES' MOLECULAR PATHWAYS

One particular aspect of our approach was the use of effector cells from patients suffering from various primary immune deficiencies (PIDs), as natural human knockout models.

By definition, a cytotoxicity between effector NK cells and targets involves two cellular types. To study the precise molecular mechanisms governing NK mediated killing, many previous works used chemical approaches like the inhibition of the granule exocytosis pathway by EGTA/$MgCl_2$ (EGTA is a chelating agent of divalent cations including Ca^{2+} to block exocytosis while the presence of Mg^{2+} in excess allows to maintain adherence between effector and target cells), or by concanamycin A that degrades perforin by increasing the pH of lytic granules. However, a major concern with this strategy is the lack of specificity of these methods that affect both the effector and the target cells. In addition, the molecular selectivity of these drugs is questionable as many different processes can be impacted. For example, with EGTA/$MgCl_2$, Ca^{2+} chelation also inhibits FasL expression on the cell surface of $CD8^+$ cytotoxic T cells (He and Ostergaard, 2007), thus rendering any interpretation equivocal.

To circumvent these limits, we aimed to separate effector and target cell study. For this purpose, we used NK cells obtained from primary immune deficient patients to study effector cells, and knockouts generated by CRISPR/Cas9 genome editing technology to study the target leukemic cell lines. We used PIDs whose molecular defects could impact: (1) NK cell activation, (2) the integration of the activating and inhibitory signals and (3) the effector response *per se* (Long et al., 2013).

1.7. AIMS

Allogeneic HSCT was initially developed for two reasons (Copelan, 2006). First, it allows complete replacement of an abnormal hematopoietic system by a normal one (which is of particular interest for severe primary immune deficiencies as well as hematological malignancies) (Gooley et al., 2010). Second, it allows dose-intensive/myeloablative therapy for patients suffering from cancer, for whom these high dose regimens increase tumoral cell elimination but also induce a permanent bone marrow failure that can be rescued by HSCT.

The graft is as an immunocompetent tissue considering the immune cells it contains which are able to mediate active immune responses, either deleterious or beneficial, the so-called graft-versus-host disease (GvHD) and graft-versus-tumor (GvT) effect respectively. Both T cells and NK cells have been shown to contribute to GvT.

In 2002, Loredana Ruggeri *et al*. published an important study establishing a role for NK cell alloreactivity in mismatched hematopoietic stem cell transplantation (HSCT) (Ruggeri, 2002). Their work laid the foundations for this phenomenon which was attributed to a mismatch between killer immunoglobulin-like receptors (KIR) expressed by donor NK cells within the graft, and KIR ligands (KIRL) expressed at the surface of recipient cells, including tumor cells. Interestingly, they provided evidence in AML but not in pre-B ALL that they found to be resistant to NK-mediated killing (Ruggeri, 2002; Ruggeri et al., 1999). Since then, different models have been proposed to predict the relative risk of relapse taking into account donor and recipient's phenotype, including the "ligand-ligand" and the "receptor-ligand" models suggested by the Perugia and the Memphis groups respectively (Handgretinger et al., 2016). If the former considers KIRL expressed both by the donor and the recipient to establish a potential mismatch, the latter considers the KIRs from the donor and the absence of the corresponding KIRLs in the recipient. Of note, alternative models exist such as the "gene-gene" model which includes KIR genes from both the donor and the recipient in its prediction (Handgretinger et al., 2016). Altogether, each model performs better in specific conditions suggesting that there might be no unique rule for NK alloreactivity but instead several mechanisms which could account differently depending on the disease type and patients (childhood versus adults).

We worked on understanding NK cell alloreactivity against pre-B ALL and why do these blasts exhibit an increase resistance to effector cell killing?

Deciphering the mechanisms governing it is important from both a fundamental point of view (i.e. to understand molecular pathways which contribute to NK cell activation and/or inhibition against this type of target cells as well as control their effector functions), and considering potential future developments as an immunotherapeutic tool.

CHAPTER 2.
METHODS

2. METHODS

2.1. PATIENTS RECRUITMENT

Several centers around the world were involved in recruiting patients suffering from various primary immunodeficiencies (PID). Because of the scarcity of PIDs that were interesting for our study, we obtained samples from patients followed in many institutions over the world. Hence, we could get samples from Hôpital Necker-Enfants Malades (Paris, France), CHU Saint-Justine (Montreal, QC, Canada), Hospices Civils de Lyon (Lyon, France), Hôpital Saint-Louis (Paris, France) and Cincinnati Children's Hospital Medical Center (Cincinnati, OH, USA). Healthy control donors were sampled at the same time as the patients bearing confirmed mutations, and samples were carried together. This study was accepted by the CHU Sainte-Justine IRB (protocole number 3195) and all the involved subjects (patients and controls) signed informed consent forms reviewed and approved by the appropriate institutional medical research ethics committee (**Table 2**).

Table 2. Patients and cytotoxicity assays characteristics.

Patient ID	Recruiting center	Disorder	Genetic defect	Mutation	Sample's type	Cell lines tested in cytotoxicity assay
P01	CHUSJ	X-linked lymphoproliferative disease, Purtilo syndrome (XLP1)	*SH2D1A*		PBMCs from fresh blood	K562, REH
P02	CHUSJ	Type 2 familial hemophagocytic lymphohistiocytosis (FHL2)	*PRF1*	[c.116C>A] +[c.445G>A], [p.Pro39His] +[p.Gly149Ser]	PBMCs from fresh blood	K562, NALM6, REH, 697
P03	CHUSJ	NEMO deficiency syndrome	*IKBKG*		PBMCs from fresh blood	K562, REH
P04	CHUSJ	X-linked chronic granulomatous disease (X-CGD)	*CYBB*	c.252G>A, p.Ala84Ala	Frozen PBMCs	K562, NALM6, REH
P05	CHUSJ	Autosomic recessive chronic granulomatous disease (AR47-CGD)	*NCF1*	[c.75_76delGT] +[c.75_76delGT], [p.Tyr26HisfsX26] +[p.Tyr26HisfsX26]	PBMCs from fresh blood	K562, NALM6, REH
P06	CHUSJ	X-linked chronic granulomatous disease (X-CGD)	*CYBB*	c.252G>A, p.Ala84Ala	PBMCs from fresh blood	K562, NALM6, REH
P07	NCK	X-linked chronic granulomatous disease (X-CGD)	*CYBB*	c.217C>T, p.Arg73X	PBMCs from fresh blood	K562, NALM6, REH
P08	NCK	X-linked chronic granulomatous disease (X-CGD)	*CYBB*	c.1610_1611delGT, p.Cys537TrpfsX3	PBMCs from fresh blood	K562, NALM6, REH

Table 2. (Continued.)

Patient ID	Recruiting center	Disorder	Genetic defect	Mutation	Sample's type	Cell lines tested in cytotoxicity assay
P09	CCHMC	Type 3 familial hemophagocytic lymphohistiocytosis (FHL3)	*UNC13D*	[c.2346_2349delGGAG] +[c.3065T>C], [p.Arg782fs] +[p.Leu1022P]	Frozen PBMCs	K562, NALM6, REH, 697
P10	CCHMC	Type 3 familial hemophagocytic lymphohistiocytosis (FHL3)	*UNC13D*	[c.154-1G>C]+253kb inversion	Frozen PBMCs	K562, NALM6, REH, 697
P11	CHUSJ	X-linked chronic granulomatous disease (X-CGD)	*CYBB*	c.469C>T, p.Arg157*	Frozen PBMCs	K562, NALM6, REH
P12	NCK	X-linked chronic granulomatous disease (X-CGD)	*CYBB*	complete gene deletion	PBMCs from fresh blood	K562, NALM6, REH
P13	NCK	X-linked chronic granulomatous disease (X-CGD)	*CYBB*	c.676C>T, p.Arg226*	PBMCs from fresh blood	K562, NALM6, REH
P14	NCK	Autosomic recessive chronic granulomatous disease (AR47-CGD)	*NCF1*	[c.75_76delGT] +[c.75_76delGT], [p.Tyr26HisfsX26] +[p.Tyr26HisfsX26]	PBMCs from fresh blood	K562, NALM6, REH
P15	HCL	Protein kinase C δ deficiency	*PRKCD*	[c.1528G>A]+[c. 1528G>A], [p.Gly510Ser]+ [p.Gly510Ser]	PBMCs from fresh blood	K562, NALM6, REH, 697
P16	HSL	GATA2 haplo-insufficiency	*GATA2*	[c.1076T>C], p.Leu359Ser	PBMCs from fresh blood	K562, NALM6, REH, 697
P17	HCL	X-linked chronic granulomatous disease (X-CGD)	*CYBB*	complete gene deletion	Frozen PBMCs	K562, NALM6, REH
P18	NCK	X-linked chronic granulomatous disease (X-CGD)	*CYBB*	c.252G>A, p.Ala84Ala	Frozen PBMCs	K562, NALM6, REH
P19	NCK	X-linked chronic granulomatous disease (X-CGD)	*CYBB*	complete gene deletion	Frozen PBMCs	K562, NALM6, REH
P20	NCK	X-linked chronic granulomatous disease (X-CGD)	*CYBB*	c.481C>T, p.Arg157X	PBMCs from fresh blood	K562, NALM6, REH
P21	HCL	X-linked chronic granulomatous disease (X-CGD)	*CYBB*	c.375G>A, p.Trp125X	PBMCs from fresh blood	nc
P22	NCK	Autosomic recessive chronic granulomatous disease (AR22-CGD)	*CYBA*	[c.204-2A>G] +[c.204-2A>G], splicing site destruction	PBMCs from fresh blood	K562, NALM6, REH, 697
P23	NCK	X-linked agammaglobulinemia	*BTK*	c.1573C>G, p.Arg525Gly	Frozen PBMCs	K562, NALM6, REH, 697
P24	NCK	X-linked immunodeficiency with hyper-IgM (XHIGM)	*CD40LG*	c.682C>T, p.Gln221X	Frozen PBMCs	K562, NALM6, REH, 697

Table 2. (Continued.)

Patient ID	Recruiting center	Disorder	Genetic defect	Mutation	Sample's type	Cell lines tested in cytotoxicity assay
P25	NCK	X-linked moesin-associated immunodeficiency (X-MAID)	*MSN*	c.511C>T, p.Arg171Trp	PBMCs from fresh blood	K562, NALM6, REH
P26	NCK	Hyper-IgE syndrome (HIES), Job-Buckley syndrome	*STAT3*	c.1144C>T, p.Arg382Trp	PBMCs from fresh blood	K562, NALM6, REH
P27	CHUSJ	Type 2 familial hemophagocytic lymphohistiocytosis (FHL2)	*PRF1*	[c.673C>T]+[c.673C>T], [p.Arg225Trp] +[p.Arg225Trp]	PBMCs from fresh blood	K562, NALM6, REH, 697

CHUSJ denotes CHU Sainte-Justine, NCK Hôpital Necker-Enfants Malades, CCHMC Cincinnati Children's Hospital Medical Center, HCL Hospices Civils de Lyon, HSL Hôpital Saint-Louis and PBMCs peripheral blood mononuclear cells.

2.2. PERIPHERAL BLOOD MONONUCLEAR CELLS ISOLATION

Peripheral blood from patients and controls were collected in heparin tubes and followed the same procedure. Whole blood was diluted 1:1 in Dulbecco's phosphate buffer saline (D-PBS, Gibco™) supplemented with 0.6% CPDA (citrate phosphate dextrose adenine solution) and carefully layered on top of Ficoll-Paque PLUS (GE Healthcare Life Sciences) in 50 mL tubes at a ratio of 3 volumes of diluted blood to 1 volume of Ficoll. After spinning (400 g for 30 minutes with brakes off), the Ficoll interphase was recovered and washed in 50 mL Falcon tubes with D-PBS/0.6% CPDA (400 g for 10 minutes). Cells were then resuspended in complete medium (RPMI (Gibco™) supplemented with 10% heat-inactivated fetal bovine serum (FBS) and penicillin-streptomycin (100 IU/mL)) before counting on a hemocytometer (Neubauer improved cell counting chamber); dead cells were excluded by the trypan blue viability test. PBMCs in excess were frozen down in FBS with 10% dimethylsulfoxide (DMSO) and stored in liquid nitrogen for long term preservation.

2.3. CELL CULTURE

2.3.1. CELL LINES

Human cell lines were purchased from the American Type Culture Collection (ATCC) and the *Deutsche Sammlung von. Mikroorganismen und Zellkulturen GmbH* (DSMZ). B cell precursor leukemias REH (DSMZ no. ACC 22), NALM6 (DSMZ no. ACC 128), 697 (DSMZ no. ACC 42), and RS4;11 (DSMZ no. ACC 508); and chronic myelogenous leukemia K562 (ATCC CCL-243) were cultured and maintained in complete RPMI (RPMI 1640 supplemented with 10% FBS and penicillin-streptomycin (100 IU/mL)) according to manufacturer's instructions.

K562-mb15-41BBL or K562-tCD19-CD64-CD86-CD137L-mbIL21 (Clone9.mbIL21) feeder cells used for NK cells expansion were kindly provided by Pr Dario Campana (National University of Singapore, Singapore) and Dr. Dean Lee (Nationwide Children's Hospital, OH, USA) respectively, and cultured and maintained in complete RPMI medium.

2.3.2. *IN VIVO* EXPANSION OF PRIMARY PRE-B ALL BLASTS AND CELL CULTURE

Deidentified diagnostic bone marrow samples were obtained from patients after written informed consent in accordance with the Declaration of Helsinki. Following bone marrow mononuclear cells (BMMCs) isolation, cells were either directly injected into NSG (NOD/LtSz-scid/IL2Rγ$^{-/-}$) mice (Jackson Laboratory) or frozen down and stored in liquid nitrogen.

An optimal blast expansion was achievable by injecting intravenously 5.10^6 ALL blasts. Depending on the cell recovery after Ficoll, it was common to inject only one NSG mouse with a suboptimal dose of blasts (total unpurified BMMCs are used). For primary expansion, we injected the highest possible cell number to a maximum of 5 x 10^6 cells and three mice. At the same time, we performed a flow cytometry analysis of the recovered BMMCs to evaluate the CD3$^+$ cells proportion among injected cells. To avoid a xenogeneic graft-versus-host disease (GvHD), mice were treated with anti-human CD3 (50 µg/mouse, OKT3) intraperitoneally on days 1, 3 and 5 after human cells injection. Time to engraftment following xenotransplantation was dependent on the injected total BMMCs number as well as on interindividual variations. Development of human ALL in mice was followed by using peripheral blood sampling, and mice were euthanized when they reached endpoints that met accepted animal care guidelines. Expanded primary blasts were recovered from the spleen and used for further *in vivo* expansion by secondary xenotransplantations or frozen down and stored for long term preservation.

For cytotoxicity assay, expanded blasts were thawed and kept in culture a few hours to get rid of the dying cells, in X-VIVO^{TM} 15 (Lonza) medium supplemented with 10% fetal bovine serum and penicillin-streptomycin (100 IU/mL). Although it is known that primary pre-B acute lymphoblastic cells are difficult to keep in culture, we observed that the remaining cells following this resting passage could survive for the time of the assay. Cells were then used for a flow cytometry-based assay following a regular protocol (**§2.5**).

2.4. NK ACTIVATION AND EXPANSION SYSTEMS (NKAES)

Highly activated NK cells were generated either from fresh or frozen PBMCs, using a previously described co-culture system. Briefly, 100 Gy irradiated K562-mb15-41BBL or Clone9.mbIL21 feeder cells (0.5 x 10^5 cells/mL) were used to stimulate mononuclear cells (0.75 x 10^5 cells/mL) in RPMI medium supplemented with L-glutamine, 10% fetal bovine serum, penicillin-streptomycin (100 IU/mL) and 40 IU/mL recombinant human IL-2 (Proleukin®, Novartis), in a 20 mL final volume T75 flask. After 3 and 5 days, an equivalent volume of fresh complete medium (containing rhIL-2) was added. Cells were eventually harvested after 7 days and NK cells expansion and purity were assessed by flow cytometry and either directly used for functional assays after CD3-depletion or put back in culture for a new expansion week.

For subsequent expansion weeks, irradiated feeder cells (0.5 x 10^5 cells/mL) were used to stimulate NKAES-NK (0.5 x 10^4 cells/mL) at a ratio of 1 $CD56^+CD3^-$ cell to 10 feeder cells (with a 20 mL starting volume in a T75 flask), and rhIL-2 concentration was increased to 100 IU/mL. NKAES-NK cells were harvested after 14 days and purity was assessed by flow cytometry (**Figure 9**).

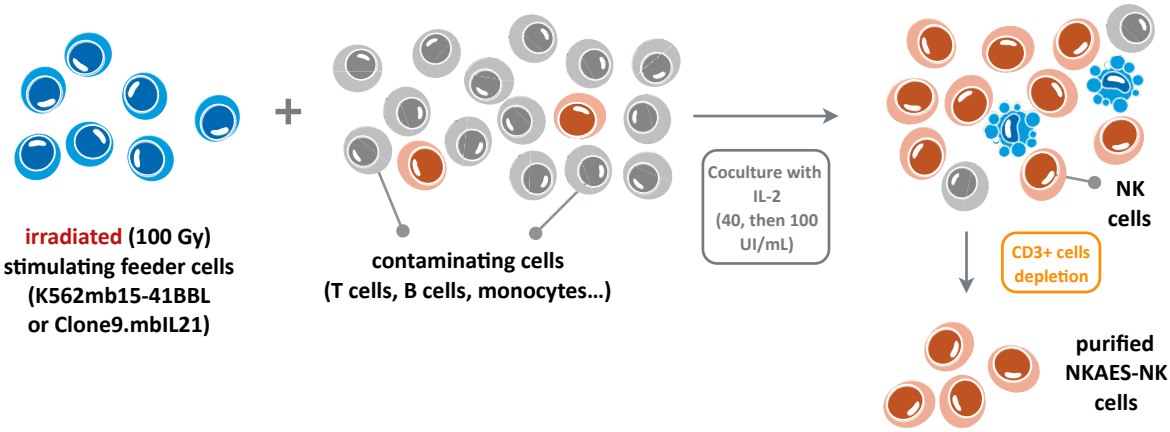

Figure 9. NK cells activation and expansion system (NKAES) from PBMCs.
The final purity of the effector cells (> 80%) is assessed by flow cytometry before using the NK cells for further functional assays.

2.5. CYTOTOXICITY ASSAY

First introduced in the 60's, the radioactive chromium (^{51}Cr)-release has been considered as the gold standard assay to measure cytolytic activity of effector cells against ^{51}Cr labeled target cells. This radioisotope passively diffuses across the cell membrane and binds to intracellular proteins. Target cells are then cocultured with effector cells and ^{51}Cr release in the medium (as measured by the amount of radioactivity in the supernatant) is used as an indicator of the amount of lysis which has occurred.

Although a reliable assay, the ^{51}Cr-release method suffers from a number of limitations including: (i) technical disadvantages taking into account the regulatory procedure for radiation safety training and licensing, the hazardousness to health, the cost, as well as the short half-life of the radioisotope which make it impractical for unplanned experiments; (ii) intrinsic disadvantages depending on target cells like a variability in the ability to uptake a sufficient amount of ^{51}Cr for a reliable detection of lysis or a strong background due to a high spontaneous ^{51}Cr release which make the assay uninterpretable; (iii) biological concerns regarding the technical readout since not only the results are uniparametric (meaning death is not quantified at a single-cell level) but also some types of cell death might not been detected because they do not involve a rupture in cell membrane integrity (and consequently do not induce ^{51}Cr release in the supernatant) or require longer coincubation times which will be associated with an excessive background.

Taken together, these reasons prompted us to consider a flow cytometry-based cytotoxicity assay as a better alternative (**Figure 10**).

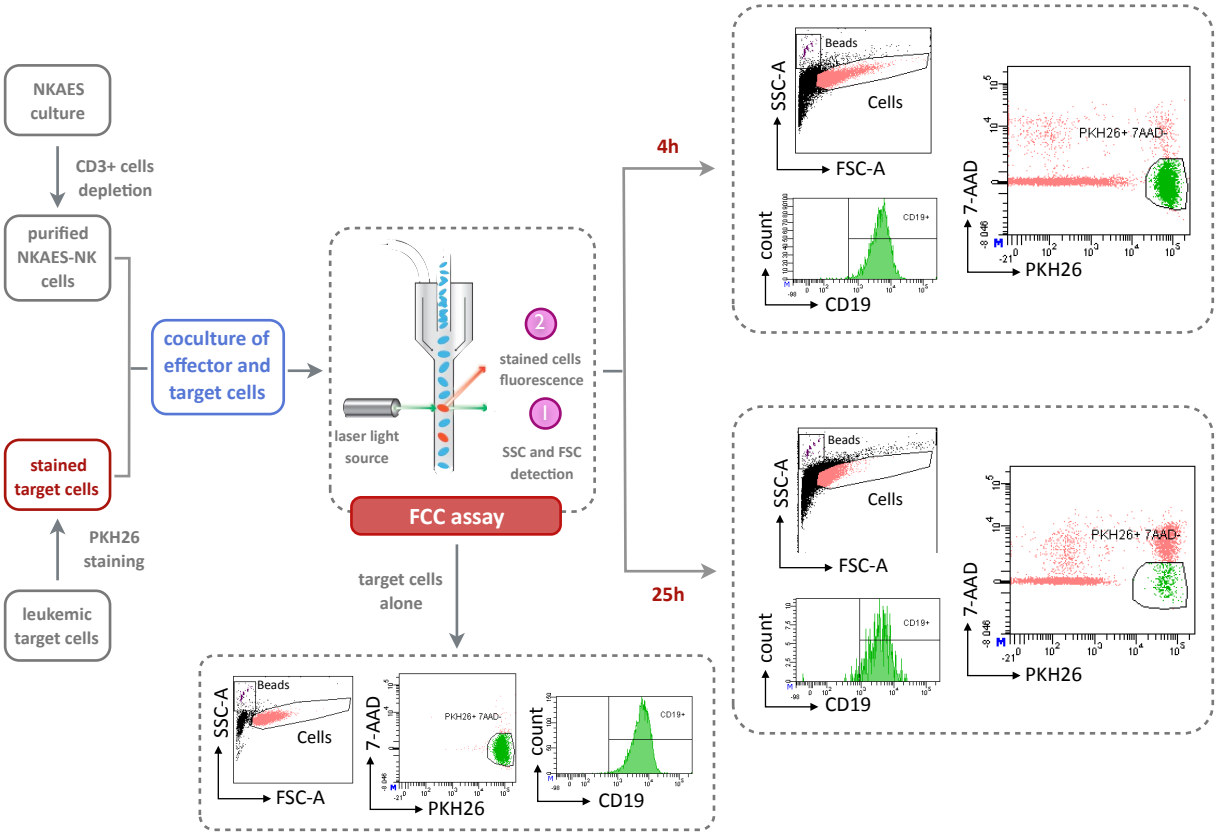

Figure 10. Flow cytometry-based cytotoxicity (FCC) assay (representative dot plots with REH cell line as target and an E:T ratio = 4:1).

NKAES-NK cells were purified from the cell culture by CD3 positive cells depletion while target cells were stained with PKH26. Cytotoxicity assays included effector:target ratios from 4:1 to 1:2 and at least two time points (4h and 25h) to assess short and long term cytotoxicity. Specific lysis was calculated by determining the absolute count of targets ($PKH26^+$ $7\text{-}AAD^-$ $CD19^+$) in presence or in absence of effector cells.

Briefly: target cells were stained with PKH26, a membrane labeling dye with long aliphatic tails which stably stains cell membrane. Following coincubation with effector cells, the absolute count of living targets was calculated thanks to the addition of fluorescent microspheres (CountBright^{TM} Absolute Counting Beads, ThermoFisher) as well as the use of a viability dye (7-AAD and fixable viability dyes were used independently depending on the experiments) and a lineage specific target cells marker (CD19 for pre-B ALL).

2.5.1. PKH26 STAINING OF THE TARGET CELLS

The day (or a few hours) before the FCC assay, a maximum of 2 x 10^6 target cells were washed twice in RPMI 1640 or D-PBS and resuspended in 100 µL of diluent C, then 100 µL of PKH26 (8 µM in diluent C) was added and cells were incubated 5 min at room temperature. The staining was stopped by adding 200 µL of FBS with a supplemental incubation for 1 min. Cells were then washed three times in RPMI 1640 or D-PBS, and resuspended in complete medium for cell culture.

2.5.2. CD3 POSITIVE CELLS DEPLETION

Our protocol used the Miltenyi magnetic system with LD columns. Expanded NK cells were harvested, washed in complete medium and absolute count determined by flow cytometry. Magnetic depletion was performed according to manufacturer's instructions: cells were resuspended in D-PBS supplemented with 0.5% bovine serum albumin (BSA) and 0.6% CPDA (up to 10 x 10^6 cells per 80 µL) and anti-CD3 beads were added to the suspension (20 µL per 10 x 10^6 cells). Cells were incubated 15 min at 4°C in the dark, then washed (1 to 2 mL for 10 x 10^6 cells) and resuspended in 500 µL of buffer. The magnetic column was rinsed with 2 mL of buffer, then cell suspension was applied and two washes (1 mL each) were done. CD3 positive cells were retained on the column (positive fraction) while NK cells were harvested in the negative fraction. Depletion efficiency was assessed by flow cytometry on recovered cells with $CD3^+$ cells < 10% and $CD3^-$ $CD56^+$ > 80% required for further functional assays.

2.5.3. FLOW CYTOMETRY-BASED CYTOTOXICITY (FCC) ASSAY

The day of the FCC assay, effector cells were harvested and their absolute count was calculated by flow cytometry. Cells were then resuspended in a cytotoxicity assay medium (RPMI 1640 supplemented with 2% FBS, penicillin-streptomycin (100 IU/mL) and rhIL-2 (20 IU/mL) at a concentration of 4 x 10^5 $CD3^-$ $CD56^+$ per mL and diluted 1:1 to prepare supplemental ratios (we systematically performed the following effector to target ratios: 4:1,

2:1, 1:1, 1:2). Target cells were harvested, counted on a hemocytometer, and resuspended in the same medium at a concentration of 1 x 10^5 per mL.

The assay was performed in 96 wells round bottom plates with 100 µL of the targets suspension (i.e. equivalent to 10^4 cells) and 100 µL of the effector cells suspension for a final volume of 200 µL per well. The plate was centrifuged at 200 g for 1 minute and incubated (37°C and 5% CO_2).

After various incubation times, plates were recovered: cells were centrifuged at 400 g for 5 minute, stained for 25 min at 4°C in the dark with a viability dye and a lineage specific marker (most often CD19), washed with 175 µL of FACS buffer (D-PBS supplemented with 2% FBS and sodium azide) and finally resuspended in 215 µL of FACS buffer per well. Prior to acquisition, 5 µL of CountBright™ beads (equivalent to 5 x 10^3 cells) were added in each well and cells acquisition was performed on a BD LSRFortessa™ X-20 cytometer equipped with a high throughput sampler (HTS). Stopping gate was fixed by the acquisition of 2500 beads per well which consequently allowed to calculate the absolute count of remaining living targets.

Specific lysis was calculated with the following formula: % Specific lysis = 100-[(absolute count of PKH26$^+$ 7-AAD$^-$ CD19$^+$ targets after incubation with effector cells) / (absolute count of PKH26$^+$ 7-AAD$^-$ CD19$^+$ targets after incubation alone) X 100].

2.6. DEVELOPMENT OF A VERSATILE LENTIVIRAL PLATFORM

Our first lentiviral transductions of the pre-B leukemic cell lines faced previously described difficulties associated with this technology, i.e. variegation and silencing of the integrated transgene whose expression was actively and dynamically repressed. Therefore, we developed a homemade lentiviral platform with the aim to efficiently transduce effector NK cells as well as target cells.

Ubiquitous chromatin opening elements (UCOEs) have been intensively investigated as a solution to these obstacles, showing promising results in maintaining high levels of transgene expression in cells over extended periods of time, both *in vitro* and *in vivo*.

Lentiviral Destination vector pHRSIN UCOE SFFV DEST (compatible with the Gateway™ cloning system) was constructed by modifying a pHRSIN SFFV GFP expression vector, kindly provided by Dr. Els Verhoeyen (ENS Lyon, France). A 0.7-kb UCOE fragment within the human HNRPA2B1/CBX3 housekeeping gene locus was amplified from NALM6 genomic DNA using the following primers: [UCOE/Fw] 5'-ctagtgaattccgcgtgtggcatctgaagca-3' and [UCOE/Rv] 5'-ctagtgaattcttccggaaacacccgaatcaacttcta-3' and EcoRI digested to be inserted into the EcoRI digested pHRSIN SFFV GFP vector, which generated the so-called pHRSIN UCOE SFFV GFP

vector. The GFP sequence of this vector was removed by a BamHI/SbfI digestion followed by blunt-end digestion and replaced by a DEST cassette extracted from the pLenti CMV_TO Puro DEST vector (Addgene #17293) by a EcoRV digestion. The forward orientation of the DEST cassette was confirmed by restriction mapping; the final construct was designated pHRSIN UCOE SFFV DEST (**Appendix 1**).

The final home-made lentiviral vector system (**Figure 11**) was based on InVitrogen's Gateway™ technology: the cDNA of interest was cloned into an Entry vector and then recombined with a Destination vector. This technology employs two sets of reactions which can be used independently: LR and BP recombinations. The BP reaction is catalyzed by the BP clonase enzyme mix to recombine *att*B sites with *att*P sites which leads to the formation of an Entry vector bearing the insert of interest flanked by *att*L sites. The LR clonase mix is used for recombination of *att*L sites from an Entry vector with *att*R sites from a Destination vector.

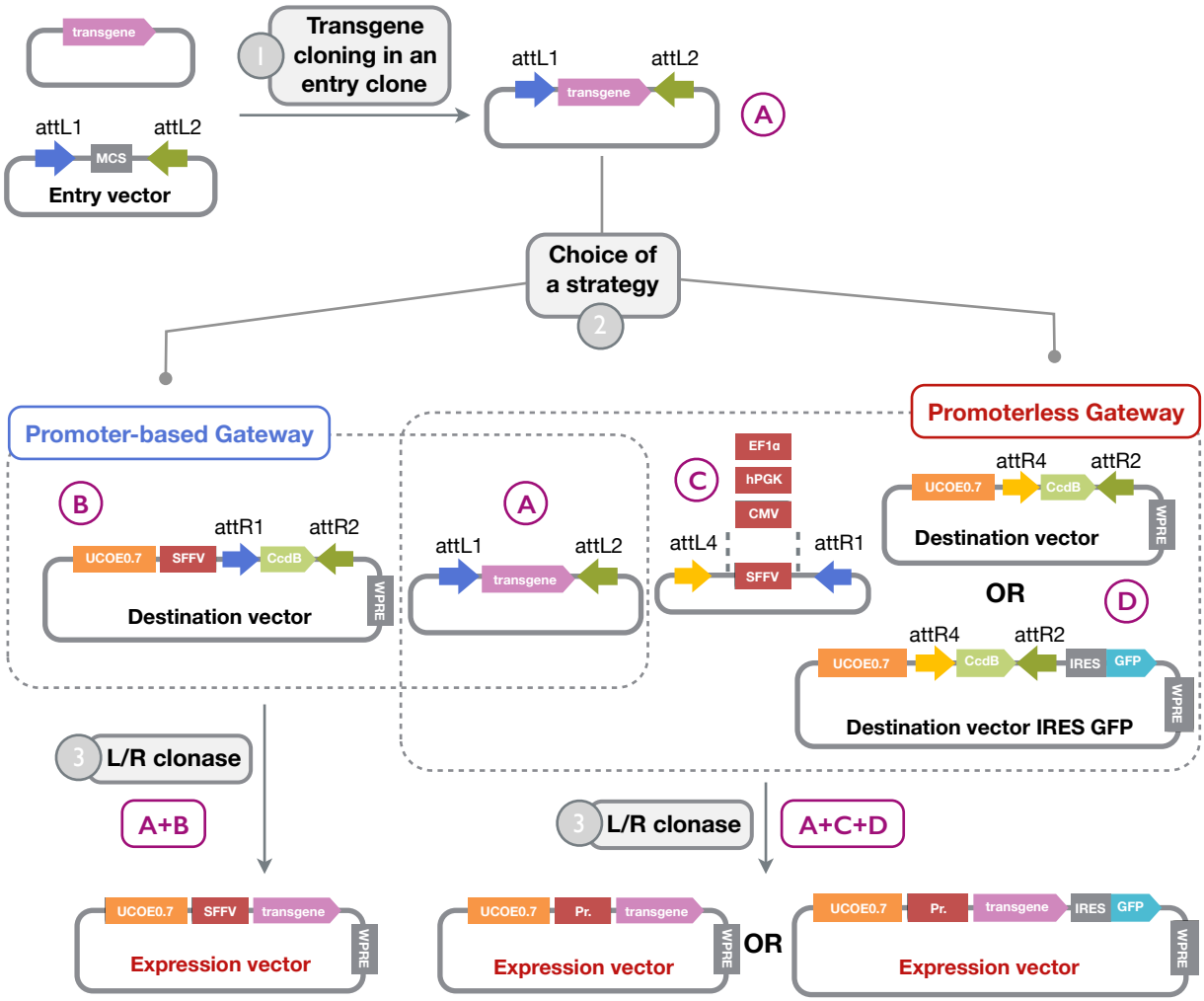

Figure 11. Homemade Gateway based lentiviral platform.
Lentiviral vectors for transgene overexpression were generated using the promoter (SFFV) based solution.

We developed two systems, namely a promoter-based Gateway cloning system with a SFFV expressing Destination vector (pHRSIN UCOE SFFV DEST plasmid) as well as a promoterless one which is based on a MultiSite Gateway approach and has been developed to allow the cloning of multiple DNA fragments. In the promoterless setting, it is possible to choose the promoter which will drive the expression of the insert of interest, as well as to use a Destination vector expressing an IRES GFP fragment.

The final lentiviral platform is offering several advantages: (i) Entry vectors are small so that the cDNA cloning is easier, (ii) LR cloning efficiency is extremely high (> 90%) with a strong decrease in the generation of unwanted cloning artifacts and (iii) its versatility offers the possibility to easily change the promoter, the expression vector type (lentiviral or retroviral vectors) or the detection of the transgene expression (with the IRES GFP cassette).

2.6.1. TRANSDUCTION OF PRE-B ALL CELL LINES

In order to transduce pre-B ALL cell lines, we used vesicular stomatitis virus (VSV) G-protein pseudotyped self-inactivating HIV-1-derived lentiviral vectors (VSV-G LVs). Transgene expression is under the control of a spleen focus foamy virus (SFFV) promoter and vectors were modified with the UCOE element to maintain long term transgene expression.

VSV-G LVs were generated by transfection of 2.4 x 10^6 HEK 293T cells per 10 cm culture plate in DMEM medium (Dulbecco's Modified Eagle's medium, Gibco™) supplemented with 10% FBS and penicillin-streptomycin (100 IU/mL). Co-transfection with polyethylenimine (PEI, a stable cationic polymer) was performed with the Gag-Pol packaging construct 8.91 (8.6 µg) and the self-inactivating (SIN) HIV-1-derived vector (pHRSIN; 8.6 µg). For VSV-G-LV production, 5.5 µg of VSV-G encoding plasmid were co-transfected. 24h later, the supernatant was replaced by Opti-MEM or DMEM. Viral supernatant was harvested 48h later (72h post-transfection) and filtrated through a 0.45 µm pore-sized membrane. If needed, ultracentrifugation (2h, 4°C, 25000 rpm) was performed to concentrate vectors 300-fold. We also directly used filtrated culture supernatant to perform cell lines transduction. In any case, concentrated vectors were aliquoted and stored at -80°C.

Cell lines transduction was performed by plating 200 x 10^3 blasts per well in a 48 wells plate and adding 1 mL of non-concentrated viral supernatant with protamine sulfate (8 µg/mL). The plate was then centrifuged (700 g, 45 min) and the supernatant is replaced 24h later by fresh culture medium. Depending on the lentiviral vector, cells were either FACS-sorted or selected with the appropriate antibiotic selection starting 72h post transduction.

2.6.2. TRANSDUCTION OF PRIMARY ACTIVATED NK CELLS

It is notoriously difficult to efficiently transduce NK cells. However, we developed a protocol showing strong and reproducible transduction rates in NKAES-NK cells with the use of lentiviral vectors pseudotyped with a baboon retroviral envelope glycoprotein, kindly provided by Dr. Els Verhoeyen (ENS Lyon, France), and further displayed BaEVRless-LVs (BaEVRless-gp was constructed by deletion of the R peptide sequence from BaEVwt-gp). For lentiviral production, 7 µg of plasmid coding for this glycoprotein was co-transfected (the procedure was otherwise exactly the same than with VSV-G LVs).

NK cells transductions were performed in a 12 wells non-treated tissue-culture plate previously coated for 2h at room temperature with retronectin solution (1 µg/µL) followed by coating with 2% BSA solution for 30 min. Viral particles were plated onto the retronectin-coated wells for 4h at 37°C. 250 x 10^3 NKAES-NK cells were added per well with protamine sulfate (8 µg/mL), rhIL-2 (100 IU/mL) and IL-15 superagonist/IL-15RαSushi-Fc fusion complex (10 ng/mL, IL-15SA/IL-15RαSu-Fc; ALT-803, Altor BioScience Corporation, USA). The plate was then centrifuged (1000 g, 1h) before an overnight incubation; 24h later, fresh complete RPMI 1640 medium was added and 72h post-transduction, lentiviral transduction efficiency was assessed by FACS.

2.6.3. CRISPR/CAS9-BASED GENOME ENGINEERING

Two complementary strategies, adapted from the dual vector system developed by Dr. Feng Zhang lab (MIT, MA, USA) (Shalem et al., 2014) based on lentiviral delivery of the CRISPR/Cas9 components in the pre-B ALL cell lines, were used depending on the experiments and the number of delivered single guide RNAs (sgRNAs): an uniplex (**Figure 12**) and a multiplex genome engineering methods (**Figure 13**).

2.6.3.1. UNIPLEX GENOME ENGINEERING

Figure 12. Uniplex genome engineering strategy.
Lentiviral expression vectors for Cas9 and sgRNA mammalian delivery using a dual vector system.

For individual gene knockout (KO), cell lines were first transduced with the lentiCas9-Blast plasmid (Addgene #52962, **Appendix 2** and **Figure 12**) to derive stably expressing Cas9 cell lines after blasticidin selection (5 µg/mL). The appropriate sgRNA was cloned into lentiGuide-Puro (Addgene #52963, **Appendix 3**) and the final expression vector was used to transduce Cas9-expressing cell lines. After puromycin selection (5 µg/mL), single clones were isolated by FACS sorting into 96 wells plates.

2.6.3.2. MULTIPLEX GENOME ENGINEERING

For multiple gene knockouts (double KO or DKO in this study), we combined two previously published strategies (**Figure 13**) (Shalem et al., 2014; Kabadi et al., 2014).

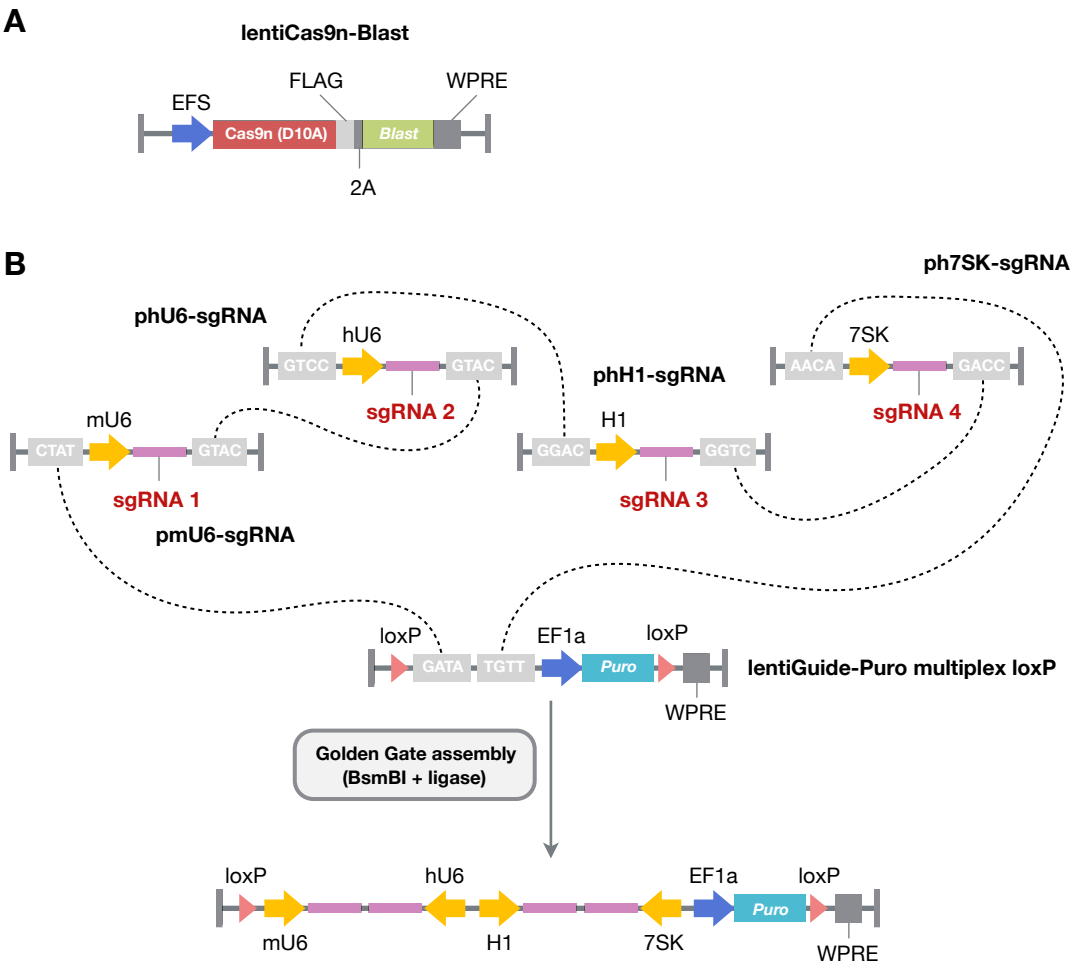

Figure 13. Multiplex genome engineering strategy.
Lentiviral expression vectors for Cas9n (D10A mutated nickase) (**A**) and multiple sgRNAs mammalian delivery using a dual vector system (**B**).

Cell lines were first transduced with the lentiCas9n-Blast plasmid (Addgene #63593, **Appendix 4** and **Figure 13**) to derive stably expressing Cas9n (D10A mutated nickase) cell lines after blasticidin selection (5 µg/mL).

For the final sgRNAs expression vector, we modified the protocole from Dr. Charles Gersbach lab ((Kabadi et al., 2014) and **Figure 13**). We created the lentiGuide-Puro multiplex loxP vector (**Appendix 10**) by PCR-cloning the Gloden Gate Assembly compatible cassette from the pLV hUbC-Cas9-T2A-GFP vector (Addgene #53190, **Appendix 9**) using the following primers: [Multiplex/Fw] 5'-GATGCCACATGCGTGTGCGCCAATTCTGCAGAC-3' and [Multiplex/ Rv] 5'- GAGTACCCGGGgctgcacccTTAatTAATTGTGGAG-3' and then AleI / XmaI digested to be inserted into the XmaI digested lentiGuide-Puro. The forward orientation of the DEST cassette was confirmed by restriction mapping. The final lentiGuide-Puro multiplex loxP vector was generated by replacing the WPRE cassette with a loxP-WPRE one.

According to the published protocol (Kabadi et al., 2014), the appropriate sgRNAs were cloned into pmU6-sgRNA (Addgene #53187, **Appendix 5**), phU6-sgRNA (Addgene #53188, **Appendix 6**), phH1-sgRNA (Addgene #53186, **Appendix 7**) and ph7SK-sgRNA (Addgene #53189, **Appendix 8**). The final expression vector was created by Golden Gate assembly of each of these single vectors with the lentiGuide-Puro multiplex loxP vector using a BsmBI digestion, and then used to transduce Cas9n-expressing cell lines. After puromycin selection (5 µg/mL), single clones were isolated by FACS sorting into 96 wells plates.

2.6.3.3. SGRNA CLONING

We listed the primers used for sgRNA cloning in both the uniplex and multiplex expression systems (**Table 3**).

Table 3. List of oligonucleotides related to sgRNA cloning.

Gene target	Expression system	Cloning vector	Primer	Sequence (5'→3')
CTRL	Uniplex	lentiGuide Puro	CTRL_sgE0_Fw1	CACCG**ACGGAGGCTAAGCGTCGCAA**
CTRL	Uniplex	lentiGuide Puro	CTRL_sgE0_Rv1	AAAC**TTGCGACGCTTAGCCTCCGT**C
CASP9	Uniplex	lentiGuide Puro	CASP9_sgE3_Fw1	CACCG**GGACACAGGCCAGGACATGC**
CASP9	Uniplex	lentiGuide Puro	CASP9_sgE3_Rv1	AAAC**GCATGTCCTGGCCTGTGTCC**C
CTRL	Multiplex	pmU6-sgRNA	CTRL_sgE0_Fw2	TTGTTTG**CGCTTCCGCGGCCCGTTCAA**
CTRL	Multiplex	pmU6-sgRNA	CTRL_sgE0_Rv2	AAAC**TTGAACGGGCCGCGGAAGCG**CAA
CTRL	Multiplex	phU6-sgRNA	CTRL_sgE0_Fw3	CACCG**ATCGTTTCCGCTTAACGGCG**
CTRL	Multiplex	phU6-sgRNA	CTRL_sgE0_Rv3	AAAC**CGCCGTTAAGCGGAAACGAT**C

Table 3. (Continued.)

Gene target	Expression system	Cloning vector	Primer	Sequence (5'→3')
CTRL	Multiplex	phH1-sgRNA	CTRL_sgE0_Fw4	TCCCAGTAGGCGCGCCGCTCTCTAC
CTRL	Multiplex	phH1-sgRNA	CTRL_sgE0_Rv4	AAACGTAGAGAGCGGCGCGCCTACT
CTRL	Multiplex	ph7SK-sgRNA	CTRL_sgE0_Fw5	CCTCGCCATATCGGGGCGAGACATG
CTRL	Multiplex	ph7SK-sgRNA	CTRL_sgE0_Rv5	AAACCATGTCTCGCCCCGATATGGC
CASP3	Multiplex	phU6-sgRNA	CASP3_sgE4_Fw4_p1	CACCGGGAAGCGAATCAATGGACTC
CASP3	Multiplex	phU6-sgRNA	CASP3_sgE4_Rv4_p1	AAACGAGTCCATTGATTCGCTTCCC
CASP3	Multiplex	ph7SK-sgRNA	CASP3_sgE4_Fw5_p1	CCTCGATTATACATAAACCCATCTC
CASP3	Multiplex	ph7SK-sgRNA	CASP3_sgE4_Rv5_p1	AAACGAGATGGGTTTATGTATAATC
CASP7	Multiplex	pmU6-sgRNA	CASP7_sgE5_Fw6_p1	TTGTTTGACTTTGATAAAGTGACAGGT
CASP7	Multiplex	pmU6-sgRNA	CASP7_sgE5_Rv6_p1	AAACACCTGTCACTTTATCAAAGTCAA
CASP7	Multiplex	phH1-sgRNA	CASP7_sgE6_Fw5_p1	TCCCAGAAGCACTTGAAGAGCGCCT
CASP7	Multiplex	phH1-sgRNA	CASP7_sgE6_Rv5_p1	AAACAGGCGCTCTTCAAGTGCTTCT
CASP8	Multiplex	pmU6-sgRNA	CASP8_sgE5_Fw2_p1	TTGTTTGATGGGTTCTTGCTTCCTTTG
CASP8	Multiplex	pmU6-sgRNA	CASP8_sgE5_Rv2_p1	AAACCAAAGGAAGCAAGAACCCATCAA
CASP8	Multiplex	phU6-sgRNA	CASP8_sgE5_Fw2_p2	CACCGGATGTTATTCCAGAGACTCC
CASP8	Multiplex	phU6-sgRNA	CASP8_sgE5_Rv2_p2	AAACGGAGTCTCTGGAATAACATCC
CASP10	Multiplex	phH1-sgRNA	CASP10_sgE2_Fw3_p1	TCCCAGGACTTCTCCAGCTTCTTGT
CASP10	Multiplex	phH1-sgRNA	CASP10_sgE2_Rv3_p1	AAACACAAGAAGCTGGAGAAGTCCT
CASP10	Multiplex	ph7SK-sgRNA	CASP10_sgE2_Fw3_p2	CCTCGTTTTGAACATCTCTTGGCAG
CASP10	Multiplex	ph7SK-sgRNA	CASP10_sgE2_Rv3_p2	AAACCTGCCAAGAGATGTTCAAAAC
BAK1	Multiplex	pmU6-sgRNA	BAK1_sgE3_Fw1_p1	TTGTTTGCACTCCTGCCTGGGAGGACC
BAK1	Multiplex	pmU6-sgRNA	BAK1_sgE3_Rv1_p1	AAACGGTCCTCCCAGGCAGGAGTGCAA
BAK1	Multiplex	phU6-sgRNA	BAK1_sgE3_Fw1_p2	CACCGCTGCCCTCTGCTTCTGGTAA
BAK1	Multiplex	phU6-sgRNA	BAK1_sgE3_Rv1_p2	AAACTTACCAGAAGCAGAGGGCAGC
BAX	Multiplex	phH1-sgRNA	BAX_sgE4_Fw1_p1	TCCCAAGTAGAAAAGGGCGACAACC
BAX	Multiplex	phH1-sgRNA	BAX_sgE4_Rv1_p1	AAACGGTTGTCGCCCTTTTCTACTT
BAX	Multiplex	ph7SK-sgRNA	BAX_sgE4_Fw1_p2	CCTCGTGCTCAAGGTGGGCAGCTGC
BAX	Multiplex	ph7SK-sgRNA	BAX_sgE4_Rv1_p2	AAACGCAGCTGCCCACCTTGAGCAC

Control sgRNAs are depicted in blue.
Regions of the sgRNA complementary to the protospacer are shown in red.

2.6.3.4. IMMUNOBLOT SCREENING OF CANDIDATE CLONES

For immunoblots, total protein was extracted with 1× RIPA lysis buffer (Millipore) with 1× protease inhibitor (Roche) and protein concentration was determined using the BCA assay (Thermo/Pierce). Cell lysates were resolved on 12% SDS-PAGE gels (Bio-Rad), transferred to PVDF membranes (Millipore) which were blocked overnight at 4°C, and incubated 1h30 at room temperature with the appropriate primary antibodies: anti-Caspase-3 (clone 3G2; Cell Signaling 9668), anti-Caspase-7 (clone 4G2; MBL International M053-3), anti-Caspase-8 (clone 5F7; MBL International M032-3), anti-Caspase-9 (clone 5B4; MBL International M054-3), anti-Caspase-10 (clone 4C1; MBL International M059-3), anti-BAX (clone 3/Bax; BD Biosciences), anti-BAK (clone G317-2; BD Biosciences) and anti-β-actin (clone AC-15, Novus Biologicals). Signals were detected using a HRP-conjugated secondary antibody (sc-2005; Santa Cruz Biotechnology) and SuperSignal West Pico Chemiluminescent Substrate (Thermo/Pierce). Images were captured using G:BOX Chemi WRQ imaging system (Syngene).

2.7. CELL CONJUGATION ASSAY

NKAES-NK cells were labeled with PKH26 as previously described (**§2.5.1**) and target cells were stained with 5-6 carboxyfluorescein diacetate succinimidyl ester (CFSE; BD Biosciences). Briefly: targets were washed in D-PBS and then resuspended in a solution of CFSE diluted in D-PBS at 0,625 nmol/mL for 7 min at room temperature in the dark, vortexing cells every 1-2 min. The staining was stopped by adding 1 mL of cold FBS for 1 min on ice. Targets were washed twice with culture medium.

For the assay, both effector and target cells are resuspended at 2 x 10^6 cells/mL and mixed with a 1:1 ratio using 100 µL of each suspension (equivalent to 2 x 10^5 cells). Cell mix was spun at 1000 rpm for 5 min and incubated for 1, 2, 5, 10, or 20 min at 37°C. After gentle resuspension, cells were analyzed by flow cytometry.

In this assay, we studied as targets K562 with (negative control) or without (positive control) EDTA 1 mM, as well as NALM6 and REH cell lines.

2.8. DEGRANULATION ASSAY

Evaluation of NK cells degranulation was performed via the detection of CD107a and CD107b on the cell surface after stimulation with various target cells. Unstained effector and target cells were cultivated at an E:T ratio of 1:1 in a final volume of 200 µL following the same cell culture conditions than a conventional cytotoxicity assay (**§2.5**). A mix of anti-CD107a (clone H4A3; BD Biosciences) and anti-CD107b (clone H4B4; BD Biosciences) antibodies were added

from the beginning of the assay. After a 1h incubation, 13.3 µL of a diluted 1:100 monensin solution (GolgiStop, BD Biosciences) were added per well and incubation was pursued 3 h. At the end of the assay, cells were washed in D-PBS and a cell surface staining was performed with anti-CD3 (clone UCHT1; BD Biosciences) and anti-CD56 (clone B159; BD Biosciences) antibodies before acquisition at the FACS. The percentage of NK degranulation was compared between effector cells stimulated with various conditions against targets or medium alone.

2.9. BLOCKING EXPERIMENTS

In these experiments, NK cells FcR blockade was performed with FcR blocking reagent from Miltenyi Biotec according to manufacturer's instructions to avoid induced antibody-dependent cell-mediated cytotoxicity (ADCC). Up to 10 x 10^6 cells were resuspended in 90 µL of a D-PBS/0.5% BSA/0.6% CPDA buffer and 20 µL of FcR blocking reagent, then incubated for 15 min at 4°C in the dark and washed with buffer.

To study their relative contribution to the cytotoxicity effect, unconjugated antibodies directed against NKG2D (clone M585; Amgen) and DNAM-1 (clone DX11; BD Biosciences) on NK cells, or against DR4 (TRAIL-R1, clone HS101; Enzo Life Sciences) and DR5 (TRAIL-R2, clone HS201; Enzo Life Sciences) on target cells were preincubated with the appropriate cells at a final concentration of 20 µg/mL for 30 min at room temperature. An irrelevant isotype antibody (MOPC21; BD Biosciences) was used as control.

In some experiments, NKp30, NKp44, NKp46 and NKp80 surface markers were blocked with Fc chimera proteins (**Figure 14**) to prevent these NCRs engagements.

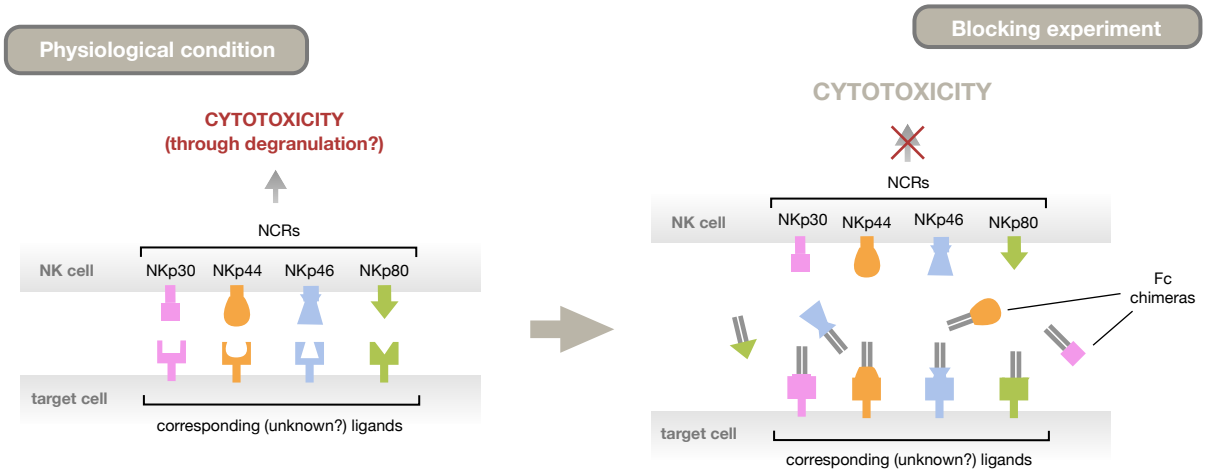

Figure 14. NCRs blockade using Fc chimeras.
Natural Cytotoxicity Receptors (NCRs) engagement was blocked by saturation of the corresponding ligands with a large excess of NCRs chimera proteins.

Targets were pre-incubated with a saturating Ig Fc concentration (5 µg/mL per chimera) for 30 min at room temperature before pursuing a conventional cytotoxicity assay.

2.10. FLOW CYTOMETRY STAININGS

Regular cell surface staining was performed by incubating cells for 25 min at 4°C with antibodies and a viability dye in D-PBS/2% FBS/sodium azide (0.2 mg/mL) in a final volume of 50 µL. Cells are then washed with this buffer.

For intracellular staining (BD Cytofix/Cytoperm; BD Biosciences), cells were fixed and permeabilized with 100 µL of Cytofix/Cytoperm buffer for 20 min at 4°C, then washed twice in Perm/Wash buffer. Conjugated antibodies were then added in 50 µL of Perm/Wash buffer for 20 min at 4°C. Cells were finally washed twice with Perm/Wash buffer and resuspended in regular FACS buffer before acquisition. The following PE-conjugated antibodies were purchased from Santa Cruz Biotechnology: anti-p22-phox (clone 44.1), anti-p47-phox (clone D-10), anti-p67-phox (clone D-6) and irrelevant isotype control antibodies IgG1 and IgG2a. Anti-flavocytochrome b558 (clone 7D5; MBL International D162-5) was used both for intracellular and cell surface stainings.

2.10.1. ANNEXIN V STAINING

Cells were harvested, washed in D-PBS and resuspended in Binding Buffer (BD Biosciences). Staining was performed (15 min at room temperature in the dark) adding 2 µL of annexin-V and others cell surface antibodies. After washing, cells were resuspended in Binding Buffer with 7-AAD and acquisition to the flow cytometer was performed within 1h (**Figure 15**).

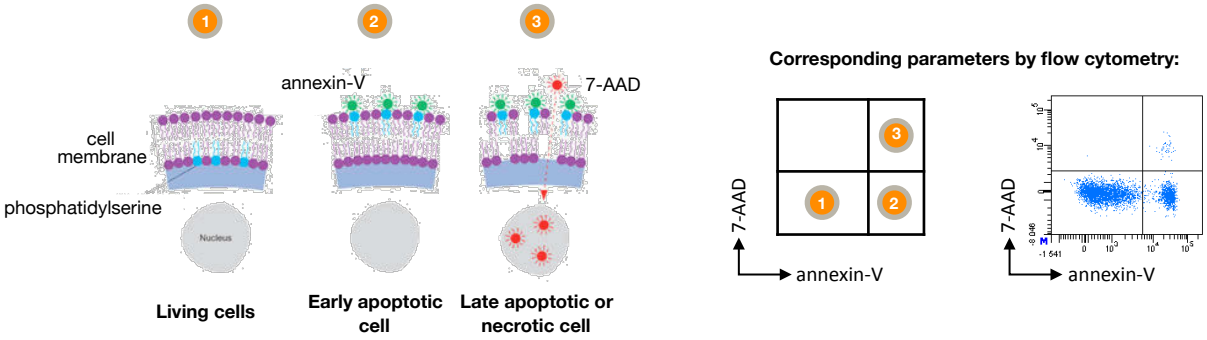

Figure 15. Parameters for the annexin-V staining.

2.10.2. MITOCHONDRIAL DEPOLARIZATION ASSAY

We used the ratiometric fluorescent dye JC-1 to assess mitochondrial potential, a key readout of mitochondrial function. Briefly: we prepared a JC-1 stock solution by diluting a vial of dye in 230 µL of DMSO (then kept at 4°C). Staining was performed by adding 2 µL of a working solution (stock solution diluted 1:10 in cell culture medium) into a final volume of 200 µL per well. Cells were incubated 25 min at 37°C, then washed twice in D-PBS and finally resuspended in FACS buffer (or Binding Buffer if an annexin-V staining was performed subsequently) before acquisition. Protonophore carbonyl cyanide m-chlorophenylhydrazone (CCCP), an uncoupler of mitochondrial respiration was used as a positive control.

2.11. PRIME FLOW RNA ASSAY

Following a regular cell surface staining, unstimulated PBMCs or NKAES-NK cells were stained with viability dye (Fixable Viability Dye eFluor 450; ThermoFisher) and a panel of surface antibodies (anti-CD3 (clone SK7; BioLegend), anti-CD56 (clone REA196; Miltenyi Biotech), anti-CD16 (clone 3G8; BioLegend), anti-CD14 (clone M5E2; BioLegend), anti-CD19 (clone SJ25C1; ThermoFisher)).

Cells were then fixed with a first fixation buffer, permeabilized and fixed a second time according to manufacturer's instructions (PrimeFlow RNA Assay, ThermoFisher). Following washing, cells were then incubated with both CYBB RNA target probe and a RLP13A control probe sets for 2h at 40 °C, allowing effective target probes hybridization. Following several washing steps, cells were successively incubated with Pre-Amplifier and Amplifier molecules for 1.5h at 40 °C. Finally, after washing, cells were incubated for 1h with Alexa Fluor 647 and Alexa Fluor 488 labelled probe sets (**Figure 16**). Following several washing steps, antibody and probe fluorescent signals were finally analyzed by flow cytometry.

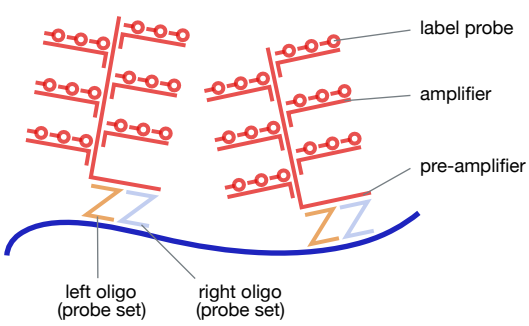

Figure 16. Principle of the Prime Flow RNA assay. It combines paired oligonucleotide probe design with branched DNA (bDNA) signal amplification to robustly detect gene expression at the single-cell level: high target specificity is achieved with the use of oligonucleotide pairs: signal amplification occurs only when two adjacent target probe oligonucleotides (left oligonucleotide and right oligonucleotide) bind to the specific target.

2.12. MEASUREMENT OF INTRACELLULAR CASPASES ACTIVATION

To determine intracellular activation of specific caspases, fluorescent labelled inhibitors of caspases (FLICA) probe assays (ImmunoChemistry Technologies) were performed. Each FLICA probe contains a 3 or 4 amino acid sequence targeted by a specific activated caspase (there is no interference from pro-caspases or the inactive form of the enzymes). FLICA probes are cell-permeable and covalently bind to the active forms of specific caspases. After washing, FLICA fluorescent signal is specifically retained within cells containing the appropriate active form of the caspase while the reagent is washed away in cells lacking the appropriate active caspase.

Briefly: we prepared FLICA stock solutions by diluting vial of probes in 50 µL of DMSO (then kept at -20°C). Staining was performed by adding 2 µL of a working solution (stock solution diluted 1:5 in D-PBS) into a final volume of 200 µL per well. Cells were incubated 15 min at 37°C, then washed twice in Apoptosis Wash Buffer from the kit and finally resuspended in the same buffer before acquisition. If required, subsequent cell surface as well as annexin-V stainings were performed in the same buffer.

2.13. CHARGE-BASED CAPILLARY NANO-IMMUNOASSAY (NANOPRO ASSAY)

The NanoPro 1000 system (ProteinSimple) is built on an automated, capillary-based immunoassay platform and enables a rapid and quantitative analysis of specific proteins. Assay were performed thanks to the Paris Descartes University Proteomic Platform (3P5) (Institut Cochin, INSERM U1016, CNRS UMR 8104, Université Paris Descartes Sorbonne Paris Cité, Paris, France).

Nanofluidic proteomic immunoassays were done according to the manufacturer's instructions. Briefly, cells were washed twice in ice cold PBS followed by another wash in 20mM Bicine pH7.6, 250mM sucrose and subsequently lysed in lysis buffer [20mM Bicine pH7.6, 0.6% CHAPS supplemented with 1X DMSO inhibitor mix (ProteinSimple; 040-510) and 1x aqueous inhibitor mix (Protein Simple; 040-482)], 20 µL / 10^6 cells. Lysates were centrifuged at 15,000 x g for 15 min at 4°C. Clarified lysates were then stored at -80°C until used. Lysates were run on the NanoPro 1000 instrument at 0.1 mg/mL final concentration in the capillary along with Premix G2, Pharmalyte pH 3-10 separation gradient and pI standard ladder 3 from ProteinSimple. Isoelectric focusing of proteins was performed by applying 21,000 µW for 40 minutes and then, UV light exposure for 100 seconds was used to cross-link proteins to the inner capillary wall. Fixed proteins were probed with primary antibodies for either CYBB (clone 54.1; Biolegend) or HSP70 (sc-32239; Santa Cruz Biotechnology) all at

1:50 dilution and incubated for 240 minutes. Secondary HRP-conjugated antibodies, 1:100 dilution, were incubated in the capillary for 1h. Finally, luminol reagent was added to generate chemiluminescence captured by CCD camera. Result were analyzed with Compass software v 2.7.1 for MacOS (ProteinSimple).

2.14. SEAHORSE ANALYSIS

The Oxygen Consumption Rate (OCR) and Extracellular Acidification Rate (ECAR) were measured in XF medium (unbuffered DMEM containing 2 mM glutamine, pH7.4) under basal conditions and in response either to oligomycin (1 μM), FCCP (1 μM) and antimycin A (1 μM) for OCR, or glucose (10 mM), oligomycin (1 μM) and 2-deoxyglucose (2-DG; 50mM) for ECAR, with an XFe96 Extracellular Flux Analyzer (Agilent). NKAES-NK cells were isolated after incubation with target cells or medium only (control) by CD56 positive selection using the Miltenyi magnetic system. Cells were plated in triplicates per condition (500,000 and 750,000 cells per well for the OCR and ECAR measurements respectively) in Seahorse plates coated with CellTak (Corning). After adhesion, the OCR and ECAR were analyzed in real time during 84 min. Measurements were performed thanks to Dr. Ivan Nemazanyy, associate professor (Faculté de Médecine, Université Paris Descartes).

2.15. RNA-SEQUENCING

2.15.1. EXPERIMENTAL DESIGN

Blood mononuclear cells from three patients suffering from X-linked chronic granulomatous disease (X-CGD) with complete CYBB gene deletion (depicted P12, P17 and P19 in **Table 2**) , as well as those from four normal donors, were isolated by Ficoll-Paque centrifugation (**§2.2**). Resting NK cells were purified from PBMCs cells by negative selection with magnetic MicroBeads (Miltenyi Biotech) using LS columns. The purity of the isolated cells was verified by flow cytometry and used as a correction factor in downstream bioinformatics analysis (**Figure 17**).

CD3 depleted NKAES-NK cells, either after a 2 weeks expansion or following respective exposure to a sensitive (REH) or a resistant (RS4;11) pre-B ALL cell line, were isolated by CD56 positive selection. Magnetic MicroBeads (Miltenyi Biotech) using LD (for $CD3^+$ depletion) and MS (for $CD56^+$ selection) columns were used. The purity of the isolated cells was verified by flow cytometry and used as a correction factor in downstream bioinformatics

analysis (see below). Cells (approximately 1 x 10^6 per condition) were immediately lysed in 600 µL of QIAzol and frozen at -80°C.

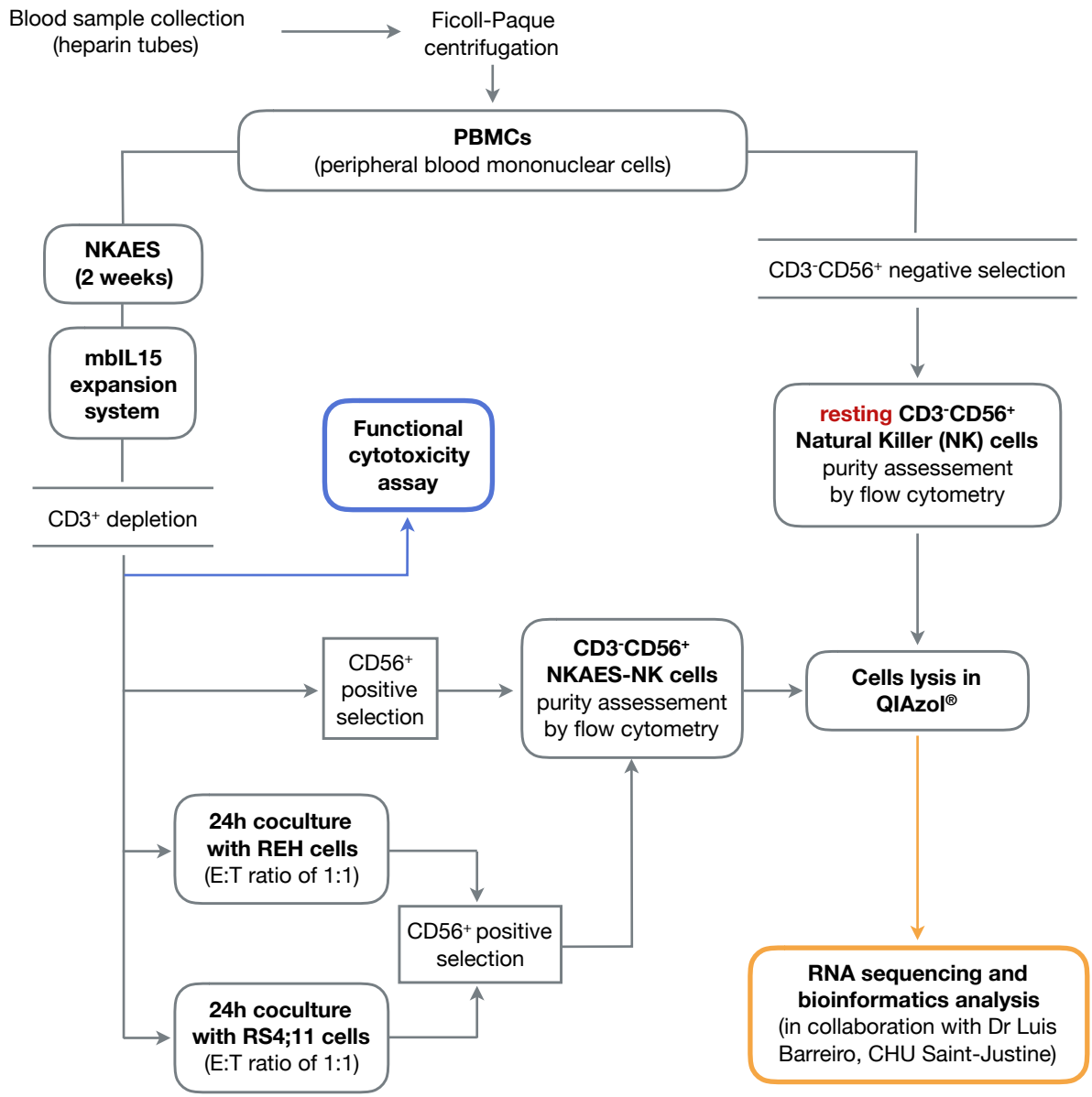

Figure 17. Experimental design for sample processing in the RNA-sequencing experiment. A total of seven donors (3 X-CGD and 4 normal donors) were recruited which represented 24 samples for further sequencing and analytic steps.

2.15.2. RNA EXTRACTION, LIBRARY PREPARATION AND SEQUENCING

Once recruitment was completed, samples were all shipped to Montreal. Total RNA was extracted using the miRNeasy kit (QIAGEN) and RNA quantity was evaluated spectrophotometrically. The quality was assessed with the Agilent 2100 Bioanalyzer (Agilent Technologies) and only samples with no evidence for RNA degradation (RNA integrity number > 8) were kept for further experiments. RNA-sequencing libraries were prepared using the Illumina TruSeq protocol. Once prepared, indexed cDNA libraries were pooled (6

libraries per pool) in equimolar amounts and were sequenced with single-end 100bp reads on an Illumina HiSeq2500. We thank Calcul Québec and Compute Canada for providing access to the supercomputer Briaree from the University of Montreal.

2.15.3. DATA PROCESSING

Samples were used to define eight different groups (**Figure 18**).

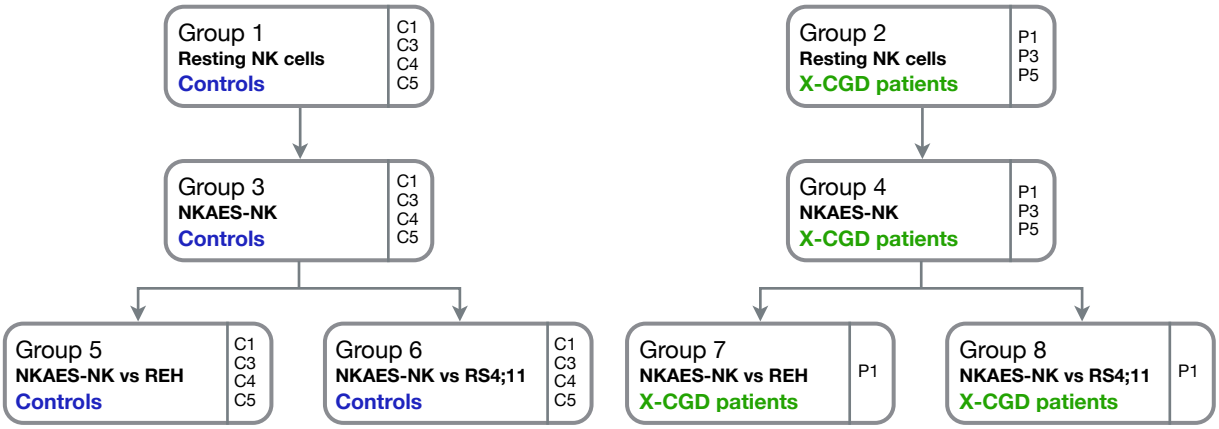

Figure 18. Group design in the RNA-sequencing experiment analysis.
Normal donors and X-CGD patients defined respectively groups 1, 3, 5, 6, and 2, 4, 7, 8.

The sequences were treated following the following pipeline. The reads within the samples were trimmed using TrimGalore! (v0.2.7, using Cutadapt v.1.11) to remove any adapter sequence or bad quality (BQ>20) left within the sequencing read. The sequences were then aligned to the reference transcriptome on the hg19 release and using gene definition file based on ENSEMBL v75 using kallisto (v. 0.43.0). The tximport (v. 1.0.3) R package was used to reconstruct from the isoforms-levels the gene-level counts.

We used mixed models (package EMMREML), to fit two models:

- **Model 1**: NKAES-model: all groups but 1 and 2 (to deal with NKAES behavior pre and post exposure to leukemia in healthy donors versus patients);
- **Model 2**: resting NK vs NKAES (no exposure to leukemia) to explore effects of NK cells activation on gene expression, and how it varies between controls and patients.

In each model, the gene-set to analyze was selected independently, by filtering out low-expressed genes. To do that, in each of them, we get the within-group median gene expression, per each gene and group, for all groups present in the model, and selected only genes with a median>2 (log2 cpm) in at least one of the groups present in the model

In both cases, using EMMREML, the models have the following structure:

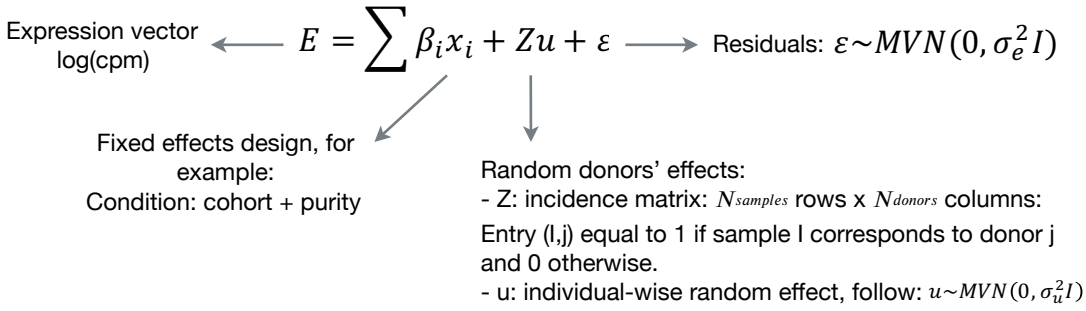

Fixed effects nested design for deconvolve samples content: Model 1

We assumed that each sample had two components (a fraction of pure NKAES-NK cells and a fraction of impurities, whatever those are made of), each of which could be modeled independently through two auxiliar models M_nk and M_imp:

- M_nk: to model the fraction of interest (NK cells), as follows: E~cohort+Condition*cohort

$$M_{nk}: E \sim \begin{cases} \beta_o & G3: NKAES@CTL \\ \beta_o + \beta_{REH} & G5: NKAES - VS - REH@CTL \\ \beta_o + \beta_{RS4} & G6: NKAES - VS - RS4@CTL \\ \beta_o + \beta_P & G4: NKAES@PAT \\ \beta_o + \beta_P + \beta_{REH} + \beta_{REH\,x\,P} & G7: NKAES - vs - REH@PAT \\ \beta_o + \beta_P + \beta_{RS4} + \beta_{RS4\,x\,P} & G8: NKAES - vs - RS4@PAT \end{cases}$$

- M_imp: to model the complementary fraction (impurities before exposure and/or cancer cells after). Modeled as E~Cytotoxic_target

$$M_{imp}: E \sim \begin{cases} \beta_o^{comp} & G3: NKAES@CTL \\ \beta_{REH}^{comp} & G5: NKAES - VS - REH@CTL \\ \beta_{RS4}^{comp} & G6: NKAES - VS - RS4@CTL \\ \beta_o^{comp} & G4: NKAES@PAT \\ \beta_{REH}^{comp} & G7: NKAES - VS - REH@PAT \\ \beta_{RS4}^{comp} & G8: NKAES - VS - RS4@PAT \end{cases}$$

Once defined M_nk and M_imp, we defined the complete model as follows:

$$M = pM_{nk} + (1-p)M_{imp}: E \sim \begin{cases} (\beta_o)p + (1-p)\beta_o^{comp} & G3: NKAES@CTL \\ (\beta_o + \beta_{REH})p + (1-p)\beta_{REH}^{comp} & G5: NKAES - VS - REH@CTL \\ (\beta_o + \beta_{RS4})p + (1-p)\beta_{RS4}^{comp} & G6: NKAES - VS - RS4@CTL \\ (\beta_o + \beta_p)p + (1-p)\beta_o^{comp} & G4: NKAES@PAT \\ (\beta_o + \beta_p + \beta_{REH} + \beta_{REHx\,p})p + (1-p)\beta_{REH}^{comp} & G7: NKAES - VS - REH@PAT \\ (\beta_o + \beta_p + \beta_{RS4} + \beta_{RS4\,x\,p})p + (1-p)\beta_{RS4}^{comp} & G8: NKAES - VS - RS4@PAT \end{cases}$$

Which could be declared like this: (Purity_comp=1-p, Purity_raw=p).

We defined eleven contrasts following Model 1 (**Table 4**).

Table 4. Differential expression contrasts retrieved from Model 1.	
Contrast 2	disease effect on NKAES cells: (G4-G3)
Contrast 3	disease effect on NKAES cells exposed to REH: (G7-G5)
Contrast 4	disease effect on NKAES cells exposed to RS4;11: (G8-G6)
Contrast 8	REH effect in controls' NKAES's: (G5-G3)
Contrast 9	REH effect in patient' NKAES's: (G7-G4)
Contrast 10	Difference between REH effect in patient minus controls' NKAES's: (G7-G4)-(G5-G3)
Contrast 11	RS4;11 effect in controls' NKAES's: (G6-G3)
Contrast 12	RS4;11 effect in controls' NKAES's: (G8-G4)
Contrast 13	Difference between RS4;11 effect in patient minus controls' NKAES's: (G8-G4)-(G6-G3)
Contrast 14	RS4;11 minus REH effect in controls' NKAES's: (G6-G5)
Contrast 15	RS4;11 minus REH effect in patient' NKAES's: (G8-G7)

Groups used for contrasts' definition are depicted in **Figure 18**.

Fixed effects nested design for deconvolve samples content: Model 2

Again, we have two auxiliar models M_nk and M_imp:

- M_nk: to model the fraction of interest (NK cells), as follows: E~cohort+Condition*cohort
- M_imp: to model the complementary fraction (impurities before exposure to leukemia). Modeled as E~Intercept

$$M_{nk}: E\sim \begin{cases} \beta_o & G1: NK@CTL \\ \beta_o+\beta_{NKAES} & G3: NKAES@CTL \\ \beta_o+\beta_p & G2: NK@PATIENT \\ \beta_o+\beta_p+\beta_{NKAES}+\beta_{P\ x\ NKAES} & G4: NKAES@PATIENT \end{cases}$$

$$M_{imp}: E\sim \begin{cases} \beta_o^{comp} & G1: NK@CTL \\ \beta_o^{comp} & G3: NKAES@CTL \\ \beta_o^{comp} & G2: NK@PATIENT \\ \beta_o^{comp} & G4: NKAES@PATIENT \end{cases}$$

$$M_2 = pM_{nk} + (1-p)M_{imp}:$$

$$E\sim \begin{cases} p\beta_o+(1-p)\beta_o^{comp} & G1: NK@CTL \\ p(\beta_o+\beta_{NKAES})+(1-p)\beta_o^{comp} & G3: NKAES@CTL \\ p(\beta_o+\beta_p)+(1-p)\beta_o^{comp} & G2: NK@PATIENT \\ p(\beta_o+\beta_p+\beta_{NKAES}+\beta_{P\ x\ NKAES})+(1-p)\beta_o^{comp} & G4: NKAES@PATIENT \end{cases}$$

We defined four contrasts following Model 2 (**Table 5**).

Table 5. Differential expression contrasts retrieved from Model 2.	
Contrast 1	differential expression between patients and controls for resting NK cells: (G2-G1)
Contrast 5	activation effect on controls: (G3-G1)
Contrast 6	activation effect on patients: (G4-G2)
Contrast 7	differences in activation effects between patients and controls: (G4-G2)-(G3-G1)

Groups used for contrasts' definition are depicted in **Figure 18**.

2.16. STATISTICAL ANALYSIS

Statistical analyses were performed with Prism v6.0h for MacOS (GraphPad Software Inc.), and the open-source statistical package R (http://www.r-project.org).

CHAPTER 3.

RESULTS AND DISCUSSION

3. RESULTS AND DISCUSSION

3.1. PRE-B ALL CELLS ARE SENSITIVE TO NK CELL KILLING IN A LONG-TERM CYTOTOXICITY ASSAY

Pre-B ALL cells relative resistance to NK cell mediated cytotoxicity has been well documented (Imai et al., 2005; Kübler et al., 2014; Romanski et al., 2005; Ruggeri, 2002; Ruggeri et al., 1999). We studied NK cell cytotoxicity against pre-B ALL cell lines as well as primary blasts amplified *in vivo* (**Figure 19**) by using a flow cytometry-based assay (FCC).

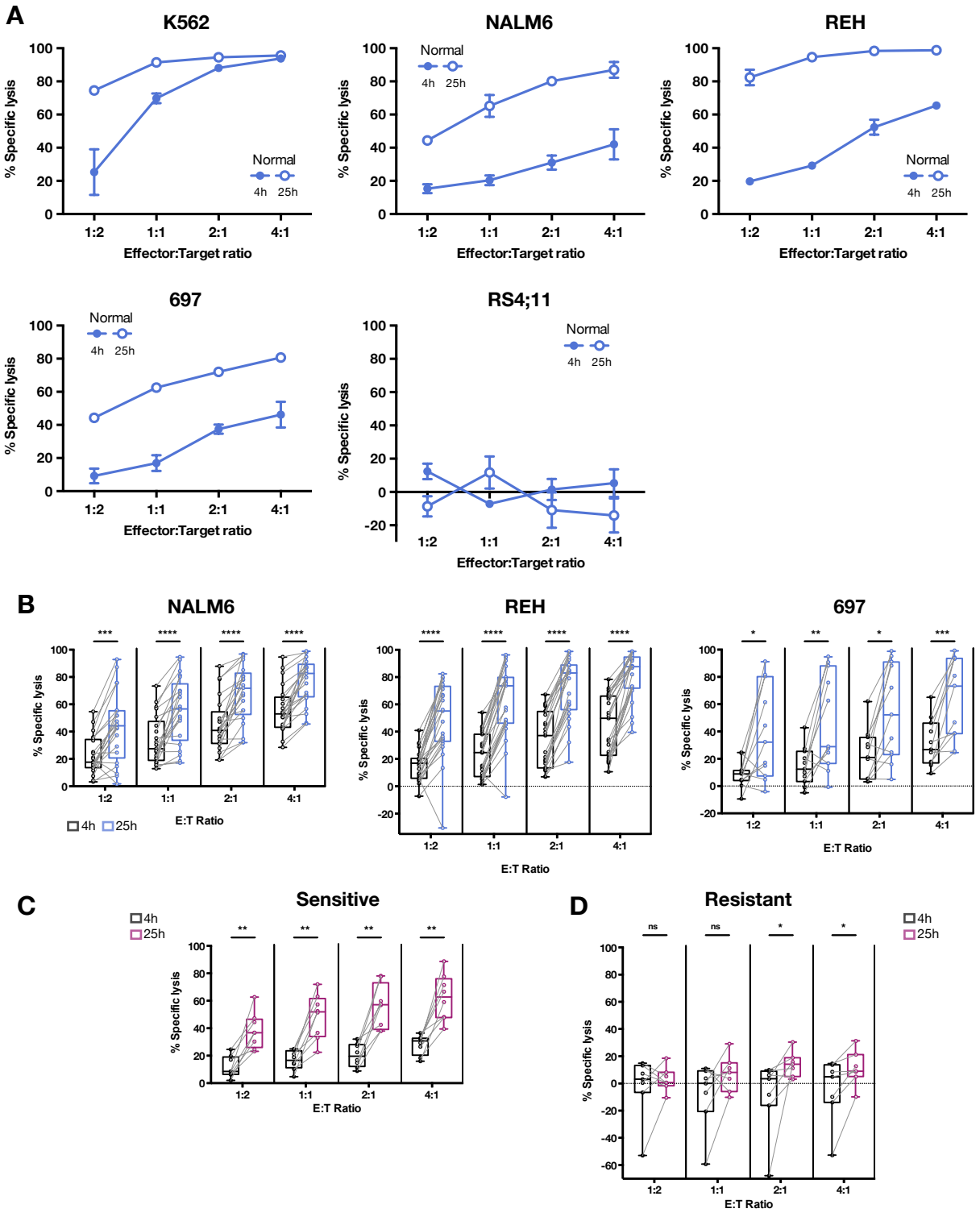

(legend on next page)

In agreement with previous studies, we observed markedly impaired killing of pre-B ALL following a 4h incubation with allogeneic NK cells in comparison to the cytotoxicity measured against the HLA-I negative, positive control K562 cell line, a condition which is similar to a conventional short term cytotoxicity assay. However, we observed a strong increase of ALL target cells' death when the assay was pursued up to 25h (**Figures 19**A and **19**B). Of note, we confirmed the specificity of this delayed killing because one cell line (RS4;11) was constantly resistant and blasts were not affected by a 25h coculture with allogeneic $CD4^+$ cells (data not shown). The late increase of NK cytotoxicity was not restricted to NK cells activated in our IL-15-based system (Imai et al., 2005) since the same result was observed when using resting NK cells from peripheral blood as well as NK cells activated in an IL-21-based system (Denman et al., 2012) (**Figures S1**A and **S1**B).

We then addressed the important question of the relevance of this observation by using patients' primary leukemic blasts. Since pre-B ALL blasts are known to be difficult to keep in culture *in vitro,* we used as target cells in a FCC assay primary cells from pediatric pre-B ALL patients which had been previously amplified in Nod/SCID/IL2R$\gamma^{-/-}$ (NSG) mice. Primary blasts could be separated in two groups respectively identified as sensitive and resistant based on NK mediated cytotoxicity (**Figures 19**C and **19**D), with cells initially resistant being killed in a late time point while others remained insensitive after long exposure to NK cells.

This data shows that pre-B ALL cells from patients are sensitive to NK cells cytotoxicity in a prolonged assay.

3.2. CHARACTERIZATION OF THE EFFECTOR PATHWAY

NK cells can kill target cells through several effector pathways shared with effector CD8 T cells (Lieberman, 2016; Martínez-Lostao et al., 2015; Russell and Ley, 2002; Sun and Lanier,

Figure 19. Pre-B ALL are not intrinsically resistant to NK cell mediated cytotoxicity.
(**A**) Representative graphs showing early and late leukemic killing by NKAES-NK cells. Shown are percentages of cytotoxicity (relative to cultures with no effector cells) in cocultures lasting 4 and 25h. Shown are mean ± SD.
(**B**) Results from twenty-one (NALM6 cell line), twenty-three (REH cell line) and eleven (697 cell line) normal donors respectively.
(**C**) Leukemic blasts from four different patients (amplified in NSG mice) were assessed using NKAES-NK from three different normal donors. Each primary blasts were tested against two different NK donors.
(**D**) Leukemic blasts from three different patients (amplified in NSG mice) were assessed using NKAES-NK from three different normal donors. Each primary blasts were tested against two or three different NK donors.
Statistics: Wilcoxon matched-pairs signed rank test (* = $p < 0.05$, ** = $p < 0.01$, *** = $p < 0.001$ and **** = $p < 0.0001$).

2011). Schematically, three main pathways are known to be engaged by cytotoxic cells: 1- granule exocytosis of lytic molecules (perforin, granzymes and granulysin); 2- death receptors mediated killing; and 3- secretion of soluble factors like cytokines that may exert direct as well as indirect (sensitization of target cells) effects (**Figure 20**). We aimed to decipher the relative contribution to each separate pathway to the late killing of pre-B ALL cells by NK cells by a methodical, systematical and dual approach exploring both molecular requirements of NK cells activation and effector response, as well as those of engaged cell death among blasts. To do so, we studied this cytotoxic interaction assessing each steps of a simplified model (**Figure 20**).

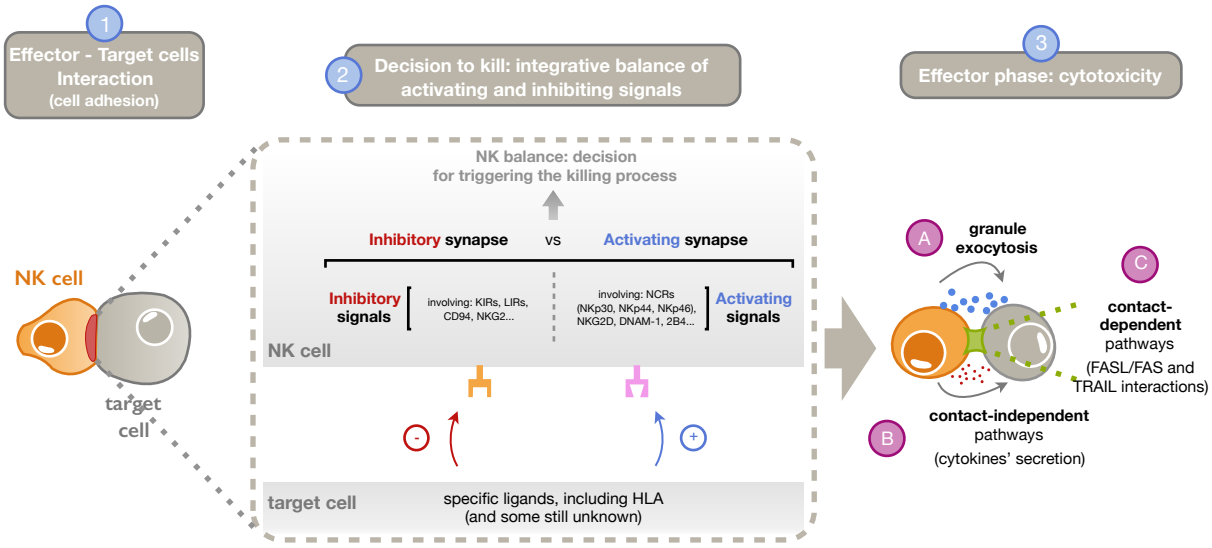

Figure 20. A simplified three-step model of the NK killing process.
In this model, one can distinguish the following sequence of events: adhesion between NK and target cells (**1**), signals integration leading to either an activation or an inhibitory synapse (**2**) and effector phase *per se*, i.e. mechanisms responsible for targets' death (**3**).

3.2.1. A CONTACT-DEPENDENT MECHANISM

We first assessed the requirement of a contact between NK cells and blasts. It has been previously postulated that the relative resistance to pre-B ALL cells was due to a defective adhesion step (Ruggeri et al., 1999), although further works tended to exclude this hypothesis as a major systematical mechanism of resistance (Mengarelli et al., 2001; Romanski et al., 2005). Albeit lower with pre-B ALL cells than with K562, early formation of conjugates by NK cells was still detectable (**Figure 21**A) and higher than in a condition preventing cell adhesion (**Figure 21**B). Exploring the hypothesis of a potential requirement for an initial NK cells priming, we also measured early conjugates formation with NK cells

previously incubated for 25h with the same target cells but didn't detect any difference (data not shown), i.e. the pre-incubation step did not increase the formation of conjugates.

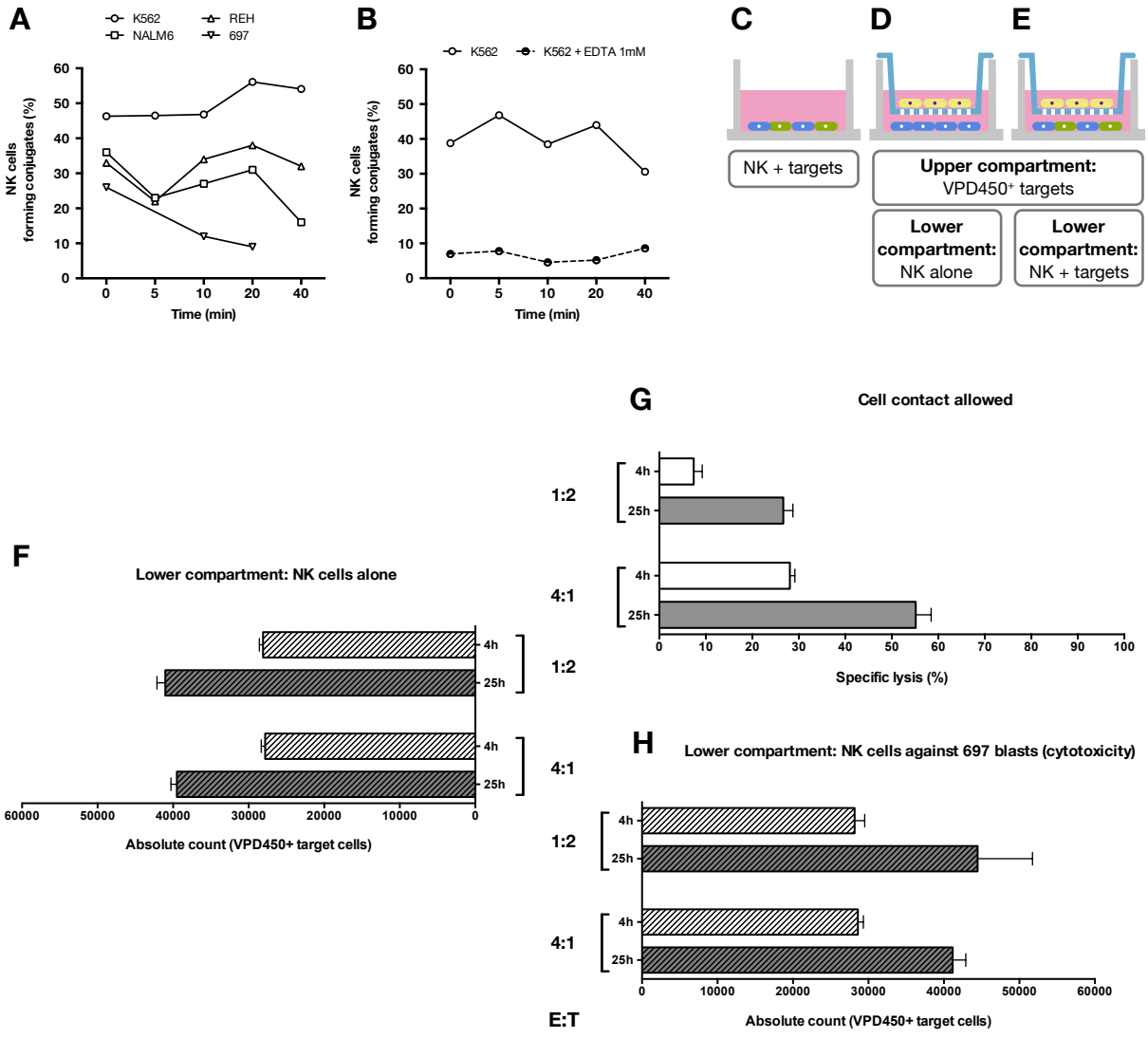

Figure 21. Killing initiation and effector phase are contact-dependent.

(**A** and **B**) Conjugate formation was measured within minutes following NK and target cells co-incubation. K562 (with - negative control - or without - positive control - EDTA 1mM), NALM6, REH and 697 cell lines were studied. NK and target cells were stained with PKH26 and CFSE respectively, and double positive conjugates were quantified by flow cytometry.

(**C**-**E**) Experimental conditions used for the transwell experiment. The lower compartment contained 30 x 10^3 NK cells (blue cells on the scheme) and blasts (green cells, **C** and **E**) according to the E:T ratio (15 x 10^3 and 120 x 10^3 targets for 1:2 and 4:1 ratios). The upper compartment contained a fixed number of 20 x 10^3 VPD450$^+$ blasts (yellow cells, **D** and **E**). 697 cell line was used as target.

(**F** - **H**) Cell contact between target and NK cells was either allowed (**G**, control) or prevented by a transwell membrane and the lower compartment seeded with NK cells alone or co-incubated with targets (**F** and **H**), corresponding to **C**, **D** and **E** respectively.

Shown are percentages of cytotoxicity (**G**) or VPD450$^+$ target cells absolute counts in the upper compartment (**F** and **H**), relative to cultures with no effector cells in co-cultures lasting 4 and 25h.

Representatives results shown are mean ± SD.

We then performed a transwell experiment choosing the 697 leukemic cell line which had shown the lower proportion of NK and target cells conjugates (**Figures 21**C-**21**E). When cell contact was prevented, blast killing was fully abrogated as shown by the absolute count of targets in the transwell upper compartment which remained unchanged in the presence of an increasing quantity of NK cells in the lower compartment, at 4h as well as 25h incubation times (**Figure 21**F). One assumption could have been that NK cells activation step was contact-dependent while the effector phase would have relied on a produced soluble factor such as cytokines. Therefore, we compared the absolute counts of targets in the upper compartment when the lower one was either seeded with NK cells only or with NK and target cells (i.e. an ongoing cytotoxicity). In both conditions, absolute counts were comparable at 4h and 25h incubation times (**Figures 21**F and **21**H), suggesting that no soluble factor could explain the late killing effect.

The precise cytotoxicity kinetics was explored to assess whether the killing increased at 25h was sudden or progressive over the course of the experiment. We designed a FCC assay with multiple time point readouts together with a quantification of apoptosis at 4h, 12h and 25h (**Figure 22**A).

Additionally, we used XVA143, an allosteric LFA-1 inhibitor (Shimaoka et al., 2003), to study the temporal impact of NK and target cells interaction. XVA143, which has been shown to be a potent modulator of NK cell function, is not only able to prevent cell aggregation but also to disaggregate existing clusters as well as to interfere with NK cell killing and activation (Weitz-Schmidt et al., 2009). We took advantage of these properties to interrupt effector and target cells interaction after various incubation times while assessing the delayed cytotoxicity (**Figure 22**A). When XVA143 was added to the culture following 3h incubation, killing was measured at the usual 4h and 25h time points corresponding to settings in which cells were allowed to interact 3h and then left together without further cell contact for 1h and 22h respectively. Proceeding this way, we addressed whether the late killing that we measured at 25h was resulting from an early signal received by NK cells during the co-culture or was requiring a permanent cell contact.

Real-time cytotoxicity assessment revealed a continuous, progressive and cumulative killing effect with a final plateau corresponding to a maximal effect (**Figure 22**B), together with a constant decrease in the target absolute counts over the 25h incubation (**Figure 22**C). Blasts were undergoing apoptosis with Annexin-V^+ 7-AAD^- cells (**Figure 22**D), suggesting that 4h classical cytotoxicity assay underestimated cells engaged in a cell-death process.

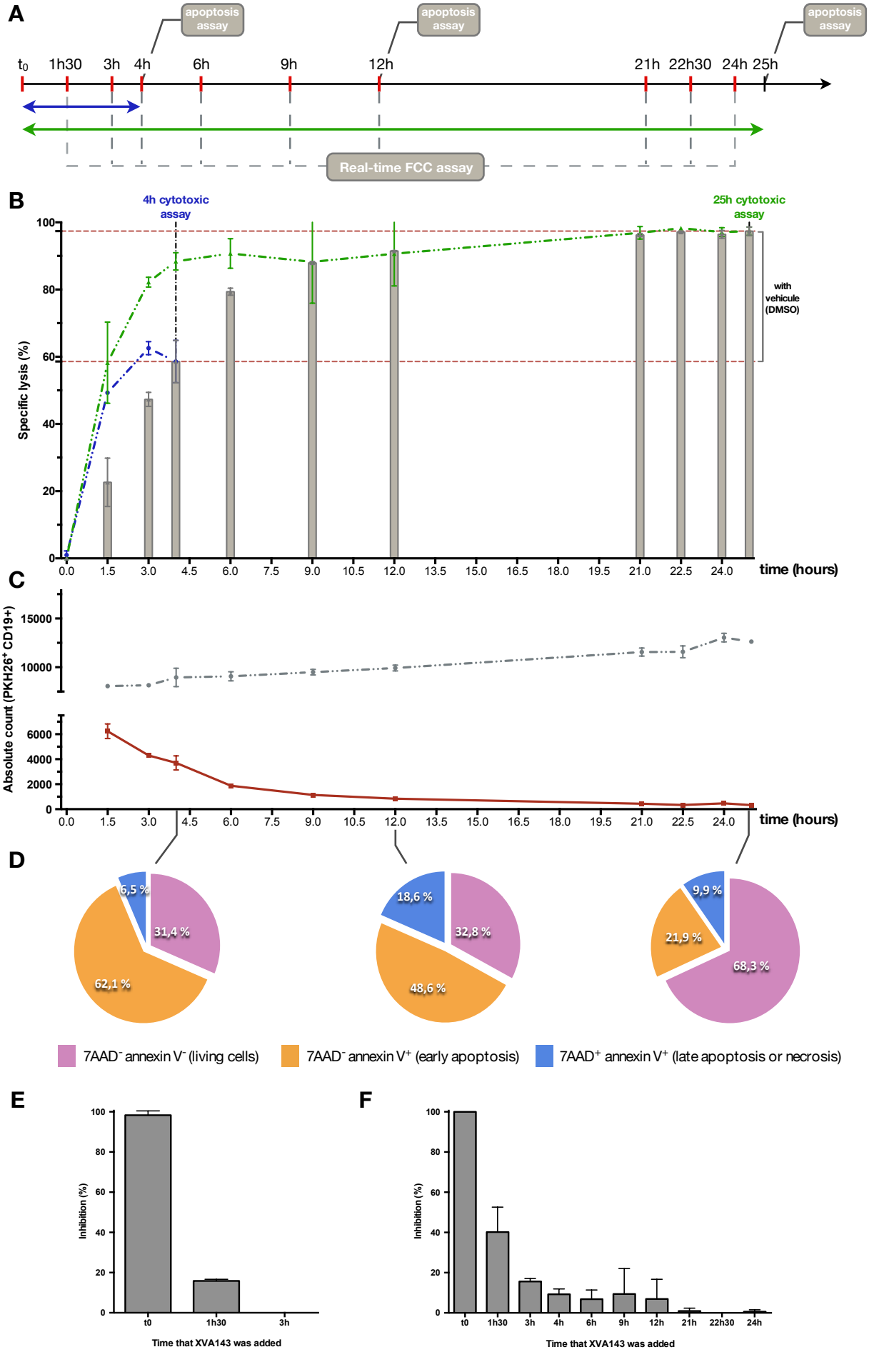

(legend on next page)

Cell adhesion inhibition with XVA143 fully abrogated short term as well as long term NK killing when the allosteric inhibitor was added at the beginning of the co-culture (**Figure 22**E and **22**F), confirming cell contact requirement. Interestingly, we observed that further adhesion inhibition following an initial cell contact was stopping the killing at its real-time value (once included the part of apoptotic cells engaged in the cell death process), suggesting that cell adhesion was required throughout the co-culture (**Figure 22**B-**22**F).
In summary, we established permanent cell contact requirement between NK and target cells for a progressive and cumulative killing.

3.2.2. A DEGRANULATION-INDEPENDENT MECHANISM

We then searched for evidence regarding the involvement of the degranulation pathway which is the main cytotoxic arm used by CD8 T cells and NK cells (Lieberman, 2016; Sun and Lanier, 2011). We observed that NK cells had a strongly reduced CD107a/b expression when co-cultivated with pre-B ALL in a 4h conventional degranulation assay: less than 10% cells were positive while more than 40% against K562, positive control (**Figures 23**A and **23**B). Previous reports demonstrated that the NK killing potential is not equally shared among effector cells with a minority of so-called serial killer cells responsible for a majority of the measured cytotoxicity (Choi and Mitchison, 2013; Vanherberghen et al., 2013). This led us to hypothesize that the small proportion of degranulating NK cells could still be responsible for the 25h killing, with the idea that a smaller fraction of effector cells could require more time to achieve the same effect. To confirm or rule out this hypothesis, we interfered with the degranulation pathway through different approaches: 1- cell surface blockade of known key receptors of this pathway; 2- target cells genetic modification to increase their resistance; and 3- use of effector cells from patients with selected immune deficiencies.

Figure 22. NK cell killing is cumulative and requires permanent cell adhesion.
(**A**) Experimental design. Red lines represent times that XVA143 was added to co-cultures. Blue and green arrows depict the two referential 4h and 25h incubations.
(**B**) Real-time killing measurements (gray bars; 4h and 25h incubation values are shown by red dashed lines as references). Blue and green dashed curves depict cytotoxicity values measured after 4h and 25h respectively (**A**) for each time point XVA143 was added.
(**C**) Evolution of target cell ($PKH26^+$ $CD19^+$) absolute counts (gray dashed line: control, i.e. targets alone; red line: targets with NK cells).
(**D**) Annexin-V staining assay was performed at 4h, 12h and 25h to precise cell death process.
(**E** and **F**) Histograms show the killing inhibition of the 4h and 25h cytotoxicity (respectively **E** and **F**) achieved by XVA143 addition at different time points.
Representative results of one experiment shown are mean ± SD against REH cell line and 4:1 effector to target ratio.

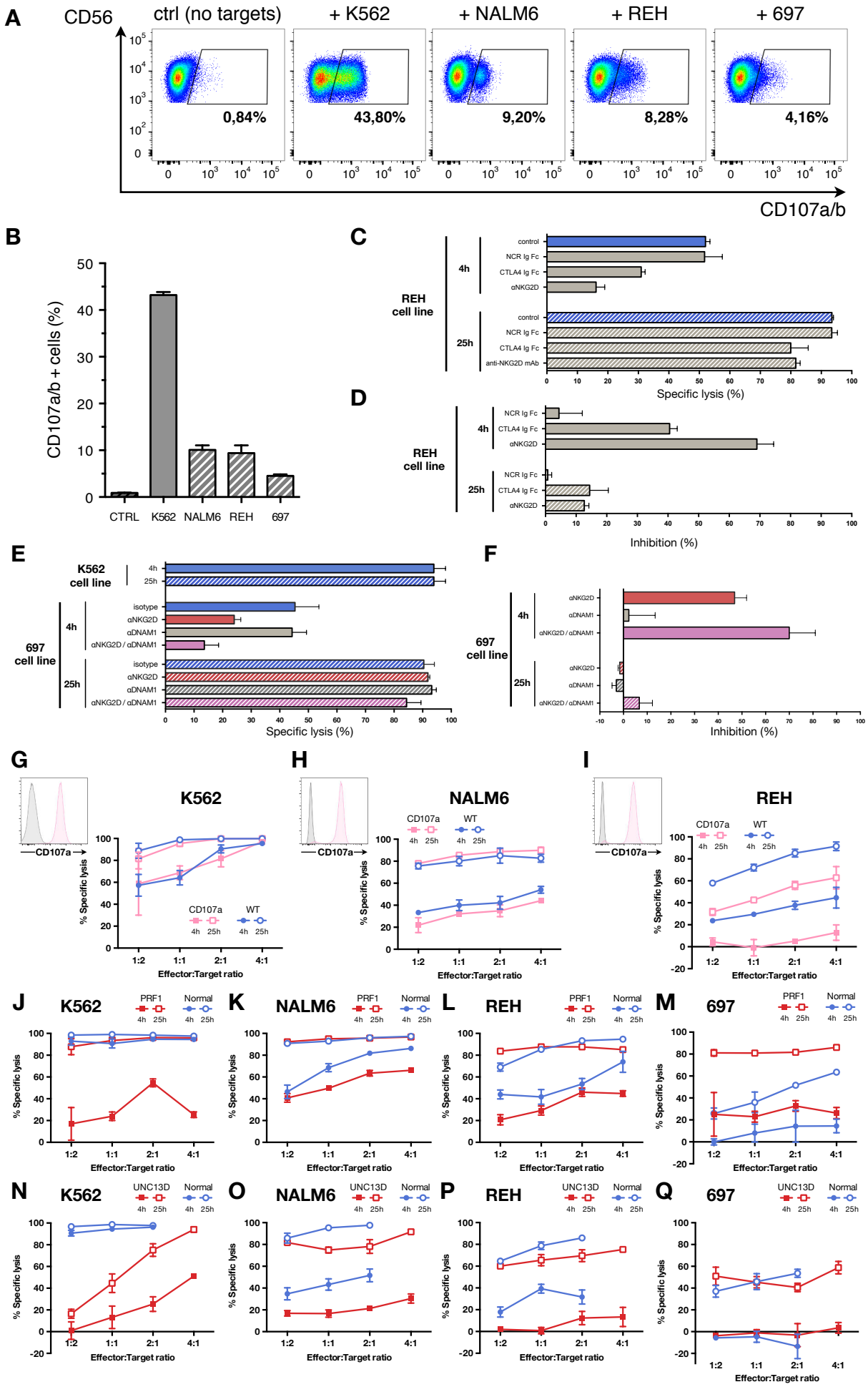

(legend on next page)

Among surface receptors, NKG2D and DNAM-1 have been shown to be crucial to trigger NK cells degranulation through the signaling-competent adaptor DNAX-activating protein 10 (DAP10) (Billadeau et al., 2003) although signals from co-activating receptors are necessary too (Bryceson et al., 2009; Lanier, 2005; Long et al., 2013). Thus, as a prototypic model, deficiency in the *MAGT1* gene causing XMEN disease with altered cell surface NKG2D expression among patient T and NK cells is associated with a defective degranulation (Chaigne-Delalande et al., 2013). We assessed this triggering pathway by interfering with NKG2D and NCRs (NKp30, NKp44, NKp46 and NKp80) engagement using blocking antibody or Fc chimera proteins respectively (**Figures 23**C and **23**D). Interestingly, we observed a biphasic response with a strong inhibition (~70%) of the 4h killing when NKG2D receptor was blocked, and almost no inhibition of the 25h killing. This observation was further confirmed by NKG2D and DNAM-1 co-blockade (**Figures 23**E and **23**F), suggesting that at least two mechanisms could have been engaged, the early one relying more on degranulation than the latter one.

Cell surface expression of CD107a (LAMP1) by NK cells has been shown to protect effector cells from self-killing (Cohnen et al., 2013). Therefore, we transduced ALL target cells with the same sCD107a (the cytoplasmic domain was truncated by removing the cytoplasmic motif implicated in lysosomal targeting of newly synthesized molecules; the construction was kindly provided by Pr. Carsten Watzl (IfADo, Leibniz, Germany)).

Figure 23. NK cell killing is independent of the perforin and degranulation pathway.
(**A**) Dot plots show CD107a/CD107b surface expression on NK cells left alone or exposed for 4h to K562 (positive control), NALM6, REH and 697 cell lines (**A**).
(**B**) The graph depicts frequencies of NK cell subsets positive for CD107a/CD107b (related to **A**).
(**C** and **D**) Effect of the NCRs (NKp30, NKp44, NKp46 and NKp80) or NKG2D blockade was evaluated on the cytotoxicity against REH cell line, at 4h and 25h (**C**). The corresponding percentage of inhibition was calculated (**D**).
(**E** and **F**) Effect of the blockade of NKG2D and DNAM-1 alone or in combination was evaluated on the cytotoxicity against 697 cell line, at 4h and 25h (**E**). The corresponding percentage of inhibition was calculated (**F**).
(**G**-**I**) Graphs showing early and late leukemic killing of K562, NALM6 and REH cell lines either unmodified or transduced with sCD107a. Shown are percentages of cytotoxicity (relative to cultures with no effector cells) in cocultures lasting 4 and 25h. Overlays showing sCD107a expression on transduced targets are also shown.
(**J**-**M**) Graphs showing early and late leukemic killing of K562, NALM6, REH and 697 cell lines using NK cells from a normal donor or a PRF1 deficient patient. Shown are percentages of cytotoxicity (relative to cultures with no effector cells) in cocultures lasting 4 and 25h. Two patients were tested with the same results.
(**N**-**Q**) Graphs showing early and late leukemic killing of K562, NALM6, REH and 697 cell lines using NK cells from a normal donor or a UNC13D deficient patient. Shown are percentages of cytotoxicity (relative to cultures with no effector cells) in cocultures lasting 4 and 25h. Two patients were tested with the same results.
(**A**-**Q**) Shown are mean ± SD.

When used as targets in a FCC assay, sCD107a expressing blasts were killed as efficiently as untransduced cells (**Figures 23**G and **23**H, see NALM6 cell line), or if an early inhibition was detected following a 4h incubation, it didn't prevent the 25h increase in killing (**Figure 23**I, see REH cell line). In line with the CD107a/CD107b assay and blocking experiments, these observations suggest that degranulation is not the main cytotoxic pathway involved in the observed 25h killing.

Cytotoxic lymphocytes granule exocytosis has been extensively studied and well characterized (de Saint Basile et al., 2010). Since we wanted to address decisively this key feature, we took advantage of the access to patients suffering from primary immunodeficiencies (PIDs) with genetically defined mutations causing degranulation or perforin expression defects. Genetic defects in granule biogenesis, content, transport and delivery have been well described (de Saint Basile et al., 2010). Perforin (encoded by the *PRF1* gene) is a crucial protein contained in the granules and released after targets cells recognition (Voskoboinik et al., 2015) while MUNC13-4 (encoded by the *UNC13D* gene) is critically involved in granule docking and fusion (de Saint Basile et al., 2010). Familial hemophagocytic lymphohistiocytosis (FHL) type 2 and type 3 are caused by PRF1 and UNC13D deficiency respectively. Affected patients present with severe defects in the granule exocytosis (Feldmann et al., 2003; Stepp et al., 1999) and life-threatening HLH.

We amplified NK cells from PRF1 and UNC13D deficient patients and used them in a FCC assay against K562, NALM6, REH and 697 cell lines with 4h and 25h co-incubations. As expected, FHL patients exhibited a severe defect in K562 killing in a conventional 4h assay, compared to a normal donor (**Figures 23**J and **23**N). Defect was also noticed against pre-B ALL blasts although more importantly with FHL3 NK cells (**Figures 23**K-**23**M and **23**O-**23**Q). However, all FHL patient NK cells showed a strong increase against all tested targets after 25h incubation (**Figures 23**J-**23**Q), ruling out the possibility that the delayed detected cytotoxic effect was dependent on granule exocytosis.

Thus, taking together, our results demonstrate that NK cells can induce target cells to die through a late mechanism which is independent of the degranulation pathway.

3.2.3. APOPTOSIS-LIKE CELL DEATH OF THE TARGET CELLS

To gain further insight into the mechanism used by NK cells to kill targets over a prolonged incubation, we performed an annexin-V staining after 4h, 10h and 25h incubation with effector cells, postulating that distinction between apoptotic and necrotic like cell deaths would orientate our working hypothesis.

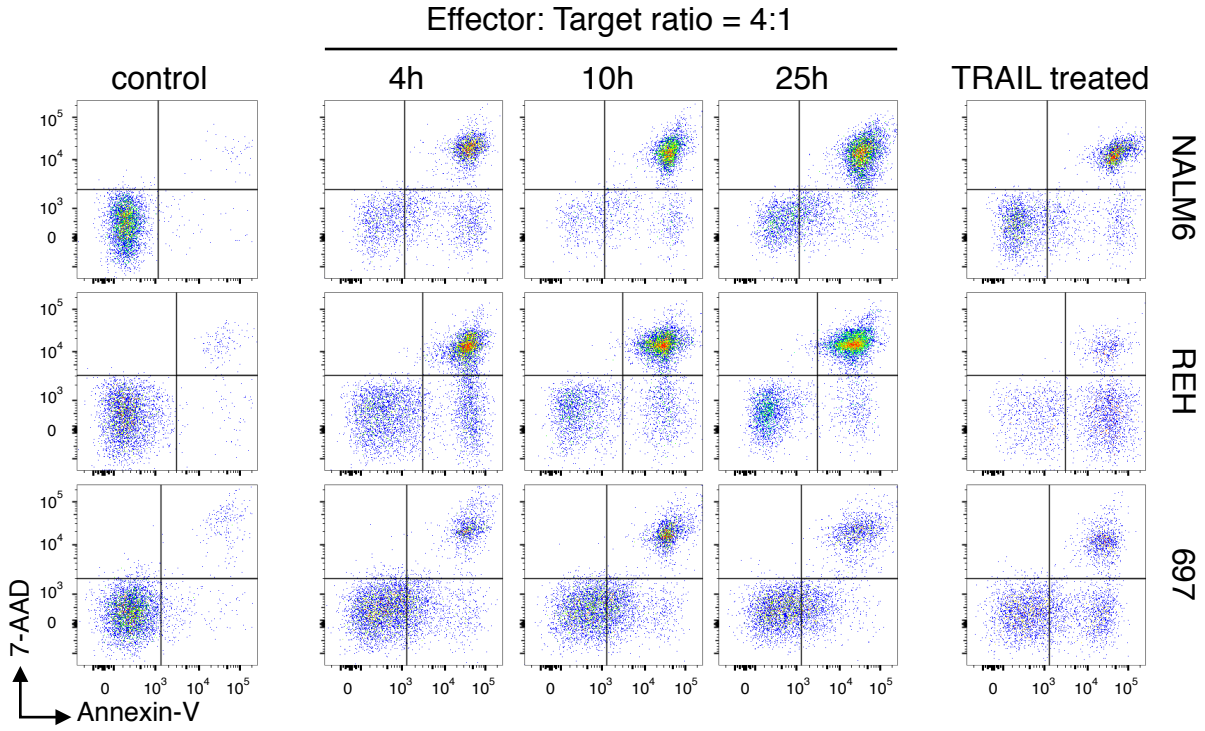

Figure 24. Apoptotic-like flow cytometry profile of pre-B ALL cells.
Representative dot plots show target cells annexin-V / 7-ADD co-staining following 4h, 10h and 25h incubation with NK cells (4:1 effector to target ratio). Soluble human recombinant SuperKillerTRAIL (250 ng/mL; Enzo Life Sciences) was used as positive control.

Results showed an apoptotic-like induced cell death among pre-B ALL targets with annexin-V$^+$ 7-AAD$^-$ single positive cells (early apoptotic-like) preceding annexin-V$^+$ 7-AAD$^+$ double positive cells (late apoptotic-like) (**Figure 24**). Apoptosis is a form of programmed cell suicide linked to the activation of the cysteine-dependent aspartate-driven proteases (caspases), which cleave key intracellular substrates to promote cell death (Green, 2011; Taylor et al., 2008). Apoptosis is controlled in mammals through two major cellular signaling pathways, namely the intrinsic and the extrinsic pathways. The former relies on mitochondria while the latter is associated to the transmission of signals from extracellular death ligands. However, both pathways often act directly and/or indirectly to reinforce one another (Ashkenazi and Salvesen, 2014). Caspase proteins are highly regulated from the moment of their synthesis. They are produced in zymogen form lacking protease activity (Parrish et al., 2013). Intrinsic and extrinsic apoptotic pathways relie on distinct initiator caspases whose activation will then trigger effector caspases through a cascade-like proteolytic stimulation.

We found evidence for pan-caspase activation among pre-B ALL cells which were harboring apoptotic-like features (**Figures 25**A and **25**B). A detailed study of initiator (caspases 8, 9 and 10) and executioner (caspases 3 and 7) caspases revealed a global activation profile (**Figure 25**C) as well as mitochondrial depolarization assessed by a JC-1 staining (**Figure 25**D), compatible with concomitant activation of both apoptotic cellular signaling pathways.

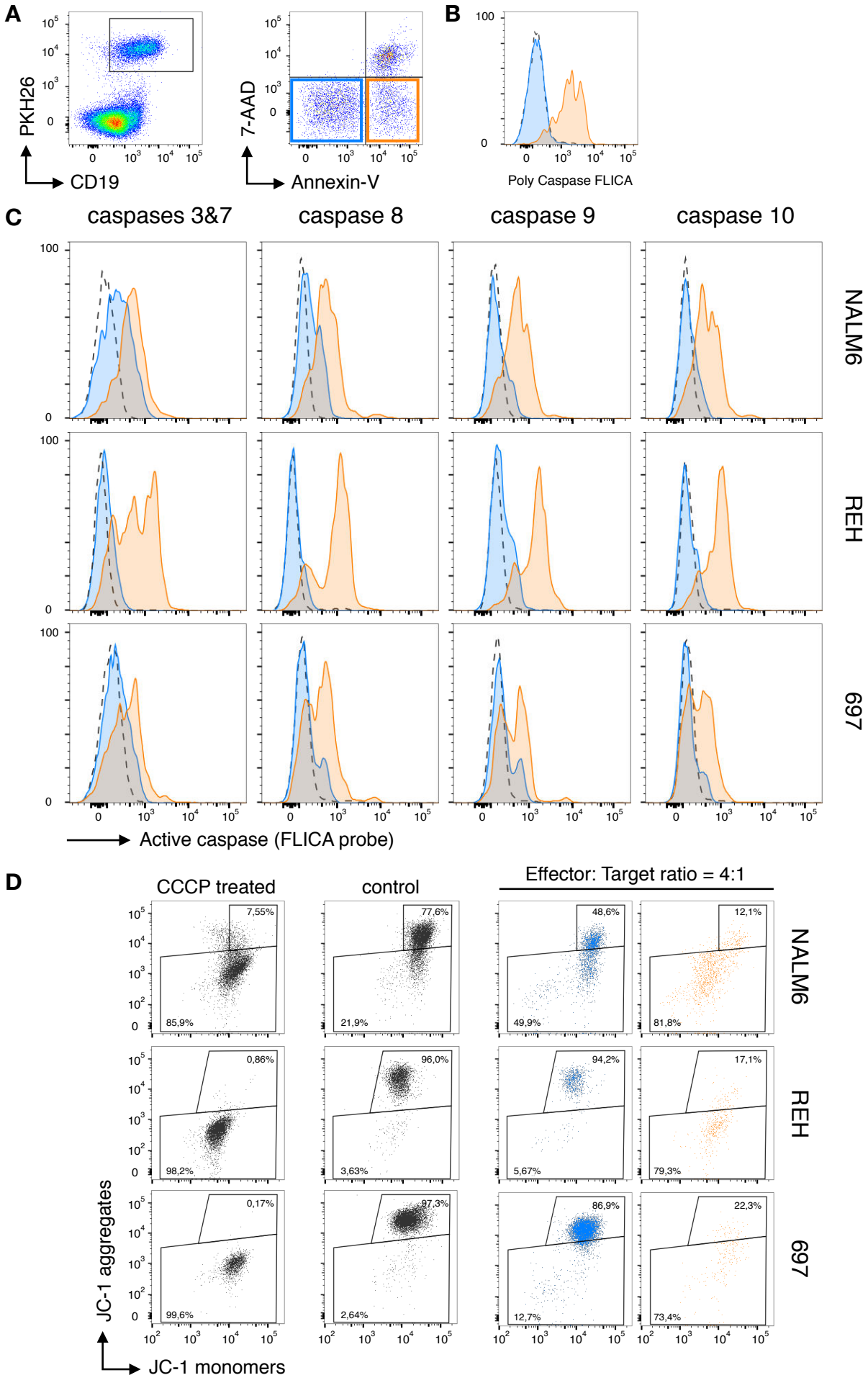

(legend on next page)

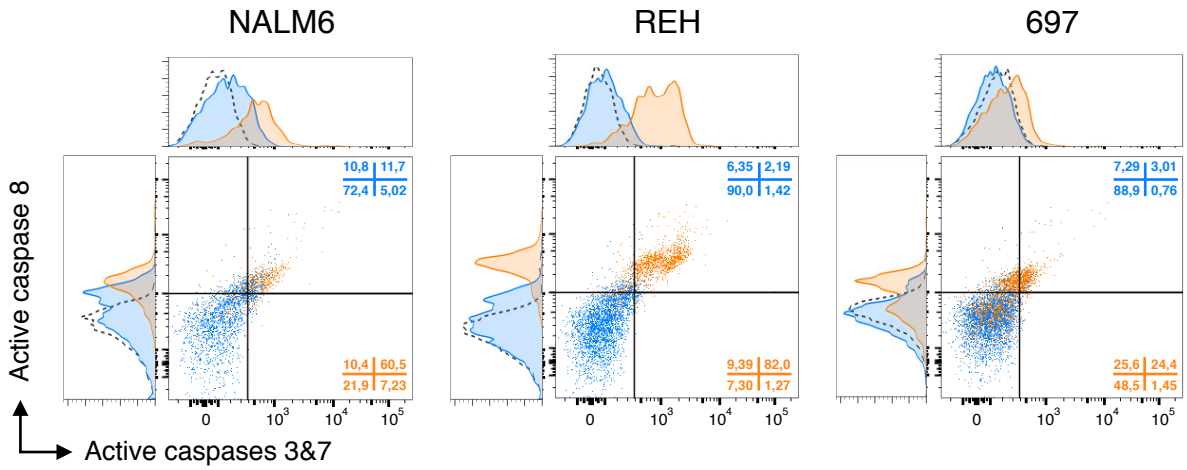

Figure 26. Hierarchical ordering of the activation of the apoptotic extrinsic pathway.
Representative dot plots show target cells active caspase 8 / caspases 3&7 co-staining (FLICA) following incubation with NK cells (4:1 effector to target ratio). Blue and orange histograms depict living and early apoptotic cells respectively (**Figure 25**A). NALM6, REH and 697 cell lines were used as targets. Observations were the same following 4h, 10h and 25h incubation.

Active caspases 8 and 10 are reminiscent of the involvement of the extrinsic apoptotic pathway but can also be a late consequence in the hierarchical ordering of caspases activation following engagement of the intrinsic pathway (Inoue et al., 2009; Slee et al., 1999). Because the study of caspases activity was compatible with activation of both apoptotic cellular signaling pathways (**Figure 25**C), we performed a caspase 8 vs caspases 3&7 co-staining by flow cytometry to further characterize the ordering in their activation. We didn't highlight a clear active caspase 8, unactive caspases 3&7 population (**Figure 26**) but our results could suggest activation of the extrinsic pathway considering that the profile was similar to the one induced by the SuperKillerTRAIL positive control (data not shown).

Thus, these results suggest that NK cells trigger an apoptotic-like cell death among pre-B ALL targets with poly-caspase activation and mitochondrial depolarization.

Figure 25. Apoptotic pre-B ALL cells activate both intrinsic and extrinsic pathways.
(**A**) Representative dot plots show target cells annexin-V / 7-ADD co-staining among pre-B ALL targets ($PKH26^+$ $CD19^+$). Blue and orange rectangles depict living and early apoptotic cells respectively: these two colors are used to define these two same populations in the other panels (**B**-**D**) and **Figure 26**.
(**B**) Representative overlay histogram of poly-caspase activity (FLICA). Gray dashed line histogram show the target cells alone control condition.
(**C**) Representative overlay histograms of caspases 3&7, 8, 9 and 10 activities (FLICA). Gray dashed line histogram show the target cells alone control condition. Gray dashed line histogram show the target cells alone control condition.
(**D**) The ratiometric ΔΨm indicator JC-1 was used to evaluate mitochondrial outer membrane permeabilization (MOMP). CCCP treatment was used as positive control.
Representative results against NALM6, REH and 697 cell lines and 4:1 effector to target ratio are shown. Observations were the same following 4h, 10h and 25h incubation.

3.2.4. A DEATH RECEPTOR PATHWAY-INDEPENDENT MECHANISM

At this point, we established that our killing mechanism was contact-dependent, did not rely on granule exocytosis and induced an apoptotic-like cell death with caspases and mitochondria alterations. Consequently, we next aimed to study whether death receptor pathway could be involved.

$CD8^+$ T cells and NK cells are known to express several death ligands including FASL and TRAIL which can trigger target cells apoptosis through death receptors engagement (Ashkenazi and Salvesen, 2014; Guicciardi and Gores, 2009; Martínez-Lostao et al., 2015; Russell and Ley, 2002). Besides, induced cell death through this pathway can take from 12h to 24h (Jedema, 2004), substantially longer than perforin and granzymes induced cell death which typically occurs within minutes following contact between effector and target cells (Jedema, 2004; Lopez et al., 2013; Voskoboinik et al., 2015; Vrazo et al., 2015).

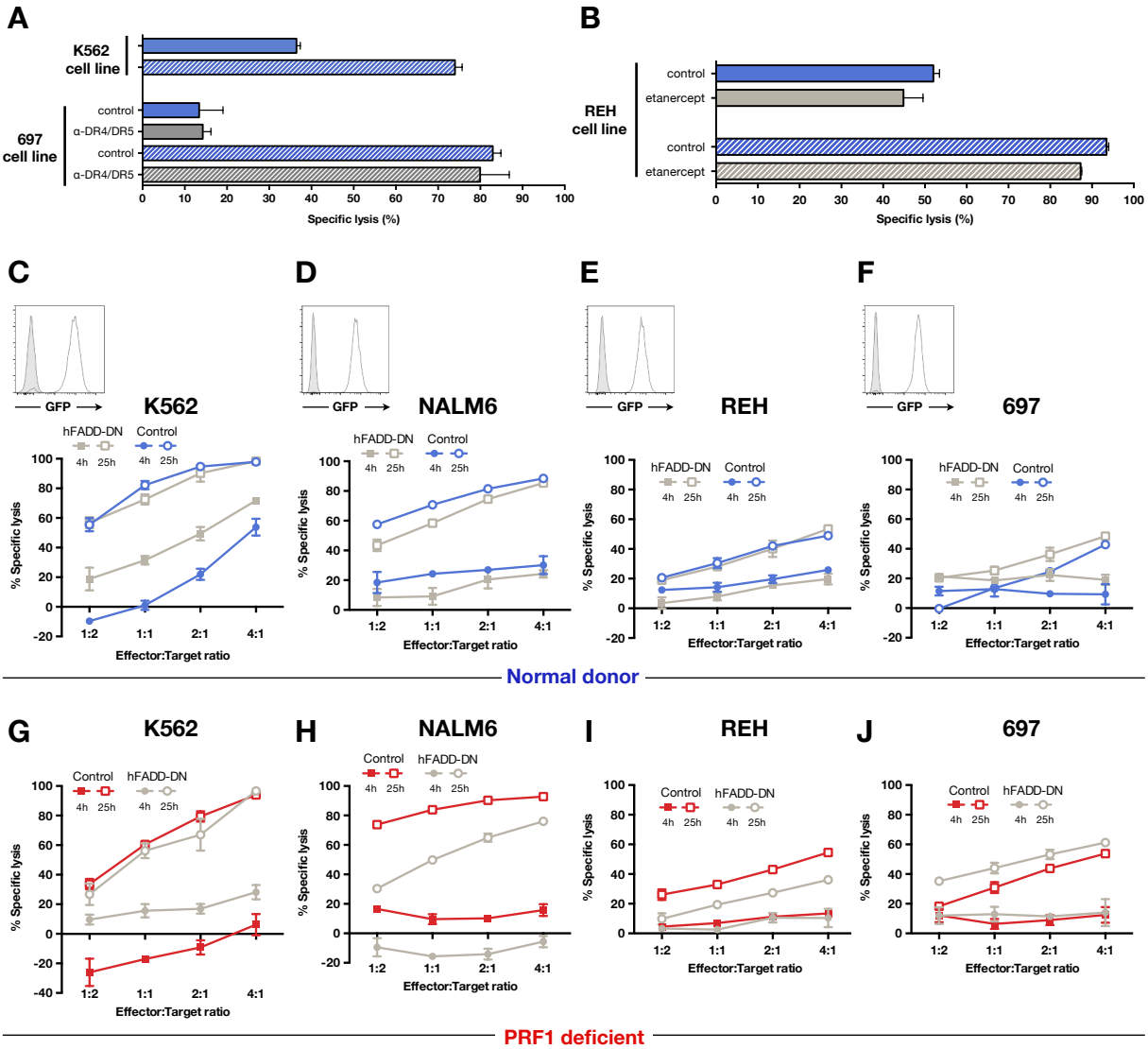

(legend on next page)

We first evaluated the expression of FAS, DR4 (TRAIL-R1) and DR5 (TRAIL-R2) death receptors on pre-B ALL cell lines by flow cytometry (**Figures S2**A-**S2**C). We observed that each one showed a weak expression of FAS and a variable expression of DR4 and/or DR5, prompting us to test cell lines sensitivity to FASL and TRAIL mediated apoptosis. APO-1 and SuperKillerTRAIL treatments respectively revealed a resistance to FASL and a strong sensitivity to TRAIL mediated apoptosis among the three pre-B cell lines (**Figures S2**D-**S2**G).

Based on these observations, we tried to block DR4 and DR5 on ALL cell lines targets. Indeed, these two receptors mediate TRAIL induced death signals while the other TRAIL receptors are considered as nondeath ones (Guicciardi and Gores, 2009; Walczak, 2013). We observed no inhibition of the NK killing when blocking antibodies against DR4 and DR5 were added to the assay (**Figure 27**A) while these blocking antibodies could significantly inhibit TRAIL-induced ALL cell death. Since TNFα can also induce leukemic cells apoptosis (Schimmer et al., 2001), we decided to block membrane bound TNFα, which is expressed and used by NK cells to induce target cells death (Caron et al., 1999). Contrary to infliximab, etanercept does not induce reverse signaling and apoptosis of effector cells (Horiuchi et al., 2010; Mitoma et al., 2008). Therefore, we decided to use etanercept to block membrane bound TNFα. Although we could not set up a control condition demonstrating the efficacy of our blocking experiment, no inhibition of the NK killing was noticed when etanercept was added during the experiment (**Figure 27**B). Although our pre-B cell lines were not sensitive *in vitro* to APO-1 mediated apoptosis (**Figures S2**D and **S2**E), we decided to use a broader and more reliable strategy to inhibit death receptor mediated death.

Figure 27. Pre-B ALL cell killing is independent of the death receptor pathway.

(**A**) Effect of the TRAIL receptors (DR4 and DR5) blockade was evaluated on the cytotoxicity against 697 cell line following 4h and 25h incubation. K562 cell line was used as a positive control.

(**B**) Effect of etanercept pre-treatment was evaluated on the cytotoxicity against REH cell line following 4h and 25h incubation.

(**C**-**F**) Graphs showing early and late leukemic killing of K562, NALM6, REH and 697 cell lines (control or hFADD-DN transduced) using NK cells from a normal donor. Shown are percentages of cytotoxicity (relative to cultures with no effector cells) in cocultures lasting 4 and 25h. Results are representative of three different donors. Overlays showing GFP expression on sorted targets transduced with the hFADD-DN IRES GFP transgene are also shown (unstransduced controls are depicted in gray).

(**G**-**J**) Graphs showing early and late leukemic killing of K562, NALM6, REH and 697 cell lines (control or hFADD-DN transduced) using NK cells from a perforin deficient patient. Shown are percentages of cytotoxicity (relative to cultures with no effector cells) in cocultures lasting 4 and 25h.

(**A**-**J**) Shown are mean ± SD.

To do so, we genetically modified target cells to make them resistant to death receptor apoptotic signaling. FADD and TRADD are two keys death receptor signal transducers, the former being associated with cell death signalling whereas the latter is linked to cell proliferation and survival (Strasser et al., 2011; Wilson et al., 2009). Also, when TRADD is involved in death signaling, it has been described to involve FADD (Strasser et al., 2011; Wilson et al., 2009). We transduced pre-B ALL cells with a dominant-negative FADD to induce stable resistance (Wajant et al., 1998) (**Appendix 12** modified from LMBP #4627 plasmid, BCCM, and **Figure S2**H). As expected and as a control of our strategy, FADD-DN expressing target cells became resistant to TRAIL mediated apoptosis (**Figure S2**H). However, they remained efficiently killed by NK cells in a long-term FCC assay (**Figures 27**C-**27**F), suggesting that cytotoxicity was independent of the death receptor pathway.

To definitely prove that our mechanism was distinct from the two main described contact-dependent killing pathways and was not partially caused by each of them, we amplified NK cells from a PRF1 deficient patient and used them in a 4h and 25h FCC assay against K562, NALM6, REH and 697 cell lines transduced with a control GFP or hFADD-DN IRES GFP vector (**Appendices 11** and **12**). As previously observed (**Figures 23**J-**23**N), perforin-deficient NK cells exhibited a severe killing defect in a conventional 4h assay against K562, compared to a normal donor (**Figures 27**G-**27**J). However, perforin-deficient NK cells showed an increased cytotoxicity against all tested ALL targets after 25h incubation, which was comparable to the increased cytotoxicity observed with normal donor cells (**Figures 27**G-**27**J). Thus, we demonstrated in a same assay that NK cells which couldn't efficiently engage the granule exocytosis cytotoxic pathway were able to kill target cells rendered resistant to death receptor induced cell death, ruling out the possibility that our mechanism was dependent, even partially, on any of them.

3.2.5. MINIMAL MOLECULAR REQUIREMENTS AMONG EFFECTOR CELLS

Our results tend to demonstrate that NK cells can kill ALL target cells through an unconventional contact-dependent pathway. To gain insight into both molecular control of this pathway by NK cells as well as the sequence of events inducing target cell death, we used a complementary approach studying either NK cells from patients suffering from molecularly characterized primary immunodeficiencies which could affect effector cells function, or genetically modified target cells whose we altered key molecular nodes. Of note, isolated NK cells deficiencies have not been reported so far (Fischer and Rausell, 2016) meaning that other immune cell subsets are also affected among these patients.

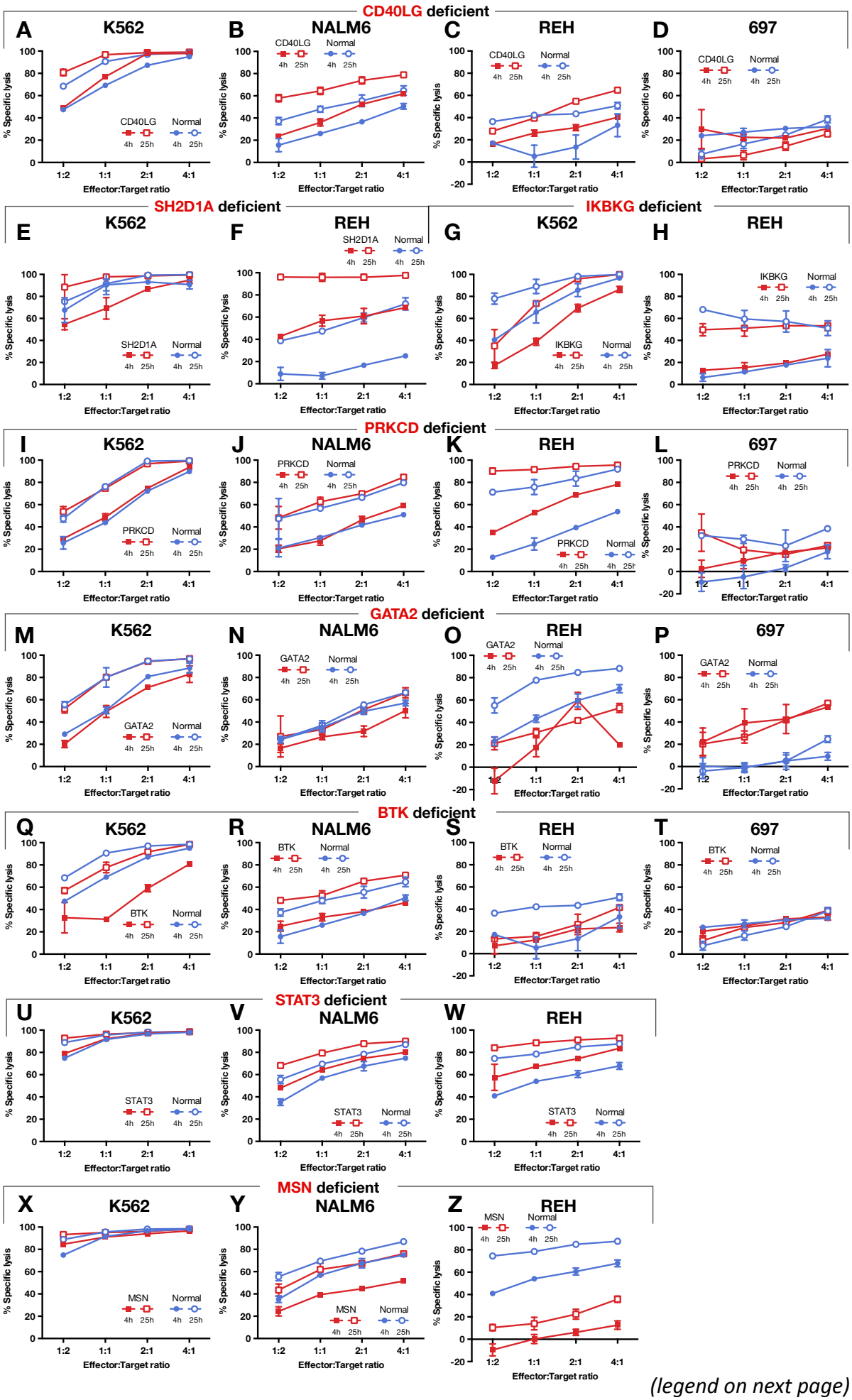

(legend on next page)

Using PIDs as a screening platform, we decided to select molecular defects which were described to impact NK cell cytotoxicity (**Table 6**). Some NK deficiencies were described to be (sometimes partially) rescued by IL-2: because we were using an activation and expansion system with exogenous rhIL-2, these ones were excluded.

Table 6. Tested genetic defects with published NK cell deficiency.

Genetic defect	Disorder	Selected references of interest (relevant for NK cell cytotoxicity deficiency)
UNC13D	Type 3 familial hemophagocytic lymphohistiocytosis (FHL3)	Bryceson et al., 2012; de Saint Basile et al., 2010; Feldmann et al., 2003; Marcenaro et al., 2006
PRF1	Type 2 familial hemophagocytic lymphohistiocytosis (FHL2)	Bryceson et al., 2012; de Saint Basile et al., 2010; Marcenaro et al., 2006; Stepp et al., 1999
CD40LG	X-linked immunodeficiency with hyper-IgM (XHIGM)	Carbone et al., 1997
SH2D1A	X-linked lymphoproliferative disease, Purtilo syndrome (XLP1)	Benoit et al., 2000; Kwon et al., 2016; Parolini et al., 2000
IKBKG	NEMO deficiency syndrome	Kwon et al., 2016; Orange et al., 2002; Pannicke et al., 2013
PRKCD	Protein kinase C δ deficiency	Kuehn et al., 2013
GATA2	GATA2 haplo-insufficiency	Mace et al., 2013
BTK	X-linked agammaglobulinemia	Bao et al., 2012
STAT3	Hyper-IgE syndrome (HIES), Job-Buckley syndrome	Zhu et al., 2014
MSN	X-linked moesin-associated immunodeficiency (X-MAID)	Lagresle-Peyrou et al., 2016

Following reviews are of particular interest for PIDs with NK cell deficiency: Ham and Billadeau, 2014; Orange, 2012; 2013.

Our previous results showed that the three used pre-B ALL cell lines were not equally sensitive to NK mediated killing, with 697 being the more resistant (with inter-individual variability) while NALM6 and REH are more constantly killed (**Figure 19**B). Besides, relative contribution to the various cytotoxic pathways (granule exocytosis, death receptors and our unconventional pathway, although minor in the late killing for the first two (**Figures 23** and **27**)) differed. Depending on the samples, we sometimes had limited number of NK cells so that we decided, when limited, to privilege K562 (positive control) and REH cell lines before NALM6 and then 697 in FCC assays. Based on these observations, REH was a good candidate to further characterize our pathway.

Figure 28. NK cell mediated cytotoxicity towards pre-B ALL targets: PIDs' screening.
Representative graphs showing early and late leukemic killing by NKAES-NK cells. Shown are percentages of cytotoxicity (relative to cultures with no effector cells) in cocultures lasting 4 and 25h (mean ± SD). NK cells were amplified from CD40L (**A**-**D**), SH2D1A (**E** and **F**), NFκB (**G** and **H**), PKCδ (**I**-**L**), GATA2 (**M**-**P**), BTK (**Q**-**T**), STAT3 (**U**-**W**) and MSN (**X**-**Z**) deficient patients and tested against K562, NALM6, REH and/or 697 cell lines.
Control normal donors and patients are respectively displayed in blue and in red.

Some of the genetic defects were also of interest because previous works suggested altered NK cell response to B-EBV lymphoblastoid cell lines (**Table 6**). We postulated these cells to be a relevant model with shared ontogeny with pre-B cells and because we also observed an increase in B-EBV LCL killing by NK cells following a 25h incubation (data not shown).

None of the tested molecular defect exhibited a constant inhibition in the late killing of pre-B ALL cell lines (**Figure 28**), with the notable exception of moesin (MSN) deficient NK cells. Moesin is a member of the ezrin-radixin-moesin (ERM) family of proteins that are important for organizing membrane domains and receptor signaling. For example, CD43 removal at the T cell immune synapse has been shown to be regulated by moesin (Delon et al., 2001), while CD43 could be an activating receptor in NK cells (McCann et al., 2003; Nieto et al., 1999). Moesin is expressed in resting and activated NK cells (Ramoni et al., 2002; Schmidt et al., 2008). MSN deficient patients have low circulating NK count (Lagresle-Peyrou et al., 2016), which made our expansion system crucial to assess their cytotoxic function. NK cells from a MSN deficient showed impaired killing of the REH ALL cell line compared to a normal donor (**Figure 28**Z), which could suggest an actin-dependent receptor clustering (Orange, 2008) at an activating immune synapse (McCann et al., 2003) although more patients should be tested.

In addition to the exclusion of the granule exocytosis contribution, we concluded from these experiments that NK activation and effector response to leukemic blasts was independent of the SLAM family receptors, CD40L, NFκB, STAT3, BTK or PKCδ mediated signaling, nor required GATA2 protein.

3.2.6. MINIMAL MOLECULAR REQUIREMENTS AMONG TARGET CELLS

We then focused on trying to characterize the induced cell death mechanism among ALL target cells. A better understanding of the molecular events leading to pre-B ALL death would also help elucidating NK cell effector mechanism.

We previously discussed that NK cells trigger an apoptotic-like cell death among pre-B ALL targets with poly-caspase activation and mitochondrial depolarization (**Figures 25**C and **25**D). Using CRISPR/Cas9 generated KO, we assessed the pre-B ALL target cell killing by NK cells by knocking out key selected genes: caspase 9 KO to interfere with the intrinsic apoptotic pathway; BAX/BAK double KO (DKO) to block mitochondrial depolarization; caspases 8 and 10 DKO to inhibit the extrinsic apoptotic pathway; and caspases 3 and 7 DKO to block effector caspase activation. Again, we initially focused on REH cell line.

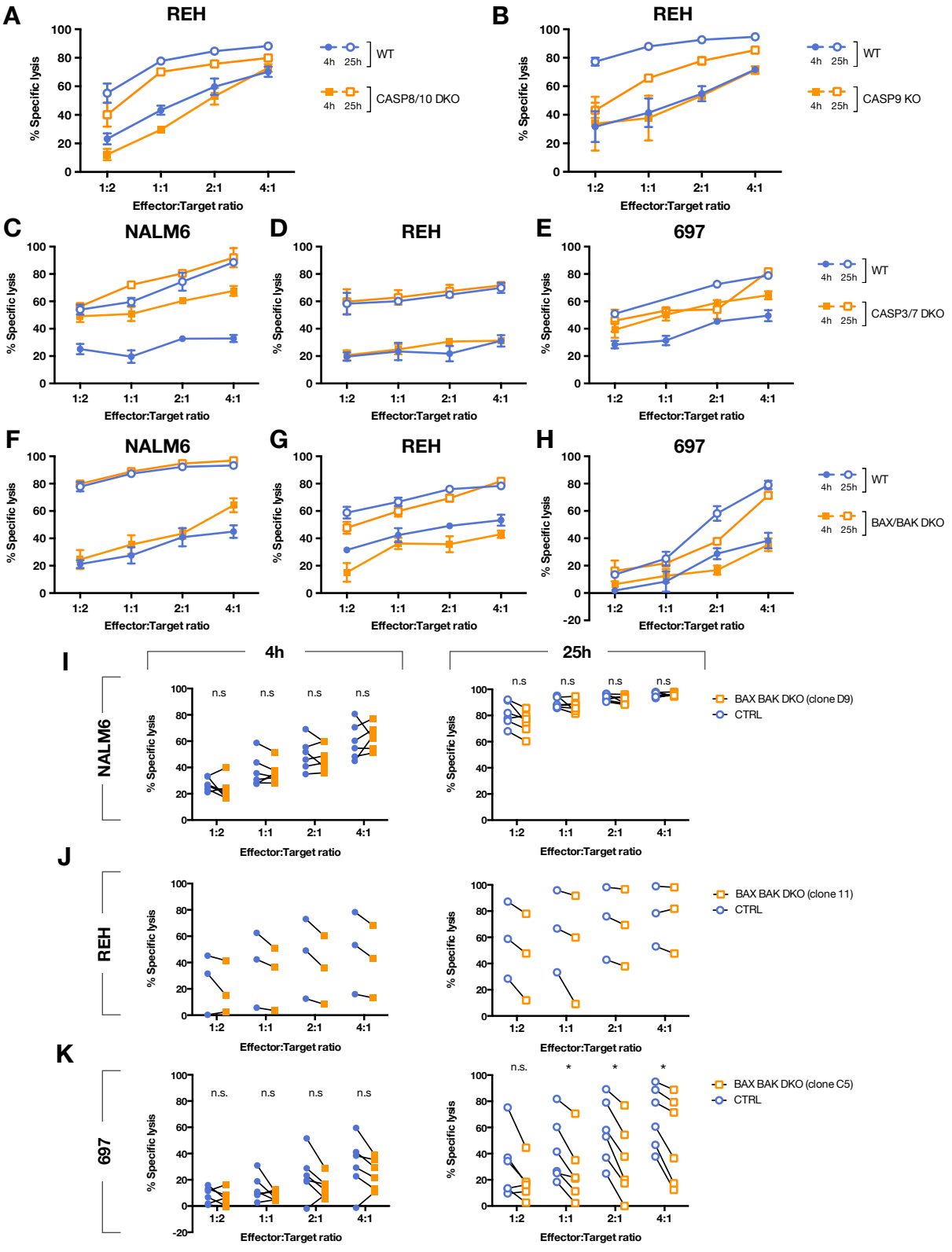

Figure 29. Active caspases and mitochondrial depolarization in pre-B ALL cell death are not mandatory for NK cell induced killing.

Representative graphs showing early and late leukemic killing by NKAES-NK cells. Shown are percentages of cytotoxicity (relative to cultures with no effector cells) in cocultures lasting 4 and 25h (mean ± SD). Caspases 8 and 10 DKO (**A**), caspase 9 KO (**B**), caspases 3 and 7 DKO (**C**-**E**, 3 tested donors) and BAX BAK DKO (**F**-**H**) NALM6, REH and/or 697 cell lines (or control sgRNA cell lines) were used as targets.

(legend continued on next page)

Although resistant to SuperKillerTRAIL induced apoptosis (data not shown), caspases 8 and 10 DKO blasts were killed as efficiently as control cells (**Figure 29**A), thus confirming results we obtained with hFADD-DN transduced targets (**Figures 29**C-**29**J) and ruling out death receptor pathway.

Interestingly, caspase 9 KO ALL target killing was not affected following 4h incubation but displayed a lower cytotoxicity at 25h (**Figure 29**B), suggesting that mitochondria could amplify the death signaling.

We assessed the role of mitochondrial depolarization with BAX/BAK DKO cells. Upon SuperKillerTRAIL treatment or in presence of effector cells, these ALL target cells did not depolarize anymore (data not shown) although they were still killed by NK cells as efficiently as control pre-B ALL cells (**Figures 29**F-**29**K). Of note, a notable exception was observed with 697 cell line: following 25h incubation, DKO targets killing was significantly reduced, showing that, albeit MOMP was not a strict requirement to cell death it instead tended to accelerate it to some extent (**Figure 29**K).

Apoptosis is defined as a programmed cell death with several possible caspase activation routes but irrespectively, these pathways lead to activation of the major effector caspases, i.e. caspase 3, caspase 6 and caspase 7 (Taylor et al., 2008). Caspase 6 is cleaved by caspases 3 and 7 but can also undergo self-activation in some settings (Inoue et al., 2009; Parrish et al., 2013).

Caspases 3 and 7 DKO cells have deep defects in their ability and kinetics to apoptosis (Lakhani et al., 2006): we studied cell death among these targets co—incubated with NK cells. Strikingly, caspases 3 and 7 DKO pre-B ALL targets were killed by NK cells as efficiently as their control counterparts, demonstrating that these terminal effector proteases were not required for late NK killing (**Figures 29**C-**29**E).

Taken together, our results showed that NK cells induced pre-B ALL cell death with detectable poly caspase activation and mitochondrial depolarization but neither one nor the other were strictly required since selected KO targets with defective signaling pathway were still efficiently killed.

(**I**-**K**) Pooled results from BAX BAK DKO targets (**I**, NALM6, n = 6 tested donors; **J**, REH, n = 3 tested donors; **K**, 697, n = 6 tested donors). Statistics: Wilcoxon matched-pairs signed rank test (* = $p < 0.05$, n.s. = non significant). For REH cell line, the sample size was not sufficient to perform statistics.
K562 cytotoxicity was assessed as a positive control (not shown). Control and (D)KO cell lines are respectively displayed in blue and in orange.

3.2.7. ROLE OF REACTIVE OXYGEN SPECIES (ROS)

Apart from a pivotal role of mitochondria during the intrinsic apoptosis, reactive oxygen species (ROS) produced by the mitochondria can be involved in cell death, as well as extra-mitochondrial ROS (Galluzzi et al., 2014; Klamt et al., 2009; Martínez-Lostao et al., 2015; Tabas and Ron, 2011).

We decided to explore a potential contribution to ROS in our killing by incubating cells with the ROS scavenger N-acetylcystein (NAC). In our hands, experiments using NAC (whose pH once reconstituted is acidic and has to be strongly buffered) were sometimes difficult to perform with a variability and a sensitivity of pre-B ALL cell lines which could die of ROS scavenging, especially for long term incubations. However, preliminary experiments suggested that ROS inhibition could increase blasts survival when exposed to NK cells (**Figure 30**). We then decided to explore oxidative metabolism in a systematic way.

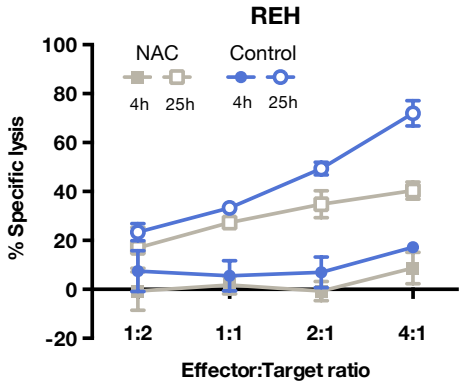

Figure 30. Preliminary experiment suggesting a potential implication of ROS.
Early and late leukemic killing by NKAES-NK cells, with or without NAC (5mM, pH = 7.71) during the co-incubation. Shown are percentages of cytotoxicity (relative to cultures with no effector cells) in cocultures lasting 4 and 25h (mean ± SD).
REH cell line was used as target.

First, we assessed cell lines sensitivity to H_2O_2 as an indicator of their ability to manage oxidative stress and indirectly to reflect antioxidant potential.

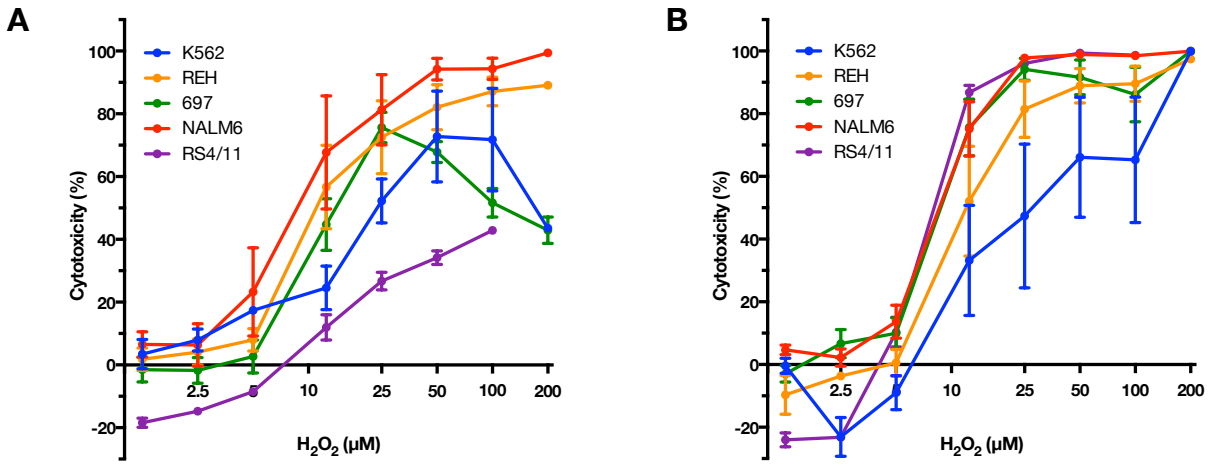

Figure 31. Different sensitivity to H_2O_2 among leukemic cell lines.
Dose response curves of K562 (blue), REH (yellow), 697 (green), NALM6 (red) and RS4;11 (purple) to hydrogen peroxyde following 4h (**A**) and 25h (**B**) incubation. Mean ± SEM is displayed.

Interestingly, pre-B ALL cells were differently sensitive to hydrogen peroxyde and we observed that it was mimicking their relative resistance to NK cell, with RS4;11 (the only tested pre-B cell line which was constantly resistant to NK cells) being the less sensitive to H_2O_2 induced stress (**Figures 31**A and **31**B). These preliminary results prompted us to modify targets to make them better to manage oxidative stress, and then assess their sensitivity or resistance to NK cell killing. We adapted a series of previously reported genetic tools (Walter et al., 2015): pre-B ALL cell lines were transduced to stably express a CAT-2A-SOD IRES GFP transgene allowing combined overexpression of the ROS-detoxifying enzymes manganese superoxide dismutase (SOD2) and catalase (**Appendix 13**, provided by Dr. Michael Milsom (HI-STEM, Germany); a roGFP-based sensor of glutathione redox potential either expressed in the cytosol (Grx1-roGFP2, **Appendix 14**) or in the mitochondria (Mito-Grx1-roGFP2, **Appendix 15**); and a roGFP-based sensor to measure hydrogen peroxide in the cytosol (roGFP2-ORP1, **Appendix 16**) or in the mitochondria (Mito-roGFP2-ORP1, **Appendix 17**). These four biosensors are based on genetically encoded redox-sensitive green fluorescent proteins (roGFPs), which allow sensitive and compartment-specific insights into redox homeostasis, and were provided by Pr. Tobias Dick (DKFZ, Germany).

We couldn't detect any difference among living targets (Annexin-V^- 7-AAD^-) which were in contact with effector cells, neither exploring glutathione redox potential nor hydrogen peroxide level (data not shown). However, apoptotic Annexin-V^+ 7-AAD^- cells displayed altered phenotype for both readouts but this observation appears to be a general property of apoptotic cells since we observed it regardless of the inducing stimulus (targets treated with SuperKillerTRAIL gave the same results, data not shown).

To our surprise, combined overexpression of the SOD2 and the catalase didn't confer protection from NK killing (**Figure 32**).

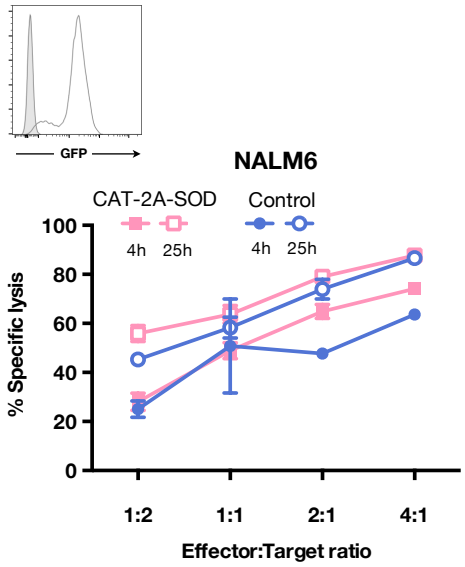

Figure 32. Catalase and SOD2 over-expressing targets do not show increased resistant to NK killing.

Early and late leukemic killing by NKAES-NK cells against NALM6 cell line (control or CAT-2A-SOD transduced). Shown are percentages of cytotoxicity (relative to cultures with no effector cells) in cocultures lasting 4 and 25h (mean ± SD).

Overlays showing GFP expression on sorted targets transduced with the CAT-2A-SOD IRES GFP transgene are also shown (unstransduced control is depicted in gray).

These results, together with the experiment using NAC, raised the hypothesis that ROS production could be important in NK cells and not in pre-B ALL targets.

3.2.8. EVIDENCE FOR A NADPH COMPLEX IN NK CELLS

All experiments exploring biological interference through chemical inhibition were of limited interest in our project because of effector and target cells were both impacted. To address the role of ROS in NK cell function, we looked for primary cells which could present a genetic defect in their production.

Patients with chronic granulomatous disease (CGD) have a well-described hereditary defect in reactive oxygen intermediates production by neutrophils and monocytes (Kuhns et al., 2010): NADPH oxidase activity is drastically impaired due to mutations in any one of five subunits of phagocyte-derived NADPH oxidase, including gp91^{phox} (*CYBB*, ~65% of patients), p22^{phox} (*CYBA*, <5%), p47^{phox} (*NCF1*, ~30%), p67^{phox} (*NCF2*, <5%), and p40^{phox} (*NCF4*, one case identified). We decided to assess whether NK cells from CGD patients displayed normal killing activity in our FCC assay against pre-B ALL cells

Surprisingly, we observed a significative defect in NK cell mediated late killing of pre-B ALL cells using effector cells from a X-CGD patient (**Figure 33**A). To further characterize our mechanism, we decided to increase patient recruitment: we tested ten different X-CGD patients and observed a significant decrease in cytotoxic abilities against NALM6 and REH cell lines, more specifically following 25h incubation (**Figures 33**D and **33**E). Of note, we noticed that NK cells from X-CGD patients proliferated less than cells from controls or other PIDs (data not shown). Then, we tested cells from CGD patients harboring mutations affecting another protein of the phagocytic NADPH oxidase complex, to see whether altered cytotoxicity was a shared characteristic among CGD patients. We included two patients with *NCF1* mutations (AR47-CGD) and one with *CYBA* mutations (AR22-CGD). Not only all of them were proliferating very well in our system (data not shown), but they displayed strong cytotoxicity against pre-B ALL blasts (**Figures 33**B and **33**C).

These results suggest that CYBB could play a role in NK cell function. However, to our knowledge, neither biological role nor NADPH expression have been reported in NK cells. We first assessed CYBB mRNA expression in PBMCs, resting and amplified NK cells, as well as those of the main components of the NADPH oxidase and NOX1 and NOX4, two NOX2 (CYBB) homologues which can interact with p22^{phox} too (**Figures 34**A-**34**C) (Chuong Nguyen et al., 2015; Lambeth et al., 2007).

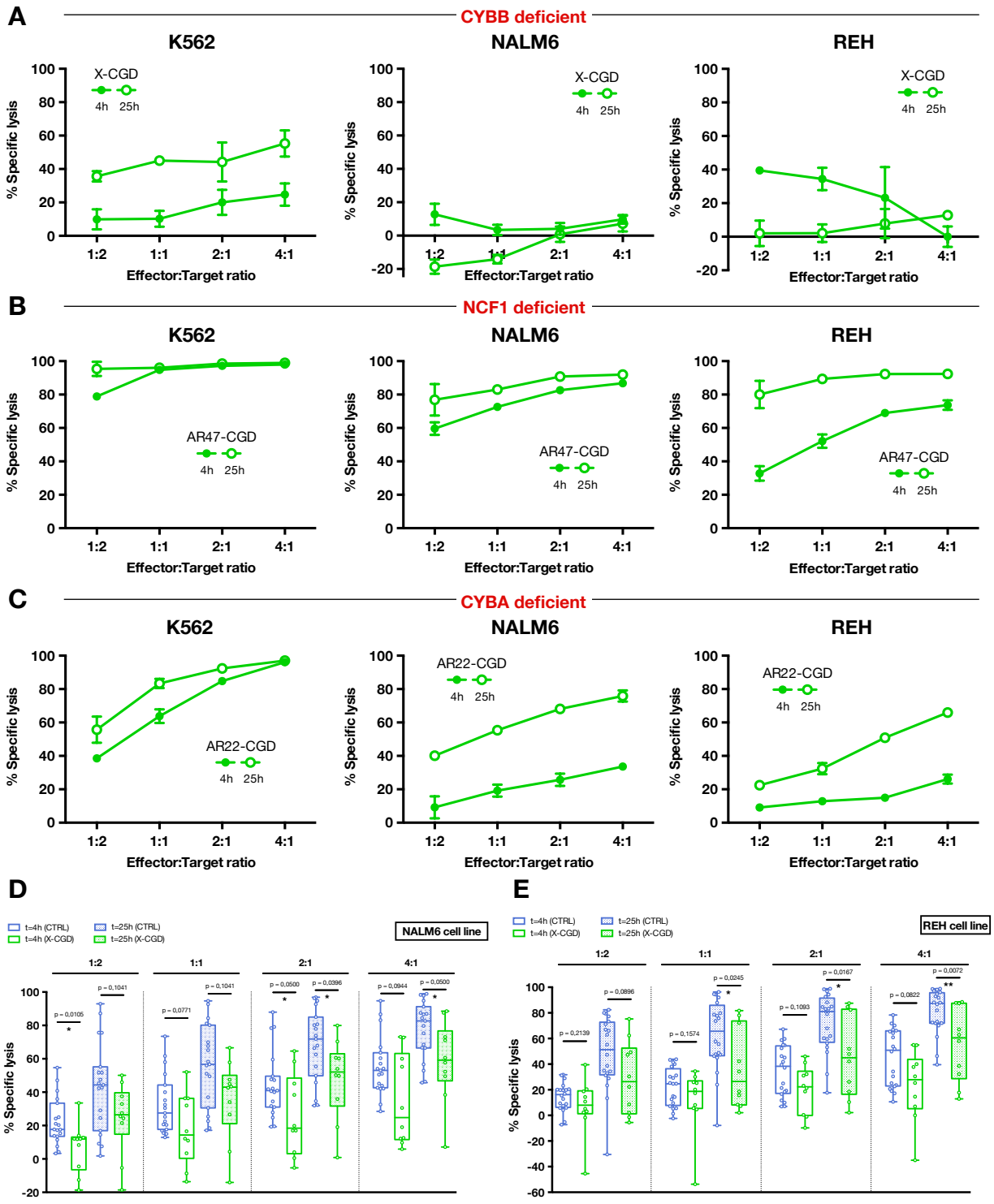

Figure 33. CYBB deficient NK cells display significantly decreased cytotoxicity against pre-B ALL cells.

(**A**-**C**) Representative graphs showing early and late leukemic killing by NKAES-NK cells from a CYBB deficient patient (X-CGD) (**A**), a NCF1 deficient patient (AR47-CGD) (**B**) and a CYBA deficient patient (AR22-CGD) (**C**). Shown are percentages of cytotoxicity (relative to cultures with no effector cells) in cocultures lasting 4 and 25h (mean ± SD).

(**D**) Results from nineteen normal donors and ten X-CGD patients against NALM6 cell line.

(**E**) Results from twenty normal donors and ten X-CGD patients against REH cell line.

Statistics: Mann-Whitney test (* = $p < 0.05$, ** = $p < 0.01$).

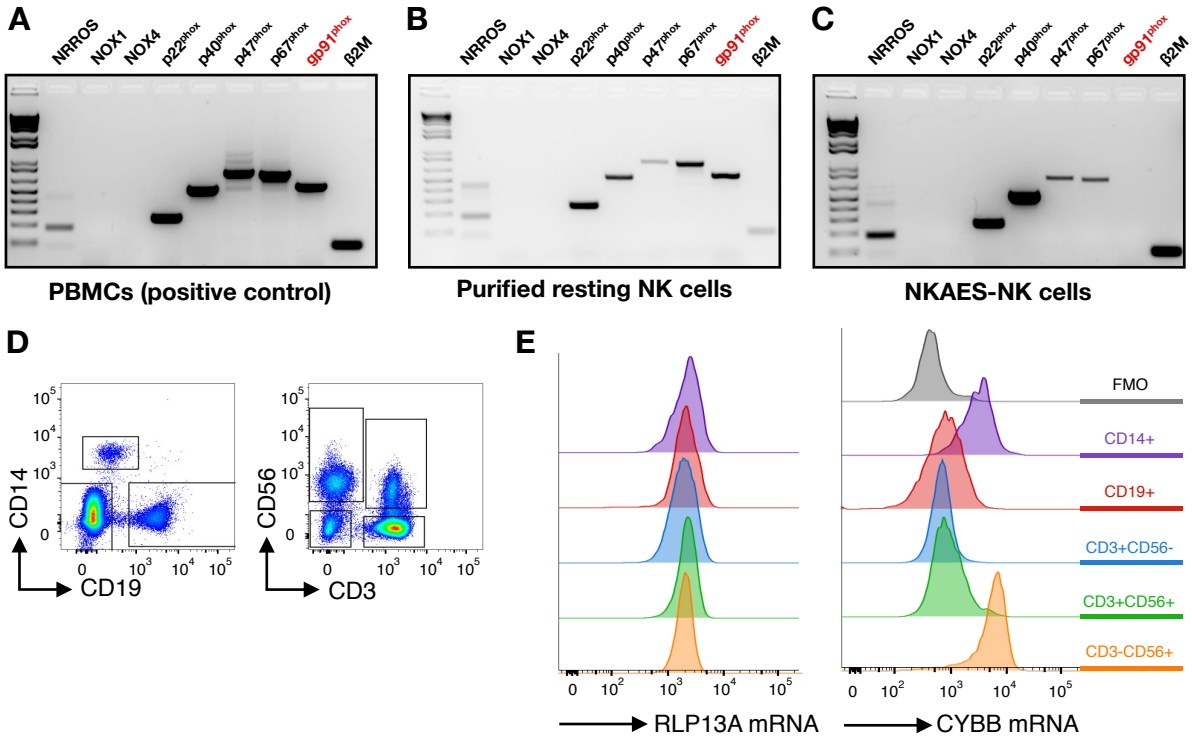

(legend continued on next page)

Apart from NOX1 and NOX4 whose expression was reported only in non-immune cells, resting NK cells expressed all the genes at the transcriptomic level, but activated NK cells displayed a selective loss of CYBB mRNA expression (**Figures 34**B and **34**C).

A previous study from Dr. Dario Campana lab explored genetic features of NKAES-NK cells, comparing the global gene expression profiles of these cells with those of unstimulated NK cells (Fujisaki et al., 2009). Supplemental data from their work reported a 55 fold repression of CYBB in NKAES-NK compared to resting cells. Besides, we confirmed this observation by performing a PrimeFlow RNA assay on PBMCs with a CYBB targeting probe. We observed that resting NK cells (both $CD56^{bright}$ and $CD56^{dim}$) expressed CYBB mRNA at a similar level as monocytes, and stronger than $CD19^{+}$ B cells which are known to express a phagocyte-type NADPH oxidase complex (Cotugno et al., 2015) (**Figures 34**D and **34**E).

$gp91^{phox}$ and $p22^{phox}$ are the two subunits of flavocytochrome b558, a heterodimeric integral membrane protein which is the key component of the phagocyte NADPH oxidase system (Jesaitis, 1995). Its expression has been reported both at the cell surface of neutrophils, monocytes and B cells, as well as intracellularly in those same cell types. We evaluated flavocytochrome b558 expression using the 7D5 monoclonal antibody which recognizes an epitope on $gp91^{phox}$ when its conformation is within the $gp91^{phox}$ / $p22^{phox}$ heterodimer (Burritt et al., 2001; Campion et al., 2007). To ensure that the antibody was specific, we tested as a negative control a CYBA deficient patient (AR22-CGD) together with a normal donor.

Figure 34. NK cells express $gp91^{phox}$ and $p22^{phox}$ but do not display a phagocyte-type NADPH oxidase complex.

(**A**-**C**) End-point PCR was performed on PBMCs (**A**, positive control), sorted resting NK cells (**B**) and sorted NKAES-NK cells (**C**) to check mRNA expression of the following genes related to NADPH oxidase: *NRROS*, *NOX1*, *NOX4*, *CYBA* ($p22^{phox}$), *NCF4* ($p40^{phox}$), *NCF1* ($p47^{phox}$), *NCF2* ($p67^{phox}$), *CYBB* ($gp91^{phox}$) and the *B2M* housekeeping gene. Representative gel (at least three different donors were tested per condition).

(**D** and **E**) PrimeFlow RNA assay was performed on total PBMCs (**D**, gating strategy). RLP13a mRNA was used as a positive control among PBMCs subpopulations and CYBB mRNA expression was studied (**E**). Representative histogram of one of three different donors showing similar results.

(**F**-**H**) Cell surface (**F**) and intracellular (**G**) flavocytochrome b558 expression (clone 7D5; MBL International) was assessed by flow cytometry on PBMCs, as well as intracellular $p22^{phox}$ expression (**H**) (clone 44.1; Santa Cruz Biotechnology). Normal donor and AR22-CGD patient are depicted as blue and red histograms respectively. PBMCs from four normal donors were tested with the same results.

(**I**) Nanofluidic proteomic immunoassay against CYBB (clone 54.1; Santa Cruz Biotechnology) was performed using resting NK cells (isolated by negative selection) from a normal donor (in green) and a X-CGD patient (in blue) harboring a complete *CYBB* gene deletion.

We detected flavocytochrome b558 on monocytes and B cells, both intracellularly and at the cell surface, and confirmed antibody specificity since no expression was detected for the AR22-CGD patient (**Figures 34**F and **34**G). We didn't detect any flavocytochrome b558 expression in resting NK cells from PBMCs, in agreement with another work (Wada et al., 2013) (**Figures 34**F and **34**G). Although a team previously reported an expression among $CD3^+$ T cells (Jackson et al., 2004), we did not detect any flavocytochrome expression b558 in T cells.

Then we postulated that $gp91^{phox}$ and $p22^{phox}$ are expressed in cytotoxic lymphocytes in a complex which differ from the phagocyte-type flavocytochrome b558. We looked for evidence of a $p22^{phox}$ proteic expression by flow cytometry with an antibody which recognizes an intracellular epitope of $p22^{phox}$. Again, antibody specificity was confirmed using cells from our AR22-CGD patient. Interestingly, we showed that resting NK cells (both $CD56^{bright}$ and $CD56^{dim}$), as well as monocytes, B cells and with a lower intensity T cells, did express $p22^{phox}$ (**Figure 34**H).

Since we could not find an antibody suitable for flow cytometry which could specifically recognize $gp91^{phox}$ in a conformation independent of the flavocytochrome b558, we took advantage of a nanofluidic proteomic immunoassay to evaluate $gp91^{phox}$ proteic expression with small amounts of proteins. Cells from a X-CGD patient with complete *CYBB* deletion were used to validate our approach and our antibody. We found resting NK cells to express $gp91^{phox}$ at the proteomic level (**Figure 34**I).

Thus, our results showed that NK cells from PBMCs expressed all the components of the NADPH oxidase complex at the transcriptomic level as well as NRROS which has been described to regulate flavocytochrome b558 expression in phagocytes by regulating $gp91^{phox}$ degradation (Noubade et al., 2014). They also expressed $gp91^{phox}$ and $p22^{phox}$, the two subunits of the flavocytochrome b558 which is a key component of the NADPH oxidase complex, at the proteic level but did not display a phagocyte-type flavocytochrome b558, suggesting that these proteins could be involved in an alternative complex.

We found surprising that CYBB mRNA was virtually completely absent in activated NK cells: then, how could we link the functional defect we observed in X-CGD patients considering that cells from normal donors didn't express the gene?

We decided to test CYBB mRNA expression in NKAES-NK cells from normal donors after they encountered targets (K562 or pre-B ALL cells).

Figure 35. CYBB mRNA is actively regulated by NK cells.
End-point PCR was performed on PBMCs (positive control), sorted NKAES-NK cells before and after incubation with targets (K562 or REH), to check mRNA expression of the following genes related to NADPH oxidase: *NRROS*, *CYBA* ($p22^{phox}$), *NCF4* ($p40^{phox}$), *NCF1* ($p47^{phox}$), *NCF2* ($p67^{phox}$), *CYBB* ($gp91^{phox}$) and the *B2M* housekeeping gene. Representative gel of one among several donors.
NALM6 and 697 cell lines were tested with results similar to REH.

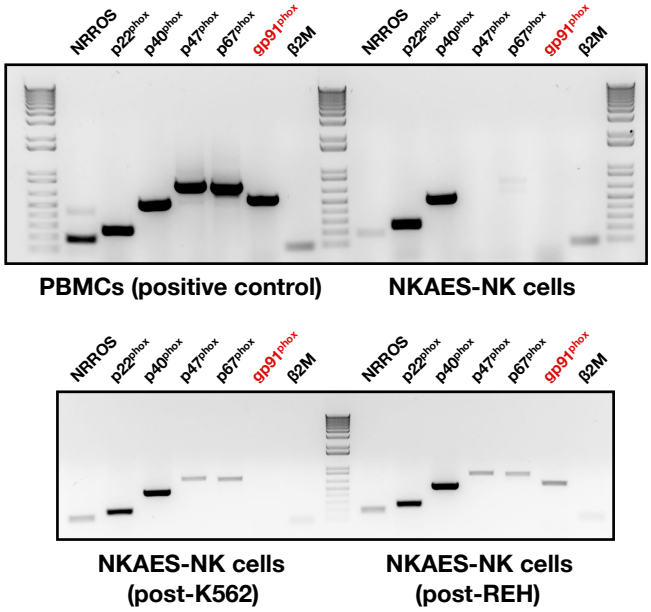

Our results showed that CYBB was re-expressed when NKAES-NK cells were incubated for 25h with pre-B ALL cells but not with K562 targets (**Figure 35**). These results demonstrated that CYBB expression is actively and dynamically regulated by proliferating NK cells and, together with our results regarding late killing of X-CGD patient NK cells against pre-B ALL blasts (**Figures 33**D and **33**E), suggested that its expression could be important for the unconventional cytotoxic pathway that we described.

To gain insight into the molecular defects among X-CGD patients, we performed RNAseq on resting NK cells and activated NKAES-NK cells either unexposed to targets or following 24h incubation with a NK-sensitive (REH) or resistant (RS4;11) pre-B ALL cell line. We tested four controls and three X-CGD patients with a complete *CYBB* gene deletion; because we had a limited amount of activated cells for patients, only one of them could be also exposed to targets.

We performed unsupervised clustering using PCA and observed a perfect separation of samples per condition and donor (**Figure 36**A). Responses to REH or RS4;11 cells are, in general, larger in effect size in the patient's sample than in the controls (data not shown) and similar among controls regardless of the cell line (**Figure 36**B).

Differentially expressed genes were plotted per contrast of interest (**Figures 36**C-**36**G and **Table S1**) and a gene ontology enrichment analysis was performed into Cytoscape using the ClueGO plugin.

For this analysis, we had contrasts with more differentially expressed genes than for others. However, the enrichment analyses work differently depending on the number of genes in the target gene sets. In our experience using this program, the most informative results were usually obtained when target gene sets are around ~500-1000 genes, so that we changed the fdr threshold between contrasts to retrieve target gene sets of sizes as comparable as possible (**Tables S2** and **S3**).

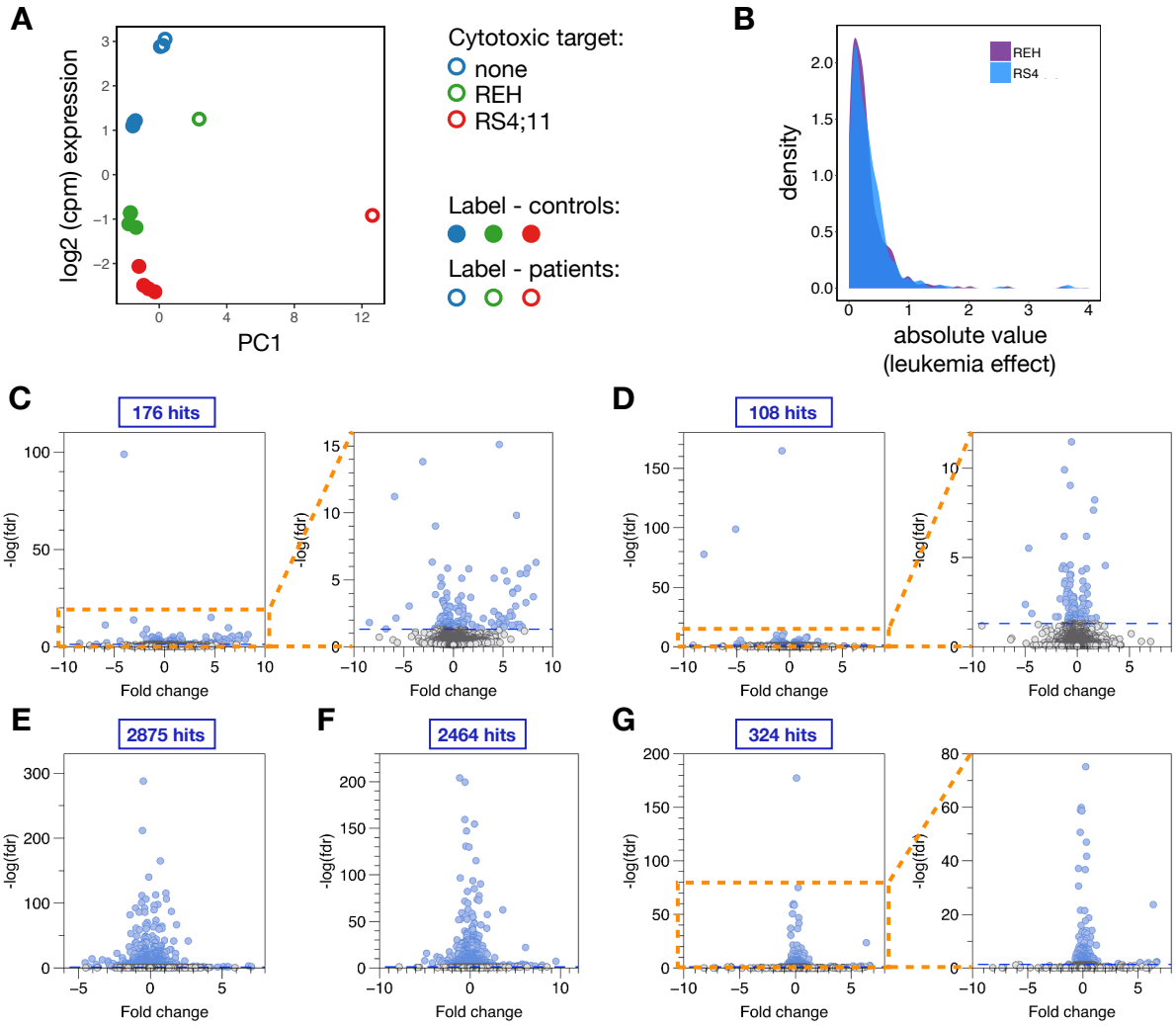

Figure 36. NK cells from X-CGD patients and normal donors have different transcriptomic expression profile.

(**A**) Principal component analysis was performed on tested samples.

(**B**) Comparison of effect sizes for response to REH (and RS4;11, and their difference) for NKAES-NK cells from controls (n = 4 per condition).

(**C**-**G**) Volcano plots showing differentially expressed genes (FDR < 0.05) between resting NK cells (**C**) or NKAES-NK cells (**D**) from X-CGD patients vs controls (**C**); NKAES-NK cells from controls exposed to REH (**E**) or RS4;11 (**F**) vs unstimulated NKAES-NK cells; and NKAES-NK cells stimulated with REH vs RS4;11 (**G**). The number of hits is also given.

GO Biological process terms

Resting NK cells (X-CGD vs controls)

A upregulated

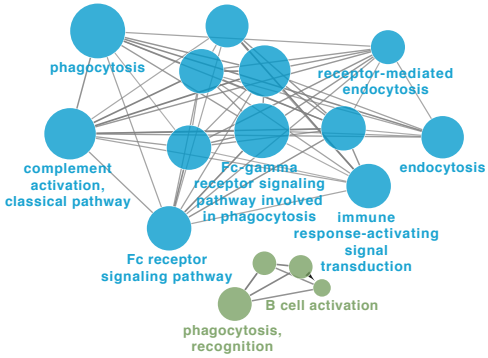

B downregulated

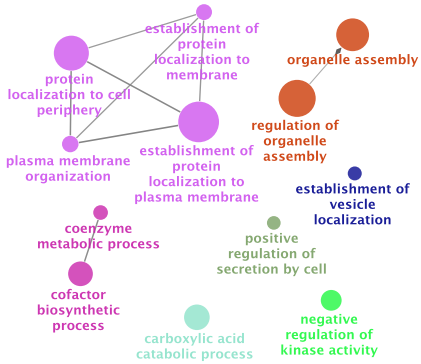

control NKAES-NK cells (post-REH vs unstimulated)

C upregulated

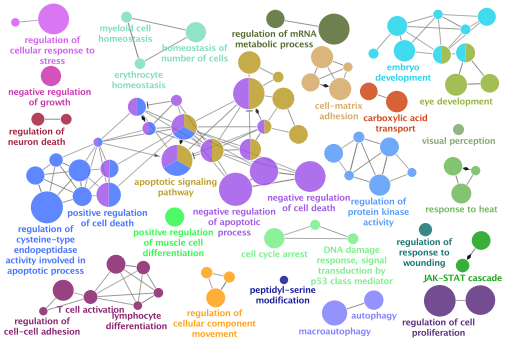

D downregulated

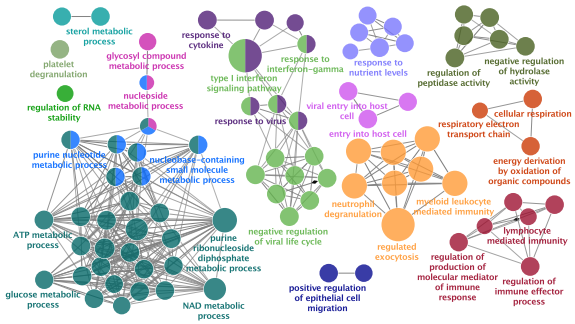

control NKAES-NK cells (post-RS4;11 vs unstimulated)

E upregulated

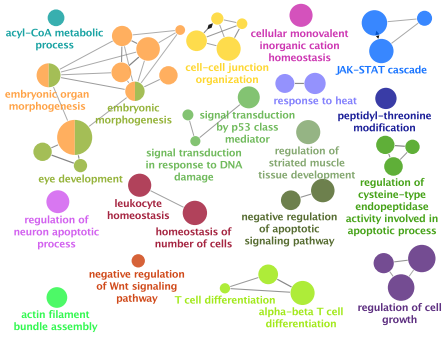

F downregulated

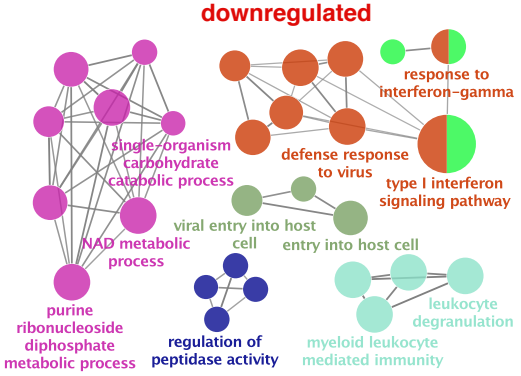

control NKAES-NK cells (post-RS4;11 vs post-REH)

G upregulated

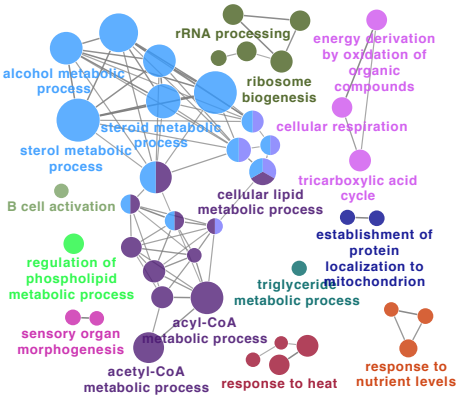

H downregulated

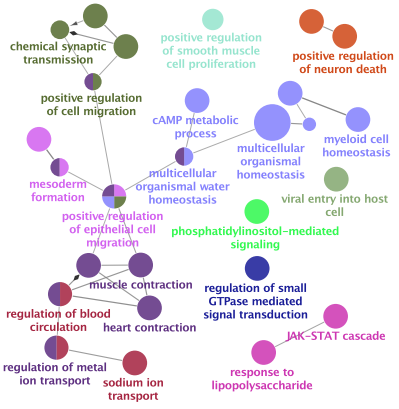

(figure continued on next page)

GO Cellular compartments terms

Resting NK cells (X-CGD vs controls)

I upregulated

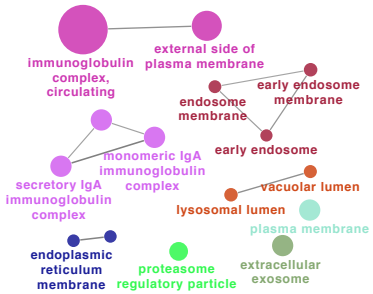

J downregulated

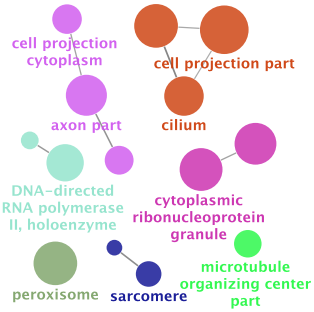

control NKAES-NK cells (post-REH vs unstimulated)

K upregulated

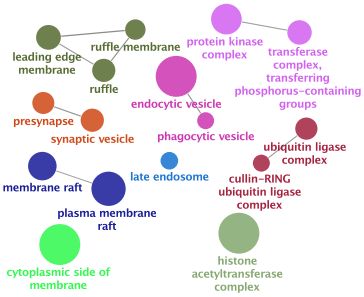

L downregulated

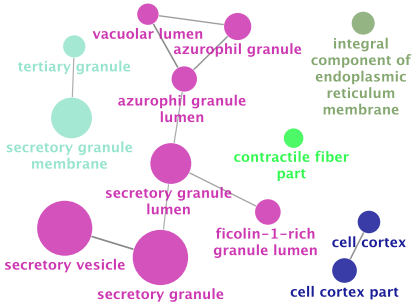

control NKAES-NK cells (post-RS4;11 vs unstimulated)

M upregulated

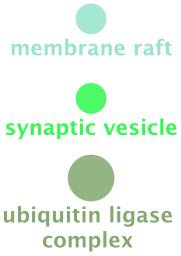

N downregulated

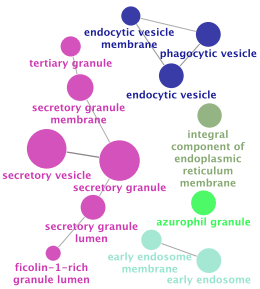

control NKAES-NK cells (post-RS4;11 vs post-REH)

O upregulated

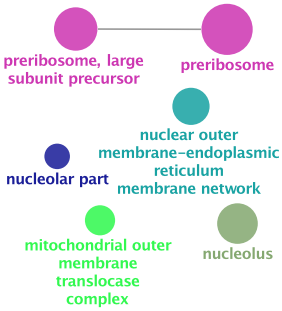

P downregulated

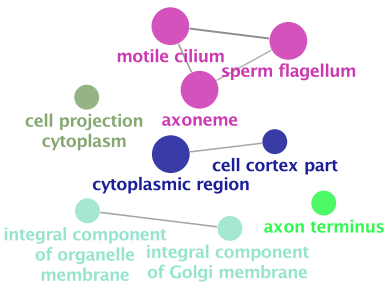

(legend continued on next page)

Regarding the comparison of resting NK cells from X-CGD patients to normal donors, results showed that functions (strongly) enriched among genes more expressed in patient cells were related to *phagocytosis* (which is directly evocative of the pathophysiology of the CGD), *endocytosis*, *receptor-mediated endocytosis* and *Fc receptor signaling* (**Figure 37**A). Functions (slightly) enriched among genes less expressed in NK from patients were associated to *protein localization to membrane* (**Figure 37**B).

Responses to REH and RS4;11 were highly similar in intensity and the category of the functions enriched, the main difference being the increased number of terms in response to REH, both up and down-regulated. Shared functions enriched among up-regulated genes in response to either REH or RS4;11 included *regulation of apoptosis-related terms*, *T cell activation*, *JAK-STAT cascade*, *leukocyte homeostasis* and *response to DNA damage* (**Figures 37**C and **37**E). Shared functions enriched among down-regulated genes in response to either REH or RS4;11 were related to *carbohydrates metabolism*, *degranulation* (of different cell types, though), *type I IFN response* and *response to virus* (**Figures 37**D and **37**F). When looking at the differential expression between NKAES-NK cells exposed to RS4;11 vs REH among controls, an interesting pattern appeared: functions enriched among genes more highly when stimulated with RS4;11 were mainly metabolic (**Figure 37**G) while those enriched with REH as a stimulus included *sodium ion transport*, *regulation of metal ion transport*, *water homeostasis*, and other terms closely related to ion pumping processes (**Figure 37**H). For cellular components terms, the enrichment was weaker; however there was a huge enrichment of immunoglobulin complex genes in the target gene set comparing resting NK cells from X-CGD patients to normal donors (**Figure 37**I).

Thus, our RNAseq study highlighted strong differences between X-CGD patients and controls. It also showed that NK cell responses either to a NK-sensitive (REH) or resistant (RS4;11) pre-B ALL cell line were similar in effect size, which could be indicative that their differential behavior in sensitivity to NK cells was intrinsic to targets. Besides, our results suggested a role of metabolic processes in NK cells responses.

Figure 37. Gene ontology functional network of biological process and cellular components terms.

ClueGO analysis was performed for resting NK cells from X-CGD patients vs controls (**A** and **B**; **I** and **J**) and NKAES-NK cells (**C** and **D**; **K** and **L**) from X-CGD patients vs controls as well as NKAES-NK from controls exposed to REH (**E** and **F**; **M** and **N**) or RS4;11 (**G** and **H**; **O** and **P**) vs unstimulated NKAES-NK.

Biological process (**A**-**H**) and cellular component (**I**-**P**) related terms were studied. We distinguished up-regulated and down-regulated genes for the analysis.

In the graphs, size is proportional to the fdr of the result (following a scale roughly logarithmic), but the significance scales vary from some runs to others.

3.3. METABOLIC SUPPORT OF NK CELLS ACTIVITY

In our transcriptomic study of NK cells, most of the hits were related to metabolism. We aimed to evaluate metabolic changes in NK cells that were engaged in a killing through our unconventional pathway.

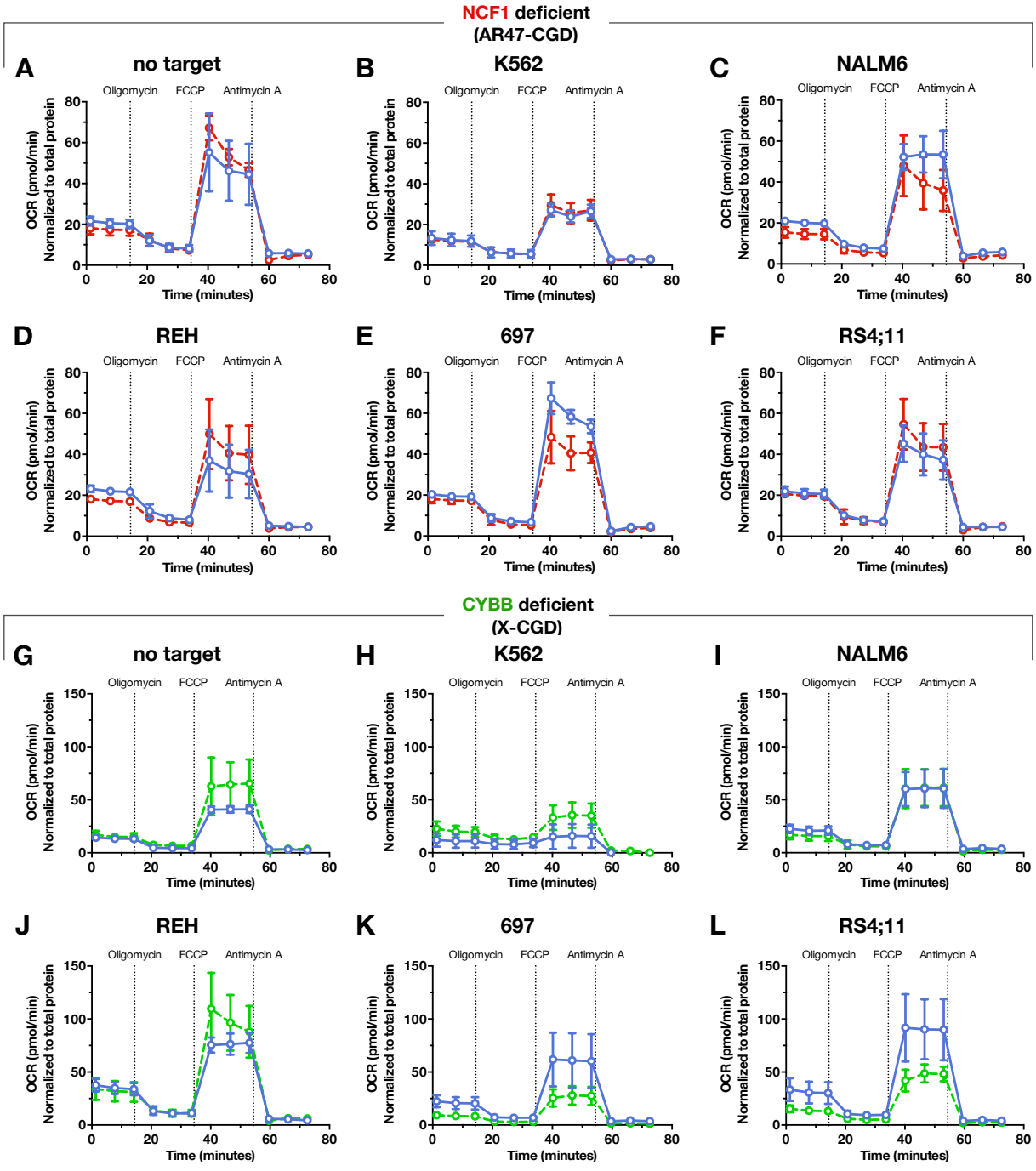

Figure 38. Oxygen Consumption Rate (OCR) among NK cells from AR47-CGD and X-CGD patients (compared to controls).

(**A**-**F**) OCR was measured using NK cells from a normal donor (in blue) and a AR47-CGD (NCF1 deficient; in red) either exposed or not to various target cell lines.

(**G**-**L**) OCR was measured using NK cells from a normal donor (in blue) and a X-CGD (CYBB deficient; in green) either exposed or not to various target cell lines.

We positively purified by magnetic separation NK cells (from normal donors or an AR47-CGD and a X-CGD patients) which had been stimulated for ~20h with various target cell lines, and then evaluated OXPHOS and glycolysis (**Figures 38** and **39**).

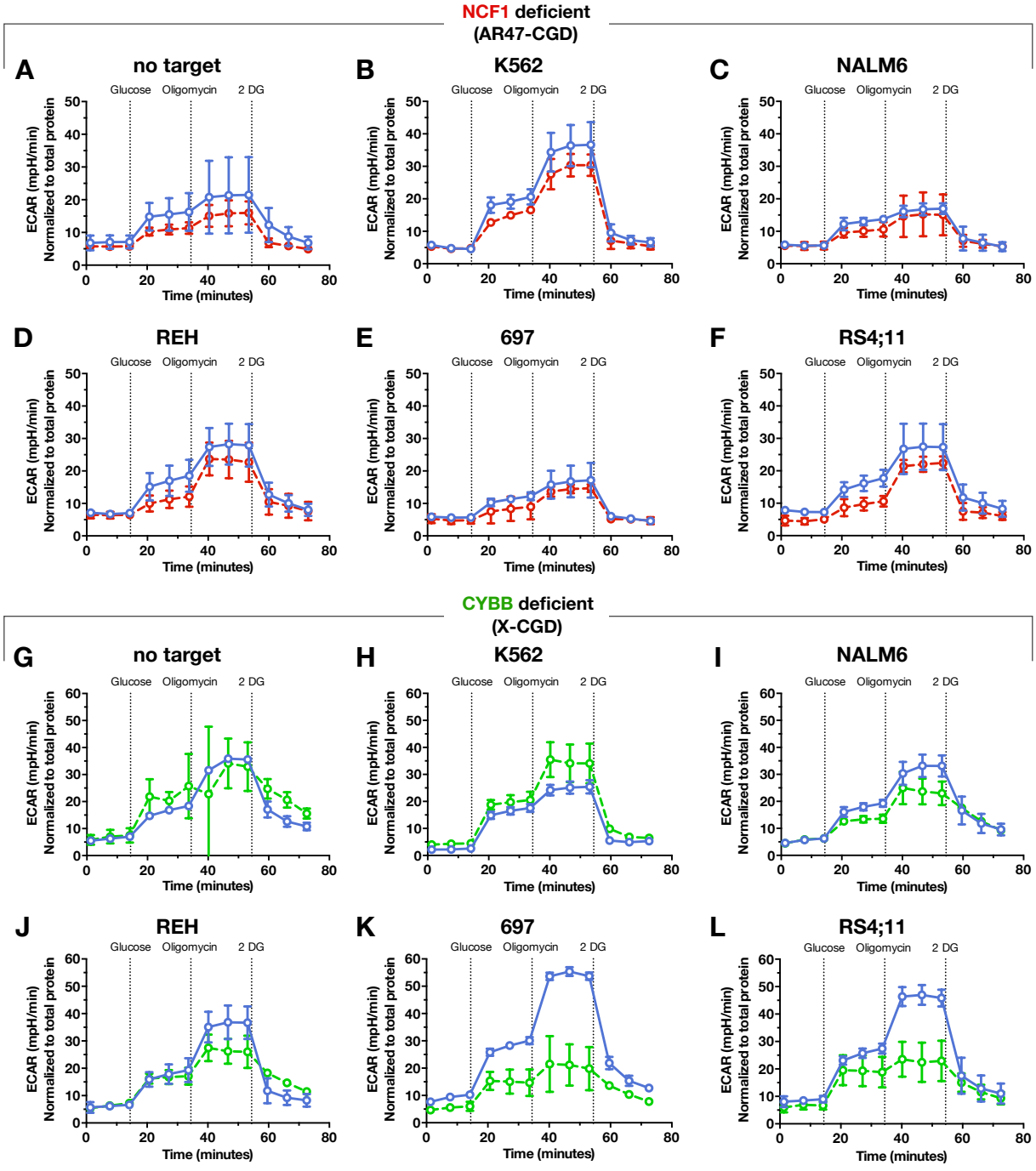

Figure 39. Extracellular Acidification Rate (ECAR) among NK cells from AR47-CGD and X-CGD patients (compared to controls).

(**A**-**F**) ECAR was measured using NK cells from a normal donor (in blue) and a AR47-CGD (NCF1 deficient; in red) either exposed or not to various target cell lines.

(**G**-**L**) ECAR was measured using NK cells from a normal donor (in blue) and a X-CGD (CYBB deficient; in green) either exposed or not to various target cell lines.

We observed that NK cells which had been exposed to K562 cell line decreased their OXPHOS use and (**Figures 38**B and **38**H) but not their glycolytic activity (**Figures 39**B and **39**H).

When stimulated with pre-B ALL cell lines, NK cells didn't strongly modify their OXPHOS activity (**Figures 38**C-**38**F and **38**I-**38**L). However, facing 697 and RS4;11 cell lines (which are the more resistant to our late NK killing), we observed an increase in NK cells glycolytic activity (**Figures 39**K and **39**L).

Interestingly, we didn't observe any difference in OXPHOS and glycolysis use by NCF1 deficient or control NK cells, which both killed efficiently pre-B ALL cells. On the other hand, CYBB deficient NK cells which were stimulated with 697 and RS4;11 targets, didn't increase their glycolytic activity, in contrast to control cells.

Our results revealed opposite metabolic profile when NK cells were engaged in K562 killing or pre-B ALL cell lines. They also suggested that a hyperglycolytic step could be required for efficient engagement of our unconventional cytotoxicity pathway.

CYBB deficient NK cells didn't exhibit hyperglycolysis, which is evocative of a work showing that NADPH oxidase has a function in supporting hyperglycolysis in stimulated neutrophils (Baillet et al., 2017).

The NK cell activation and expansion system we used relies on K562-mb15-41BBL feeder cells and therefore on IL-15 signaling. Previous works showed mTOR dependent metabolic changes induced by IL-15 signaling in murine and human NK cells (Gardiner and Finlay, 2017; Keating et al., 2016; Marçais et al., 2014).

We checked CD98 (**Figures 40**A-**40**C) and CD71 (**Figures 40**D-**40**F) expression as well as glucose uptake (**Figures 40**G and **40**H) in NK cells following incubation with K562 or pre-B ALL cell lines.

We found opposite results when effector cells were engaged in a conventional degranulation-dependent cytotoxicity against K562, with increased CD71 expression and no difference for CD98, compared to unstimulated NK cells. However, pre-B ALL cell lines induced an early CD98 up-regulation (delayed with K562) and no CD71 modulation compared to control. Glucose uptake was increased at 4h with K562 only, while we could observe a later increase (at 25h) with pre-B ALL cell lines, suggesting that both metabolic requirement and its kinetics were distinct depending on the killing pathway that NK cells were engaging.

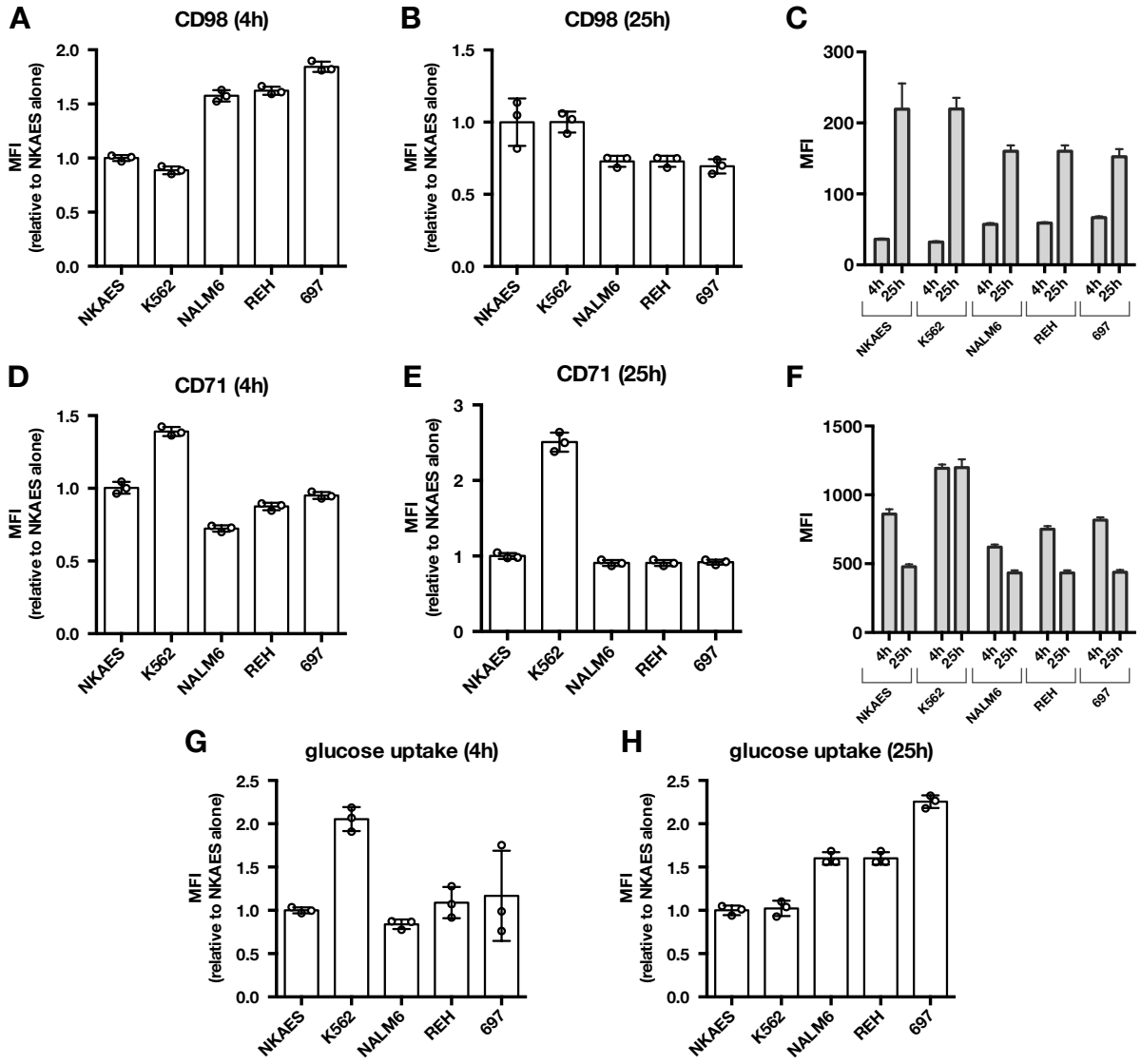

Figure 40. NK cell metabolic profile discriminates stimulation with K562 or pre-B ALL cell lines.

(**A**-**C**) Expression of CD98 on NK cells following 4h (**A**) or 25h (**B**) incubation with targets (relative to unstimulated effector cells) was assessed by flow cytometry. Absolute MFI values are also displayed (**C**).

(**D**-**F**) Expression of CD71 on NK cells following 4h (**D**) or 25h (**E**) incubation with targets (relative to unstimulated effector cells) was assessed by flow cytometry. Absolute MFI values are also displayed (**F**).

(**G** and **H**) NK cells incorporation of 2-NBDG following 4h (**G**) or 25h (**H**) incubation with targets (relative to unstimulated effector cells) was assessed by flow cytometry.

Finally, we also assessed the basal metabolism in target ALL cells. Compared to K562 cell line, pre-B ALL cells had a lower oxidative phosphorylation (OXPHOS) with glycolysis being substantially the same (**Figures 41**A and **41**B), and overall, equally relied on OXPHOS and glycolysis (**Figure 41**C). The NK-resistant cell line RS4;11 showed a very low OXPHOS and we generally observed that pre-B ALL cell lines which were relying mainly on glycolysis because

of this low OXPHOS were also the more resistant to NK killing (**Figure 41**C).

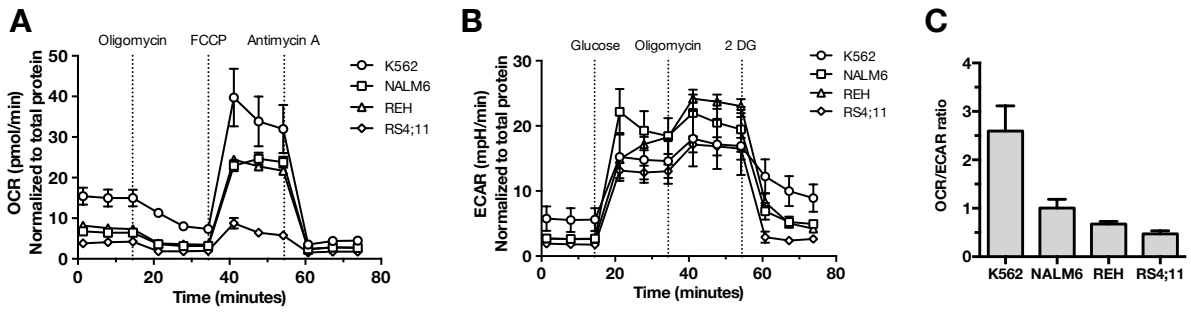

Figure 41. Metabolic profile of target cell lines.

(**A**) Oxygen Consumption Rate (OCR) at baseline among K562, NALM6, REH and RS4;11 cell lines.

(**B**) Extracellular Acidification Rate (ECAR) at baseline among K562, NALM6, REH and RS4;11 cell lines.

(**C**) OCR/ECAR ratio at baseline was used as a parameter to evaluate the relative use of OXPHOS and glycolysis by target cell lines.

These preliminary results in ALL cell lines showed that spare respiratory capacity could potentially be correlated to their sensitivity to activated NK cells and suggest that target cell metabolism should be further investigated to understand NK cell induced death process.

CHAPTER 4.

CONCLUDING REMARKS AND PERSPECTIVES

4. CONCLUDING REMARKS AND PERSPECTIVES

4.1. CONCLUDING REMARKS

The work reported in this manuscript was aimed at understanding the NK-mediated killing of pre-B ALL. Previous publications indicated that these targets were resistant, but the mechanisms responsible for this resistance remain largely unknown (Imai et al., 2005; Kübler et al., 2014; Romanski et al., 2005; Ruggeri, 2002; Ruggeri et al., 1999). Our results conclusively establish that pre-B ALL are not intrinsically resistant to NK cell cytotoxicity. In our experiments, despite these blasts were poorly killed after a 4h incubation period, we found a striking increase in this killing when the incubation was extended up to 25h (**Figure 19**). Is this experimental setup biologically relevant? We believe the answer is yes, for at least two reasons: first, we observed resistant targets (both the RS4;11 cell line and some primary leukemic samples), meaning that not all long-term co-cultures with NK cells induce target death; second, when $CD4^+$ T cells were used as a negative control for effector cells, no effector-induced cell death was measured, proving that the effect was linked to the cytotoxic potential of NK cells and not simply to the prolonged allogeneic co-culture (data not shown).
In our assay, we used NK cells amplified and activated with feeder cells in a mbIL-15-dependent system; we decided to use such a protocol because of the limited number of NK cells present in the blood, particularly with patient samples. Importantly, we showed that NK cells activated in a distinct system (a mbIL-21-dependent, feeder cell-based system), as well as resting NK cells displayed the same ability to kill the pre-B ALL cells in a delayed manner (**Figure S1**). We also demonstrated that primary pediatric pre-B ALL blasts behaved similarly to cell lines and distinguished NK-sensitive and resistant primary blasts. In sum, we used NKAES-NK cytotoxicity against pediatric pre-B ALL cell lines as a model that includes a number of intrinsic limitations but allows flexible work on both effector and target cells.

Having established this cytotoxicity, we aimed to understand the precise molecular mechanisms that governing it. We found that both killing initiation and the effector phase were contact-dependent (**Figures 21** and **22**). In particular, we researched the relative contribution of the two recognized contact-dependent cytotoxicity pathways, namely the granule exocytosis and the death receptor pathway. To assess the role of these pathways, we used NK cells from PIDs with a complete absence of the granule exocytosis to demonstrate that the late killing by NK cells was still preserved (**Figure 23**). We also generated target cells resistant to death receptor mediated cell death and again, we found no inhibition in the NK mediated killing (**Figure 27**). In conclusion, our results strongly suggest that the delayed

killing of ALL cells by NK cells expanded in the NKAES system relies on a novel unconventional cytotoxicity pathway. This novel pathway is independent of both granule exocytosis and death receptor pathway.

In parallel, we became interested in the minimal molecular requirements for target cell death, postulating that understanding the engaged pathway was complementary to the study of the effector cells. We found evidence for an apoptotic-like cell death among pre-B ALL (**Figure 24**) with pan-caspase activation and mitochondrial depolarization (**Figures 25** and **26**). From these empirical observations, we wanted to establish their absolute requirement. We generated knockout cell lines using the CRISPR/Cas9 technology and, to our surprise, found that caspases 3 and 7 DKO were still efficiently killed (**Figure 29**), which demonstrates that the activation of effector caspases is not required for NK-induced cell death. Caspases 8 and 10 DKO targets were also still killed, suggesting that these initiator caspases are not required either. Finally, disruption of the mitochondrial depolarization by double knockout of BAX and BAK did not prevent cell death, nor caspase 9 KO, although there was a tendency suggesting that mitochondrial signaling amplifies the molecular signaling for cell death commitment.

We have yet to characterize the type of engaged cell death since the pre-B ALL cells consistently died regardless of the canonical apoptotic gene(s) we disrupted. Giving an appropriate name to our cell death is important but following the recommendations of the Nomenclature Committee on Cell Death (NCCD) (Kroemer et al., 2009), it does not correspond to any category (Galluzzi et al., 2012). In particular, we expect caspases 3 and 7 DKO cells to be resistant to both intrinsic and extrinsic apoptosis (Lakhani et al., 2006) leading us to limit our description to an "apoptotic-like cell death" of the pre-B ALL cells. Importantly, the observation that the killing of the BAX BAK DKO targets is preserved (**Figure 29**) excludes both the possibility of a truncated BID (tBID) mediated cell death (Wei et al., 2001) as well as the one of the unfolded protein response (UPR) consecutive to endoplasmic reticulum (ER) stress (Hetz et al., 2006), or lysosomal membrane permeabilization induced cell death (Boya et al., 2003).

In the meantime, we demonstrated that interfering with ROS with N-acetylcysteine, a ROS scavenger, partially inhibited pre-B ALL killing (**Figure 30**). However, oxidative metabolism did not play a significant role in target cell death (**Figure 32**). Because the NADPH oxidase complex is associated with oxygen-derived species in neutrophils, monocytes/macrophages and B-cells, we studied NK cells from patients suffering from chronic granulomatous disease (CGD) whose ability to produce such derivatives is severely compromised in phagocytes

(Roos, 2016). Although no NK cell deficiency has been reported to date among these patients, X-linked CGD (CYBB deficient) activated NK cells had a defect in the late killing of pre-B ALL (**Figure 33**), but not AR22 (CYBA deficient) or AR47 (NCF1 deficient)-CGD. Of note, to date, no report described a phagocyte-type NADPH complex in NK cells. We demonstrated the expression of the NADPH oxidase components in resting NK cells, in particular $gp91^{phox}$ (CYBB) and $p22^{phox}$ (CYBA). These two proteins heterodimerize to form the flavocytochrome b558 in phagocytes. We showed that these two proteins do not interact in resting NK cells in the same conformation than in phagocytes and B-cells (**Figure 34**), and concluded that they had to be part of a different, yet still uncharacterized, molecular complex.

Transcriptomic analysis comparing resting NK cells and NKAES-NK either unexposed to targets or following 24h incubation with a NK-sensitive (REH) or resistant (RS4;11) pre-B ALL cell line revealed interesting patterns which suggest deep metabolic changes in effector cells (**Figure 37**). However, this transcriptomic analysis also showed marked differences in CYBB deficient NK cells, with a strong enrichment for *phagocytosis, endocytosis*, *receptor-mediated endocytosis* and *Fc receptor signaling* related gene ontology terms (**Figure 37**). The former suggest a compensatory mechanism for NK cells in the setting of a neutrophil defect. To some extent, this observation is reminiscent of previous works establishing that NK cells express signaling proteins which are molecular signatures of other immune lineages, including myeloid cell-related proteins (e.g. FcεRγ, SYK, and EAT-2) (Schlums et al., 2015). Functional studies addressing cellular fitness in NK cells that are engaged in a killing interaction, established distinct metabolic programs depending on target cell type and, as a corollary, on the effector pathway. We found a striking difference between the metabolic profile of NKAES-NK co-cultured with K562 (which engage granule exocytosis) versus pre-B ALL cell lines (which engage our new cytotoxicity pathway). When exposed to pre-B ALL, NKAES-NK showed a higher spare respiratory capacity (the maximal oxygen consumption reachable by mitochondrial oxidative phosphorylation activity) and a higher glycolytic potential, indicating that the engagement of different cytotoxic pathways were accompanied by different energetic requirements and, as a consequence, by different metabolic profiles (**Figures 38** and **39**). Interestingly, CYBB deficient NKAES-NK cells (which display a restricted ability to kill pre-B ALL cells, **Figure 33**) showed a remarkably altered metabolic profile, with a decrease of both spare respiratory capacity and glycolytic potential when exposed to ALL targets as compared to NKAES expanded from a normal donor (**Figures 38** and **39**). These observations suggest a role for $gp91^{phox}$ in the achievement of a metabolic fitness that correlates with killing capacity and are consistent with a recent work showing that the

phagocyte-type NADPH oxidase supports hyperglycolysis in stimulated neutrophils (Baillet et al., 2017).

The work involved in this manuscript entails major paradigm shifts. First, we have conclusively demonstrated the existence of an unconventional contact-dependent cytotoxicity pathway, distinct from the granule exocytosis and death receptor pathway, which has not been described to-date. In this process, metabolic versatility appears crucial.

Second, mirroring the fact that we are facing a novel effector mechanism in NK cells, our results strongly suggest that we have identified a new death mechanism in pre-B ALL target cells, far more complex than a regular apoptotic process in the sense that neither effector caspases 3 and 7, nor mitochondrial signaling appear to be required for the process to reach completion.

Finally, we challenge the view of the CGD pathogenesis by establishing (i) that key molecular components of the NADPH oxidase are expressed in NK cells but not in a phagocyte-type complex and (ii) that the components of the complex may have a distinct function, due to their contribution to several different complexes. We found that CYBB is dynamically and specifically regulated during NK cell activation and proliferation (**Figure 35**). CYBB deficient NK cells were impacted both in their transcriptional profile and cytotoxic function (impacting our new cytotoxicity pathway) while CYBA and NCF1 deficient NK cells were not, at least for their killing behavior. Some teams reported a NADPH oxidase among $CD8^+$ T cells (Bai et al., 2015; Wen et al., 2016) and at least one publication showed T cell blast preparations expression of a phagocyte-type NADPH oxidase recognized by the 7D5 monoclonal antibody (Jackson et al., 2004), an observation that we and others (Wada et al., 2013) did not reproduce on resting $CD3^+$ T cells (**Figure 34**). We believe the molecular role of CYBB in non-phagocyte cell lineages deserves further exploration and characterization. Notably, we tested NK cells in a flow cytometric dihydrorhodamine 123 (DHR) assay (data not shown). In this test, oxidation of DHR by ROS to a fluorescent compound, rhodamine 123, can be assessed. NK cells were negative in this assay, meaning that they did not produce detectable amounts of ROS. However, although this test is important for CGD diagnosis in clinical labs, complete myeloperoxidase (MPO) deficiency can cause a false-positive result for CGD in the DHR flow cytometric assay (i.e. phagocytes do not oxidize DHR) (Mauch et al., 2007). Thus, the DHR test is not always correlated to the clinical severity of the disease since MPO deficient patients usually do not display severe symptoms (Lekstrom-Himes and Gallin, 2000) while their cells can be DHR negative similarly to CGD patients cells. In other words, some aspects could contribute to CGD physiopathology independently of their inability to produce oxygen derivatives.

What could be the relevance of our findings? Although experimental limitations should be emphasized (most of our work was performed *in vitro* and used amplified and activated effector cells), we point out what we believe are interesting considerations:

(i) previous teams reported potentiated killing abilities among cytotoxic lymphocytes ($CD8^+$ and $CD4^+$ cytotoxic T cells as well as NK cells) in long-term assays, usually with incubation periods up to 24h (Baetz et al., 1995; Konomi et al., 1995; Lee et al., 1996; Reeves et al., 2015). The interaction between activated NK cells and autologous immature dendritic cells was also intensively investigated in the early 2000s and shown to require prolonged incubation times too (Piccioli et al., 2002; Reeves et al., 2015; Walzer et al., 2005). The precise engaged cytotoxic mechanism has not been specifically addressed but it is interesting to note that CTL from Chediak-Higashi patients exhibited a delayed killing (Baetz et al., 1995) despite a strong defect in granule exocytosis among these patients (Bryceson et al., 2012; Jessen et al., 2011), which suggests the engagement of alternative cytotoxic pathway(s) in this late effect.

(ii) many paradigms in NK cell function have been established in short term co-cultures between effector and target cells. Of note, biological relevance of limiting functional studies to short incubations because of technical constraints can be (and has been) challenged. For instance, the classical dichotomy between the two main subsets, i.e. $CD56^{bright}$ and $CD56^{dim}$ NK cells respectively considered as immunoregulatory (in link to cytokine production) and cytotoxic cell subpopulations, was queried by investigating the kinetics of their effector functions. Indeed, it was shown that the $CD56^{dim}$ subset actually produces cytokines such as IFN-γ within a very short time span (2-4h) concomitant to their cytotoxic activity (De Maria et al., 2011). The authors pointed out that cytokine production by NK cells had been routinely analyzed at late intervals (≥ 16 h after cell stimulation) and that early cytokine production had not been appropriately explored before. By analogy, our results suggest that cytotoxicity could be assessed at late intervals and not only within 4h, to unravel unappreciated killing pathways.

(iii) functional exploration of NK cells usually relies on degranulation assay and, if applicable, intracellular cytokine staining to evaluate cytokine production following appropriate stimulations (Bryceson et al., 2010). The former, based on CD107a up-regulation at the cell surface, are widely and efficiently used for the rapid diagnosis of familial hemophagocytic syndromes (Alter et al., 2004; Bryceson et al., 2012). Our results demonstrate that these tests do not allow a full exploration of NK cell functions, but rather skew functional studies toward preconceived notions.

(iv) as a corollary, we suggest that the elucidation of our novel cytotoxicity pathway could find at least two further paths for development. First, it would open new fields of investigation in NK cell contribution to innate immunity and pathology beyond antiviral and antitumoral cytotoxicity; second, it would establish the need for new functional assay(s) to improve complete NK cell exploration. Nevertheless, these future developments would make sense on the condition that this novel cytotoxicity pathway could be shown to contribute significantly to clinically relevant disorders.

(v) finally, we believe that this novel effector mechanism is also engaged by $CD8^+$ T cells. These cytotoxic lymphocytes share molecular activation pathways and effector responses with NK cells (Narni-Mancinelli et al., 2011; Sun and Lanier, 2011) and no effector function was reported to be strictly specific of either one. However, their respective effector behavior are not necessarily identical. Thus, a study exploring effector lymphocytes from Chediak-Higashi patients showed that $CD8^+$ CTL, but not NK cells, could exhibit a normal cytotoxic function further correlating with late-onset or absent HLH (Jessen et al., 2011). Nevertheless, this observation could be explained by distinct activation rules and/or threshold between both effector cell types. Preliminary data in our labs showed that cytokine-induced killer cells (CIK), which are generated *in vitro* from $CD3^+$ T cells (Durrieu et al., 2014), also have an increased cytotoxicity against pre-B ALL targets when co-incubated for 24h (**Figure S3**). Interestingly, this cytotoxicity did not involve granule exocytosis since CIK cells did not significantly degranulate (data not shown).

In conclusion, we demonstrate that activated NK cells can engage a previously unappreciated contact-dependent cytotoxicity pathway which is distinct from granule exocytosis and death receptors. Furthermore, the corresponding apoptotic-like engaged cell-death appears to rely on unconventional molecular requirements. Eventually, we establish a dynamic metabolic fitness in NK cells depending on the target cells they encounter and possibly the cytotoxicity pathway they engage. Dealing with pre-B ALL target cells, $gp91^{phox}$ expression is important for the NK cell cytotoxicity. We further demonstrate that $gp91^{phox}$ is expressed and dynamically regulated among NK cells and suggest a potential role for this protein in the metabolic control of effector cell function.

These discoveries deserve further exploration and characterization to establish their contribution to the immune function.

4.2. PERSPECTIVES

A basic model for further investigation is presented in **Figure 42**. It depicts the NK killing process as a sequence of defined events providing key nodes to decipher.

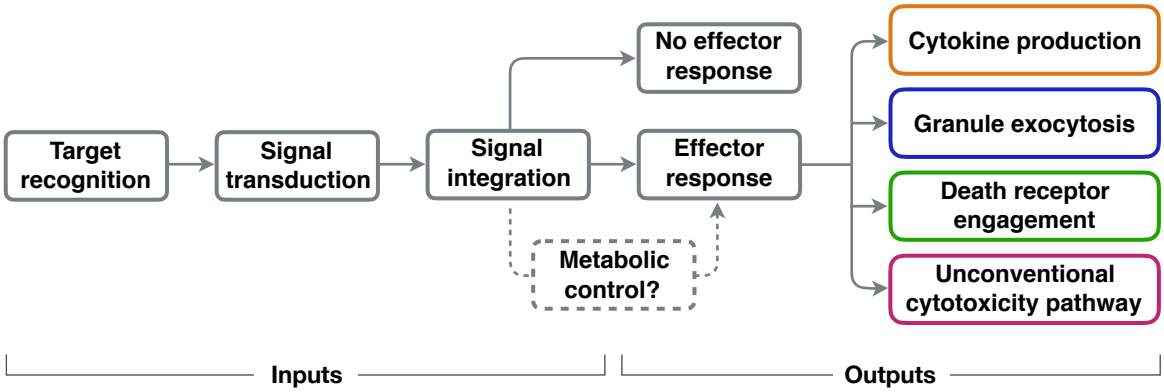

Figure 42. A proposed schematic representation of the steps involved in the NK killing process.
Effector cells recognize target cells by activating and inhibiting membrane receptors which engage various signaling pathways, all integrated in the "decision to kill" (inputs). The effector response (outputs), possibly via a metabolic control, is in the form of cytokine production, granule exocytosis, death receptor engagement and our described unconventional cytotoxicity pathway.

We initially made the choice not to work with a mouse model but instead to favor primary human NK cells that have been activated and amplified *in vitro* to generate a sufficient amount of cells (Imai et al., 2005). Murine NK cells display common features with their human counterparts but they also display noteworthy distinctions that would have limited the scope of our study. For instance, granulysin, which is an important molecule for the elimination of intracellular bacteria and parasites by cytotoxic lymphocytes in humans, has no known murine homolog (Dotiwala et al., 2016; Walch et al., 2014). Similarly for target cell death, caspase 10, which is a close homolog of caspase 8 in humans, is absent in rodents (Reed et al., 2003). Caspase 10 is considered to (1) play a role as an initiator of the extrinsic apoptotic pathway mediated by TRAIL and FASL (Sprick et al., 2002) with some similarities to caspase 8, and also to (2) participate to proper signaling involved in apoptosis and autophagy (Lamy et al., 2013; Lee et al., 2007). More recently, it has been suggested that, far from having redundant functions, caspase 10 negatively regulates DISC-mediated caspase 8 activation and contributes to cell commitment between survival and cell death (Horn et al., 2017). Also, we postulate that *in vivo* studies will be of significant relevance. Indeed, a recent study has demonstrated the ability of activated NK cells to control pediatric pre-B ALL in NSG

mice (Kübler et al., 2014). We developed expertise in humanized mice models as well as in patient-derived xenografts (PDX) and plan to validate our findings using these preclinical mouse models.

Based on our work, subsequent experiments should be performed to better assess the role of gp91^{phox} function in the above-mentioned model (**Figure 42**):

A - Biochemical characterization of gp91^{phox} in NK cells

We have demonstrated that both gp91^{phox} and p22^{phox} proteins can be detected in resting NK cells, but not within a phagocyte-type NADPH complex.

On one hand, we will establish protein subcellular localization: cellular fractionation will be performed by centrifugation on an OptiPrep gradient as described (Baginska et al., 2013; Noubade et al., 2014) and fractions will be tested by nanofluidic proteomic immunoassay.

On the other hand, to identify physiologically-relevant protein-protein interactions, we propose to perform co-immunoprecipitation coupled to mass spectrometry. This approach has already been performed with monoclonal antibodies directed against gp91^{phox} (clone 54.1, that we also used for nanofluidic proteomic immunoassays) or p22^{phox} (clone 44.1) (Noubade et al., 2014; Raad et al., 2009; Zhu et al., 2006). We will apply this protocol to both resting and activated NK cells and will use CGD cells as negative controls to determine irrelevant antibodies' binding.

This combined strategy should allow us to characterize gp91^{phox} cell localization and its molecular partners.

B - Investigation of NK cells antifungal activity

CGD pathophysiology is traditionally linked to phagocytes (neutrophils, monocytes and macrophages) dysfunction due to defective NADPH oxidase activity (Kuhns et al., 2010). Clinically, it is characterized by severe recurrent bacterial and fungal infections with a limited spectrum of pathogenic species as well as dysregulated inflammatory response resulting in granuloma formation and inflammatory disorders such as colitis (Marciano et al., 2015; Song et al., 2011). The most frequently involved extracellular but also intracellular pathogens include *Staphylococcus*, *Serratia*, *Nocardia*, *Burkholderia* and *Aspergillus* species (Marciano et al., 2015). Fungal infections by *Aspergillus* species remain the leading cause of mortality (Leiding and Holland, 2016). Of note, although phagocytes of all CGD patients (regardless of the causative mutated gene) display defective NADPH oxidase function with abnormal respiratory burst (Kuhns et al., 2010), there are remarkable clinical differences between gp91^{phox}-deficient (X-linked) and other CGD patients. The former are more prone to

Aspergillus infection (Marciano et al., 2015) and display a lower survival rate (Kuhns et al., 2010). Although this observation could be explained by a generally lower residual ROS production among X-CGD patients (Kuhns et al., 2010; Marciano et al., 2015), it does not rule out a possible contribution of other immune cell populations. For instance, Kostmann's syndrome, which is caused by mutations in the *HAX1* gene and often considered as the paradigm of congenital neutropenia, usually presents with bacterial but no fungal infections except as a complication of prolonged antibiotic therapy (Antachopoulos, 2010; Donadieu et al., 2011; Skokowa et al., 2017).

We hypothesize that NK cells could be involved in the control of *Aspergillus* infection and that this role could depend on $gp91^{phox}$. NK cells cytotoxicity (either directly or through their crosstalk with neutrophils) against yeast fungus such as *Cryptococcus* and *Candida* species has been well documented (Bär et al., 2014; Li et al., 2013; Ma et al., 2004). A few works have also addressed their function against filamentous fungus such as *Aspergillus* species and suggested a link between NK-cell counts after HSCT and invasive aspergillosis (Stuehler et al., 2015) or even showed a direct NK cell antifungal activity against *Aspergillus* hyphae but not conidia (Schmidt et al., 2011; 2013). More recently, CD56 has been demonstrated to play a role in the *Aspergillus* mediated NK cell activation and was proposed as a pathogen recognition receptor (Ziegler et al., 2017). Besides, it has been widely documented that there is crosstalk between neutrophils and NK cells serving to reciprocally modulate their responses (Scapini and Cassatella, 2014).

As our data suggests that metabolism is a key feature of $gp91^{phox}$-dependent NK cell function, we propose to study two readouts using primary cells from normal donors or CGD patients: (i) NKAES-NK cells cytotoxicity against *Aspergillus fumigatus* and (ii) fungus-induced metabolic changes when resting or activated NK cells will be facing *Aspergillus* hyphae or conidia.

Furthermore, we believe that studying inflammasome-derived cytokines induced changes (such as IL-18 and IL-1β (de Zoete et al., 2014; Guo et al., 2015) on NK cells metabolism would be interesting since inflammasome-derived IL-18 has been showed to prime NK cell cytotoxicity to kill infected hepatocytes in mice infected with *Chromobacterium violaceum*, an intracellular bacteria (Maltez et al., 2015) which is an opportunistic pathogen for CGD patients (Song et al., 2011).

C - NK cells heterogeneity: identification of the novel effector mechanism

We previously discussed phenotypic as well as behavioral diversity among cytotoxic lymphocytes (**§1.4**). As shown by others (Choi and Mitchison, 2013; Vanherberghen et al.,

2013; Vasconcelos et al., 2015), cytotoxicity is not a rapid and homogeneous response to target cells. *In vitro*, some effector clones are endowed with a serial killing activity when facing target cells. However, *in vivo* studies tend to support a lower rate of killing at the single effector cell level and a sustained role for dynamic interactions and cooperation among cytotoxic cells (Halle et al., 2016). There is currently no consensus on the order of magnitude of *in vivo* killing rates in either experimental models or human diseases. *In vivo* comparative studies also showed some differences between NK cells and $CD8^+$ T cells (Deguine and Bousso, 2013; Deguine et al., 2010). In comparison to the latter, the former establish contacts which have been described as mainly dynamic.

Our RNAseq experiment showed that the responses to REH or RS4;11 cells are, in general, larger in effect size in X-linked CGD patient's samples than in the controls (**Figure 43**). Because we had only one X-CGD patient for which NK cell expansion generated a sufficient amount of cells to be tested against pre-B ALL cell lines, we still consider these results as very preliminary (even though we observed for other samples a perfect separation per condition and donor with unsupervised clustering using PCA (**Figure 36**A)).

Figure 43. Comparison of effect sizes for response to REH (and RS4;11, and their difference) for NKAES-NK cells from controls (n = 4 per condition) and a X-CGD patient.

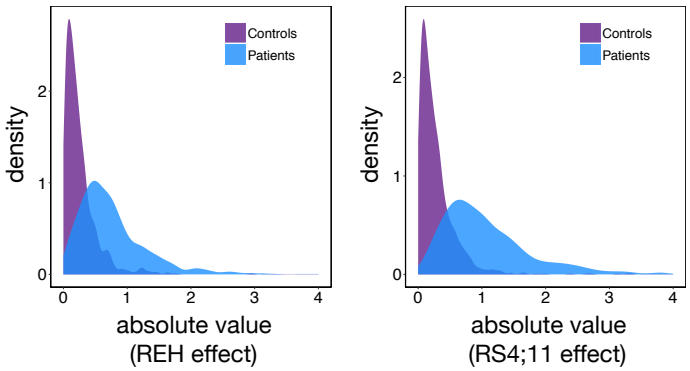

However, we observed that the specific loss of the *CYBB* gene led to a dramatic change in the effect sizes for response to sensitive or resistant pre-B ALL cell lines (**Figure 43**). In other words, this implies that among activated NK cells exposed to targets, CYBB deficiency induces many other genes to vary in terms of expression level, which could suggest a role for $gp91^{phox}$ as a node in a gene regulatory network.

Among NK cell effector functions, cytokine production and cytotoxicity have been uncoupled (Rajasekaran et al., 2013; Vivier et al., 2013). However, at the single cell level, it has not been studied whether single effector functions are characteristic of specific committed subsets or can be engaged by a same unique NK cell (**Figure 44**).

Why don't NK cells degranulate when they face pre-B ALL cells? Rouce *et al*. suggested that TGF-β is a major mediator of immune evasion in childhood pre-B ALL (Rouce et al., 2016). Deep modulation of NK cell effector functions by TGF-β has been documented and this

modulation was linked to effector cell metabolism (Gao et al., 2017; Viel et al., 2016). It is possible that leukemia-derived TGF-β is a triggering signal for a metabolic reprogramming and effector switch in NK cell functions.

Our results show different metabolic profiles depending on the target cell type co-cultured with NKAES-NK cells. They also demonstrate that gp91^{phox}/CYBB is expressed and dynamically regulated among NK cells and suggest that NKAES-NK cells from X-CGD patients have a defect in our novel cytotoxic pathway.

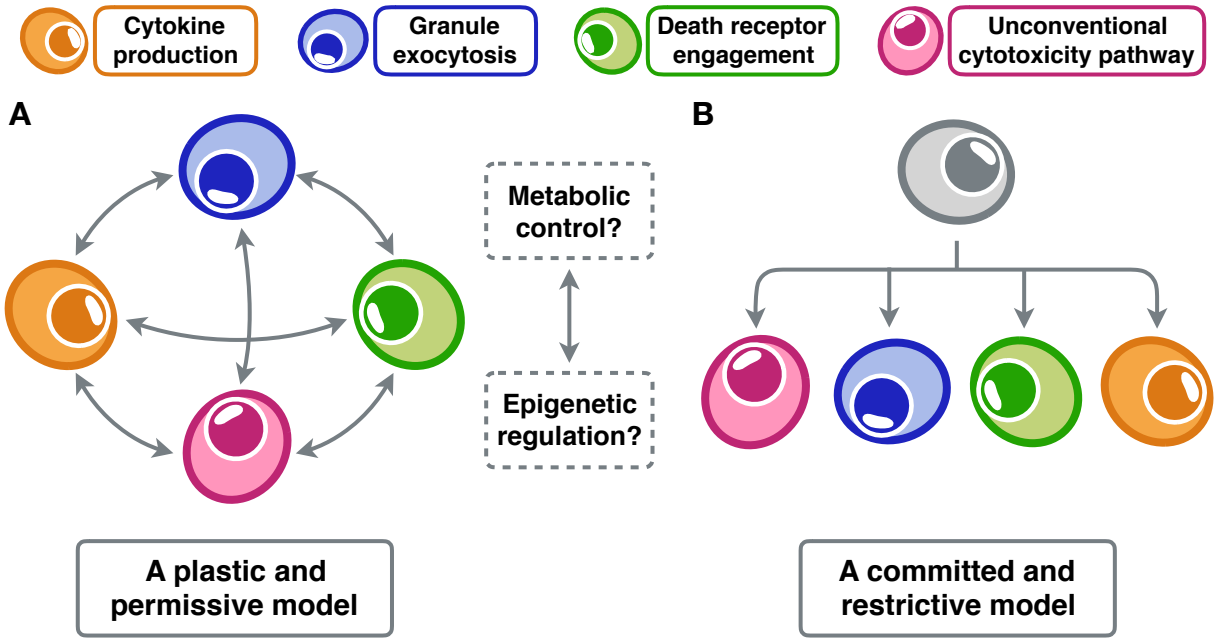

Figure 44, related to figure 42. Proposed models for NK cell effector responses at the single cell level: a metabolic fingerprinting?

Cytotoxic cell output can engage an effector response (**Figure 42**) in the form of cytokine production, granule exocytosis, death receptor engagement and our unconventional cytotoxicity pathway. At the single cell level, one may propose two alternative models: a plastic and permissive model (**A**) which postulates possible switches between effector responses, and a committed and restrictive model (**B**) which proposes that distinct NK clones engage each type of response. Whatever the model, we hypothesize the metabolic state to be a central checkpoint, possibly through a crosstalk with epigenetic regulation.

As a working hypothesis, we propose that a global and versatile metabolic platform could control NK cell effector function. In this model, gp91^{phox} could be involved in the control of our novel cytotoxicity pathway.

To gain further insight, we propose to study the respective importance of oxidative phosphorylation and glycolysis as well as to dissect the metabolic pathways through integrative metabolomics and proteomics profiling of NKAES-NK cells facing pre-B ALL targets (Geiger et al., 2016; Hukelmann et al., 2016; Ross et al., 2016; Tan et al., 2017). To precisely map each pathway, effector cells from patients with defective granule exocytosis (such as

PRF1 or UNC13D deficient ones) and the use of death receptor resistant target cells will be of significant interest.

To some extent, this view (**Figure 44**) is reminiscent of the epigenetic landscape depicted by Conrad Waddington (Waddington, 1957). Interestingly, epigenetic modifications have been linked to memory NK cell development (Lee et al., 2015; Schlums et al., 2015) and to the regulation of NK cell effector functions (Cichocki et al., 2013). Cell fate and function integrate an interplay between metabolism, epigenetics and transcription (Etchegaray and Mostoslavsky, 2016; Kaelin and McKnight, 2013; Lu and Thompson, 2012), which has also shown to be relevant for the immune system function (Xu et al., 2017). Thus, we think that studying epigenetic and metabolic control of NK cell effector functions could be an interesting and complementary approach. Eventually, understanding the precise metabolic requirements could open new perspectives to **restore** an effector function (Fisicaro et al., 2017; Kawalekar et al., 2016; Schurich et al., 2016) or **favor the switch** between effector functions by cellular reprogramming.

D - Target cell sensitivity or resistance: identification of the death process in pre-B ALL

Our results support a death mechanism which has never been reported. In the meantime, understanding the mechanism of pre-B ALL cells death is crucial to unravel the new cytotoxic pathway. When we looked at the metabolic profile of pre-B ALL and K562 cell lines, we observed that although glycolysis was similar, pre-B ALL cells had a much lower oxidative phosphorylation than K562 cells, with the lowest OXPHOS status being observed in the resistant RS4;11 cell line (**Figure 41**). Besides, we demonstrated that primary pre-B ALL blasts could be separated between sensitive and resistant cells (**Figures 19**C and **19**D). We think that a deeper investigation of pre-B ALL cells' metabolism is necessary: in particular, we propose to test whether basal metabolism could **predict** the sensitivity of blasts to NK cell killing.

To discover the main genetic components of our novel cell death pathway in pre-B ALL cells, we propose to perform a genome-scale CRISPR/Cas9-based screening (**Figure 45**).

Following this strategy, we expect that for sensitive pre-B ALL cell lines, the cell viability will be negatively impacted with the exception of the subset of cells that contain deletions in genes essential for cell death associated with our new pathway. This will enrich cells that contain sgRNAs that have produced the deficiency in expression of essential cell death genes (positive selection). On the contrary, for the resistant RS4;11 cell line, which normally survives well facing the cytotoxic insult of NKAES-NK, we expect a depletion of the cells that

contain the sgRNAs that produced the deletion of genes (negative selection) that counteract our new pathway.

Such an approach has been recently successfully used for the identification of genes which are essential for CTL effector function (Patel et al., 2017). However, it has never been employed for NK cell mediated cytotoxicity or to decipher essential genes specific of each of the engaged effector pathways.

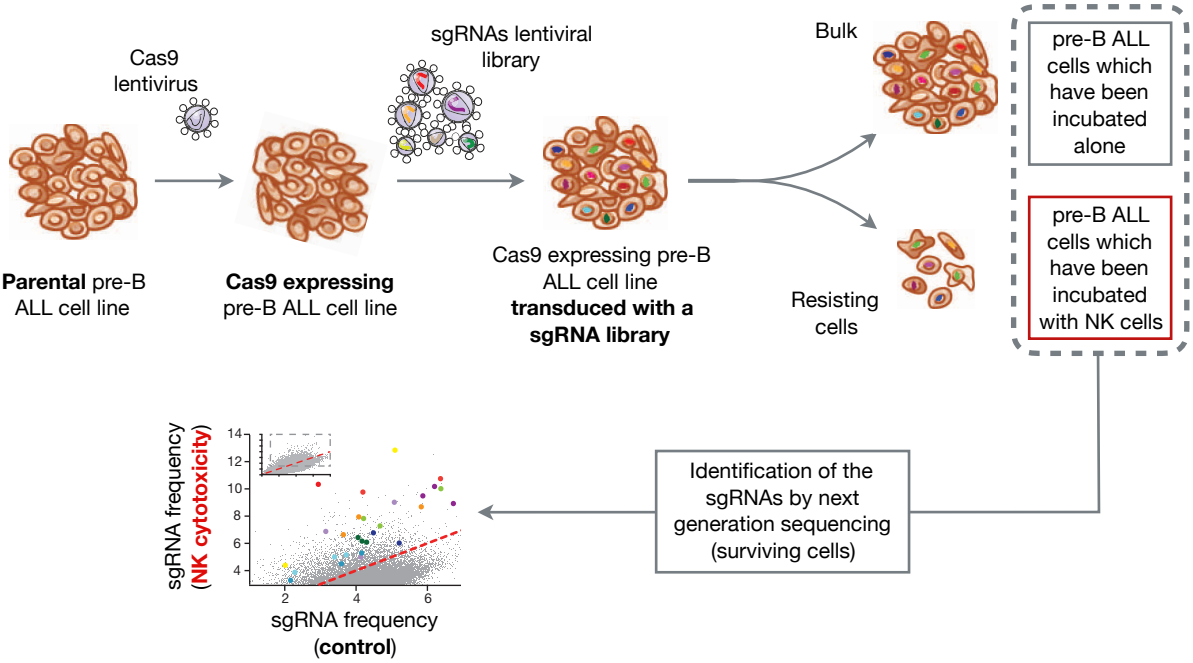

Figure 45. Experimental design for a genome-scale CRISPR/Cas9-based screening.
Sensitive and resistant pre-B ALL cell lines are infected at low multiplicity of infection (MOI) to ensure that blasts receive only a single viral particle (here, a strategy using a two-plasmid system is depicted; Shalem et al., 2014). For each cell line, a first group is exposed to NKAES-NK cells. The second group of cells, acting as the negative control group cultured under the same condition, is not exposed to effector cells. Following incubation, the genomic DNA is extracted and sgRNA amplified with specific primers.

Finally, although this screening would allow key molecular pathways to be pinpointed, we think that our results strongly support the hypothesis of a non-genetic origin of target cell resistance to NK cell mediated cytotoxicity (**Figure 46**).

Through the CRISPR/Cas9-based strategy, we generated knockout clonal target cell lines. Interestingly, when clonal pre-B cell lines have been used, we measured a similar NK killing rate compared to parental bulk cell lines (for the sensitive cell lines NALM6, REH and 697). This observation suggests that resisting pre-B target cells (among an otherwise sensitive cell line) do not display a heritable phenotype but rather a non-genetic origin of cellular variability to NK cell induced-apoptosis, which calls to mind previous works in the field of

cellular drug resistance (Flusberg and Sorger, 2015; Flusberg et al., 2013; Shaffer et al., 2017; Spencer et al., 2009). Analysis of these complex phenotypes could be conducted combining genome-scale CRISPR/Cas9-based screening and single cell RNAseq (Dixit et al., 2016), a technology that we are currently using for ongoing experiments (Macosko et al., 2015).

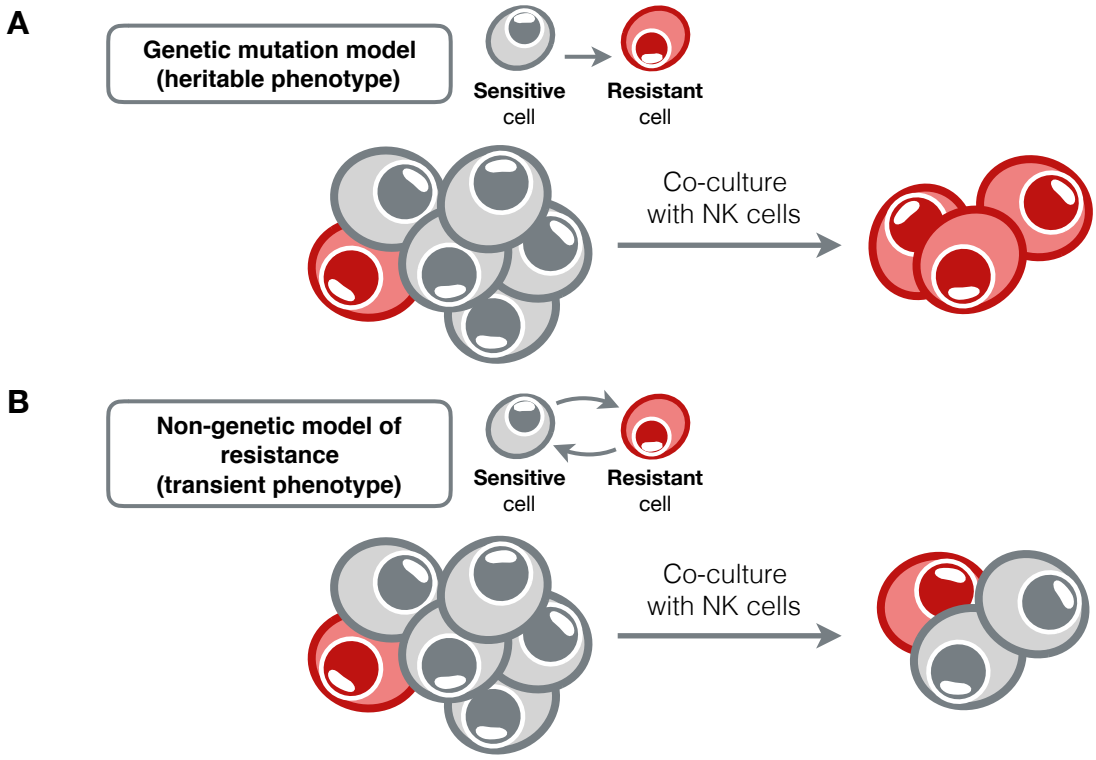

Figure 46. Alternative models for resistance to NK cell mediated cytotoxicity.
(**A**) Resistant cells are genetically distinct from their sensitive counterparts. In that model, when a saturating amount of effector cells is used only resistant clones are recovered.
(**B**) Resistant cells represent a transient state. Here, when a saturating amount of effector cells is used, both resistant and sensitive clones will be recovered following NK cell cytotoxicity.

To conclude, our findings challenge the dogma of pre-B ALL resistance to NK cell cytotoxicity; and of the absence of gp91^{phox} expression and role in NK cells. Further works should provide a more complete understanding of this novel cytotoxicity pathway and induced target cell death.

CHAPTER 5.
APPENDICES AND SUPPLEMENTARY MATERIAL

5. SUPPLEMENTARY MATERIAL AND APPENDICES

5.1. SUPPLEMENTARY MATERIAL

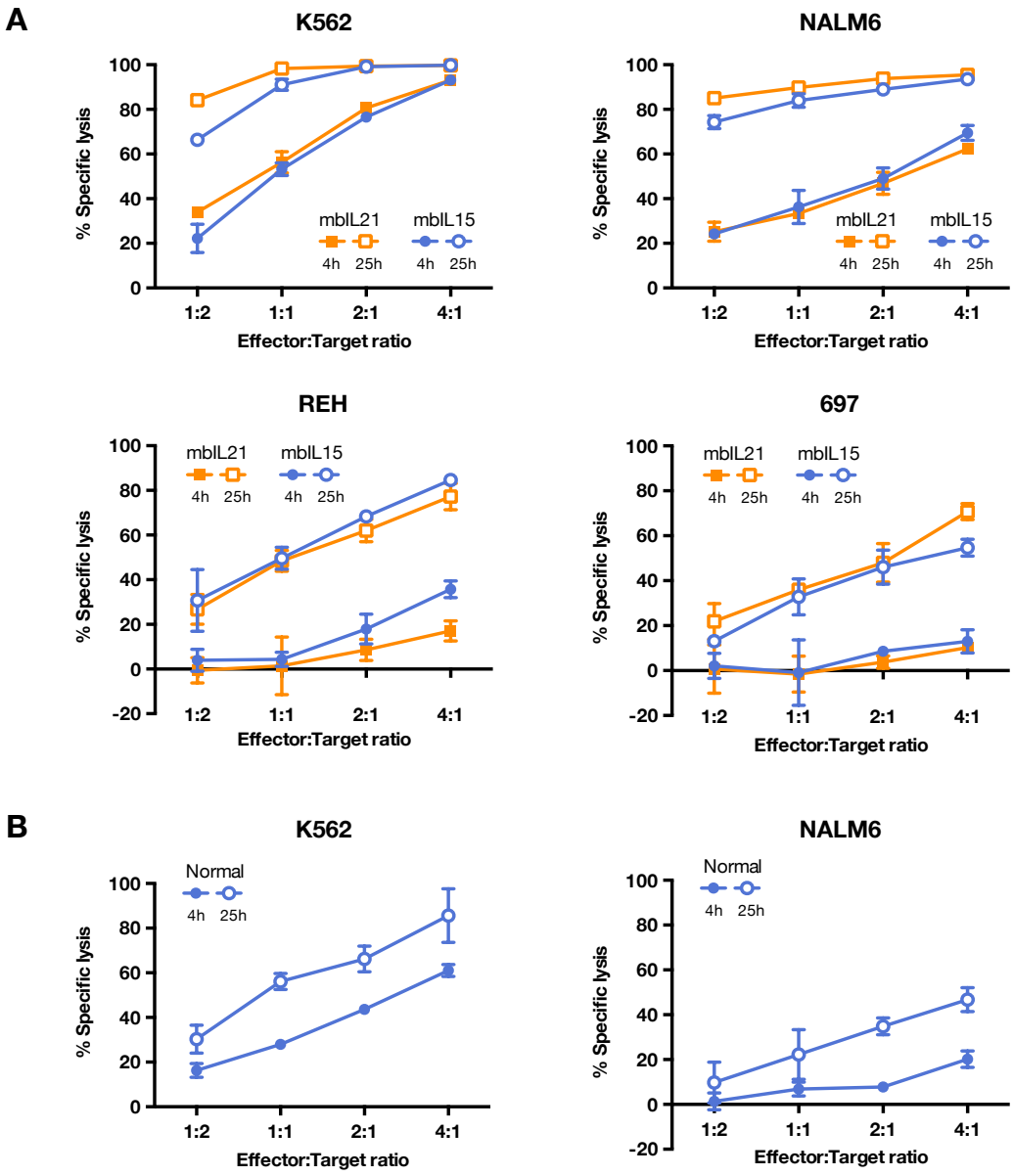

Figure S1, related to Figure 19. Killing increase against leukemic target cells is not restricted to mbIL-15 activated NK cells.

(**A**) Representative graphs showing early and late leukemic killing by mbIL-15 and mbIL-21 NKAES-NK cells against K562, REH, NALM6 and 697 cell lines. Results from two normal donors.

(**B**) Early and late leukemic killing by resting NK cells against K562 and NALM6 cell lines. Results from one normal donor.

Shown are percentages of cytotoxicity (relative to cultures with no effector cells) in cocultures lasting 4 and 25h.

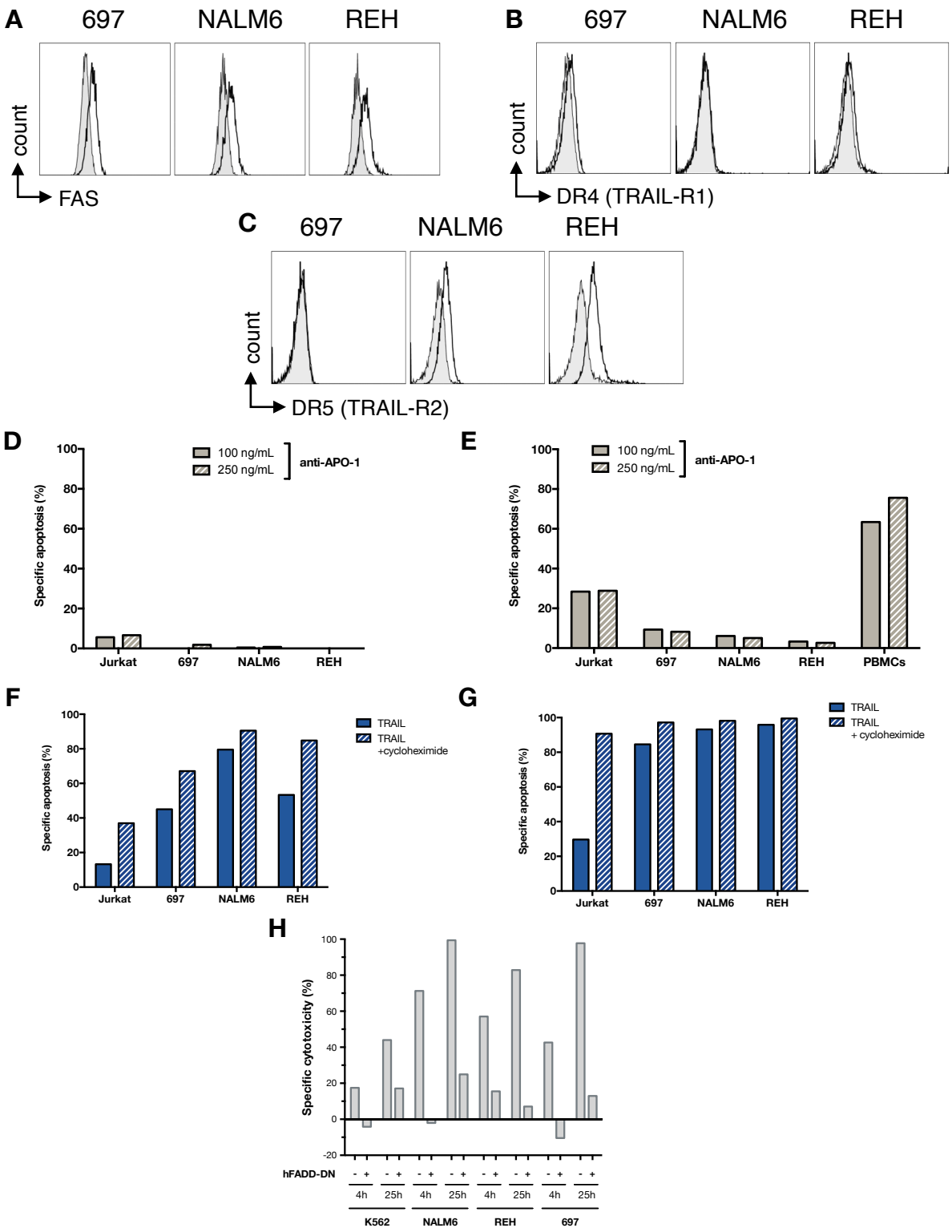

Figure S2, related to Figure 27. Pre-B ALL cell lines are sensitive to TRAIL mediated apoptosis.

(**A**-**C**) Overlay histograms showing FAS (**A**), DR4 (**B**) and DR5 (**C**) surface expression by 697, NALM6 and REH cell lines (isotype control is depicted in gray).

(**D**-**G**) Percentages of specific apoptosis among APO-1 (100 and 250 ng/mL; Jurkat cell line and PBMCs were used as positive controls) and SuperKillerTRAIL (250 ng/mL, with or without 0,1 µg/mL cycloheximide to potentiate killing effect; Jurkat cell line was used as positive control) treated 697, NALM6 and REH cell lines.

(**H**) Specific cytotoxicity of WT and hFADD-DN transduced K562, NALM6, REH and 697 cell lines following 4h and 25h incubation with SuperKillerTRAIL (250 ng/mL).

Table S1, related to Figure 36. Number of hits using the Emma nested models 1 and 2.

	Contrast	Number of hits FDR<0.1 (0.05)
1.	differential expression between patients and controls for resting NK cells	317 (176)
2.	disease effect on NKAES cells	197 (108)
3.	disease effect on NKAES cells exposed to REH	128 (67)
4.	disease effect on NKAES cells exposed to RS4;11	637 (425)
5.	activation effect on controls	9723 (8489)
6.	activation effect on patients	10480 (9434)
7.	differences in activation effects between patients and controls	464 (289)
8.	REH effect in controls' NKAES's	3713 (2875)
9.	REH effect in patient' NKAES's	981 (752)
10.	Difference between REH effect in patient minus controls' NKAES's	902 (682)
11.	RS4;11 effect in controls' NKAES's	3140 (2464)
12.	RS4;11 effect in controls' NKAES's	1219 (881)
13.	Difference between RS4;11 effect in patient minus controls' NKAES's	1257 (941)
14.	RS4;11 minus REH effect in controls' NKAES's	410 (324)
15.	RS4;11 minus REH effect in patient' NKAES's	531 (434)

FDR stands for false discovery rate.

Table S2, related to Figure 37. Enrichment of GO Biological process terms.

Contrast	FDR threshold	Number of genes in target	Number of terms
8(+)	0.01	874	97
8(-)	0.01	1033	99
11(+)	0.01	742	45
11(-)	0.01	898	30
14(+)	0.2	321	51
14(-)	0.2	217	35
1(+)	0.2	272	16
1(-)	0.2	405	12

For each contrast, + or – stand for up-regulated or down-regulated genes respectively.

Table S3, related to Figure 37. Enrichment of GO Cellular components terms.

Contrast	FDR threshold	Number of genes in target	Number of terms
8(+)	0.01	874	16
8(-)	0.01	1033	13
11(+)	0.01	742	3
11(-)	0.01	898	13
14(+)	0.2	321	6
14(-)	0.2	217	9
1(+)	0.2	272	15
1(-)	0.2	405	14

For each contrast, + or – stand for up-regulated or down-regulated genes respectively.

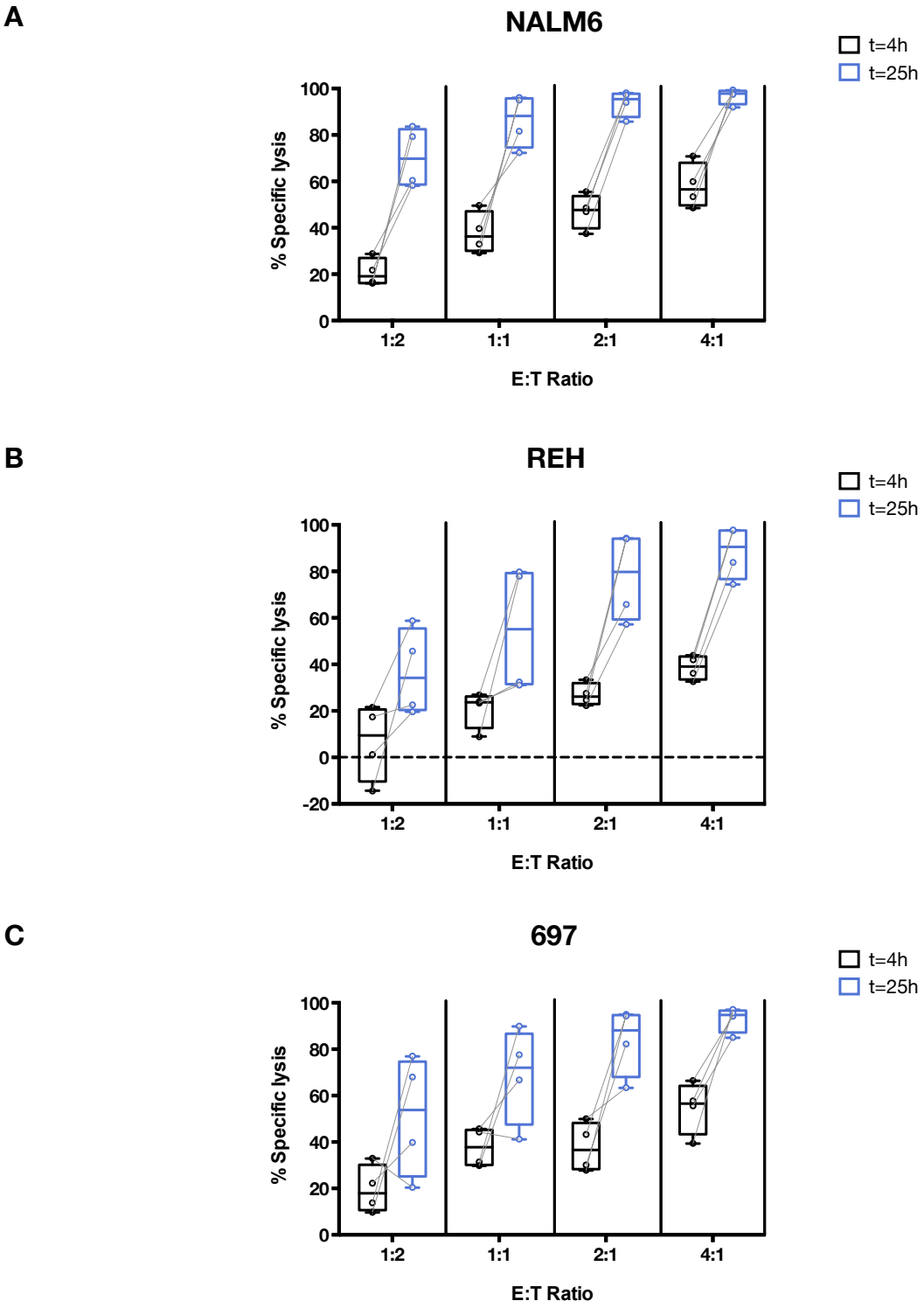

Figure S3. CIK effector cells cytotoxicity toward pre-B ALL targets increases following a prolonged incubation.

(**A**-**C**) Representative graphs showing early and late leukemic killing by CIK cells. Shown are percentages of cytotoxicity (relative to cultures with no effector cells) in cocultures lasting 4 and 25h. Shown are mean.

Results from three normal donors tested against NALM6 (**A**), REH (**B**) and 697 (**C**) pre-B ALL cell lines.

Statistics did not reach significance (Wilcoxon matched-pairs signed rank test).

5.2. APPENDICES

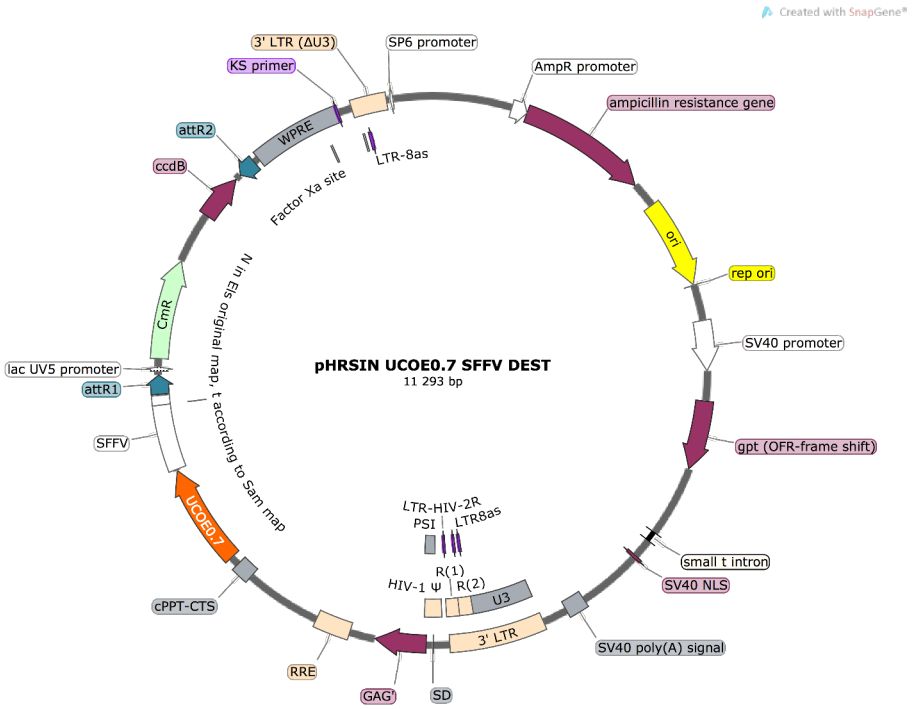

Appendix 1. pHRSIN UCOE0.7 SFFV DEST (plasmid map).

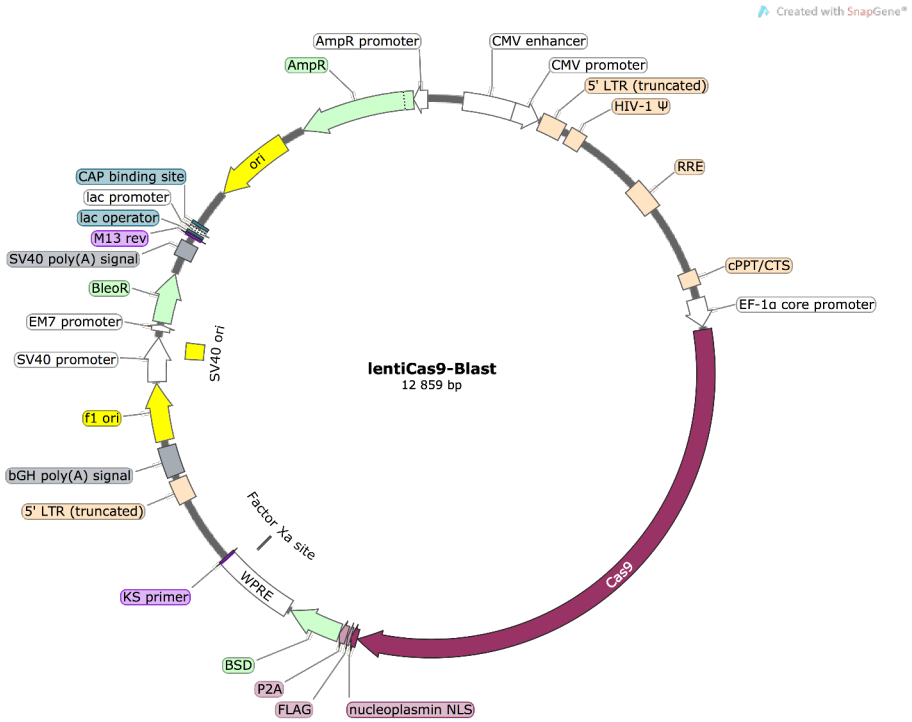

Appendix 2. lentiCas9-Blast (plasmid map).

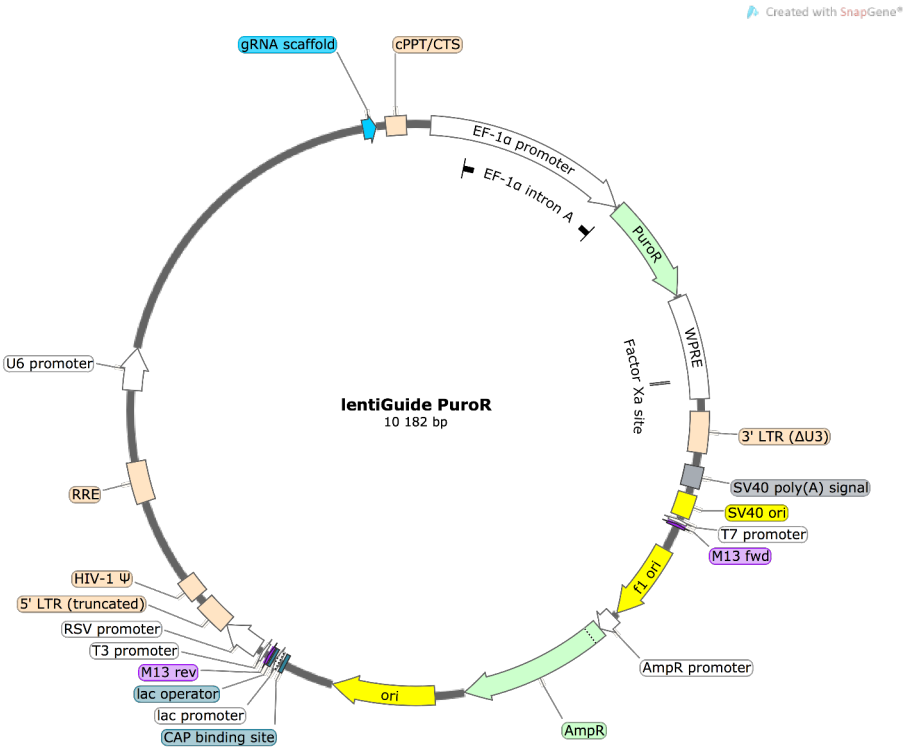

Appendix 3. lentiGuide PuroR (plasmid map).

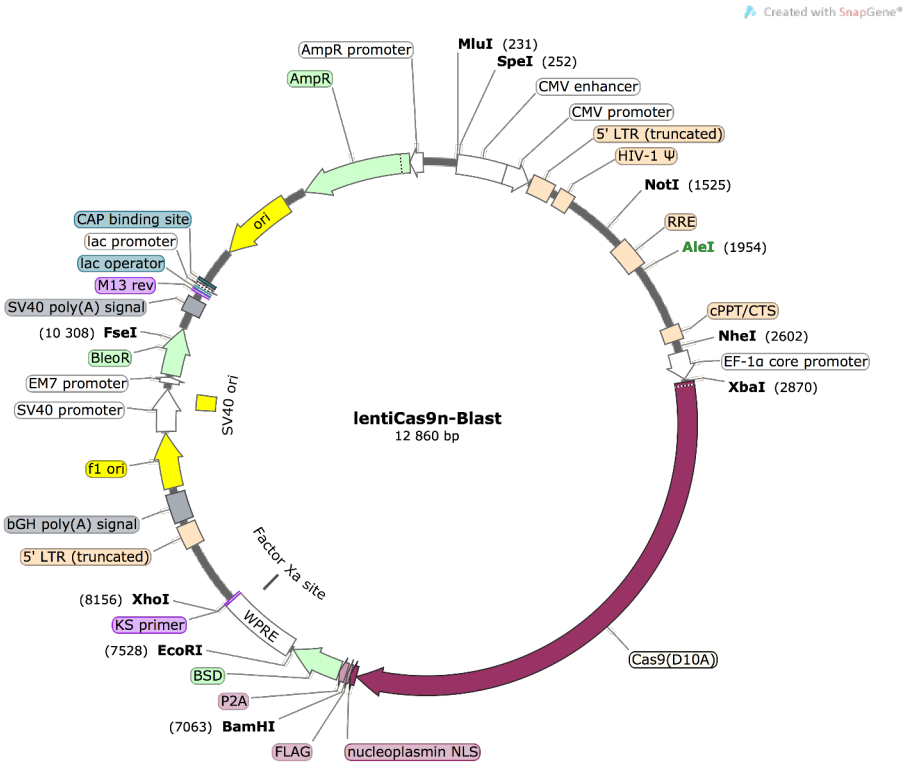

Appendix 4. lentiCas9n-Blast (plasmid map).

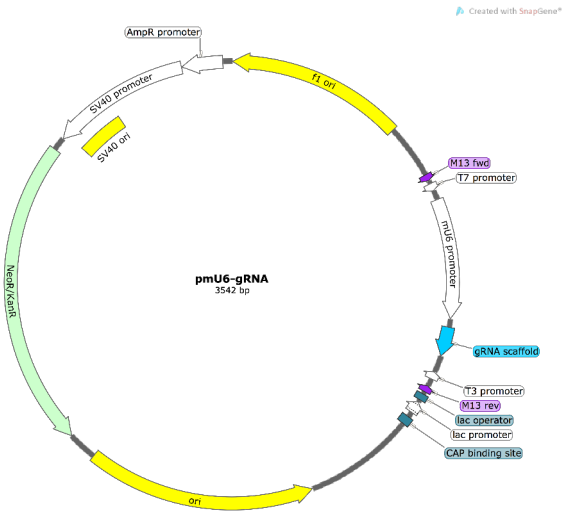

Appendix 5. pmU6-gRNA (plasmid map).

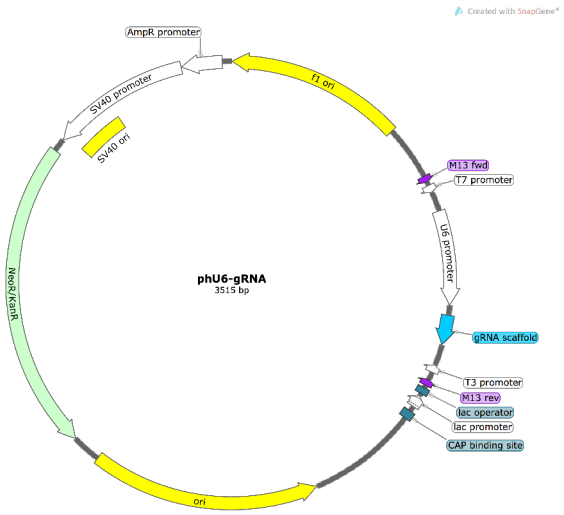

Appendix 6. phU6-gRNA (plasmid map).

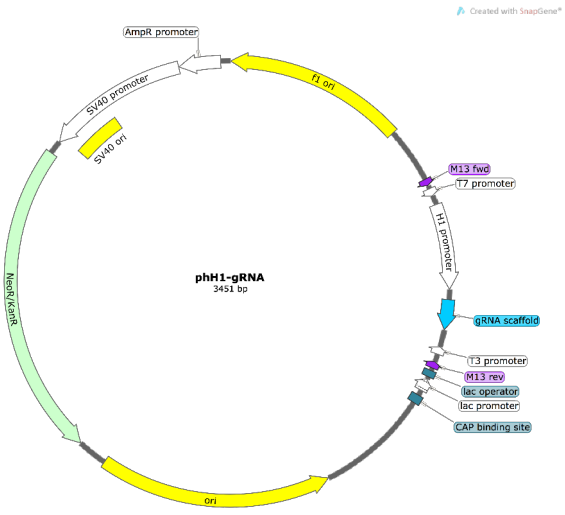

Appendix 7. phH1-gRNA (plasmid map).

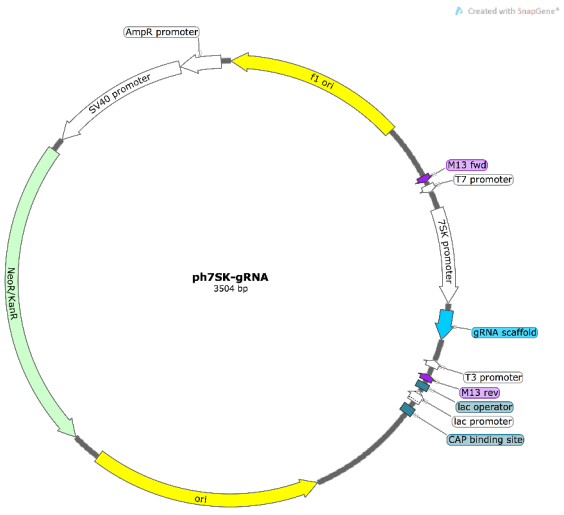

Appendix 8. ph7SK-gRNA (plasmid map).

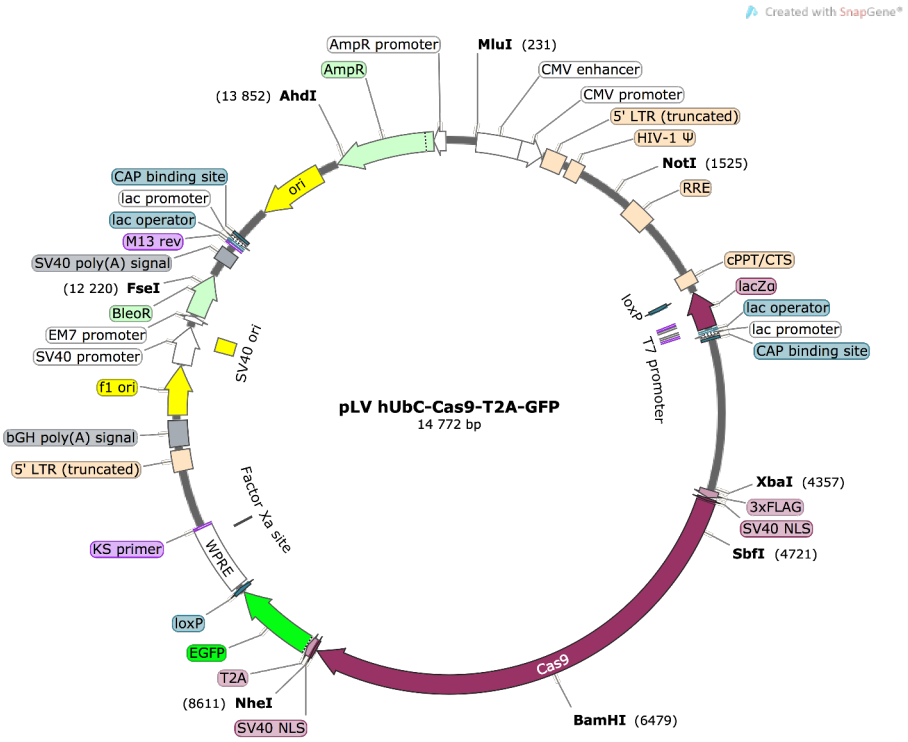

Appendix 9. pLV hUbC-Cas9-T2A-GFP (plasmid map).

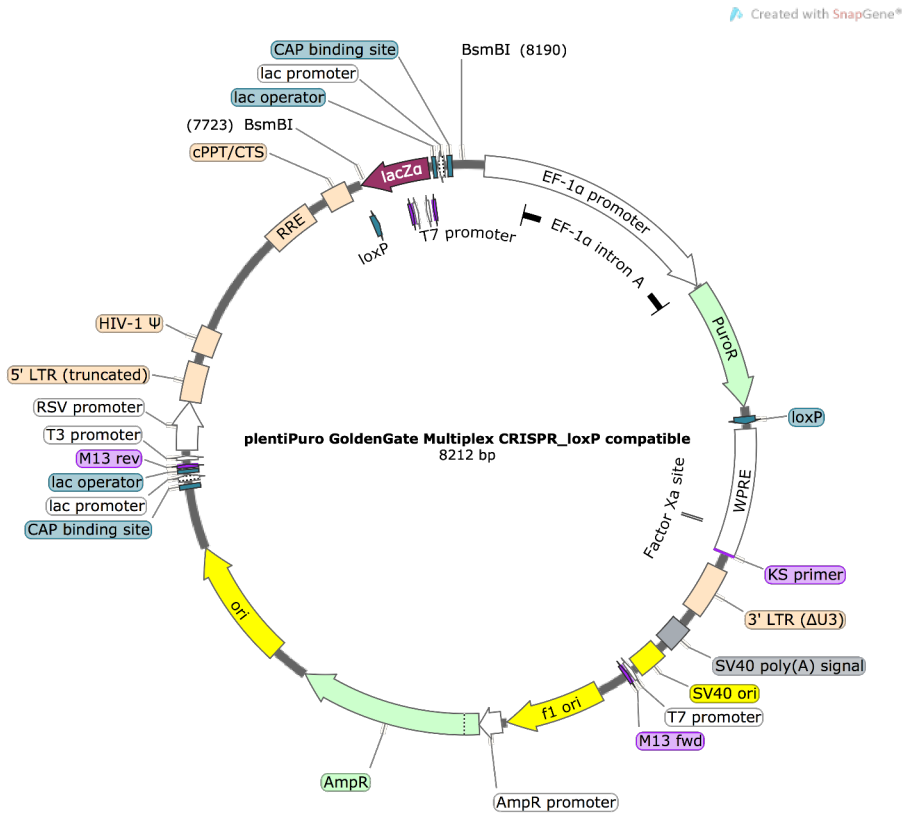

Appendix 10. lentiGuide-Puro multiplex loxP (plasmid map).

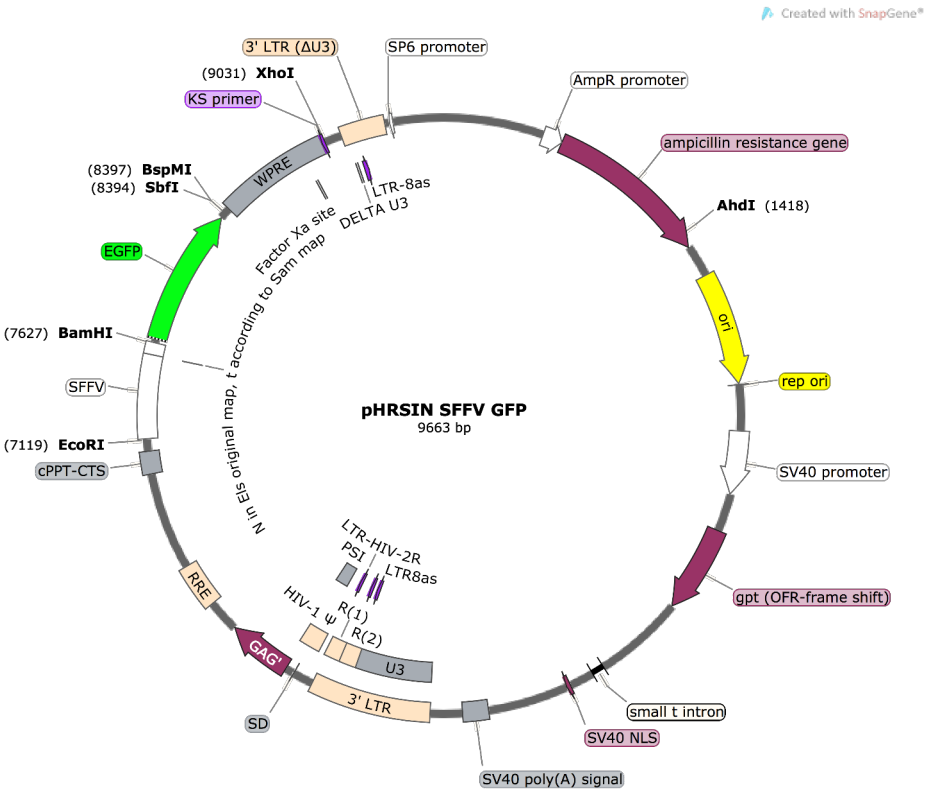

Appendix 11. pHRSIN SFFV GFP (plasmid map).

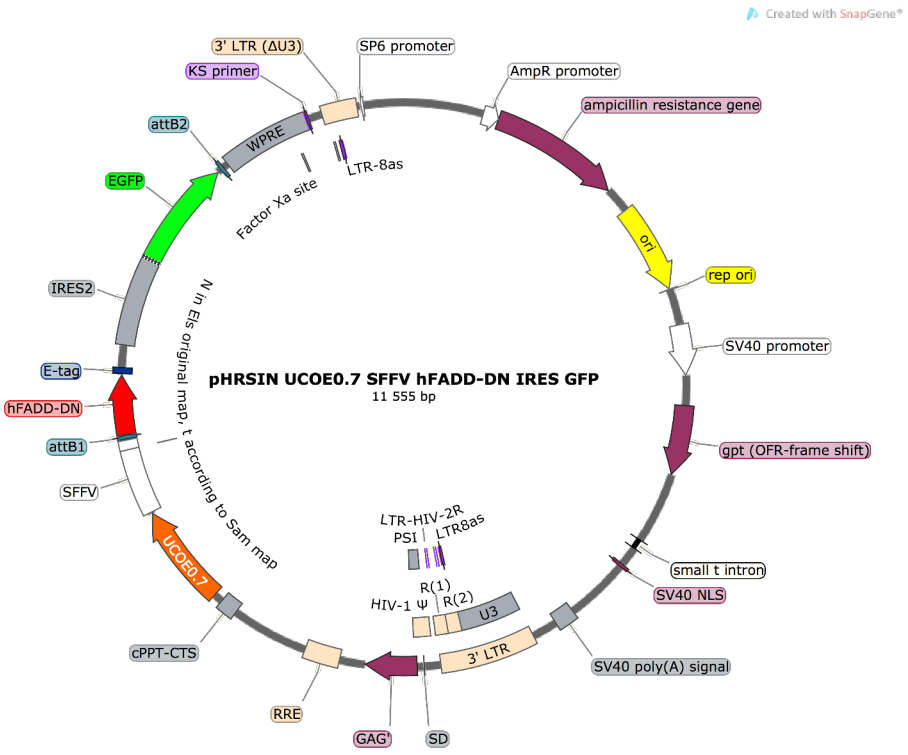

Appendix 12. pHRSIN UCOE0.7 SFFV hFADD-DN IRES GFP (plasmid map).

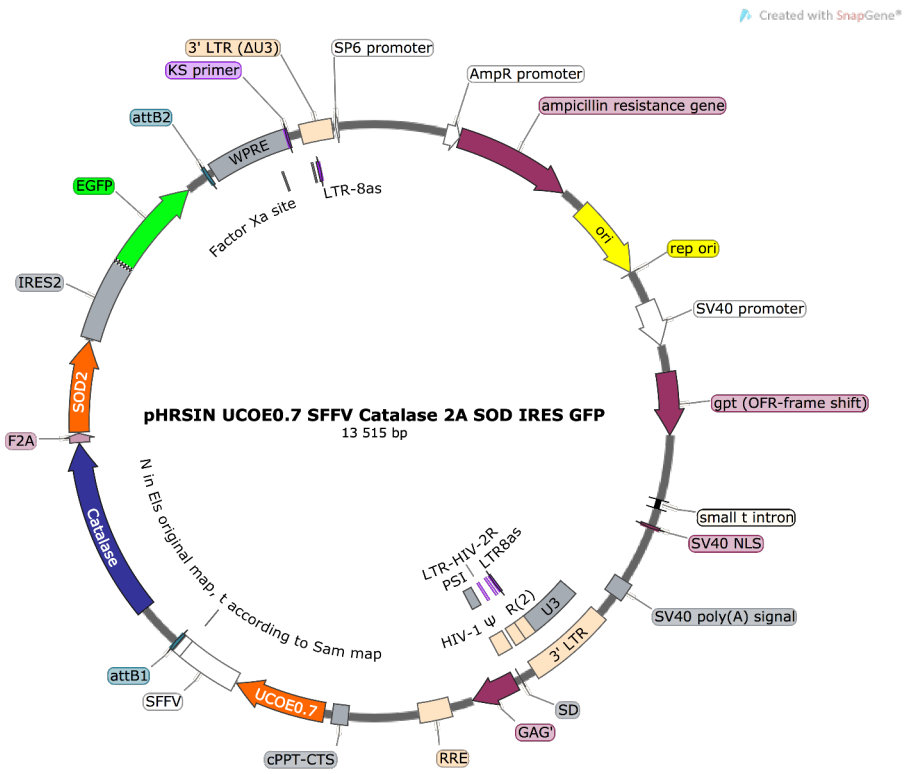

Appendix 13. pHRSIN UCOE0.7 SFFV Catalase 2A SOD IRES GFP (plasmid map).

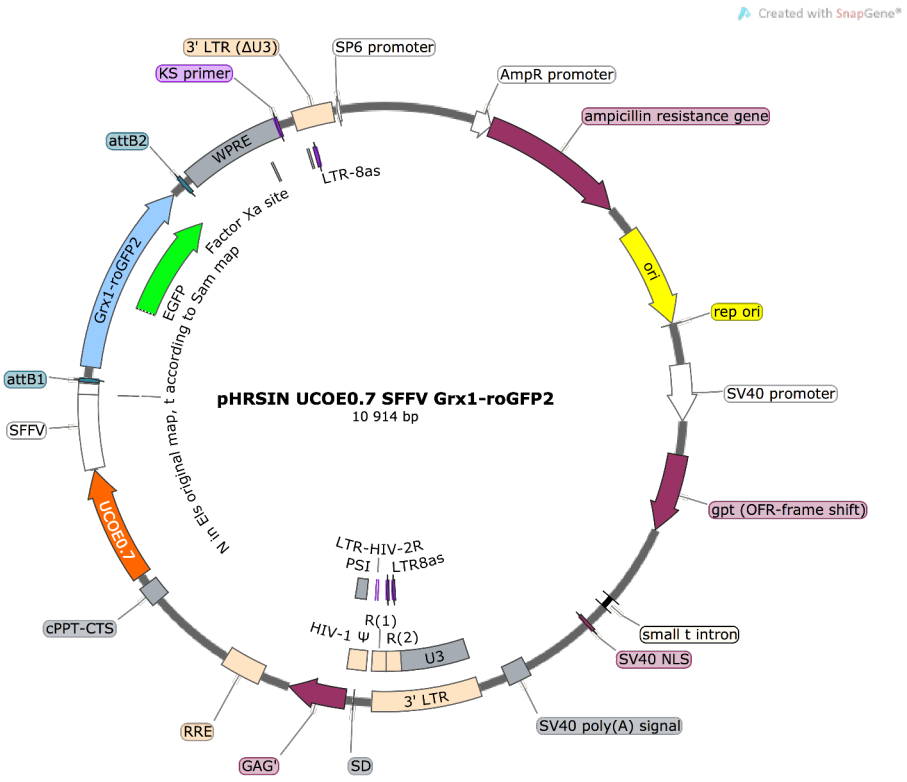

Appendix 14. pHRSIN UCOE0.7 SFFV Grx1-roGFP2 (plasmid map).

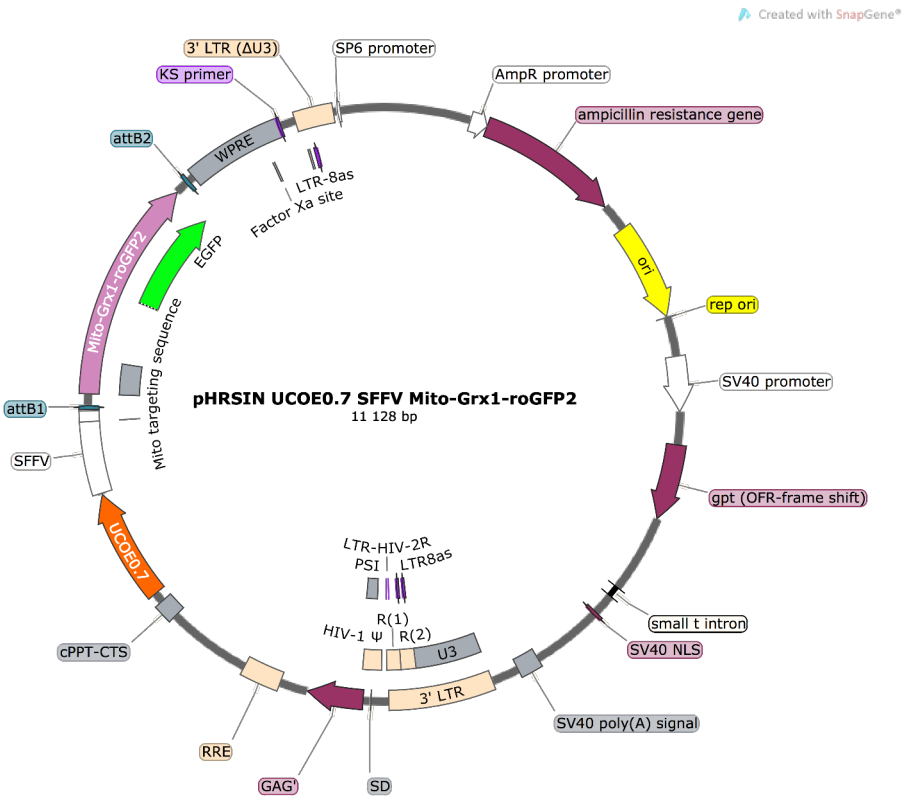

Appendix 15. pHRSIN UCOE0.7 SFFV Mito-Grx1-roGFP2 (plasmid map).

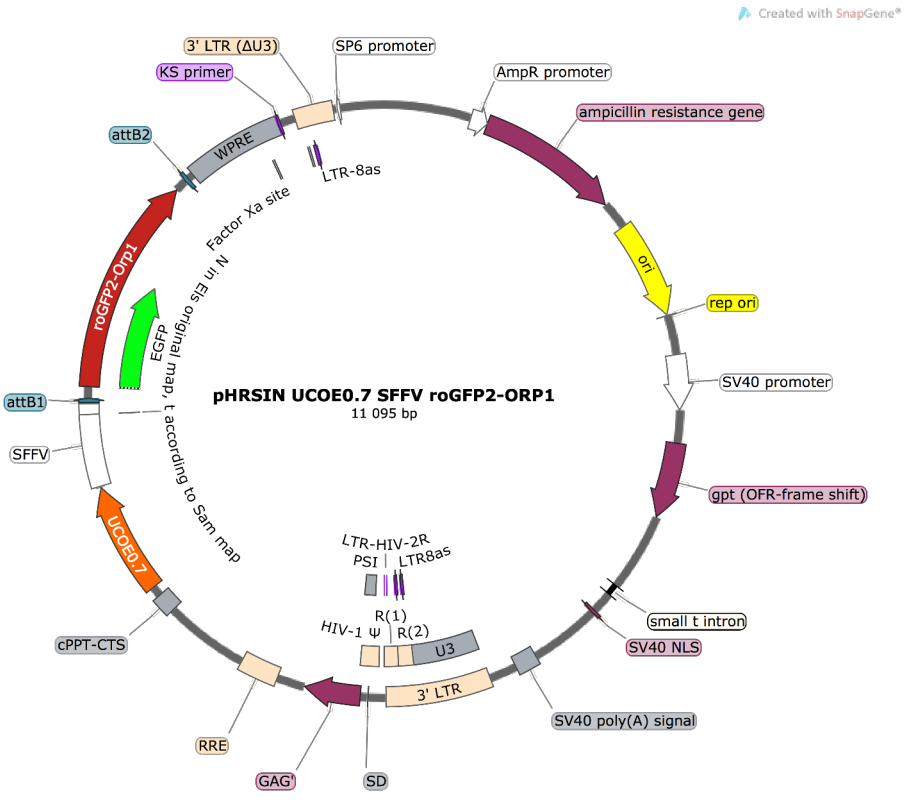

Appendix 16. pHRSIN UCOE0.7 SFFV roGFP2-ORP1 (plasmid map).

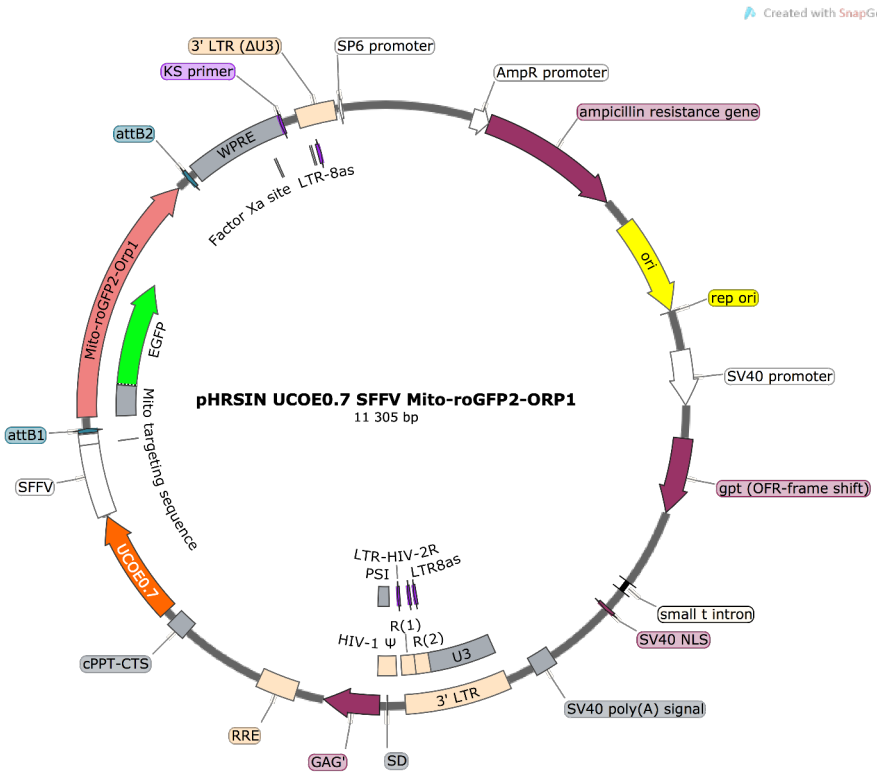

Appendix 17. pHRSIN UCOE0.7 SFFV Mito-roGFP2-ORP1 (plasmid map).

CHAPTER 6.

REFERENCES

6. REFERENCES

Alter, G., Malenfant, J.M., and Altfeld, M. (2004). CD107a as a functional marker for the identification of natural killer cell activity. J. Immunol. Methods *294*, 15–22.

Antachopoulos, C. (2010). Invasive fungal infections in congenital immunodeficiencies. Clin. Microbiol. Infect. *16*, 1335–1342.

Aquino-López, A., Senyukov, V.V., Vlasic, Z., Kleinerman, E.S., and Lee, D.A. (2017). Interferon Gamma Induces Changes in Natural Killer (NK) Cell Ligand Expression and Alters NK Cell-Mediated Lysis of Pediatric Cancer Cell Lines. Front Immunol *8*, 391.

Artis, D., and Spits, H. (2015). The biology of innate lymphoid cells. Nature *517*, 293–301.

Ashkenazi, A., and Salvesen, G. (2014). Regulated cell death: signaling and mechanisms. Annu. Rev. Cell Dev. Biol. *30*, 337–356.

Aurelius, J., Thorén, F.B., Akhiani, A.A., Brune, M., Palmqvist, L., Hansson, M., Hellstrand, K., and Martner, A. (2012). Monocytic AML cells inactivate antileukemic lymphocytes: role of NADPH oxidase/gp91(phox) expression and the PARP-1/PAR pathway of apoptosis. Blood *119*, 5832–5837.

Baetz, K., Isaaz, S., and Griffiths, G.M. (1995). Loss of cytotoxic T lymphocyte function in Chediak-Higashi syndrome arises from a secretory defect that prevents lytic granule exocytosis. The Journal of Immunology *154*, 6122–6131.

Baginska, J., Viry, E., Berchem, G., Poli, A., Noman, M.Z., Van Moer, K., Medves, S., Zimmer, J., Oudin, A., Niclou, S.P., et al. (2013). Granzyme B degradation by autophagy decreases tumor cell susceptibility to natural killer-mediated lysis under hypoxia. Proc. Natl. Acad. Sci. U.S.a. *110*, 17450–17455.

Bai, A., Moss, A., Rothweiler, S., Serena Longhi, M., Wu, Y., Junger, W.G., and Robson, S.C. (2015). NADH oxidase-dependent CD39 expression by CD8(+) T cells modulates interferon gamma responses via generation of adenosine. Nat Comms *6*, 8819.

Baillet, A., Hograindleur, M.-A., Benna, El, J., Grichine, A., Berthier, S., Morel, F., and Paclet, M.-H. (2017). Unexpected function of the phagocyte NADPH oxidase in supporting hyperglycolysis in stimulated neutrophils: key role of 6-phosphofructo-2-kinase. Faseb J. *31*, 663–673.

Bao, Y., Zheng, J., Han, C., Jin, J., Han, H., Liu, Y., Lau, Y.-L., Tu, W., and Cao, X. (2012). Tyrosine kinase Btk is required for NK cell activation. J. Biol. Chem. *287*, 23769–23778.

Bär, E., Whitney, P.G., Moor, K., Reis e Sousa, C., and LeibundGut-Landmann, S. (2014). IL-17 regulates systemic fungal immunity by controlling the functional competence of NK cells. Immunity *40*, 117–127.

Bedoui, S., Gebhardt, T., Gasteiger, G., and Kastenmüller, W. (2016). Parallels and differences between innate and adaptive lymphocytes. Nat Immunol *17*, 490–494.

Belderbos, M.E., Koster, T., Ausema, B., Jacobs, S., Sowdagar, S., Zwart, E., de Bont, E., de Haan, G., and Bystrykh, L.V. (2017). Clonal selection and asymmetric distribution of human leukemia in murine xenografts revealed by cellular barcoding. Blood *129*, 3210–3220.

Bengsch, B., Ohtani, T., Herati, R.S., Bovenschen, N., Chang, K.-M., and Wherry, E.J. (2017). Deep immune profiling by mass cytometry links human T and NK cell differentiation and cytotoxic molecule expression patterns. J. Immunol. Methods.

Benoit, L., Wang, X., Pabst, H.F., and Dutz, J. (2000). Cutting edge: defective NK cell activation in X-linked lymphoproliferative disease. The Journal of Immunology *165*, 3549–3553.

Bezman, N.A., Kim, C.C., Sun, J.C., Min-Oo, G., Hendricks, D.W., Kamimura, Y., Best, J.A., Goldrath, A.W., Lanier, L.L., Immunological Genome Project Consortium (2012). Molecular definition of the identity and activation of natural killer cells. Nat Immunol *13*, 1000–1009.

Bhojwani, D., and Pui, C.H. (2013). Relapsed childhood acute lymphoblastic leukaemia. The Lancet Oncology.

Billadeau, D.D., Upshaw, J.L., Schoon, R.A., Dick, C.J., and Leibson, P.J. (2003). NKG2D-DAP10 triggers human NK cell-mediated killing via a Syk-independent regulatory pathway. Nat Immunol *4*, 557–564.

Björkström, N.K., Ljunggren, H.-G., and Michaëlsson, J. (2016). Emerging insights into natural killer cells in human peripheral tissues. Nat Rev Immunol *16*, 310–320.

Boya, P., Andreau, K., Poncet, D., Zamzami, N., Perfettini, J.-L., Metivier, D., Ojcius, D.M., Jäättelä, M., and Kroemer, G. (2003). Lysosomal membrane permeabilization induces cell death in a mitochondrion-dependent fashion. J. Exp. Med. *197*, 1323–1334.

Bryceson, Y.T., Fauriat, C., Nunes, J.M., Wood, S.M., Björkström, N.K., Long, E.O., and Ljunggren, H.-G. (2010). Functional analysis of human NK cells by flow cytometry. Methods Mol. Biol. *612*, 335–352.

Bryceson, Y.T., Ljunggren, H.-G., and Long, E.O. (2009). Minimal requirement for induction of natural cytotoxicity and intersection of activation signals by inhibitory receptors. Blood *114*, 2657–2666.

Bryceson, Y.T., Pende, D., Maul-Pavicic, A., Gilmour, K.C., Ufheil, H., Vraetz, T., Chiang, S.C., Marcenaro, S., Meazza, R., Bondzio, I., et al. (2012). A prospective evaluation of degranulation assays in the rapid diagnosis of familial hemophagocytic syndromes. Blood *119*, 2754–2763.

Burritt, J.B., DeLeo, F.R., McDonald, C.L., Prigge, J.R., Dinauer, M.C., Nakamura, M., Nauseef, W.M., and Jesaitis, A.J. (2001). Phage display epitope mapping of human neutrophil flavocytochrome b558. Identification of two juxtaposed extracellular domains. J. Biol. Chem. *276*, 2053–2061.

Caligiuri, M.A. (2008). Human natural killer cells. Blood *112*, 461–469.

Campion, Y., Paclet, M.-H., Jesaitis, A.J., Marques, B., Grichine, A., Berthier, S., Lenormand, J.-L., Lardy, B., Stasia, M.-J., and Morel, F. (2007). New insights into the membrane topology of the phagocyte NADPH oxidase: characterization of an anti-gp91-phox conformational monoclonal antibody. Biochimie *89*, 1145–1158.

Carbone, E., Ruggiero, G., Terrazzano, G., Palomba, C., Manzo, C., Fontana, S., Spits, H., Kärre, K., and Zappacosta, S. (1997). A new mechanism of NK cell cytotoxicity activation: the CD40-CD40 ligand interaction. J. Exp. Med. *185*, 2053–2060.

Caron, G., Delneste, Y., Aubry, J.P., Magistrelli, G., Herbault, N., Blaecke, A., Meager, A., Bonnefoy, J.Y., and Jeannin, P. (1999). Human NK cells constitutively express membrane TNF-alpha (mTNFalpha) and present mTNFalpha-dependent cytotoxic activity. Eur. J. Immunol. *29*, 3588–3595.

Cerwenka, A., and Lanier, L.L. (2016). Natural killer cell memory in infection, inflammation and cancer. Nat Rev Immunol.

Chaigne-Delalande, B., Li, F.-Y., O'Connor, G.M., Lukacs, M.J., Jiang, P., Zheng, L., Shatzer, A., Biancalana, M., Pittaluga, S., Matthews, H.F., et al. (2013). Mg2+ regulates cytotoxic functions of NK and CD8 T cells in chronic EBV infection through NKG2D. Science *341*, 186–191.

Chalifour, A., Jeannin, P., Gauchat, J.-F., Blaecke, A., Malissard, M., N'Guyen, T., Thieblemont, N., and Delneste, Y. (2004). Direct bacterial protein PAMP recognition by human NK cells involves TLRs and triggers alpha-defensin production. Blood *104*, 1778–1783.

Chiang, S.C.C., Theorell, J., Entesarian, M., Meeths, M., Mastafa, M., Al-Herz, W., Frisk, P., Gilmour, K.C., Ifversen, M., Langenskiöld, C., et al. (2013). Comparison of primary human cytotoxic T-cell and natural killer cell responses reveal similar molecular requirements for lytic granule exocytosis but differences in cytokine production. Blood *121*, 1345–1356.

Choi, P.J., and Mitchison, T.J. (2013). Imaging burst kinetics and spatial coordination during serial killing by single natural killer cells. Proc. Natl. Acad. Sci. U.S.a. *110*, 6488–6493.

Chuong Nguyen, M.V., Lardy, B., Paclet, M.-H., Rousset, F., Berthier, S., Baillet, A., Grange, L., Gaudin, P., and Morel, F. (2015). [NADPH oxidases, Nox: new isoenzymes family]. Med Sci (Paris) *31*, 43–52.

Cichocki, F., Miller, J.S., Anderson, S.K., and Bryceson, Y.T. (2013). Epigenetic regulation of NK cell differentiation and effector functions. Front Immunol *4*, 55.

Clark, S.E., Filak, H.C., Guthrie, B.S., Schmidt, R.L., Jamieson, A., Merkel, P., Knight, V., Cole, C.M., Raulet, D.H., and Lenz, L.L. (2016). Bacterial Manipulation of NK Cell Regulatory Activity Increases Susceptibility to Listeria monocytogenes Infection. PLoS Pathog *12*, e1005708.

Cohnen, A., Chiang, S.C., Stojanovic, A., Schmidt, H., Claus, M., Saftig, P., Janßen, O., Cerwenka, A., Bryceson, Y.T., and Watzl, C. (2013). Surface CD107a/LAMP-1 protects natural killer cells from degranulation-associated damage. Blood *122*, 1411–1418.

Cooper, M.A. (2001). Human natural killer cells: a unique innate immunoregulatory role for the CD56bright subset. Blood *97*, 3146–3151.

Copelan, E.A. (2006). Hematopoietic stem-cell transplantation. N Engl J Med *354*, 1813–1826.

Cotugno, N., Finocchi, A., Cagigi, A., Di Matteo, G., Chiriaco, M., Di Cesare, S., Rossi, P., Aiuti, A., Palma, P., and Douagi, I. (2015). Defective B-cell proliferation and maintenance of long-term memory in patients with chronic granulomatous disease. J. Allergy Clin. Immunol. *135*, 753–61.e2.

De Maria, A., Bozzano, F., Cantoni, C., and Moretta, L. (2011). Revisiting human natural killer cell subset function revealed cytolytic CD56(dim)CD16+ NK cells as rapid producers of abundant IFN-gamma on activation. Proc. Natl. Acad. Sci. U.S.a. *108*, 728–732.

de Saint Basile, G., Ménasche, G., and Fischer, A. (2010). Molecular mechanisms of biogenesis and exocytosis of cytotoxic granules. Nat Rev Immunol *10*, 568–579.

de Saint Basile, G., Sepulveda, F.E., Maschalidi, S., and Fischer, A. (2015). Cytotoxic granule secretion by lymphocytes and its link to immune homeostasis. F1000Res *4*, 930.

de Zoete, M.R., Palm, N.W., Zhu, S., and Flavell, R.A. (2014). Inflammasomes. Cold Spring Harb Perspect Biol *6*, a016287–a016287.

Deguine, J., and Bousso, P. (2013). Dynamics of NK cell interactions in vivo. Immunol. Rev. *251*, 154–159.

Deguine, J., Breart, B., Lemaître, F., Di Santo, J.P., and Bousso, P. (2010). Intravital imaging reveals distinct dynamics for natural killer and CD8(+) T cells during tumor regression. Immunity *33*, 632–644.

Delon, J., Kaibuchi, K., and Germain, R.N. (2001). Exclusion of CD43 from the immunological synapse is mediated by phosphorylation-regulated relocation of the cytoskeletal adaptor moesin. Immunity.

Denman, C.J., Senyukov, V.V., Somanchi, S.S., Phatarpekar, P.V., Kopp, L.M., Johnson, J.L., Singh, H., Hurton, L., Maiti, S.N., Huls, M.H., et al. (2012). Membrane-Bound IL-21 Promotes Sustained Ex Vivo Proliferation of Human Natural Killer Cells. PLoS ONE *7*, e30264.

Dixit, A., Parnas, O., Li, B., Chen, J., Fulco, C.P., Jerby-Arnon, L., Marjanovic, N.D., Dionne, D., Burks, T., Raychowdhury, R., et al. (2016). Perturb-Seq: Dissecting Molecular Circuits with Scalable Single-Cell RNA Profiling of Pooled Genetic Screens. Cell *167*, 1853–1866.e17.

Dobbs, K., Tabellini, G., Calzoni, E., Patrizi, O., Martinez, P., Giliani, S.C., Moratto, D., Al-Herz, W., Cancrini, C., Cowan, M., et al. (2017). Natural Killer Cells from Patients with Recombinase-Activating Gene and Non-Homologous End Joining Gene Defects Comprise a Higher Frequency of CD56(bright) NKG2A(+++) Cells, and Yet Display Increased Degranulation and Higher Perforin Content. Front Immunol *8*, 798.

Donadieu, J., Fenneteau, O., Beaupain, B., Mahlaoui, N., and Chantelot, C.B. (2011). Congenital neutropenia: diagnosis, molecular bases and patient management. Orphanet J Rare Dis *6*, 26.

Dotiwala, F., Mulik, S., Polidoro, R.B., Ansara, J.A., Burleigh, B.A., Walch, M., Gazzinelli, R.T., and Lieberman, J. (2016). Killer lymphocytes use granulysin, perforin and granzymes to kill intracellular parasites. Nat. Med.

Durrieu, L., Lemieux, W., Dieng, M.M., Fontaine, F., Duval, M., Le Deist, F., and Haddad, E. (2014). Implication of different effector mechanisms by cord blood-derived and peripheral blood-derived cytokine-induced killer cells to kill precursor B acute lymphoblastic leukemia cell lines. Cytotherapy *16*, 845–856.

Eberl, G., Colonna, M., Di Santo, J.P., and McKenzie, A.N.J. (2015). Innate lymphoid cells. Innate lymphoid cells: a new paradigm in immunology. Science *348*, aaa6566–aaa6566.

Eberl, G., Di Santo, J.P., and Vivier, E. (2014). The brave new world of innate lymphoid cells. Nat Immunol *16*, 1–5.

Etchegaray, J.-P., and Mostoslavsky, R. (2016). Interplay between Metabolism and Epigenetics: A Nuclear Adaptation to Environmental Changes. Mol. Cell *62*, 695–711.

Fauriat, C., Long, E.O., Ljunggren, H.-G., and Bryceson, Y.T. (2010). Regulation of human NK-cell cytokine and chemokine production by target cell recognition. Blood *115*, 2167–2176.

Feldmann, J., Callebaut, I., Raposo, G., Certain, S., Bacq, D., Dumont, C., Lambert, N., Ouachée-Chardin, M., Chedeville, G., Tamary, H., et al. (2003). Munc13-4 is essential for cytolytic granules fusion and is mutated in a form of familial hemophagocytic lymphohistiocytosis (FHL3). Cell *115*, 461–473.

Fischer, A., and Rausell, A. (2016). Primary immunodeficiencies suggest redundancy within the human immune system. Sci Immunol *1*, eaah5861.

Fischer, A., Notarangelo, L.D., Neven, B., Cavazzana, M., and Puck, J.M. (2015). Severe combined immunodeficiencies and related disorders. Nat Rev Dis Primers *1*, 15061.

Fisicaro, P., Barili, V., Montanini, B., Acerbi, G., Ferracin, M., Guerrieri, F., Salerno, D., Boni, C., Massari, M., Cavallo, M.C., et al. (2017). Targeting mitochondrial dysfunction can restore antiviral activity of exhausted HBV-specific CD8 T cells in chronic hepatitis B. Nat. Med. *23*, 327–336.

Flusberg, D.A., and Sorger, P.K. (2015). Surviving apoptosis: life-death signaling in single cells. Trends Cell Biol. *25*, 446–458.

Flusberg, D.A., Roux, J., Spencer, S.L., and Sorger, P.K. (2013). Cells surviving fractional killing by TRAIL exhibit transient but sustainable resistance and inflammatory phenotypes. Mol. Biol. Cell *24*, 2186–2200.

Fujisaki, H., Kakuda, H., Shimasaki, N., Imai, C., Ma, J., Lockey, T., Eldridge, P., Leung, W.H., and Campana, D. (2009). Expansion of Highly Cytotoxic Human Natural Killer Cells for Cancer Cell Therapy. Cancer Research *69*, 4010–4017.

Galluzzi, L., Vitale, I., Abrams, J.M., Alnemri, E.S., Baehrecke, E.H., Blagosklonny, M.V., Dawson, T.M., Dawson, V.L., El-Deiry, W.S., Fulda, S., et al. (2012). Molecular definitions of cell death subroutines: recommendations of the Nomenclature Committee on Cell Death 2012. Cell Death Differ. *19*, 107–120.

Galluzzi, L., Bravo-San Pedro, J.M., and Kroemer, G. (2014). Organelle-specific initiation of cell death. Nat. Cell Biol. *16*, 728–736.

Gao, Y., Souza-Fonseca-Guimaraes, F., Bald, T., Ng, S.S., Young, A., Ngiow, S.F., Rautela, J., Straube, J., Waddell, N., Blake, S.J., et al. (2017). Tumor immunoevasion by the conversion of effector NK cells into type 1 innate lymphoid cells. Nat Immunol *18*, 1004–1015.

Gardiner, C.M., and Finlay, D.K. (2017). What Fuels Natural Killers? Metabolism and NK Cell Responses. Front Immunol *8*, 367.

Geiger, R., Rieckmann, J.C., Wolf, T., Basso, C., Feng, Y., Fuhrer, T., Kogadeeva, M., Picotti, P., Meissner, F., Mann, M., et al. (2016). L-Arginine Modulates T Cell Metabolism and Enhances Survival and Anti-tumor Activity. Cell *167*, 829–842.e13.

Gooley, T.A., Chien, J.W., Pergam, S.A., Hingorani, S., Sorror, M.L., Boeckh, M., Martin, P.J., Sandmaier, B.M., Marr, K.A., Appelbaum, F.R., et al. (2010). Reduced mortality after allogeneic hematopoietic-cell transplantation. N Engl J Med *363*, 2091–2101.

Greaves, M. (2006). Infection, immune responses and the aetiology of childhood leukaemia. Nat. Rev. Cancer *6*, 193–203.

Greaves, M., and Muschen, M. (2015). Infection and the Perils of B-cell Activation. Cancer Discov *5*, 1244–1246.

Green, D.R. (2011). Apoptosis: physiology and pathology.

Guicciardi, M.E., and Gores, G.J. (2009). Life and death by death receptors. Faseb J. *23*, 1625–1637.

Guo, H., Callaway, J.B., and Ting, J.P.-Y. (2015). Inflammasomes: mechanism of action, role in disease, and therapeutics. Nat. Med. *21*, 677–687.

Halle, S., Keyser, K.A., Stahl, F.R., Busche, A., Marquardt, A., Zheng, X., Galla, M., Heissmeyer, V., Heller, K., Boelter, J., et al. (2016). In Vivo Killing Capacity of Cytotoxic T Cells Is Limited and Involves Dynamic Interactions and T Cell Cooperativity. Immunity *44*, 233–245.

Ham, H., and Billadeau, D.D. (2014). Human immunodeficiency syndromes affecting human natural killer cell cytolytic activity. Front Immunol *5*, 2.

Hanahan, D., and Weinberg, R.A. (2011). Hallmarks of cancer: the next generation. Cell *144*, 646–674.

Handgretinger, R., Lang, P., and André, M.C. (2016). Exploitation of Natural Killer (NK) cells for the treatment of acute leukemia. Blood blood–2015–12–629055.

He, J.-S., and Ostergaard, H.L. (2007). CTLs contain and use intracellular stores of FasL distinct from cytolytic granules. The Journal of Immunology *179*, 2339–2348.

Herberman, R.B., Nunn, M.E., and Lavrin, D.H. (1975). Natural cytotoxic reactivity of mouse lymphoid cells against syngeneic acid allogeneic tumors. I. Distribution of reactivity and specificity. *16*, 216–229.

Hetz, C., Bernasconi, P., Fisher, J., Lee, A.-H., Bassik, M.C., Antonsson, B., Brandt, G.S., Iwakoshi, N.N., Schinzel, A., Glimcher, L.H., et al. (2006). Proapoptotic BAX and BAK modulate the unfolded protein response by a direct interaction with IRE1alpha. Science *312*, 572–576.

Hidalgo, L.G., Einecke, G., Allanach, K., and Halloran, P.F. (2008). The transcriptome of human cytotoxic T cells: similarities and disparities among allostimulated CD4(+) CTL, CD8(+) CTL and NK cells. Am. J. Transplant. *8*, 627–636.

Holmes, T.D., and Bryceson, Y.T. (2016). Natural killer cell memory in context. Semin. Immunol.

Horiuchi, T., Mitoma, H., Harashima, S.-I., Tsukamoto, H., and Shimoda, T. (2010). Transmembrane TNF-alpha: structure, function and interaction with anti-TNF agents. Rheumatology (Oxford) *49*, 1215–1228.

Horn, S., Hughes, M.A., Schilling, R., Sticht, C., Tenev, T., Ploesser, M., Meier, P., Sprick, M.R., MacFarlane, M., and Leverkus, M. (2017). Caspase-10 Negatively Regulates Caspase-8-Mediated Cell Death, Switching the Response to CD95L in Favor of NF-κB Activation and Cell Survival. Cell Rep *19*, 785–797.

Horowitz, A., Strauss-Albee, D.M., Leipold, M., Kubo, J., Nemat-Gorgani, N., Dogan, O.C., Dekker, C.L., Mackey, S., Maecker, H., Swan, G.E., et al. (2013). Genetic and environmental determinants of human NK cell diversity revealed by mass cytometry. Sci Transl Med *5*, 208ra145.

Hukelmann, J.L., Anderson, K.E., Sinclair, L.V., Grzes, K.M., Murillo, A.B., Hawkins, P.T., Stephens, L.R., Lamond, A.I., and Cantrell, D.A. (2016). The cytotoxic T cell proteome and its shaping by the kinase mTOR. Nat Immunol *17*, 104–112.

Hunger, S.P., and Mullighan, C.G. (2015). Acute Lymphoblastic Leukemia in Children. N Engl J Med *373*, 1541–1552.

Huntington, N.D., Legrand, N., Alves, N.L., Jaron, B., Weijer, K., Plet, A., Corcuff, E., Mortier, E., Jacques, Y., Spits, H., et al. (2009). IL-15 trans-presentation promotes human NK cell development and differentiation in vivo. Journal of Experimental Medicine *206*, 25–34.

Imai, C., Iwamoto, S., and Campana, D. (2005). Genetic modification of primary natural killer cells overcomes inhibitory signals and induces specific killing of leukemic cells. Blood *106*, 376–383.

Inaba, H., Greaves, M., and Mullighan, C.G. (2013). Acute lymphoblastic leukaemia. The Lancet.

Inoue, S., Browne, G., Melino, G., and Cohen, G.M. (2009). Ordering of caspases in cells undergoing apoptosis by the intrinsic pathway. Cell Death Differ. *16*, 1053–1061.

Jackson, S.H., Devadas, S., Kwon, J., Pinto, L.A., and Williams, M.S. (2004). T cells express a phagocyte-type NADPH oxidase that is activated after T cell receptor stimulation. Nat Immunol *5*, 818–827.

Jedema, I. (2004). New CFSE-based assay to determine susceptibility to lysis by cytotoxic T cells of leukemic precursor cells within a heterogeneous target cell population. Blood *103*, 2677–2682.

Jenkins, M.R., Rudd-Schmidt, J.A., Lopez, J.A., Ramsbottom, K.M., Mannering, S.I., Andrews, D.M., Voskoboinik, I., and Trapani, J.A. (2015). Failed CTL/NK cell killing and cytokine hypersecretion are directly linked through prolonged synapse time. Journal of Experimental Medicine.

Jesaitis, A.J. (1995). Structure of human phagocyte cytochrome b and its relationship to microbicidal superoxide production. The Journal of Immunology *155*, 3286–3288.

Jessen, B., Maul-Pavicic, A., Ufheil, H., Vraetz, T., Enders, A., Lehmberg, K., Längler, A., Gross-Wieltsch, U., Bay, A., Kaya, Z., et al. (2011). Subtle differences in CTL cytotoxicity determine susceptibility to hemophagocytic lymphohistiocytosis in mice and humans with Chediak-Higashi syndrome. Blood *118*, 4620–4629.

Kabadi, A.M., Ousterout, D.G., Hilton, I.B., and Gersbach, C.A. (2014). Multiplex CRISPR/Cas9-based genome engineering from a single lentiviral vector. Nucleic Acids Res. *42*, e147.

Kaelin, W.G., and McKnight, S.L. (2013). Influence of metabolism on epigenetics and disease. Cell *153*, 56–69.

Karo, J.M., Schatz, D.G., and Sun, J.C. (2014). The RAG Recombinase Dictates Functional Heterogeneity and Cellular Fitness in Natural Killer Cells. Cell *159*, 94–107.

Kashii, Y., Giorda, R., Herberman, R.B., Whiteside, T.L., and Vujanovic, N.L. (1999). Constitutive expression and role of the TNF family ligands in apoptotic killing of tumor cells by human NK cells. The Journal of Immunology *163*, 5358–5366.

Kawalekar, O.U., O'Connor, R.S., Fraietta, J.A., Guo, L., McGettigan, S.E., Posey, A.D., Patel, P.R., Guedan, S., Scholler, J., Keith, B., et al. (2016). Distinct Signaling of Coreceptors Regulates Specific Metabolism Pathways and Impacts Memory Development in CAR T Cells. Immunity *44*, 380–390.

Kärre, K., Ljunggren, H.G., Piontek, G., and Kiessling, R. (1986). Selective rejection of H-2-deficient lymphoma variants suggests alternative immune defence strategy. Nature *319*, 675–678.

Kärre, K. (2008). Natural killer cell recognition of missing self. Nat Immunol *9*, 477–480.

Keating, S.E., Zaiatz-Bittencourt, V., Loftus, R.M., Keane, C., Brennan, K., Finlay, D.K., and Gardiner, C.M. (2016). Metabolic Reprogramming Supports IFN-γ Production by CD56bright NK Cells. J. Immunol. *196*, 2552–2560.

Klamt, F., Zdanov, S., Levine, R.L., Pariser, A., Zhang, Y., Zhang, B., Yu, L.-R., Veenstra, T.D., and Shacter, E. (2009). Oxidant-induced apoptosis is mediated by oxidation of the actin-regulatory protein cofilin. Nat. Cell Biol. *11*, 1241–1246.

Konomi, Y., Sekine, T., Takayama, T., Fuji, M., and Tanaka, T. (1995). Cytotoxic activity of CD4+ T cells against autologous tumor cells. Jpn. J. Cancer Res. *86*, 854–860.

Kroemer, G., Galluzzi, L., Vandenabeele, P., Abrams, J., Alnemri, E.S., Baehrecke, E.H., Blagosklonny, M.V., El-Deiry, W.S., Golstein, P., Green, D.R., et al. (2009). Classification of cell death: recommendations of the Nomenclature Committee on Cell Death 2009. Cell Death Differ. *16*, 3–11.

Krzewski, K., and Coligan, J.E. (2012). Human NK cell lytic granules and regulation of their exocytosis. Front Immunol *3*, 335.

Krzewski, K., Gil-Krzewska, A., Nguyen, V., Peruzzi, G., and Coligan, J.E. (2013). LAMP1/CD107a is required for efficient perforin delivery to lytic granules and NK-cell cytotoxicity. Blood *121*, 4672–4683.

Kuehn, H.S., Niemela, J.E., Rangel-Santos, A., and Zhang, M. (2013). Loss-of-function of the protein kinase C δ (PKCδ) causes a B-cell lymphoproliferative syndrome in humans. Blood.

Kuhns, D.B., Alvord, W.G., Heller, T., Feld, J.J., Pike, K.M., Marciano, B.E., Uzel, G., DeRavin, S.S., Priel, D.A.L., Soule, B.P., et al. (2010). Residual NADPH oxidase and survival in chronic granulomatous disease. N Engl J Med *363*, 2600–2610.

Kübler, A., Woiterski, J., Witte, K.-E., Bühring, H.-J., Hartwig, U.F., Ebinger, M., Oevermann, L., Mezger, M., Herr, W., Lang, P., et al. (2014). Both mature KIR+ and immature KIR- NK cells control pediatric acute B-cell precursor leukemia in NOD.Cg-Prkdcscid IL2rgtmWjl/Sz mice. Blood *124*, 3914–3923.

Kwon, H.-J., Choi, G.-E., Ryu, S., Kwon, S.J., Kim, S.C., Booth, C., Nichols, K.E., and Kim, H.S. (2016). Stepwise phosphorylation of p65 promotes NF-κB activation and NK cell responses during target cell recognition. Nat Comms *7*, 11686.

Lagresle-Peyrou, C., Luce, S., Ouchani, F., Soheili, T.S., Sadek, H., Chouteau, M., Durand, A., Pic, I., Majewski, J., Brouzes, C., et al. (2016). X-linked primary immunodeficiency associated with hemizygous mutations in the moesin (MSN) gene. J. Allergy Clin. Immunol. *138*, 1681–1689.e1688.

Lakhani, S.A., Masud, A., Kuida, K., Porter, G.A., Booth, C.J., Mehal, W.Z., Inayat, I., and Flavell, R.A. (2006). Caspases 3 and 7: key mediators of mitochondrial events of apoptosis. Science *311*, 847–851.

Lambeth, J.D., Kawahara, T., and Diebold, B. (2007). Regulation of Nox and Duox enzymatic activity and expression. Free Radic. Biol. Med. *43*, 319–331.

Lamy, L., Ngo, V.N., Emre, N.C.T., Shaffer, A.L., Yang, Y., Tian, E., Nair, V., Kruhlak, M.J., Zingone, A., Landgren, O., et al. (2013). Control of autophagic cell death by caspase-10 in multiple myeloma. Cancer Cell *23*, 435–449.

Lanier, L.L. (2005). NK cell recognition. Annu. Rev. Immunol. *23*, 225–274.

le Viseur, C., Hotfilder, M., Bomken, S., Wilson, K., Röttgers, S., Schrauder, A., Rosemann, A., Irving, J., Stam, R.W., Shultz, L.D., et al. (2008). In childhood acute lymphoblastic leukemia, blasts at different stages of immunophenotypic maturation have stem cell properties. Cancer Cell *14*, 47–58.

Lee, H.-J., Pyo, J.-O., Oh, Y., Kim, H.-J., Hong, S.-H., Jeon, Y.-J., Kim, H., Cho, D.-H., Woo, H.-N., Song, S., et al. (2007). AK2 activates a novel apoptotic pathway through formation of a complex with FADD and caspase-10. Nat. Cell Biol. *9*, 1303–1310.

Lee, J., Zhang, T., Hwang, I., Kim, A., Nitschke, L., Kim, M., Scott, J.M., Kamimura, Y., Lanier, L.L., and Kim, S. (2015). Epigenetic Modification and Antibody-Dependent Expansion of Memory-like NK Cells in Human Cytomegalovirus-Infected Individuals. Immunity *42*, 431–442.

Lee, R.K., Spielman, J., Zhao, D.Y., Olsen, K.J., and Podack, E.R. (1996). Perforin, Fas ligand, and tumor necrosis factor are the major cytotoxic molecules used by lymphokine-activated killer cells. The Journal of Immunology *157*, 1919–1925.

Leiding, J.W., and Holland, S.M. (2016). Chronic granulomatous disease.

Lekstrom-Himes, J.A., and Gallin, J.I. (2000). Immunodeficiency diseases caused by defects in phagocytes. N. Engl. J. Med. *343*, 1703–1714.

Lettau, M., Kabelitz, D., and Janssen, O. (2015). Lysosome-Related Effector Vesicles in T Lymphocytes and NK Cells. Scand. J. Immunol. *82*, 235–243.

Li, S.S., Kyei, S.K., Timm-McCann, M., Ogbomo, H., Jones, G.J., Shi, M., Xiang, R.F., Oykhman, P., Huston, S.M., Islam, A., et al. (2013). The NK receptor NKp30 mediates direct fungal recognition and killing and is diminished in NK cells from HIV-infected patients. Cell Host and Microbe *14*, 387–397.

Lieberman, J. (2016). Cytotoxic Lymphocytes. In Encyclopedia of Immunobiology, (Elsevier), pp. 363–373.

Long, E.O., Kim, H.S., Liu, D., Peterson, M.E., and Rajagopalan, S. (2013). Controlling natural killer cell responses: integration of signals for activation and inhibition. Annu. Rev. Immunol. *31*, 227–258.

Lopez, J.A., Jenkins, M.R., Rudd-Schmidt, J.A., Brennan, A.J., Danne, J.C., Mannering, S.I., Trapani, J.A., and Voskoboinik, I. (2013). Rapid and Unidirectional Perforin Pore Delivery at the Cytotoxic Immune Synapse. The Journal of Immunology *191*, 2328–2334.

Lotze, M.T., and Thomson, A.W. (2009). Natural Killer Cells (Academic Press).

Lu, C., and Thompson, C.B. (2012). Metabolic regulation of epigenetics. Cell Metabolism *16*, 9–17.

Ma, L.L., Wang, C.L.C., Neely, G.G., Epelman, S., Krensky, A.M., and Mody, C.H. (2004). NK cells use perforin rather than granulysin for anticryptococcal activity. J. Immunol. *173*, 3357–3365.

Ma, X., Edmonson, M., Yergeau, D., Muzny, D.M., Hampton, O.A., Rusch, M., Song, G., Easton, J., Harvey, R.C., Wheeler, D.A., et al. (2015). Rise and fall of subclones from diagnosis to relapse in pediatric B-acute lymphoblastic leukaemia. Nat Comms *6*, 6604.

Mace, E.M., Dongre, P., Hsu, H.-T., Sinha, P., James, A.M., Mann, S.S., Forbes, L.R., Watkin, L.B., and Orange, J.S. (2014). Cell biological steps and checkpoints in accessing NK cell cytotoxicity. Immunol Cell Biol *92*, 245–255.

Mace, E.M., Hsu, A.P., Monaco-Shawver, L., Makedonas, G., Rosen, J.B., Dropulic, L., Cohen, J.I., Frenkel, E.P., Bagwell, J.C., Sullivan, J.L., et al. (2013). Mutations in GATA2 cause human NK cell deficiency with specific loss of the CD56(bright) subset. Blood *121*, 2669–2677.

Macosko, E.Z., Basu, A., Satija, R., Nemesh, J., Shekhar, K., Goldman, M., Tirosh, I., Bialas, A.R., Kamitaki, N., Martersteck, E.M., et al. (2015). Highly Parallel Genome-wide Expression Profiling of Individual Cells Using Nanoliter Droplets. Cell *161*, 1202–1214.

Maltez, V.I., Tubbs, A.L., Cook, K.D., Aachoui, Y., Falcone, E.L., Holland, S.M., Whitmire, J.K., and Miao, E.A. (2015). Inflammasomes Coordinate Pyroptosis and Natural Killer Cell Cytotoxicity to Clear Infection by a Ubiquitous Environmental Bacterium. Immunity *43*, 987–997.

Marcenaro, S., Gallo, F., Martini, S., Santoro, A., Griffiths, G.M., Aricò, M., Moretta, L., and Pende, D. (2006). Analysis of natural killer-cell function in familial hemophagocytic lymphohistiocytosis (FHL): defective CD107a surface expression heralds Munc13-4 defect and discriminates between genetic subtypes of the disease. Blood *108*, 2316–2323.

Marciano, B.E., Spalding, C., Fitzgerald, A., Mann, D., Brown, T., Osgood, S., Yockey, L., Darnell, D.N., Barnhart, L., Daub, J., et al. (2015). Common severe infections in chronic granulomatous disease. Clin. Infect. Dis. *60*, 1176–1183.

Marçais, A., Cherfils-Vicini, J., Viant, C., Degouve, S., Viel, S., Fenis, A., Rabilloud, J., Mayol, K., Tavares, A., Bienvenu, J., et al. (2014). The metabolic checkpoint kinase mTOR is essential for IL-15 signaling during the development and activation of NK cells. Nat Immunol *15*, 749–757.

Marshall, G.M., Carter, D.R., Cheung, B.B., Liu, T., Mateos, M.K., Meyerowitz, J.G., and Weiss, W.A. (2014). The prenatal origins of cancer. Nat. Rev. Cancer *14*, 277–289.

Martinet, L., and Smyth, M.J. (2015). Balancing natural killer cell activation through paired receptors. Nat Rev Immunol *15*, 243–254.

Martín-Lorenzo, A., Hauer, J., Vicente-Dueñas, C., Auer, F., González-Herrero, I., García-Ramírez, I., Ginzel, S., Thiele, R., Constantinescu, S.N., Bartenhagen, C., et al. (2015). Infection Exposure is a Causal Factor in B-cell

Precursor Acute Lymphoblastic Leukemia as a Result of Pax5-Inherited Susceptibility. Cancer Discov *5*, 1328–1343.

Martínez-Lostao, L., Anel, A., and Pardo, J. (2015). How Do Cytotoxic Lymphocytes Kill Cancer Cells? Clin. Cancer Res. *21*, 5047–5056.

Mauch, L., Lun, A., O'Gorman, M.R.G., Harris, J.S., Schulze, I., Zychlinsky, A., Fuchs, T., Oelschlägel, U., Brenner, S., Kutter, D., et al. (2007). Chronic granulomatous disease (CGD) and complete myeloperoxidase deficiency both yield strongly reduced dihydrorhodamine 123 test signals but can be easily discerned in routine testing for CGD. Clin. Chem. *53*, 890–896.

McCann, F.E., Vanherberghen, B., Eleme, K., Carlin, L.M., Newsam, R.J., Goulding, D., and Davis, D.M. (2003). The Size of the Synaptic Cleft and Distinct Distributions of Filamentous Actin, Ezrin, CD43, and CD45 at Activating and Inhibitory Human NK Cell Immune Synapses. The Journal of Immunology *170*, 2862–2870.

McClellan, J.S., and Majeti, R. (2013). The cancer stem cell model: B cell acute lymphoblastic leukaemia breaks the mould. EMBO Mol Med *5*, 7–9.

Melki, M.-T., Saïdi, H., Dufour, A., Olivo-Marin, J.-C., and Gougeon, M.-L. (2010). Escape of HIV-1-infected dendritic cells from TRAIL-mediated NK cell cytotoxicity during NK-DC cross-talk--a pivotal role of HMGB1. PLoS Pathog *6*, e1000862.

Mengarelli, A., Zarcone, D., Caruso, R., Tenca, C., Rana, I., Pinto, R.M., Grossi, C.E., and De Rossi, G. (2001). Adhesion molecule expression, clinical features and therapy outcome in childhood acute lymphoblastic leukemia. Leuk Lymphoma *40*, 625–630.

Mitoma, H., Horiuchi, T., Tsukamoto, H., Tamimoto, Y., Kimoto, Y., Uchino, A., To, K., Harashima, S.-I., Hatta, N., and Harada, M. (2008). Mechanisms for cytotoxic effects of anti–tumor necrosis factor agents on transmembrane tumor necrosis factor α–expressing cells: Comparison among infliximab, etanercept, and adalimumab. Arthritis Rheum *58*, 1248–1257.

Mullighan, C.G. (2012). Molecular genetics of B-precursor acute lymphoblastic leukemia. J. Clin. Invest. *122*, 3407–3415.

Mullighan, C.G., Phillips, L.A., Su, X., Ma, J., Miller, C.B., Shurtleff, S.A., and Downing, J.R. (2008). Genomic analysis of the clonal origins of relapsed acute lymphoblastic leukemia. Science *322*, 1377–1380.

Narni-Mancinelli, E., Vivier, E., and Kerdiles, Y.M. (2011). The “T-cell-ness” of NK cells: unexpected similarities between NK cells and T cells. Int. Immunol. *23*, 427–431.

Ni, J., Miller, M., Stojanovic, A., Garbi, N., and Cerwenka, A. (2012). Sustained effector function of IL-12/15/18-preactivated NK cells against established tumors. Journal of Experimental Medicine *209*, 2351–2365.

Nieto, M., Rodríguez-Fernández, J.L., Navarro, F., Sancho, D., Frade, J.M., Mellado, M., Martínez-A, C., Cabañas, C., and Sánchez-Madrid, F. (1999). Signaling through CD43 induces natural killer cell activation, chemokine release, and PYK-2 activation. Blood *94*, 2767–2777.

Noubade, R., Wong, K., Ota, N., Rutz, S., Eidenschenk, C., Valdez, P.A., Ding, J., Peng, I., Sebrell, A., Caplazi, P., et al. (2014). NRROS negatively regulates reactive oxygen species during host defence and autoimmunity. Nature *509*, 235–239.

Orange, J.S. (2008). Formation and function of the lytic NK-cell immunological synapse. Nat Rev Immunol *8*, 713–725.

Orange, J.S. (2012). Unraveling human natural killer cell deficiency. J. Clin. Invest. *122*, 798–801.

Orange, J.S. (2013). Natural killer cell deficiency. J. Allergy Clin. Immunol. *132*, 515–25–quiz526.

Orange, J.S., Brodeur, S.R., Jain, A., Bonilla, F.A., Schneider, L.C., Kretschmer, R., Nurko, S., Rasmussen, W.L., Köhler, J.R., Gellis, S.E., et al. (2002). Deficient natural killer cell cytotoxicity in patients with IKK-gamma/NEMO mutations. *109*, 1501–1509.

Oskarsson, T., Söderhäll, S., Arvidson, J., Forestier, E., Montgomery, S., Bottai, M., Lausen, B., Carlsen, N., Hellebostad, M., Lähteenmäki, P., et al. (2016). Relapsed childhood acute lymphoblastic leukemia in the Nordic countries: prognostic factors, treatment and outcome. Haematologica *101*, 68–76.

Pannicke, U., Baumann, B., Fuchs, S., Henneke, P., Rensing-Ehl, A., Rizzi, M., Janda, A., Hese, K., Schlesier, M., Holzmann, K., et al. (2013). Deficiency of innate and acquired immunity caused by an IKBKB mutation. N Engl J Med *369*, 2504–2514.

Parolini, S., Bottino, C., Falco, M., Augugliaro, R., Giliani, S., Franceschini, R., Ochs, H.D., Wolf, H., Bonnefoy, J.Y., Biassoni, R., et al. (2000). X-linked lymphoproliferative disease. 2B4 molecules displaying inhibitory rather than activating function are responsible for the inability of natural killer cells to kill Epstein-Barr virus-infected cells. J. Exp. Med. *192*, 337–346.

Parrish, A.B., Freel, C.D., and Kornbluth, S. (2013). Cellular Mechanisms Controlling Caspase Activation and Function. Cold Spring Harb Perspect Biol *5*, a008672–a008672.

Patel, S.J., Sanjana, N.E., Kishton, R.J., Eidizadeh, A., Vodnala, S.K., Cam, M., Gartner, J.J., Jia, L., Steinberg, S.M., Yamamoto, T.N., et al. (2017). Identification of essential genes for cancer immunotherapy. Nature *548*, 537–542.

Paust, S., and Andrian, von, U.H. (2011). Natural killer cell memory. Nat Immunol *131*, 500–508.

Peppa, D., Gill, U.S., Reynolds, G., Easom, N.J.W., Pallett, L.J., Schurich, A., Micco, L., Nebbia, G., Singh, H.D., Adams, D.H., et al. (2013). Up-regulation of a death receptor renders antiviral T cells susceptible to NK cell-mediated deletion. Journal of Experimental Medicine *210*, 99–114.

Perona-Wright, G., Mohrs, K., Szaba, F.M., Kummer, L.W., Madan, R., Karp, C.L., Johnson, L.L., Smiley, S.T., and Mohrs, M. (2009). Systemic but not local infections elicit immunosuppressive IL-10 production by natural killer cells. Cell Host and Microbe *6*, 503–512.

Perova, T., Grandal, I., Nutter, L.M.J., Papp, E., Matei, I.R., Beyene, J., Kowalski, P.E., Hitzler, J.K., Minden, M.D., Guidos, C.J., et al. (2014). Therapeutic Potential of Spleen Tyrosine Kinase Inhibition for Treating High-Risk Precursor B Cell Acute Lymphoblastic Leukemia. Sci Transl Med *6*, 236ra62–236ra62.

Piccioli, D., Sbrana, S., Melandri, E., and Valiante, N.M. (2002). Contact-dependent stimulation and inhibition of dendritic cells by natural killer cells. J. Exp. Med. *195*, 335–341.

Raad, H., Paclet, M.H., Boussetta, T., Kroviarski, Y., Morel, F., Quinn, M.T., Gougerot-Pocidalo, M.-A., Dang, P.M.C., and Benna, El, J. (2009). Regulation of the phagocyte NADPH oxidase activity: phosphorylation of gp91phox/NOX2 by protein kinase C enhances its diaphorase activity and binding to Rac2, p67phox, and p47phox. The FASEB Journal *23*, 1011–1022.

Rajasekaran, K., Kumar, P., Schuldt, K.M., Peterson, E.J., Vanhaesebroeck, B., Dixit, V., Thakar, M.S., and Malarkannan, S. (2013). Signaling by Fyn-ADAP via the Carma1-Bcl-10-MAP3K7 signalosome exclusively regulates inflammatory cytokine production in NK cells. Nat Immunol *14*, 1127–1136.

Ramoni, C., Luciani, F., Spadaro, F., Lugini, L., Lozupone, F., and Fais, S. (2002). Differential expression and distribution of ezrin, radixin and moesin in human natural killer cells. Eur. J. Immunol. *32*, 3059–3065.

Ramos-Casals, M., Brito-Zerón, P., López-Guillermo, A., Khamashta, M.A., and Bosch, X. (2014). Adult haemophagocytic syndrome. Lancet *383*, 1503–1516.

Reed, J.C., Doctor, K., Rojas, A., Zapata, J.M., Stehlik, C., Fiorentino, L., Damiano, J., Roth, W., Matsuzawa, S.-I., Newman, R., et al. (2003). Comparative analysis of apoptosis and inflammation genes of mice and humans. Genome Res. *13*, 1376–1388.

Reefman, E., Kay, J.G., Wood, S.M., Offenhäuser, C., Brown, D.L., Roy, S., Stanley, A.C., Low, P.C., Manderson, A.P., and Stow, J.L. (2010). Cytokine secretion is distinct from secretion of cytotoxic granules in NK cells. J. Immunol. *184*, 4852–4862.

Reeves, R.K., Li, H., Jost, S., Blass, E., Li, H., Schafer, J.L., Varner, V., Manickam, C., Eslamizar, L., Altfeld, M., et al. (2015). Antigen-specific NK cell memory in rhesus macaques. Nat Immunol.

Rehe, K., Wilson, K., Bomken, S., Williamson, D., Irving, J., Boer, den, M.L., Stanulla, M., Schrappe, M., Hall, A.G., Heidenreich, O., et al. (2013). Acute B lymphoblastic leukaemia-propagating cells are present at high frequency in diverse lymphoblast populations. EMBO Mol Med *5*, 38–51.

Romanski, A., Bug, G., Becker, S., Kampfmann, M., Seifried, E., Hoelzer, D., Ottmann, O.G., and Tonn, T. (2005). Mechanisms of resistance to natural killer cell-mediated cytotoxicity in acute lymphoblastic leukemia. Experimental Hematology *33*, 344–352.

Romee, R., Rosario, M., Berrien-Elliott, M.M., Wagner, J.A., Jewell, B.A., Schappe, T., Leong, J.W., Abdel-Latif, S., Schneider, S.E., Willey, S., et al. (2016). Cytokine-induced memory-like natural killer cells exhibit enhanced responses against myeloid leukemia. Sci Transl Med *8*, 357ra123–357ra123.

Roos, D. (2016). Chronic granulomatous disease. Br. Med. Bull. *118*, 50–63.

Ross, S.H., Rollings, C., Anderson, K.E., Hawkins, P.T., Stephens, L.R., and Cantrell, D.A. (2016). Phosphoproteomic Analyses of Interleukin 2 Signaling Reveal Integrated JAK Kinase-Dependent and -Independent Networks in CD8(+) T Cells. Immunity *45*, 685–700.

Rouce, R.H., Shaim, H., Sekine, T., Weber, G., Ballard, B., Ku, S., Barese, C., Murali, V., Wu, M.-F., Liu, H., et al. (2016). The TGF-β/SMAD pathway is an important mechanism for NK cell immune evasion in childhood B-acute lymphoblastic leukemia. Leukemia *30*, 800–811.

Ruggeri, L. (2002). Effectiveness of Donor Natural Killer Cell Alloreactivity in Mismatched Hematopoietic Transplants. Science *295*, 2097–2100.

Ruggeri, L., Capanni, M., Casucci, M., Volpi, I., Tosti, A., Perruccio, K., Urbani, E., Negrin, R.S., Martelli, M.F., and Velardi, A. (1999). Role of natural killer cell alloreactivity in HLA-mismatched hematopoietic stem cell transplantation. Blood *94*, 333–339.

Russell, J.H., and Ley, T.J. (2002). Lymphocyte-mediated cytotoxicity. Annu. Rev. Immunol. *20*, 323–370.

Scapini, P., and Cassatella, M.A. (2014). Social networking of human neutrophils within the immune system. Blood *124*, 710–719.

Schimmer, A.D., Hedley, D.W., Penn, L.Z., and Minden, M.D. (2001). Receptor- and mitochondrial-mediated apoptosis in acute leukemia: a translational view. Blood *98*, 3541–3553.

Schlums, H., Cichocki, F., Tesi, B., Theorell, J., Béziat, V., Holmes, T.D., Han, H., Chiang, S.C.C., Foley, B., Mattsson, K., et al. (2015). Cytomegalovirus infection drives adaptive epigenetic diversification of NK cells with altered signaling and effector function. Immunity *42*, 443–456.

Schmidt, H., Gelhaus, C., Nebendahl, M., Lettau, M., Watzl, C., Kabelitz, D., Leippe, M., and Janßen, O. (2008). 2-D DIGE analyses of enriched secretory lysosomes reveal heterogeneous profiles of functionally relevant proteins in leukemic and activated human NK cells. Proteomics *8*, 2911–2925.

Schmidt, S., Tramsen, L., Hanisch, M., Latgé, J.-P., Huenecke, S., Koehl, U., and Lehrnbecher, T. (2011). Human natural killer cells exhibit direct activity against Aspergillus fumigatus hyphae, but not against resting conidia. J. Infect. Dis. *203*, 430–435.

Schmidt, S., Zimmermann, S.-Y., Tramsen, L., Koehl, U., and Lehrnbecher, T. (2013). Natural killer cells and antifungal host response. Clin. Vaccine Immunol. *20*, 452–458.

Schurich, A., Pallett, L.J., Jajbhay, D., Wijngaarden, J., Otano, I., Gill, U.S., Hansi, N., Kennedy, P.T., Nastouli, E., Gilson, R., et al. (2016). Distinct Metabolic Requirements of Exhausted and Functional Virus-Specific CD8 T Cells in the Same Host. Cell Rep *16*, 1243–1252.

Shaffer, S.M., Dunagin, M.C., Torborg, S.R., Torre, E.A., Emert, B., Krepler, C., Beqiri, M., Sproesser, K., Brafford, P.A., Xiao, M., et al. (2017). Rare cell variability and drug-induced reprogramming as a mode of cancer drug resistance. Nature *546*, 431–435.

Shalem, O., Sanjana, N.E., Hartenian, E., Shi, X., Scott, D.A., Mikkelsen, T.S., Heckl, D., Ebert, B.L., Root, D.E., Doench, J.G., et al. (2014). Genome-Scale CRISPR-Cas9 Knockout Screening in Human Cells. Science *343*, 84–87.

Shi, F.-D., Ljunggren, H.-G., La Cava, A., and Van Kaer, L. (2011). Organ-specific features of natural killer cells. Nat Rev Immunol *11*, 658–671.

Shimaoka, M., Salas, A., Yang, W., Weitz-Schmidt, G., and Springer, T.A. (2003). Small Molecule Integrin Antagonists that Bind to the β 2 Subunit I-like Domain and Activate Signals in One Direction and Block Them in the Other. Immunity *19*, 391–402.

Shlush, L.I., Mitchell, A., Heisler, L., Abelson, S., Ng, S.W.K., Trotman-Grant, A., Medeiros, J.J.F., Rao-Bhatia, A., Jaciw-Zurakowsky, I., Marke, R., et al. (2017). Tracing the origins of relapse in acute myeloid leukaemia to stem cells. Nature *547*, 104–108.

Sieni, E., Cetica, V., Hackmann, Y., Coniglio, M.L., Da Ros, M., Ciambotti, B., Pende, D., Griffiths, G., and AricÃ², M. (2014). Familial Hemophagocytic Lymphohistiocytosis: When Rare Diseases Shed Light on Immune System Functioning. Front Immunol *5*, 44.

Skokowa, J., Dale, D.C., Touw, I.P., Zeidler, C., and Welte, K. (2017). Severe congenital neutropenias. Nat Rev Dis Primers *3*, 17032.

Slee, E.A., Harte, M.T., Kluck, R.M., Wolf, B.B., Casiano, C.A., Newmeyer, D.D., Wang, H.-G., Reed, J.C., Nicholson, D.W., Alnemri, E.S., et al. (1999). Ordering the Cytochrome c–initiated Caspase Cascade: Hierarchical Activation of Caspases-2, -3, -6, -7, -8, and -10 in a Caspase-9–dependent Manner. J. Cell Biol. *144*, 281–292.

Song, E., Jaishankar, G.B., Saleh, H., Jithpratuck, W., Sahni, R., and Krishnaswamy, G. (2011). Chronic granulomatous disease: a review of the infectious and inflammatory complications. Clin Mol Allergy *9*, 10.

Spencer, S.L., Gaudet, S., Albeck, J.G., Burke, J.M., and Sorger, P.K. (2009). Non-genetic origins of cell-to-cell variability in TRAIL-induced apoptosis. Nature *459*, 428–432.

Sprick, M.R., Rieser, E., Stahl, H., Grosse-Wilde, A., Weigand, M.A., and Walczak, H. (2002). Caspase-10 is recruited to and activated at the native TRAIL and CD95 death-inducing signalling complexes in a FADD-dependent manner but can not functionally substitute caspase-8. Embo J. *21*, 4520–4530.

Stepp, S.E., Dufourcq-Lagelouse, R., Le Deist, F., Bhawan, S., Certain, S., Mathew, P.A., Henter, J.-I., Bennett, M., Fischer, A., de Saint Basile, G., et al. (1999). Perforin Gene Defects in Familial Hemophagocytic Lymphohistiocytosis. Science *286*, 1957–1959.

Strasser, A., Cory, S., and Adams, J.M. (2011). Deciphering the rules of programmed cell death to improve therapy of cancer and other diseases. Embo J. *30*, 3667–3683.

Stuehler, C., Kuenzli, E., Jaeger, V.K., Baettig, V., Ferracin, F., Rajacic, Z., Kaiser, D., Bernardini, C., Forrer, P., Weisser, M., et al. (2015). Immune Reconstitution After Allogeneic Hematopoietic Stem Cell Transplantation and Association With Occurrence and Outcome of Invasive Aspergillosis. J. Infect. Dis. *212*, 959–967.

Sun, J.C., and Lanier, L.L. (2011). NK cell development, homeostasis and function: parallels with $CD8^+$ T cells. Nat Rev Immunol *11*, 645–657.

Sun, J.C., Beilke, J.N., and Lanier, L.L. (2009). Adaptive immune features of natural killer cells. Nature *457*, 557–561.

Swaminathan, S., Klemm, L., Park, E., Papaemmanuil, E., Ford, A., Kweon, S.-M., Trageser, D., Hasselfeld, B., Henke, N., Mooster, J., et al. (2015). Mechanisms of clonal evolution in childhood acute lymphoblastic leukemia. Nat Immunol *16*, 766–774.

Tabas, I., and Ron, D. (2011). Integrating the mechanisms of apoptosis induced by endoplasmic reticulum stress. Nat. Cell Biol. *13*, 184–190.

Takeda, K., Smyth, M.J., Cretney, E., Hayakawa, Y., Kayagaki, N., Yagita, H., and Okumura, K. (2002). Critical Role for Tumor Necrosis Factor–related Apoptosis-inducing Ligand in Immune Surveillance Against Tumor Development. J. Exp. Med. *195*, 161–169.

Tan, H., Yang, K., Li, Y., Shaw, T.I., Wang, Y., Blanco, D.B., Wang, X., Cho, J.-H., Wang, H., Rankin, S., et al. (2017). Integrative Proteomics and Phosphoproteomics Profiling Reveals Dynamic Signaling Networks and Bioenergetics Pathways Underlying T Cell Activation. Immunity *46*, 488–503.

Taylor, R.C., Cullen, S.P., and Martin, S.J. (2008). Apoptosis: controlled demolition at the cellular level. Nat Rev Mol Cell Biol *9*, 231–241.

Thiery, J., Keefe, D., Boulant, S., Boucrot, E., Walch, M., Martinvalet, D., Goping, I.S., Bleackley, R.C., Kirchhausen, T., and Lieberman, J. (2011). Perforin pores in the endosomal membrane trigger the release of endocytosed granzyme B into the cytosol of target cells. Nat Immunol *12*, 770–777.

Thoren, F.B., Romero, A.I., and Hermodsson, S. (2007). The CD16−/CD56bright subset of NK cells is resistant to oxidant-induced cell death. The Journal of Immunology.

Vanherberghen, B., Olofsson, P.E., Forslund, E., Sternberg-Simon, M., Khorshidi, M.A., Pacouret, S., Guldevall, K., Enqvist, M., Malmberg, K.-J., Mehr, R., et al. (2013). Classification of human natural killer cells based on migration behavior and cytotoxic response. Blood *121*, 1326–1334.

Vasconcelos, Z., Müller, S., Guipouy, D., Yu, W., Christophe, C., Gadat, S., Valitutti, S., and Dupré, L. (2015). Individual Human Cytotoxic T Lymphocytes Exhibit Intraclonal Heterogeneity during Sustained Killing. Cell Rep *11*, 1474–1485.

Vély, F., Barlogis, V., Vallentin, B., Neven, B., Piperoglou, C., Ebbo, M., Perchet, T., Petit, M., Yessaad, N., Touzot, F., et al. (2016). Evidence of innate lymphoid cell redundancy in humans. Nat Immunol *17*, 1291–1299.

Viel, S., Marçais, A., Guimaraes, F.S.-F., Loftus, R., Rabilloud, J., Grau, M., Degouve, S., Djebali, S., Sanlaville, A., Charrier, E., et al. (2016). TGF-β inhibits the activation and functions of NK cells by repressing the mTOR pathway. Sci Signal *9*, ra19–ra19.

Vivier, E., Di Santo, J., and Moretta, A. (2016). Natural Killer Cells.

Vivier, E., Raulet, D.H., Moretta, A., Caligiuri, M.A., Zitvogel, L., Lanier, L.L., Yokoyama, W.M., and Ugolini, S. (2011). Innate or adaptive immunity? The example of natural killer cells. Science *331*, 44–49.

Vivier, E., Ugolini, S., and Nunès, J.A. (2013). ADAPted secretion of cytokines in NK cells. Nat Immunol *14*, 1108–1110.

Voskoboinik, I., Whisstock, J.C., and Trapani, J.A. (2015). Perforin and granzymes: function, dysfunction and human pathology. Nat Rev Immunol.

Vrazo, A.C., Hontz, A.E., Figueira, S.K., Butler, B.L., and Ferrell, J.M. (2015). Live cell evaluation of granzyme delivery and death receptor signaling in tumor cells targeted by human natural killer cells. Blood.

Wada, T., Muraoka, M., Toma, T., Imai, T., Shigemura, T., Agematsu, K., Haraguchi, K., Moriuchi, H., Oh-Ishi, T., Kitoh, T., et al. (2013). Rapid detection of intracellular p47phox and p67phox by flow cytometry; useful screening tests for chronic granulomatous disease. J. Clin. Immunol. *33*, 857–864.

Waddington, C.H. (1957). The strategy of the genes. A discussion of some aspects of theoretical biology. With an appendix by H. Kacser. The Strategy of the Genes a Discussion of Some ….

Wajant, H., Johannes, F.J., Haas, E., and Siemienski, K. (1998). Dominant-negative FADD inhibits TNFR60-, Fas/Apo1-and TRAIL-R/Apo2-mediated cell death but not gene induction. Current Biology.

Walch, M., Dotiwala, F., Mulik, S., Thiery, J., Kirchhausen, T., Clayberger, C., Krensky, A.M., Martinvalet, D., and Lieberman, J. (2014). Cytotoxic cells kill intracellular bacteria through granulysin-mediated delivery of granzymes. Cell *157*, 1309–1323.

Walczak, H. (2013). Death receptor-ligand systems in cancer, cell death, and inflammation. Cold Spring Harb Perspect Biol *5*, a008698–a008698.

Walter, D., Lier, A., Geiselhart, A., Thalheimer, F.B., Huntscha, S., Sobotta, M.C., Moehrle, B., Brocks, D., Bayindir, I., Kaschutnig, P., et al. (2015). Exit from dormancy provokes DNA-damage-induced attrition in haematopoietic stem cells. Nature.

Walzer, T., and Marçais, A. (2016). [Memory NK cells discovered in non-human primates]. Med Sci (Paris) *32*, 246–248.

Walzer, T., Dalod, M., Robbins, S.H., Zitvogel, L., and Vivier, E. (2005). Natural-killer cells and dendritic cells: "l'union fait la force". Blood *106*, 2252–2258.

Wang, R., Jaw, J.J., Stutzman, N.C., Zou, Z., and Sun, P.D. (2012). Natural killer cell-produced IFN-γ and TNF-α induce target cell cytolysis through up-regulation of ICAM-1. J Leukoc Biol *91*, 299–309.

Watzl, C., Urlaub, D., Fasbender, F., and Claus, M. (2014). Natural killer cell regulation - beyond the receptors. F1000Prime Rep *6*, 87.

Wei, M.C., Zong, W.X., Cheng, E.H., Lindsten, T., Panoutsakopoulou, V., Ross, A.J., Roth, K.A., MacGregor, G.R., (null), and Korsmeyer, S.J. (2001). Proapoptotic BAX and BAK: a requisite gateway to mitochondrial dysfunction and death. Science *292*, 727–730.

Weitz-Schmidt, G., Chreng, S., and Riek, S. (2009). Allosteric LFA-1 Inhibitors Modulate Natural Killer Cell Function. Molecular Pharmacology *75*, 355–362.

Wen, Z., Shimojima, Y., Shirai, T., Li, Y., Ju, J., Yang, Z., Tian, L., Goronzy, J.J., and Weyand, C.M. (2016). NADPH oxidase deficiency underlies dysfunction of aged CD8+ Tregs.

Wilson, N.S., Dixit, V., and Ashkenazi, A. (2009). Death receptor signal transducers: nodes of coordination in immune signaling networks. Nat Immunol *10*, 348–355.

Wu, C., Li, B., Lu, R., Koelle, S.J., Yang, Y., Jares, A., Krouse, A.E., Metzger, M., Liang, F., Loré, K., et al. (2014). Clonal Tracking of Rhesus Macaque Hematopoiesis Highlights a Distinct Lineage Origin for Natural Killer Cells. Cell Stem Cell *14*, 486–499.

Xu, T., Stewart, K.M., Wang, X., Liu, K., Xie, M., Kyu Ryu, J., Li, K., Ma, T., Wang, H., Ni, L., et al. (2017). Metabolic control of TH17 and induced Treg cell balance by an epigenetic mechanism. Nature *548*, 228–233.

Zhu, S., Phatarpekar, P.V., Denman, C.J., Senyukov, V.V., Somanchi, S.S., Nguyen-Jackson, H.T., Mace, E.M., Freeman, A.F., Watowich, S.S., Orange, J.S., et al. (2014). Transcription of the activating receptor NKG2D in natural killer cells is regulated by STAT3 tyrosine phosphorylation. Blood *124*, 403–411.

Zhu, Y., Marchal, C.C., Casbon, A.-J., Stull, N., Löhneysen, von, K., Knaus, U.G., Jesaitis, A.J., McCormick, S., Nauseef, W.M., and Dinauer, M.C. (2006). Deletion mutagenesis of p22phox subunit of flavocytochrome b558: identification of regions critical for gp91phox maturation and NADPH oxidase activity. J. Biol. Chem. *281*, 30336–30346.

Ziegler, S., Weiss, E., Schmitt, A.-L., Schlegel, J., Burgert, A., Terpitz, U., Sauer, M., Moretta, L., Sivori, S., Leonhardt, I., et al. (2017). CD56 Is a Pathogen Recognition Receptor on Human Natural Killer Cells. Sci Rep *7*, 6138.

CHAPTER 7.
RÉSUMÉ DE LA THÈSE EN FRANÇAIS

7. RÉSUMÉ DE LA THÈSE EN FRANÇAIS

Les cellules Natural Killer (NK) ont été initialement décrites en 1975 (Herberman et al., 1975), caractérisées par leur capacité cytotoxique spontanée face à des cellules cibles sans étape préalable de sensibilisation ni restriction aux molécules du complexe majeure d'histocompatibilité. Au sein du système immunitaire, elles contribuent à défendre l'organisme face aux infections et transformations tumorales, et participent à la régulation de la réponse immunitaire adaptative et au maintien de l'homéostasie via l'élimination sélective des cellules ayant pris part à cette réponse immunitaire (Lieberman, 2016).

Dans le sang périphérique, les cellules NK représentent de 5 à 15% des cellules mononucléées (Lotze and Thomson, 2009). Elles sont également retrouvées dans certains organes (foie, tissus lymphoïdes secondaires, muqueuses, peau, poumons, utérus, pancréas, système nerveux central…) où leur proportion peut être significativement plus élevée.

De par leurs fonctions en miroir de celles des lymphocytes T $CD8^+$, les cellules NK sont considérées comme des cellules lymphoïdes innées cytotoxiques (Eberl et al., 2015; 2014). Lorsqu'elles interagissent avec une cellule cible, c'est la balance des signaux médiés par les récepteurs activateurs et inhibiteurs de surface qui détermine l'engagement des fonctions effectrices des cellules NK. Celles-ci comprennent la production (indépendante du contact cellulaire) de cytokines solubles ainsi que les voies (associées au contact entre cibles et effecteurs) de l'exocytose de granules cytotoxiques (ou dégranulation) et des récepteurs de mort cellulaire.

Les leucémies aiguës lymphoblastiques (ou LAL) pré-B représentent la cause la plus fréquente de décès par cancer avant l'âge de 20 ans (Hunger and Mullighan, 2015; Inaba et al., 2013; Oskarsson et al., 2016). Les données de survie se sont améliorées avec 85 à 90% de survie chez les enfants atteints mais également des complications sur le long terme liées au traitement par chimiothérapie (Hunger and Mullighan, 2015; Inaba et al., 2013; Oskarsson et al., 2016). La rechute survient chez environ 20% des patients pédiatriques et 60% des patients adultes (Perova et al., 2014) et est associée à un mauvais pronostic (Bhojwani and Pui, 2013).

L'allogreffe de cellules souches hématopoïétiques est l'une des approches thérapeutiques pouvant être proposées aux patients. Elle fut initialement développée pour deux raisons (Copelan, 2006) : tout d'abord, elle permet le remplacement complet d'un système hématopoïétique anormal par celui d'un donneur sain (ce qui s'avère pertinent dans le cas

de déficits immunitaires primitifs ainsi que dans celui des hémopathies malignes) (Gooley et al., 2010) ; ensuite, elle autorise le recours à un traitement myéloablatif "à haute dose" pour les patients atteints de cancer, pour lesquels cela permet d'accentuer l'élimination des cellules tumorales mais conduit aussi à une perte de fonction médullaire permanente nécessitant donc le secours d'une allogreffe.

Dans ce contexte, l'immunobiologie de l'allogreffe de cellules souches hématopoïétiques implique une reconnaissance et une réponse immune potentielle entre donneur et receveur, et réciproquement. Elle se manifeste ainsi par deux effets étroitement corrélés et liés à la présence de cellules immunocompétentes dans le greffon : l'effet délétère du greffon contre l'hôte (ou GvHD pour *graft-versus-host disease*) et celui bénéfique du greffon contre la tumeur (ou GvT pour *graft-versus-tumor*). Les lymphocytes T et les cellules NK sont deux populations cellulaires du greffon contributives de ces effets. Concernant les cellules NK, la base de leur alloréactivité repose sur l'engagement ou non de récepteurs présents à la surface de ces cellules et capables de reconnaître les déterminants polymorphiques des molécules du complexe majeur d'histocompatibilité (CMH) de classe I. Par ailleurs, des récepteurs activateurs entrent également en jeu et c'est la balance entre signaux activateurs et signaux inhibiteurs qui déterminent la réponse effectrice des cellules NK.

En 2002, Loredana Ruggeri *et al.* ont rapporté le rôle important joué par les cellules NK dans le cadre de l'allogreffe de cellules souches hématopoïétiques (Ruggeri, 2002). Leurs travaux ont établi que les leucémies aiguës myéloïdes (ou LAM) du receveur peuvent être éliminées par les cellules NK du donneur présentes dans le greffon. Cependant, les LAL pré-B ont été décrites résistantes à cet effet cytotoxique (Imai et al., 2005; Kübler et al., 2014; Romanski et al., 2005; Ruggeri, 2002; Ruggeri et al., 1999).

Ce travail de thèse s'intéresse à la compréhension des mécanismes qui gouvernent l'alloréactivité des cellules NK face aux LAL pré-B ainsi que ceux expliquant la résistance de ce type de cellules cibles.

Nos résultats ont permis de démontrer que les LAL pré-B ne sont pas intrinsèquement résistantes à l'action cytotoxique des NK. Une exposition prolongée des blastes leucémiques (de lignées ou primaires) à des cellules NK amplifiées et activées *in vitro* (NKAES-NK) permet de surmonter cette résistante de façon efficace. Surtout, nous avons constaté que cette cytotoxicité ne reposait pas sur des mécanismes classiques tels que l'exocytose de granules cytotoxiques ou l'engagement de la voie des récepteurs de mort cellulaire mais sur un

nouveau mécanisme effecteur puisque : (1) les cellules NKAES-NK n'expriment pas le CD107a lors des tests de cytotoxicité ; (2) les cellules NKAES-NK obtenues à partir des patients déficients en perforine ou en Munc13.4 (molécule nécessaire à la dégranulation) ne perdent pas leur capacité à tuer les cellules LAL ; et (3) les cellules NKAES-NK tuent les cellules LAL pré-B exprimant un dominant négatif de FADD.

En étudiant le processus de mort induit dans les cellules cibles leucémiques, nous montrons que le mécanisme est contact-dépendant mais que, bien qu'ayant un profil de type apoptotique avec une activation des caspases et une dépolarisation mitochondriale, il est indépendant de ces deux processus biologiques. En effet, des cellules cibles rendues double déficientes grâce à la technologie CRISPR/Cas9 pour les caspases 3 et 7 (et donc résistantes à l'apoptose), ou pour BAX et BAK (et donc incapables de dépolariser leur mitochondrie), meurent de façon identique lorsqu'elles sont exposées aux cellules NK activées allogéniques. Dans leur ensemble et de façon complémentaire à nos observations sur les cellules NK, nos résultats suggèrent l'engagement d'un nouveau processus de mort dans les cellules cibles qui sont éliminées.

Nous avons ensuite étudié la contribution du stress oxidant et observé qu'un pré-traitement par le N-acétylcystéine (ou NAC), un inhibiteur des "espèces réactives de l'oxygène" (ROS), inhibait partiellement la cytotoxicité des NKAES-NK suggérant que notre nouveau mécanisme cytotoxique pouvait impliquer les ROS. Les blastes leucémiques rendus davantage résistants au stress oxidant par transduction avec la catalase et la superoxide dismutase 2 sont éliminés de façon identique par les cellules NKAES-NK. Nous avons donc ensuite exploré la voie de production des ROS dans les cellules effectrices en testant les cellules NKAES-NK de patients atteints de granulomatose septique chronique (CGD), porteurs de mutations dans un des gènes codant pour les protéines du complexe NADPH oxydase ($p22^{phox}$, $p40^{phox}$, $p47^{phox}$, $p67^{phox}$ et $gp91^{phox}$). Nous avons constaté que seules les cellules NKAES-NK déficitaires en $gp91^{phox}$ présentaient une fonction cytotoxique altérée contre les cellules LAL pré-B, suggérant un rôle de cette protéine dans notre nouveau mécanisme cytotoxique.

Dans les phagocytes, la NADPH oxydase est un complexe qui comprend notamment un hétérodimère membranaire, le flavocytochrome b558, formé par l'association de $p22^{phox}$ et $gp91^{phox}$. L'expression de de cet hétérodimère peut être vérifiée grâce à l'utilisation d'un anticorps monoclonal spécifique (clone 7D5). L'existence d'un complexe de type NADPH oxydase dans les cellules NK n'est pas documentée à notre connaissance. Nos résultats

démontrent que les cellules NK expriment bien au niveau transcriptomique mais aussi protéique, $p22^{phox}$ et $gp91^{phox}$, mais pas le flavocytochrome b558 exprimé par les phagocytes et les lymphocytes B. Le complexe moléculaire précis présent dans les cellules NK reste ainsi à caractériser de façon approfondie.

Notre étude s'est poursuivie par une analyse transcriptomique des cellules NK non activées ainsi que NKAES-NK de contrôles sains et de patients atteints d'une granulomatose septique chronique liée à l'X (due à un déficit en $gp91^{phox}$), éventuellement post-exposition à une lignée LAL pré-B sensible (REH) ou résistante (RS4;11) à l'action cytotoxique des NKAES-NK. Les résultats suggèrent des modifications métaboliques importantes parmi les NKAES-NK exposées ou non aux différentes cibles leucémiques. Nous avons pu le confirmer par une étude fonctionnelle de la glycolyse et de la phosphorylation oxidative des cellules NKAES-NK, révélant une signature métabolique distincte selon l'engagement des voies effectrices par les cellules NK. Lorsque les cellules ont été exposées à la lignée K562 (où la voie de l'exocytose des granules cytotoxiques prédomine), les modifications métaboliques sont distinctes de celles mesurées après coculture avec des LAL pré-B. Dans ce dernier cas, une utilisation accrue de la glycolyse est observée. De façon intéressante, les cellules NKAES-NK de patients déficitaires en $gp91^{phox}$ ont montré un défaut de cette hyperglycolyse, suggérant une altération de la capacité d'adaptation métabolique de ces cellules.

Dans leur ensemble, les résultats présentés dans cette thèse remettent en cause le dogme de la résistance des LAL pré-B à l'action cytotoxique des cellules NK, ainsi que l'absence d'expression ou d'un rôle de la protéine $gp91^{phox}$ dans ces mêmes lymphocytes cytotoxiques. La poursuite de ces travaux devrait permettre une meilleure compréhension des mécanismes moléculaires contribuant à la nouvelle voie de cytotoxicité que nous décrivons, et en corollaire, au type de mort cellulaire induit dans les cellules de LAL pré-B.

Titre : Cellules Natural Killer et leucémies aiguës lymphoblastiques pré-B : éléments de preuve d'une voie de cytotoxicité non conventionnelle

Mots clés : Cellules NK ; leucémie aiguë lymphoblastique ; cytotoxicité ; mort cellulaire ; granulomatose septique chronique ; déficits immunitaires

Résumé : Les cellules Natural Killer (NK) représentent une population de cellules innées lymphoïdes aux fonctions anti-infectieuses et antitumorales. Les leucémies aiguës lymphoblastiques pré-B (LAL pré-B) constituent le cancer de l'enfant le plus fréquent et ont été décrites comme résistantes à la cytotoxicité médiée par les NK bien que les bases moléculaires demeurent inconnues.
L'objectif de ces travaux a été de caractériser cette résistance. En développant un essai de cytotoxicité par cytométrie en flux et en utilisant des cellules effectrices activées *in vitro*, nous avons établi la sensibilité retardée des LAL pré-B à la cytotoxicité NK : initialement résistantes après 4h d'incubation, elles sont fortement tuées après 25h.
Cette cytotoxicité est contact-dépendante mais ni la voie de l'exocytose des granules cytotoxiques ni celle des récepteurs de mort n'y contribuent. La mort cellulaire des cibles est de profil apoptotique mais indépendante des caspases ; la signalisation mitochondriale l'amplifie partiellement. Interférer avec les dérivés de l'oxygène par un antioxydant diminue la cytotoxicité. Nous montrons que les cellules NK de patients atteints de granulomatose septique chronique liée à l'X présentent un défaut de cette nouvelle cytotoxicité. Nous démontrons l'expression par les NK des composants clefs d'une NADPH oxydase distincte du complexe utilisé par les phagocytes. Nos travaux établissent l'existence d'une voie de cytotoxicité non conventionnelle et en définissent les principaux prérequis moléculaires.

Title: Natural Killer cells and pre-B acute lymphoblastic leukemia: evidence for an unconventional cytotoxicity pathway

Keywords: Natural Killer cells; acute lymphoblastic leukemia; cytotoxicity; cell death; chronic granulomatous disease; immune deficiencies

Abstract: Natural Killer (NK) cells are innate lymphoid cells with anti-infectious and anti-tumoral activities. Among neoplasia, pre-B acute lymphoblastic leukemias (pre-B ALL) represent the most common form of cancer in childhood and were shown to be resistant to NK cell mediated cytotoxicity although the mechanisms explaining this phenomenon are incompletely understood.
In the present work, we investigated the relative immune resistance of pediatric pre-B ALL targets to activated NK cells. We developed a flow cytometry based cytotoxicity assay to assess the NK activity and the involvement of long term cytotoxic pathways. Although pre-B ALL blasts were strongly resistant at 4h, we found a considerable delayed NK killing at 25h.
Further investigations revealed that cell contact was mandatory for efficient killing but also that neither the granule exocytosis nor the death receptor pathway were involved. Target cell death was caspase independent but mitochondria signaling amplified it. We then showed that NK cells from patients with X-linked chronic granulomatous disease could not kill efficiently ALL blasts and that NK cells expressed key components of a NADPH oxidase complex that was distinct from the phagocyte type.
Our work reveals an uncharacterized effector pathway among cytotoxic lymphocytes and establishes key molecular requirements for this unconventional pathway.